

BRAIN- SPINE- MUSCLE INTERFACES

BY: JACKSON POWELL
FOR: **FUTURE** JACKSON

root@/last_updated: **November 15, 2023**

Once you know the way broadly, you can see it in all things.
– The Book of Five Rings by Miyamoto Musashi

Contents

0.1	Overview	1
0.1.1	Purpose	1
0.2	To Do:	1
I	Electronics	2
1	Background Information	3
1.0.1	Overview	3
1.1	How Electricity Works	3
1.1.1	The misconception	3
1.2	Laws and Devices	4
1.2.1	Thevenin and Ideality	5
1.2.2	LED Circuits and PNP	7
1.3	Resistor Lattice Digression	8
2	Capacitors, Inductors, Filters	14
2.1	Overview	14
2.2	Capacitor Behavior	15
2.3	Filtration Conceptually	16
2.3.1	Integration and Differentiation	16
2.4	Frequency Dependence	18
2.4.1	Imaginary Numbers Digression.	19
2.5	Impedance	20
2.6	Filtration Quantitatively	21
2.6.1	Corner Frequency and Phase Shift	22
2.6.2	Summarizing Thoughts	22
2.7	Inductors	23
2.8	Peak Detection	24
2.9	Input and Output Resistance	25
3	Opamps	27
3.1	Introduction and Gold	27
3.1.1	Golden Rules	28
3.2	Simple Opamp Circuits	28
3.3	Opamp Imperfections	33
4	Transistors	35
4.0.1	Transistor Overview	35

4.1	Transistor Circuits	35
4.1.1	A Follower	35
4.1.2	Amplifiers	38
4.1.3	Current Sources	39
4.1.4	The Components of an OpAmp	40
5	Writing Hardware	44
5.1	Introduction	44
5.1.1	Creating Modules	44
5.1.2	Bus Notation	45
5.1.3	Constants and Variables	46
5.1.4	Logic	46
5.1.5	Adder	47
II	Math and Models	48
5.2	Perspective	49
6	Math Essentials	50
6.1	Linear Algebra	50
6.1.1	Cross Products, Dot Products, and Gradients	50
6.2	Markov-chains	50
7	Neuron Modeling	52
7.1	Hodgkin-Huxley	52
7.1.1	The Main Form	52
7.1.2	Gating and Conductance	52
7.2	Fitzhugh-Nagumo Reduction	53
7.2.1	Why would we simplify this system?	53
7.2.2	How to Reduce	54
7.3	Diffusion	56
7.3.1	Diffusion Equation Derivation	56
7.3.2	Forward Euler's	57
7.3.3	Backward Euler's	58
8	Modeling Circuits	60
9	Fluid Mechanics and Cell Motility	62
9.1	Introduction	62
9.2	Cell Motility	62
9.3	Fluid Mechanics	62
9.3.1	Conservation of Mass	65
9.3.2	Stress Tensor	66
9.3.3	Conservation of Momentum	67
9.3.4	Navier-Stokes Equations	68
9.3.5	Propulsion	70
9.4	Literature	71
9.4.1	CSF Flow	71

10 Machine Learning	73
10.0.1 Models	74
III Physiology	76
10.1 Perspective	77
11 Biochemistry	78
11.1 Membranes, Ions, and Potentials	78
11.1.1 Action Potentials	80
11.2 Ion Channels	81
11.2.1 Voltage Gated Channels	81
11.3 Current Literature	82
11.3.1 Piezo	85
12 Muscles	86
12.1 Skeletal Muscle	86
12.1.1 A Cellular Level	86
12.1.2 Disorders Digression	87
12.2 Smooth Muscle	88
12.2.1 A Cellular Level	88
12.3 Cardiac Muscle	89
12.3.1 A Cellular Level	89
13 Sensory Processing	91
13.1 Various Senses	92
13.1.1 Touch	92
13.1.2 Temperature	92
13.1.3 Pain	92
13.1.4 Olfaction	92
13.1.5 Ears in Hearing and More	92
13.1.6 Vision	94
14 The Central Nervous System	96
14.1 Spinal Cord General Structure	96
14.2 Autonomic Nervous System	97
14.2.1 Sympathetic Nervous System	97
14.2.2 Parasympathetic Nervous System	98
14.3 Somatic Nervous System	98
14.4 Acetylcholine, Nicotinic Receptors, and Muscarinic Receptors	99
14.5 Cerebrospinal Fluid	100
14.5.1 Structure Overview	100
14.5.2 CSF Contacting Cells	100
14.6 Myelin in Health and Regeneration	101
14.6.1 Initiation of Demyelination	102
14.7 Central Pattern Generation	102

IV Spinal Cord Injury	103
15 The Injury Itself	104
15.1 Cell Specific Responses	104
15.1.1 Immune Response	104
15.1.2 Neural Response	105
15.1.3 IL-12 Sensing Neurons Promote Neuroprotection	106
16 In The Clinic & Therapeutic Approaches	108
16.1 Clinical Presentation	108
16.2 Auxiliary Management	109
16.3 Treatments	110
16.3.1 Electrical Stimulation	110
16.3.2 Biomaterials	111
16.3.3 Drug Treatment	111
16.3.4 Surgery	111
16.3.5 Rehabilitation	112
16.4 Complications After SCI	112
17 Approaches to Researching SCI	114
17.1 SCI Injury Models	114
17.2 The Basso Scale	115
17.3 Traumatic and Nontraumatic SCI	116
18 Broad Coverage of Axonal Regeneration	118
18.1 Intrinsic Factors	118
18.2 Extrinsic Factors	120
18.3 Recovery of Walking via Target Reconnection	121
18.4 Neuronal Excitability and Regeneration	122
19 Metabolism of Neurons	123
19.1 Programming Mitochondrial Maintenance	123
19.1.1 Mitochondrial Generation and Degredation	123
19.1.2 Mitochondrial Trafficking	124
19.1.3 Response to Stress	124
19.1.4 Neuronal Injury and Regeneration	125
20 Circuit Reorganization and Plasticity	126
20.1 Reorganization After Injury	126
20.1.1 Interneurons and KCC2	128
20.2 Non-coding RNA in Rewiring and Plasticity	129
20.3 Synaptic Pruning	130
20.3.1 Ube3a E3 Ligase Promotes Pruning in Flies	130
21 Stem Cell and Tissue Engineering	132
21.1 Cell Transplantation Therapy	132
21.1.1 Long Distance Growth of Stem Cells	133
21.1.2 3D Printed Spinal Scaffolds	133

V	Brain-Spine-Muscle Interfaces	135
21.2	Perspective	136
22	Interfacing with Nerves	137
22.1	Historical Dealings	137
22.2	Electrostimulation	138
22.2.1	Background	138
22.2.2	Biomaterials Used	138
22.2.3	Flexible Brain-Computer Interfaces	139
23	Peripheral Nerve Stimulation	141
23.0.1	Adaptive, Conductive, and Electrotherapeutic Scaffolds	141
23.0.2	Vagus Nerve Modulates Circuits via Acetylcholine	142
23.0.3	Hand Movement Recovery via Intrafascicular Stimulation	143
24	Spinal Cord Stimulation	144
24.0.1	Electronic Dura Mater	144
24.0.2	Electronics with Shape Actuation	145
24.0.3	SCI Specific Cells	146
24.1	Clinical Applications	147
24.2	Advancements in Parkinson’s Disease	148
24.2.1	SCS-DBS Intersection	149
25	Brain Stimulation	150
25.1	Deep Brain Stimulation	150
25.1.1	Technology Overview	150
25.1.2	In the Clinic—Parkinson’s and Essential Tremor	151
25.1.3	The Surgery Itself	151
25.1.4	Living Electrodes	152
26	Reading Thoughts	154
26.0.1	Different Reading Devices	154
26.0.2	Reading LFPs Without Surgery	155
26.0.3	Neurograin	156
26.0.4	Robotic Control with Eye.	156
26.0.5	WIMAGINE ECoG	157
27	Synthesis	158
27.1	Lorach et al. 2023	158
27.1.1	Overview	158
27.1.2	Shortcomings	158
VI	Some Ideas	160
28	Ramblings	161
28.1	Idealized World	161
28.2	Device Idea	162
28.2.1	Motivation	162

28.2.2 Framework	162
VII Addendum	165
29 Neurodegeneration	167

0.1 Overview

0.1.1 Purpose

The purpose of this book is to aggregate all of the content and tools I will need in forging the future I desire: building better brain-spine-muscle interfaces. Interestingly, I already find myself referencing the information here quite a bit! It has already paid back itself in full.

0.2 To Do:

1. More neuron regeneration models (SCN, etc.).
2. Wrap-up electronics intro (Thev., Nort., etc.).
3. Diodes section :(
4. Markov Models :(
5. Sensory processing :(
6. Better breakdown of cellular localization in the spinal cord.
7. Clinical outcomes section.
8. Giovanni age-dependent regeneration article.
9. Deepen neuron activity section with focus on Bradke, Munc-13 paper, alpha2delta2, and their L-type vgcc work
10. Sections for: Minassian, Rossignol, and the other titans.

Part I

Electronics

Like many of the vagabonds who live in the fields, stray horses seemed to him to be good-natured things. When you're through with them, they ask for nothing; they just go off quietly somewhere by themselves.

– Musashi by Eiji Yoshikawa

Chapter 1

Background Information

1.0.1 Overview

The bulk of this information comes from the Lab Electronics course at the University of Pennsylvania, taught to me by Professor Ashmanskas^{1,2}. As a comment on notation: V represents a variable value, while V represents a unit (or at least, that's what it should be; sometimes I forget proper notation). Graphics like this were made using CircuitTikz, whose manual can be found here³.

1.1 How Electricity Works

1.1.1 The misconception

One often represents electricity with the canonical metaphor of water flowing in a tube, equating the flow of water, which powers a wheel of some sort, as being the equivalent of electrons pushing through a wire. Incidentally, this simplifying schema illustrates a key misconception in the nature of electricity. This is easiest exemplified in the mode with which electricity reaches one's house from a power-plant, which before arriving will be subject to breaks in the circuit (transformers). In the traditional viewing of electricity, that is taught in early education, this is disconcerting as if electrons can not physically go from a power plant to the lights in your home, then how can their kinetic energy be transferred to them and turn them on?

Regarding the flow of *energy*: when a battery sits without wires attached, around it is an electric field. This field does not dissipate because no electrons flow from it. When wires are attached, charge accumulates on the surface of the wires. This causes a small electric field within the wires, but the drift velocity of electrons within the wire is quite slow—nowhere near the speed of light that you might expect electricity to flow. However, the flow of electrons within the wire is sufficient to drive an electric field which exists all around the wires. From this, we can determine the direction that energy will flow by taking the cross product of the electric and magnetic fields. In fact, if an lightbulb is attached, this means that energy flows from the battery to the bulb in all directions, not through the wires itself. This energy flow induces the vibration of electrons within the bulb's filament, thereby causing light. This means that a net flow of electrons is not required to power a bulb—but rather

¹https://www.hep.upenn.edu/Courses/Phys364_spring23/

²<http://www.hep.upenn.edu/~ashmansk/>

³<https://texdoc.org/serve/circuitikzmanual.pdf/0>

only their vibrations. Thus is illustrated next:

Let us consider now what will happen with an AC circuit (120V AC outlets around your home), where the electromotive force flips with each cycle. In this case, both the electric and magnetic fields switch directions, meaning that their cross product will remain the same and, again, energy flows in all directions to power the lightbulb. Notably, the electrons do not move much (if at all) in this setup—but this is not a surprise, as it is not the electrons that carry the energy anyway. Now, it is still essential to recognize that it is the movement of electrons within the filament of a lightbulb that creates light. This is, indeed, from kinetic energy transferred from electrons bouncing against the metals lattice, dissipating energy in the form of light. The necessary distinction is that it is not electrons that flow all the way from the battery, but rather it is vibrations of those that were, and always will be, within the bulb itself. When you consider it like this, it is straightforward—as the electric field derived from the battery is what provides the electrons with enough kinetic energy to power the bulb.

Interestingly, comparisons to the “water flow” model fail dramatically in the traditional sense, but the Venturi Effect used to describe fluid flow actually succeeds. In adding a bulb you add a resistor, which is comparable to adding a part of a pipe with a smaller diameter. As water will flow faster in this section of the tube, so too will electrons. In order to maintain the same current as is through the rest of the tube, the drift velocity, V_d , must be higher. V_d is proportional to the electromotive force, E , meaning the force is highest within the bulb. Things like V_d are simplified into Ohm’s Law ($V = IR$) and not often discussed.

Of course you may say: “well, then why do we use wires at all?” The answer is that wires are helpful in channeling the fields, thereby making them more efficient. But, we do not *need* wires, per se. Think of wireless charging, for example. Knowing all of this, in this work I will almost invariably describe the flow of current as electrons moving through a wire. This is because it is much easier to think of electricity in this way, hence the ubiquitous misconception.

Nuances in the Fields.

It is worth explicitly highlighting that the electric field that causes the actual flow is from charges along the wires, rather than the battery. This is notable because if this were not the case, the proximity of the bulb to the battery would dictate its brightness. One may wonder how this type of charge distribution can be established so rapidly, and the reason is that the distance an electron needs to travel in order to create such a distribution is subatomic in size—meaning that with movement at the speed of light, the time it takes to establish a surface charge is effectively zero.

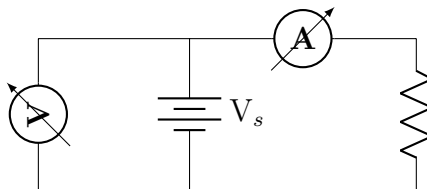
The whole idea is quite unintuitive, so it is appropriate to keep it smushed in the back of your mind, and to only draw it out when encountering things that are otherwise strange—like the aforementioned wireless charging, which should now be much more comprehensible.

1.2 Laws and Devices

The currents flowing in and out of a node will always be equal. The sum of the voltages over an entire circuit will always be equal. Kirchoff’s Voltage Law (KVL) can be used to show that wires connected in parallel will have the same voltage across them, and the current flowing in and out of a node will always be the same, defined in Kirchoff’s Current Law (KCL). In this way, we can predict the current

flowing through a circuit to be $V = IR$. The formula for power is given as: $VI = P$, which means that when one solves for voltage, and knowing that current is in units of charge/time and power in work/time, voltage is work per unit charge.

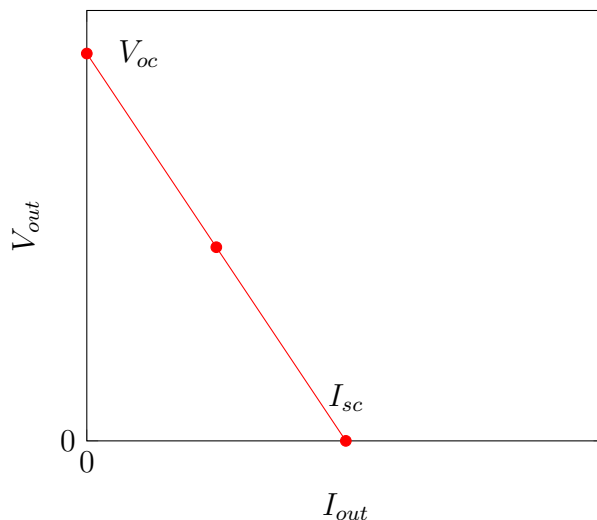
Voltage is measured using a voltmeter, a device in parallel with the load you are interested in measuring. An ammeter is used to measure current, which will be in series with the current you are trying to measure. This means that the voltmeter should have an extremely high resistance, so as to not draw any current, and an ammeter to have a low resistance, so as to not have any voltage drop. These are important considerations, as if the resistance of the load you are measuring is large (say, $1\text{M}\Omega$), it is possible that the voltmeter will have some non-negligible current flow through it. The same goes for if your circuit has very low resistance and you use an ammeter. To illustrate, one would measure the voltage and current coming from a battery as seen below:



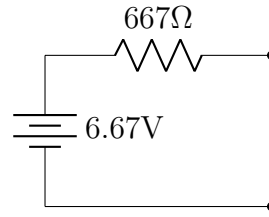
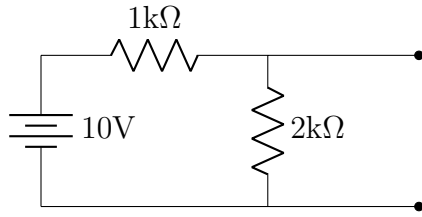
1.2.1 Thevenin and Ideality

A Thevenin Circuit simplifies the circuit to have a single resistance, R_{th} , and a single voltage, V_{th} . R_{th} can be calculated via replacing all of the voltage sources with a wire, and disconnecting all of the current sources. This “short circuits” your circuit and leaves you with only resistors, which can be used to calculate R_{th} using the familiar resistor rules. One can also short circuit the terminals, and determine the current flow, giving us $R_{th} = V_{th}/I_{sc}$.

R_{th} can be measured in a circuit by varying the R_{load} added to a circuit. In this case, you will see the voltage supplied (and corresponding current) change. The slope of this change ($\Delta V/\Delta I$) will equal R_{th} . If you vary the load through the two terminals and measure the voltage across it, you will get a graph that looks something like this:

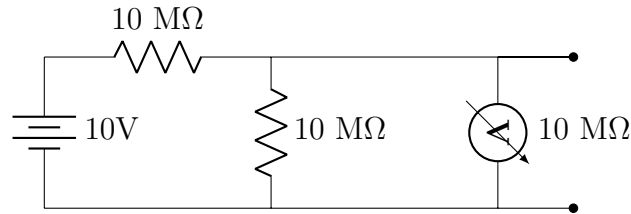


Again, the slope is what gives you R_{th} . I_{sc} is an important value which allows you to calculate V_{th} . The current that flows when you short circuit the load (I_{sc}), multiplied by R_{th} , gives you V_{th} .



The ideality of sources.

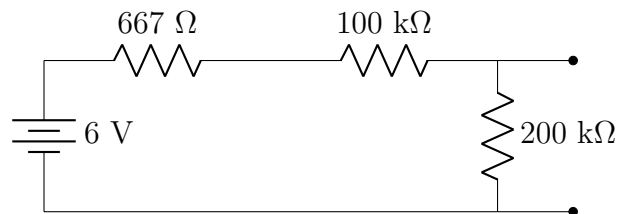
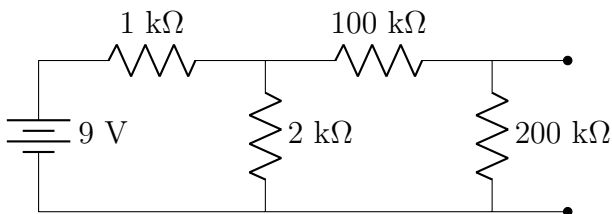
This coaxes us lightly into the topic of source ideality. Imagine all voltage or current sources as having a resistor in parallel with it, but inside of the component itself. An ideal battery, or voltage source, would be able to drive the same voltage, irrespective of the resistor/current. This would be like having a battery whose internal resistance is 0, causing the entirety of the voltage drop to occur on the circuit fragments outside of the battery. In the real world, batteries are not ideal. The canonical illustration of a batteries ideality is in trying to use a 9V battery to start your car. Naturally, the voltage dwindles as the current supplied increases. You can calculate the internal resistance of a battery by adding increasingly large loads to it, thereby giving you the batteries IV curve. It is worth considering this, as if your R_{load} is only $\approx 10 \times R_{th}$, then you may see drooping in the voltage supplied. Another way to state this is to make sure that the *input resistance* of your voltage source is much smaller than the *output resistance* of the upcoming circuit fragment you are attempting to drive. An example of when this fails is as follows:



Because the circuit has a non-negligible resistance relative to the voltmeter, you should expect to read something inconsistent with using an ideal voltmeter. As we are adding a $10\text{ M}\Omega$ voltmeter in parallel to our $10\text{ M}\Omega$ resistor, we expect that the “ R_{load} ” in this case will now be $5\text{ M}\Omega$, so the voltage divider at V_{out} will now be $1/3 \times 20\text{V}$, or 6.67V .

This contrasts to a current source, whose desired internal resistance is ∞ , as you will want no current to flow through it, and to flow entirely through the circuit fragments outside of the component. Once again, as the real world is not ideal, your goal in this case will be to have downstream circuit components whose input resistance is much smaller than the components output resistance.

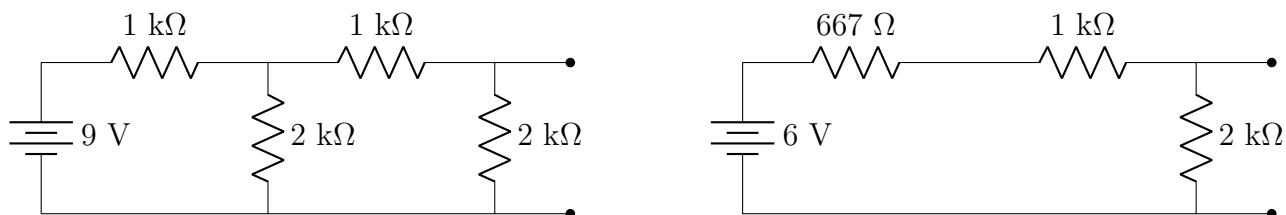
Let us consider another example of input resistance vs. output resistance:



If we draw a black box around the first voltage divider, we can convert it to the circuit schematic on the right because $1\text{ k}\Omega || 2\text{ k}\Omega = 667\text{ k}\Omega$ just as before. We can find the V_{th} by first finding I_{sc} , when

we short the black box's load. So, $I_{sc} = 9V/1k\Omega = 0.9mA$. We multiply I_{sc} (9 mA) by R_{th} (6.67 k Ω) to get a V_{th} of 6 V. If you were to compare the output resistance of the black box, 6.67 k Ω , to the input resistance of the upcoming voltage divider, 300 k Ω , you would find that it is much smaller. This naturally means that the entirety of the 6 V drop will occur over this part of the circuit.

Another way to think about this is as two successive voltage dividers, and qualitatively noting that the second's total resistance is much higher allows us to simplify things greatly. As a reminder, a voltage divider can be solved as $R_A I = R_A \times V_{total}/R_{total} = V_{total} \times R_A/(R_A + R_B)$. If you redraw as the Thevenin equivalent, the first voltage divider can effectively be ignored, because the voltage drop across this component will be minimal. Not by coincidence, since the first voltage divider is a 2/3 divider, and the second is a 2/3 divider, the voltage measured between our two terminals is $2/3 \times 2/3 \times 9V$, or alternatively, $2/3 \times 6V$ (V_{th}). This equivalency does not work when the input and output resistances of each fragment are comparable, here is an example:

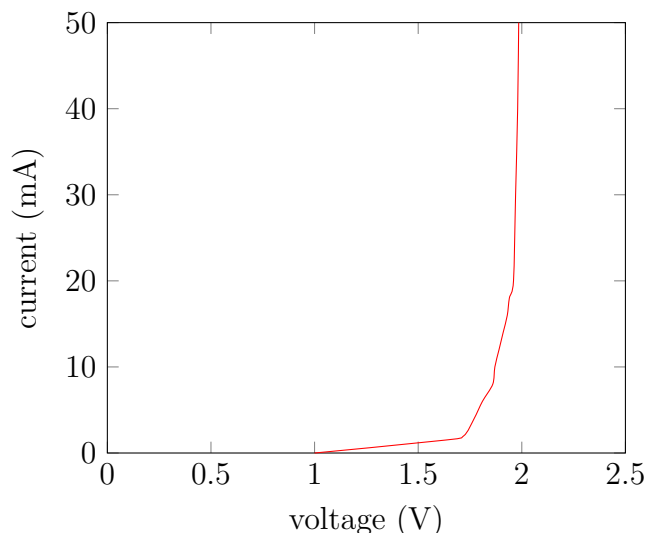


In this case, R_{th} will be the same, and R_{load} will be 3 k Ω . $V_{th} \times R_A/(R_A + R_B) = 3,000/3,667 \approx 5.45V$ for the output of the first divider (i.e., between R_{th} and the 1 k Ω resistor). And then naturally, if you were to measure the voltage between the 1 k Ω and 2 k Ω resistors, it would be $2/3 \times 5.45V \approx 3.63V$ for the voltage at the second divider.

This kind of Thevenin analysis only works when you have a linear IV curve. When might you have a non-linear IV curve?

1.2.2 LED Circuits and PNP

The IV curve across a light emitting diode (LED) should look something like this:

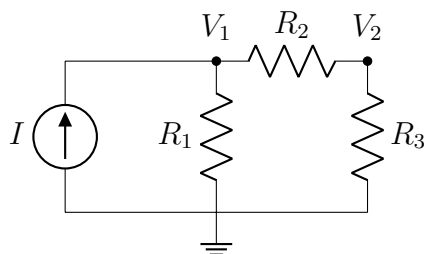


The IV curve for a diode, like an LED, is exponential in that the current slowly increases after the voltage across a diode hits some “threshold,” after which the current rises exponentially with voltage. Why is this the case? A diode is a P-N junction bridged by some depletion zone. The P side of the diode contains positively charged elements that act as “holes” (a silly way to say there is an absent electron position). The N side contains elements whose outer layers are loosely filled with electrons (i.e., low ionization energy). Effectively, the P side is devoid of electrons, while the N side has many free to give. What does this mean with regard to current and voltage? It means that the “depletion zone” between the two requires electrons to be able to bridge the gap. This really can’t happen unless they have a certain amount of energy, so increasing the voltage helps reach the “threshold” energy requires to pass the depletion zone (think of $P = IV$). Thus, as the electrons somewhat saturate the diode, you can theoretically pass an infinite current through it, as it will be effectively a short circuit.

1.3 Resistor Lattice Digression

One issue with modern BSIs is the usage of ECoGs, or EEGs, or other large measuring devices⁴. Too, they are almost universally hard electronics that require intense surgeries to implant. Therefore, if we could replace with soft electronics, we can cover considerable ground. For example, if one could drill a small hole into a patient’s skull and spread over the cortex a fabric that contained electrodes, one could achieve a similar amount of readings with a minimally invasive surgery. It is probable that there will be electrodes small enough to accomplish this, but let’s say there aren’t. Another way that this could be solved is using a lattice of resistors, with probes at either corner. These corners can exit the brain and be the points at which a computer interfaces with them.

Don’t be annoying, just go with the process.



Please, don’t be annoying—the solution is trivial but we will be talking about methods you can generalize. This example is from the SPICE method⁵. Considering KCL at the nodes gives us these two equations:

$$\begin{aligned} I &= \frac{V_1}{R_1} + \frac{V_1 - V_2}{R_2} \\ \frac{V_1 - V_2}{R_2} &= \frac{V_2}{R_3} \end{aligned} \tag{1.1}$$

As it goes, we can reformat this so as to easily turn it into a matrix in the following way:

⁴This is expanded on in the later parts.

⁵Thank you Prof. Ashmanskas, <http://www.ecircuitcenter.com/SpiceTopics/Overview/Overview.htm>

$$\begin{aligned}
I &= \frac{1}{R_1}V_1 + \frac{1}{R_2}(V_1 - V_2) \\
I &= \frac{1}{R_1}V_1 + \frac{1}{R_2}V_1 - \frac{1}{R_2}V_2 \\
I &= \left(\frac{1}{R_1} + \frac{1}{R_2}\right)V_1 - \frac{1}{R_2}V_2
\end{aligned} \tag{1.2}$$

$$\begin{aligned}
\frac{V_1 - V_2}{R_2} &= \frac{V_2}{R_3} \\
0 &= -\frac{1}{R_2}V_1 + \frac{1}{R_2}V_2 + \frac{1}{R_3}V_2 \\
0 &= -\frac{1}{R_2}V_1 + \left(\frac{1}{R_2} + \frac{1}{R_3}\right)V_2
\end{aligned} \tag{1.3}$$

These sorts of equations will usually be simplified using conductance as below:

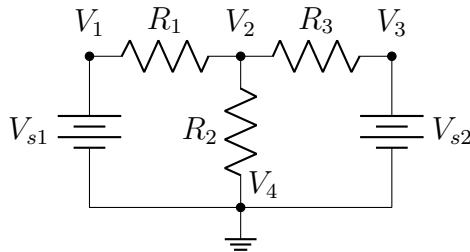
$$\begin{aligned}
(G_1 + G_2)V_1 - G_2V_2 &= I \\
-G_2V_1 + (G_2 + G_3)V_2 &= 0
\end{aligned} \tag{1.4}$$

$$\begin{bmatrix} G_1 + G_2 & -G_2 \\ -G_2 & G_2 + G_3 \end{bmatrix} \begin{bmatrix} V_1 \\ V_2 \end{bmatrix} = \begin{bmatrix} I \\ 0 \end{bmatrix} \tag{1.5}$$

So if $R_{1,2,3} = 100\Omega$, and $I = 1\text{mA}$, then:

$$x = A^{-1}B = \begin{bmatrix} 67\text{mV} \\ 33\text{mV} \end{bmatrix} \tag{1.6}$$

This method is called *nodal analysis*. You'll find more trouble trying to use a voltage source rather than a current source, and in fixing this, a method of *modified nodal analysis* was invented. Let us take the below example⁶:



In this system, we have 4 nodes, but node 4 largely functions as a reference for the other 3 nodes. A small note to make this a tad clearer is that in thinking about the current flowing into a node, such as into V_1 , you will view this as current going from V_2 to V_1 , but because everything in electronics is backwards, this is calculated as $(V_1 - V_2)/R_1$, and the opposite for current flowing into V_2 . Annoyance aside, using KCL, and then our definitions, we can gather these equations:

⁶<https://cheever.domains.swarthmore.edu/Ref/mna/MNA2.html>

$$\begin{aligned}
I_1 + \frac{V_1 - V_2}{R_1} &= 0 \\
\frac{V_2 - V_1}{R_1} + \frac{V_2}{R_2} + \frac{V_2 - V_3}{R_3} &= 0 \\
I_2 + \frac{V_3 - V_2}{R_3} &= 0 \\
V_1 &= V_{s1} \\
V_3 &= V_{s2}
\end{aligned} \tag{1.7}$$

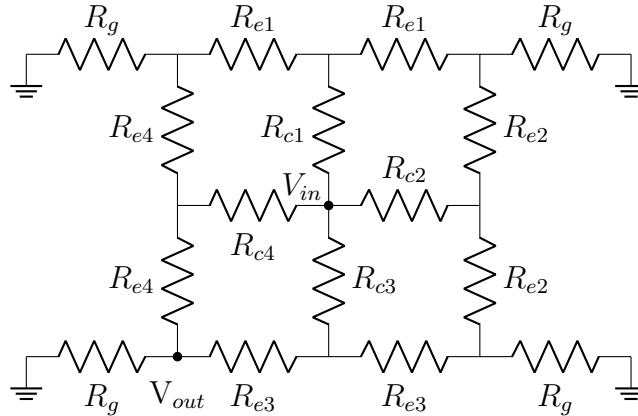
Which we convert to:

$$\begin{aligned}
I_1 + G_1 V_1 - G_1 V_2 &= 0 \\
G_1 V_1 + (-G_1 + G_2 + G_3) V_2 - G_3 V_3 &= 0 \\
I_3 - G_3 V_2 + G_3 V_3 &= 0 \\
V_1 &= V_{s1} \\
V_3 &= V_{s2}
\end{aligned} \tag{1.8}$$

And then:

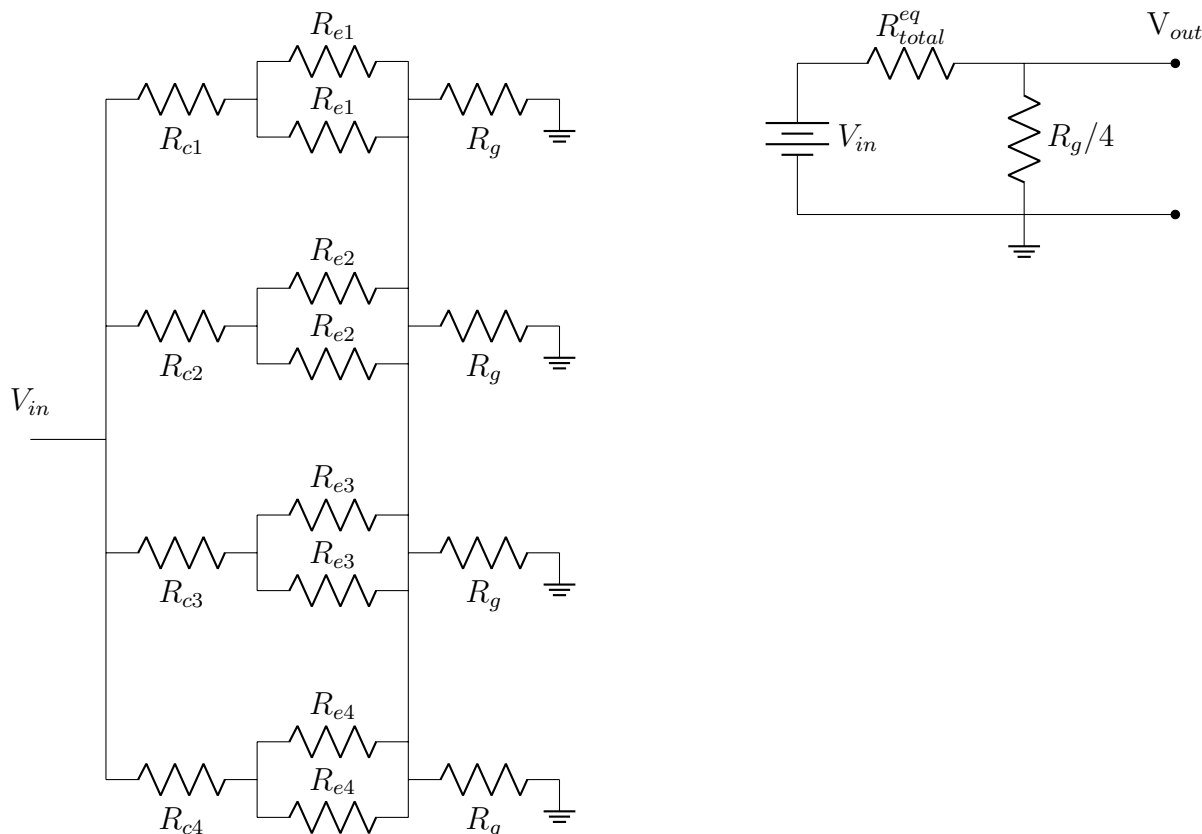
$$\begin{bmatrix} G_1 & -G_1 & 0 & 1 & 0 \\ -G_1 & G_1 + G_2 + G_3 & -G_3 & 0 & 0 \\ 0 & -G_3 & G_3 & 0 & 1 \\ 1 & 0 & 0 & 0 & 0 \\ 0 & 0 & 1 & 0 & 0 \end{bmatrix} \begin{bmatrix} V_1 \\ V_2 \\ V_3 \\ I_1 \\ I_3 \end{bmatrix} = \begin{bmatrix} 0 \\ 0 \\ 0 \\ V_{s1} \\ V_{s2} \end{bmatrix} \tag{1.9}$$

Now, I realize that one doesn't need to build a system of equations for most problems of small size, and they can be generally solved at a glance. Too, in many cases building a system is more hassle than it's worth. But, this will be important to keep in mind for the upcoming chapter **Modeling Circuits**. Let's look at some examples that are easier dealt with in the traditional way:

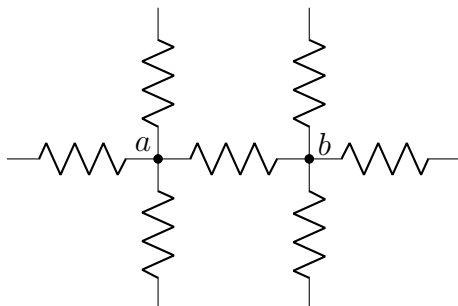


Firstly, apologies for the mess in labeling. The most difficult thing about this problem, in actuality, is how you look at it. Redrawing the circuit helps a great deal. I'll guide you through how one

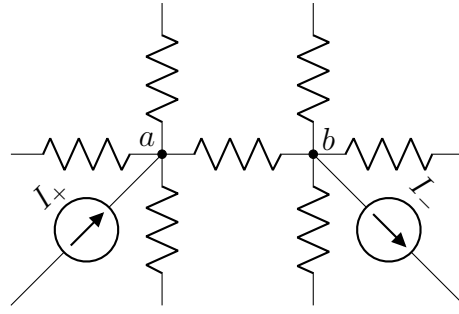
might do this. In truth, the four grounded resistors are in parallel and can be simplified to one wire ($R_g || R_g || R_g || R_g$, or $R_g/4$). You can probably realize that the edge resistors, for example the pair of R_{e1} , are also in parallel and are in series with R_{c1} . Therefore, we have $(R_{e1} || R_{e1}) + R_{c1}$. I'll call this R_1^{eq} . Then you'll realize simply that all of the equivalent R are also in parallel. This gives us $R_1^{eq} || R_2^{eq} || R_3^{eq} || R_4^{eq}$, which I will call R_{total}^{eq} . Now, our circuit simplifies to:



You may have had trouble at first glance because of all the “looped” sections of the circuit. It appears that current can flow any which way. Keep KVL in mind, and recall that current will only flow from high to low voltage. Therefore, you would never have current flowing from, say, R_{e2} to R_{e3} . A popular problem of the same flavor is the *infinite resistor grid*, which looks something like this:

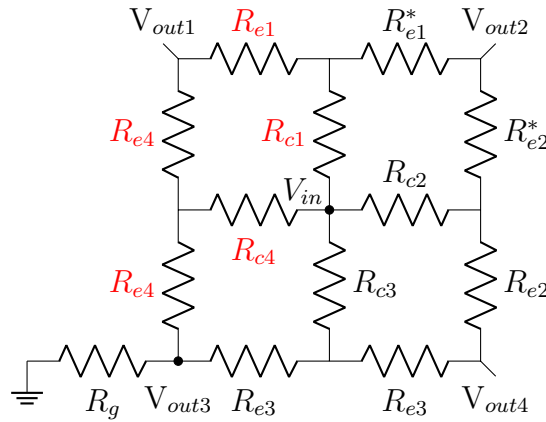


Imagine that the lattice of resistors continues out in every direction infinitely, in a grid-like fashion. The problem asks you to determine the equivalent resistance between points a and b . Considering the infinite nature, the more immediate method to solve would be to take some limit of parallel and series resistors. I actually think this is an important solution to keep in mind, as it can be generalized to other systems better. However, in this case the easiest solution is to use *superposition*. It goes as follows:

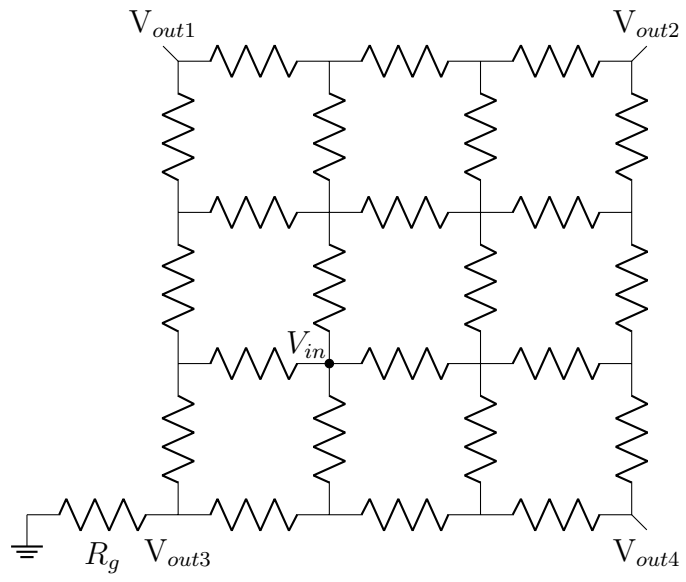


If you were to wire a positive current source to node a , you can immediately know that the current will be split equally in 4 ways, as the lattice is infinite. Then, if you apply a negative current source to node b , you can immediately know that it will draw $1/4I$ from each resistor as well. The total current flowing between nodes a and b will then be $1/2I$. Given that $V = IR$, and by superposition, we can know that $V_{ab} = (I/2)R$, so $R_{ab} = V_{ab}/I = (I/2)R/I = R/2$. The in-line math is kind of ugly, but I think you get the gist.

Another option of a similar flavor is:



In this case, we will think about what each V_{out} will read. One thing to note immediately is that the net current at V_{out2} will be 0. Therefore, R_{e1}^* and R_{e2}^* don't really matter, and can be neglected in our calculations. This once again is easiest to solve when re-visualized. The gist being that you have two quadrants (the R_{c1}, R_{c4} , which I colored to have red labels, and the R_{c2}, R_{c3} quadrants) where V_{in} is split into. The voltage drop across these quadrants being $3R \parallel R$. We then add another R , for the one that connects to R_g , and voila, we are done. Let's call this R_q , so to find the equivalent resistance from V_{in} to V_{out3} it is $R_{q1} \parallel R_{q2}$. I think you get the idea. The reason for going through these simple models is to prepare ourselves for some of the upcoming, more complicated ones. Let us level up now:



Chapter 2

Capacitors, Inductors, Filters

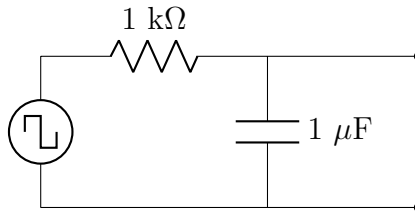
2.1 Overview

Getting a good intuition of capacitor behavior is an essential part of understanding electronics. A capacitor is a storer of charge, which allows it maintain a voltage for a period after the voltage source originally supplying the circuit is cut off. The basic structure of a capacitor is an anode and a cathode separated by a dielectric plate. Charge will be stored across it, and is released when the voltage supply dwindles. Once a capacitor is fully charged, there will be no current. However, if the voltage oscillates, the capacitor will follow V_{in} . Effectively, capacitors filter out DC voltage.

Capacitor discharge will be exponential decay in the form:

$$\begin{aligned} V_C &= V_S \times e^{-t/RC} \\ \tau &= RC \\ V_C &= V_S \times e^{-t/\tau} \end{aligned} \tag{2.1}$$

This is quite similar to neurons, isn't it! Let's consider some examples to further our intuition. Let's say you have the following circuit:

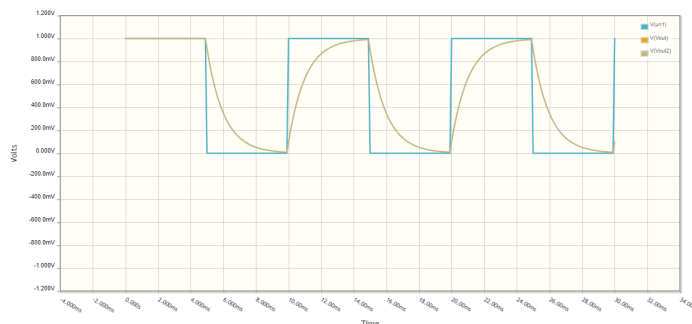
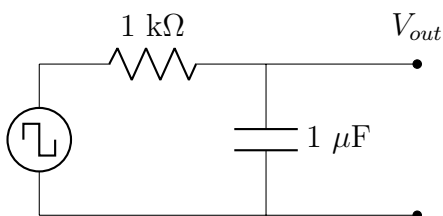


RC will be $1\text{k}\Omega \times 1\mu\text{F} = 1 \times 10^{-3}$, or $\tau = 1\text{ms}$. What does this actually mean, though? It means that if you charge this capacitor up to 10V , then $V_C = V_S \times e^{-t/RC} \rightarrow 10\text{V} \times e^{-t/1\text{ms}}$. So, 1 ms after voltage is removed, and or, one time constant, τ , after voltage is removed, the voltage at the capacitor will be $10 \times e^{-1} \approx 10 \times 0.367 = 3.67\text{V}$. If you were using a square wave which oscillated between 0 and 10V with a very high frequency (100 kHz , for example), then the period would be $1/100\text{kHz} = 0.01\text{ ms}$. Therefore, you would not expect the capacitor to ever fully discharge, and it would maintain a constant, high voltage. Perhaps you can intuitively predict that it would get stuck near a voltage of 5V , in the middle of our square wave input.

This circuit happens to be what is called a *low-pass filter*, which we will discuss in-depth later. But, you can see how it might get this moniker, as this very high frequency is not allowed to pass due to the capacitor's time constant. This was meant to serve as a basic intro to what a capacitor is. Now we can begin discussing the nuances.

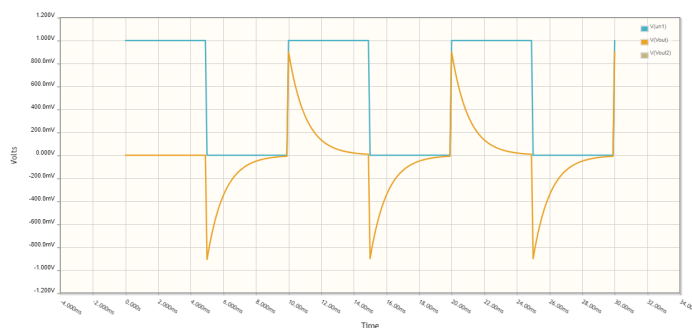
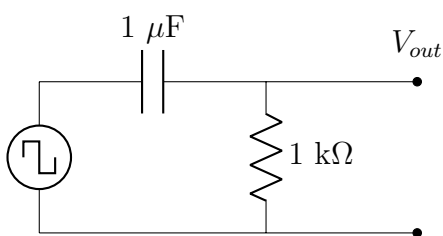
2.2 Capacitor Behavior

Let's look at the circuit below and its output (the same circuit as before)⁷. Only think about the shape of the output, no number. Only work on building up the conceptual understanding. This time our V_{in} (the blue square wave) is 100Hz.



Think about how the capacitor will behave. At time $t = 0$, the capacitor is fully charged. No current will flow at this time, meaning it will act as an open circuit, and therefore have a “resistance” of ∞ . You can think of the circuit as being like a voltage divider whose $R_2 = \infty$, and or $V_{out} = V_{in}$. At $t = (1/2)\omega$, the capacitor is able to discharge, and dissipates charge according to its decay curve. At $t = \omega$, the capacitor is subject to voltage again and begins to charge up. At first it acts like a wire, since it draws current proportional to the input voltage. As it becomes fully charged, it will again act like an open circuit.

Let's now consider swapping positions:



At $t = 0$, the capacitor is fully charged, so no current flows at all, and $V_{out} = 0$. This is expected, since capacitors are meant to filter out DC voltage. At $t = (1/2)\omega$, the capacitor shoots down to $-V_{pp}$. This is because V_{in} becomes negative relative to the voltage that the capacitor is held at. I.e., one plate of the capacitor is held at this V_{pp} value, so when V_{in} goes to 0, the voltage is negative between the plates of the capacitor, which draws negative current to the plate on the right side, making the voltage drop

⁷I really dislike needing to include .png images in works like this, but I believe I have no choice in this case.

across the $1k\Omega$ resistor equal to $-IR$. It then undergoes its standard decay curve, following this rule. Again, the decay will end at 0 because capacitors filter out DC voltage.

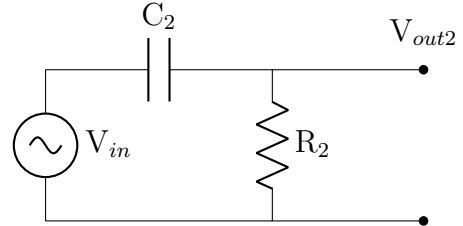
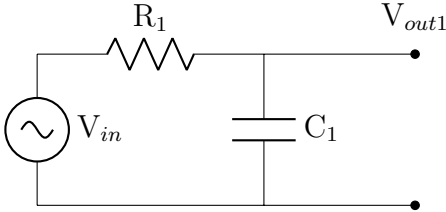
2.3 Filtration Conceptually

Firstly, what is filtration? Filtration refers to our filtering out of background signal, or any undesired signal, in order to isolate our signal of interest. For example, perhaps you are interested in a sine wave whose period is 1 ms, but this is superimposed on a bunch of other sine waves of variable periods. You can extract the 1ms sine wave with some clever circuits, and build your downstream circuit fragments based on it. It's like an analog version of the Fourier Transform!

Let's consider a specific example given by Professor Ashmanskas: imagine you are building a sensor that tests the water level in a pool. You don't want the pool to overflow when it rains, or get too low when the Summer comes and water evaporates—so you devise an automatic system to add or take out water as needed. One could simply add a sensor to the side of the pool, but it will be subject to the constant waves formed by people swimming, and its readings will be horribly variable and uninterpretable, as they do not reflect the so-called *steady-state* value of the water level. Each time someone cannon-balls in and splashes it, the sensor will think that the pool is greatly overflowing. Thus, one can devise a circuit that filters out all of these little fluctuations (this would be called a *low-pass filter*, for passing variations that occur on a long time-scale—low frequency).

2.3.1 Integration and Differentiation

Capacitors have this incredible ability to perform complex math, including taking derivatives or integrals of your wave form. Let's think about how this may occur using the circuit mentioned in the previous part. Firstly, recall that the current flowing through the resistor must equal the current flowing through the capacitor, and that $Q = CV$:



We can then solve for the voltage drop across R_1 as:

$$\begin{aligned} Q &= C_1 V_{out1} \\ \frac{d}{dt} Q &= \frac{d}{dt} C_1 V_{out1} \\ I &= C_1 \frac{dV_{out1}}{dt} \end{aligned} \tag{2.2}$$

$$\begin{aligned} IR_1 &= V_{in} - V_{out1} \\ \frac{dV_{out1}}{dt} &= \frac{1}{R_1 C_1} (V_{in} - V_{out1}) \end{aligned} \tag{2.3}$$

Therefore, if V_{out} is very small compared to V_{in} , you get:

$$\begin{aligned}\frac{dV_{out1}}{dt} &= \frac{1}{R_1 C_1} V_{in} \\ \int \frac{dV_{out1}}{dt} &= \int \frac{1}{R_1 C_1} V_{in} \\ V_{out1} &= \frac{1}{R_1 C_1} \int V_{in}\end{aligned}\tag{2.4}$$

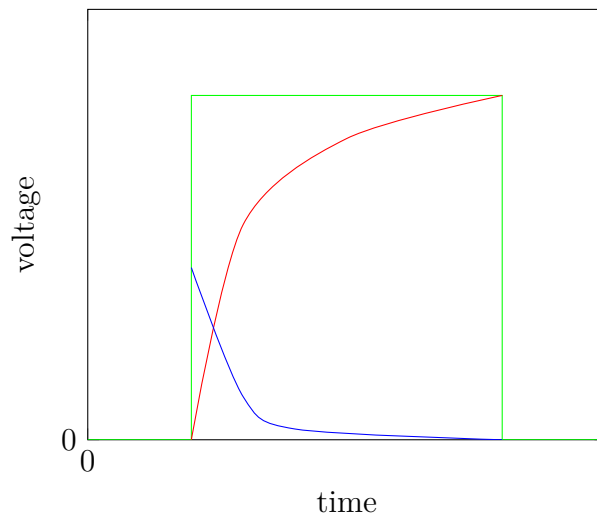
And or, that V_{out} integrates V_{in} . How will this change if we swap the positions of the resistor and capacitor in circuit 2? Once again, consider when V_{out} is much smaller than the input.

$$\begin{aligned}I &= C_2 \frac{d}{dt} (V_{in} - V_{out2}) \\ \frac{V_{out2}}{R_2} &= C_2 \frac{d}{dt} (V_{in} - V_{out2}) \\ \frac{V_{out2}}{R_2} &= C_2 \frac{dV_{in}}{dt} \\ V_{out2} &= R_2 C_2 \frac{dV_{in}}{dt}\end{aligned}\tag{2.5}$$

Thus, in this case V_{out} approximates the derivative of V_{in} .

Qualitative Thinking.

The best lead in to thinking about filtration, to me, is thinking simply about how the graphs look like when something integrates or differentiates a square wave, combined with our understanding of capacitor behavior from above. Let us not do any math, and think only qualitatively.

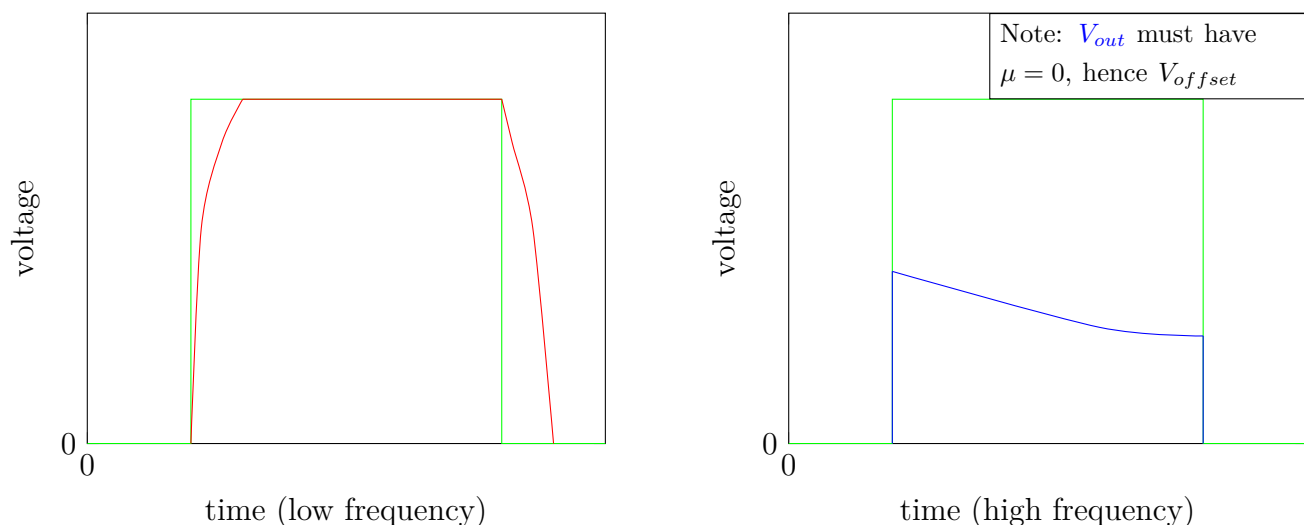


If the green waveform is our V_{in} from the previous example, then our red curve is similar to how V_{out1} may look, and the blue curve is similar to how V_{out2} . That is, the blue curve *kind of* differentiates

the green curve, because the relatively instant rise signifies a very positive derivative, marked by this blue spike. Similarly, the red curve *kind of* integrates the green curve, because the area under the green curve slowly accumulates, hence the overall positive slope of the red curve.

Something interesting you might notice, though, about the blue curve is that it seems centered around 0, while the red curve seems centered around the midway point of the green V_{in} . You can realize that the capacitor being before V_{out} means it'll filter out all DC voltage, thereby centering V_{out} about 0. Thus, you can expect there to be a symmetric, negative curve on the downward edge of the green curve, as mentioned and discussed in section 2.2.

So if we say that the frequency is extremely slow, and the red curve is the voltage being measured at V_{out2} , how might the red curve look?



Similarly, if the frequency is very high, how might the blue curve look? Take a second to ponder the two graphs above and gather a bit of intuition on it. This should allow you to qualitatively state that an integrating circuit will be a *low-pass filter* (because V_{out} matches V_{in}), and a differentiating circuit will be a *high-pass filter* (except that there's an offset when the long-term average of $V_{in} \neq 0$). As in the left graph, as the frequency gets smaller and smaller, the red plot will more and more closely match the green plot. This is the basis of capacitor filtration, an essential tool in electronics!

2.4 Frequency Dependence

This section will primarily be quantitative. The important bits, though, are the qualitative understandings, and the final results of this quantitative section. What you find in the interim is likely not worth understanding fully. Let's begin by supposing we apply a cos wave to a resistor. The relationship between current and voltage is as follows:

$$\begin{aligned}
 f &= \frac{\omega}{2\pi} \\
 V(t) &= V_{pp} \cos(\omega t) \\
 V(t) &= I(t)R \\
 I(t) &= (V_{pp}/R) \cos(\omega t)
 \end{aligned} \tag{2.6}$$

Therefore, if you were to solve something like V_{out}/V_{in} your pesky cos terms will cancel. This simply means that V_{in} and V_{out} will be in phase, only changed by some scaling factor. Unfortunately, this is not so for capacitor equations. We can see this below:

$$\begin{aligned} Q &= CV \\ I(t) &= C \frac{d(V_{pp} \cos(\omega t))}{dt} \\ I(t) &= -\omega CV_{pp} \sin(\omega t) \end{aligned} \tag{2.7}$$

This means that the current and the voltage will be 90° out of phase. Another way would be to write this as $A \cos(\omega t + \phi)$. Let us think about what will happen with our standard low-pass filter. Using KVL, we can state that:

$$\begin{aligned} V_{pp} \cos(\omega t) &= RC \frac{dv_C}{dt} + v_c \\ v_c &= A \cos(\omega t + \phi) \\ V_{pp} \cos(\omega t) &= RC \frac{d}{dt} A \cos(\omega t + \phi) + A \cos(\omega t + \phi) \end{aligned} \tag{2.8}$$

2.4.1 Imaginary Numbers Digression.

Maybe looked at the previous equation and thought it is solvable (probably?) but that it would be not worth your while to do so, and that there is likely a better way to go about it. Recall Euler's Relation⁸:

$$e^{j\omega t} = \cos(\omega t) + j \sin(\omega t) \tag{2.9}$$

One of the requirements of a linear circuit is superposition, and that is *kind of* the argument that allows us to use imaginary numbers. You can think that if you are using math that includes both a real and imaginary component, as long as you keep track of the real, your output will still be correct—but, don't think too hard about this. In the upcoming sections, I will use \mathbf{v}_c to denote the complex number. Let us examine:

$$\begin{aligned} V_{pp} e^{j\omega t} &= RC \frac{d\mathbf{v}_c}{dt} + \mathbf{v}_c \\ \mathbf{v}_c &= A e^{j\omega t} \\ V_{pp} e^{j\omega t} &= RC \frac{d}{dt} A e^{j\omega t} + A e^{j\omega t} \end{aligned} \tag{2.10}$$

We can differentiate, and then obtain an expression for A , and solve for the voltage at the capacitor as:

⁸Electrical Engineers use j instead of i for imaginary numbers. The claim is that it is easier to keep track of in the math. Other's claim it's because i is sometimes used to represent currents, particularly small ones.

$$\begin{aligned}
V_{pp}e^{j\omega t} &= j\omega RC A e^{j\omega t} + A e^{j\omega t} \\
V_{pp} &= j\omega RC A + A \\
V_{pp} &= A(1 + j\omega RC) \\
\frac{V_{pp}}{(1 + j\omega RC)} &= A \\
\mathbf{v}_c &= \frac{V_{pp}}{1 + j\omega RC} e^{j\omega t}
\end{aligned} \tag{2.11}$$

We now want to find the real component, which begins by rewriting the expression in its polar form:

$$\begin{aligned}
\mathbf{v}_c &= \left(\frac{1}{\sqrt{1 + \omega^2 R^2 C^2}} e^{j\phi} \right) V_{pp} e^{j\omega t} \\
\phi &= \tan^{-1}(-\omega RC) \\
\mathbf{v}_c &= \frac{1}{\sqrt{1 + \omega^2 R^2 C^2}} V_{pp} e^{j(\omega t + \phi)}
\end{aligned} \tag{2.12}$$

From here we can simply take the real part and be on our way:

$$v_c = \frac{V_{pp}}{\sqrt{1 + \omega^2 R^2 C^2}} \cos(\omega t + \phi) \tag{2.13}$$

This is equivalent to saying:

$$A_{out} = A_{in} \sin(\omega t + \phi) \tag{2.14}$$

Where A is the amplitude at either time. This is one way to go about this problem. Another way, which will be discussed in the next section, is using impedance.

2.5 Impedance

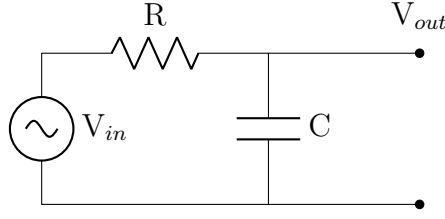
We mentioned earlier in equation (2.11) that the relationship between an input voltage and what is measured at a capacitor for a low-pass filter is:

$$V_{in} \frac{1}{1 + j\omega RC} = v_c \tag{2.15}$$

If we were to divide this fraction by $j\omega C$, and simplify using the representation Z_C , we would get:

$$\begin{aligned}
V_{in} \frac{1/j\omega C}{1/j\omega C + R} &= v_c \\
V_{in} \frac{Z_C}{Z_C + R} &= v_c
\end{aligned} \tag{2.16}$$

This looks just like a voltage divider equation! The concept of *impedance* is used to summarize other circuit fragments, like capacitors or inductors, using some resistance equivalent Z . The impedance of a resistor, Z_R , is simply R . Z_C is $1/j\omega C$. Let's think of how this pertains to our low-pass filter.



If we measure at V_{out} , we can think of it like a voltage divider, giving us:

$$V_{out} = \frac{Z_C}{Z_C + R} V_{in} \quad (2.17)$$

You may wonder if $Z_C = 1/j\omega C$ has any real basis, or if it is simply an extraction from the above math. In reality, you can find it quite simply through:

$$\begin{aligned} I_c &= C \frac{dv_c}{dt} \\ I_c e^{j\omega t} &= CA \frac{d}{dt} e^{j\omega t} \\ I_c e^{j\omega t} &= j\omega CA e^{j\omega t} \\ I_c &= j\omega CA \\ I_c \frac{1}{j\omega C} &= A \end{aligned} \quad (2.18)$$

This is the equivalent of Ohm's law, where $1/j\omega C$ is the resistance. Understanding this, we can find our high-pass filter's equation to be:

$$V_{out} = \frac{R}{Z_C + R} V_{in} \quad (2.19)$$

2.6 Filtration Quantitatively

We are finally prepared to talk about filtration quantitatively! As was mentioned in the impedance discussion, resistor-capacitor (RC) circuits can be formulated as voltage dividers. We know that the impedance of a capacitor is $1/j\omega C$, which has some frequency dependence from ω (or, $2\pi f$). Therefore, we can get the sense that V_{out} may change depending on this frequency. With a bit of re-writing, we find:

$$\begin{aligned} \frac{V_{out}}{V_{in}} &= \frac{Z_C}{Z_C + R} \\ \frac{V_{out}}{V_{in}} &= \frac{1}{1 + j\omega RC} \\ \frac{V_{out}}{V_{in}} &= \frac{1}{\sqrt{1 + (2\pi f RC)^2}} \end{aligned} \quad (2.20)$$

We can see that as the frequency goes up, this converges to $1/\infty$, or $1/1$ as frequency goes down. Whereas, for a high pass filter:

$$\begin{aligned}
\frac{V_{out}}{V_{in}} &= \frac{R}{Z_C + R} \\
\frac{V_{out}}{V_{in}} &= \frac{j\omega RC}{1 + j\omega RC} \\
\frac{V_{out}}{V_{in}} &= \frac{2\pi f RC}{\sqrt{1 + (2\pi f RC)^2}}
\end{aligned} \tag{2.21}$$

Which converges to ∞/∞ as frequency goes up, and $0/1$ as frequency goes down.

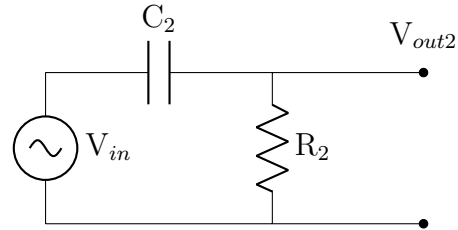
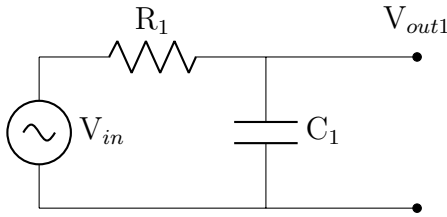
2.6.1 Corner Frequency and Phase Shift

The way one quantifies this is with the “corner frequency,” which you will more often hear as f_{3dB} . You’ll notice that for both the high-pass and low-pass filter equations described above, the ratio of V_{out} to V_{in} is $1/\sqrt{2}$ when the frequency inputted is $f = 1/2\pi RC$. $1/\sqrt{2}$ corresponds to about 0.7, meaning that at this f_{3dB} , the output is about 70% the amplitude of the input. Thus, it is a good marker of how well your filter will work. If you are trying to pick a low pass filter that filters out anything at 1000 kHz and higher, you’ll want to pick an RC circuit combination that is well below it.

Notably, filtration causes a phase shift. This shouldn’t be surprising when you recall that a low-pass and high-pass filter also integrate and differentiate respectively. Let us take, for example, a sin input. If it is passed through a low-pass filter, would expect it to be integrated to $-\cos$. If passed to a high-pass, it would be differentiated to \cos . Therefore, as $-\cos$ is -90° ($\sin(x - \frac{\pi}{2}) = -\cos(x)$) relative to \sin , and \cos is $+90^\circ$ ($\sin(x + \frac{\pi}{2}) = \cos(x)$), we would expect a low-pass filter to generate an output that lags V_{in} , while a high-pass will generate one which precedes V_{in} .

The filtration at f_{3dB} is 45° . I don’t think this has a straightfoward math explanation, but conceptually it is when the real and imaginary parts are equal. Maybe don’t think about this too hard.

2.6.2 Summarizing Thoughts



Let us look at these two circuits again, and see what we can tell just from a glance.

For the left circuit, since the current through the resistor and capacitor must be the same, we can say $Q = CV_{out}$, and thus $I = CV'_{out}$, that $V_{in} = IR = RCV'_{out}$, so V_{out} integrates V_{in} . Knowing that it integrates, we can intuit that it must be a low-pass filter, based on the graphs presented earlier. We can also know it is a low-pass filter if we recall that $Z_C = 1/j\omega C$, and that a voltage divider must look like $Z_C/R + Z_C$, which would give us $1/j\omega C + 1$. And, since it integrates, we know that $\int \sin = -\cos$, so there will be a -90° phase shift at very high frequencies.

For the right circuit, since $V_{in} - V_{out} = V_C$, we know $CV'_C = I$, so $V_{out} = RCV'_{in}$. Therefore, it differentiates, which means it must be a high-pass filter. Too, it must be of the form $R/Z_C + R$. And if it differentiates, then $\sin' = \cos$, so there must be a $+90^\circ$ phase shift at very low frequencies.

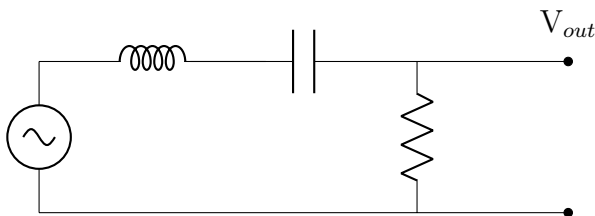
In other words, you can tell a lot just at a glance! This is without any math!

2.7 Inductors

An inductor stores energy in a magnetic field. An inductor is usually a tightly coiled bit of wire, and as you know a wire always has a magnetic field, so by coiling them and running current through it, you are summing these magnetic fields.

To conceptualize an inductor's behavior, as we will consider a water-wheel. An inductor is like a water-wheel in a pipe. As water flows through the pipe and reaches this large, heavy wheel, the speed of flow will be decreased as this wheel is pushed. Eventually, the wheel gets 'up to speed' so-to-speak, and its momentum carries it. The water's flow will not be impeded at this point. If you were to stop the flow of water, the momentum of the wheel would allow it to continue spinning, thereby continuing the water's movement for a time. If you were to have an LED in parallel with an inductor, you would expect that the LED would initially shine very brightly, as the inductor functions similarly to a large resistor its early stages. You'll see the LED dim as the inductor becomes fully charged, and now acts like a wire. If you remove the battery from the circuit, the LED will remain on for a time, as the inductor loses its charge. The rate at which the inductor dissipates its charge will depend on the total resistance of the circuit.

In fact, the magnetic field that forms as a reduce of current generates an electromotive force in the opposite direction, essentially opposing the current's flow. This field is held for some time constant, similar to a capacitor. An inductors time constant is $\tau = 2L/R$. The field is generated at at a rate of $V = L\frac{d}{dt}I$, compared to a capacitor's curve of $I = C\frac{d}{dt}V$. Therefore, you can imagine that an inductor may work opposite of a capacitor. Indeed, the impedance of an inductor is $j\omega L$, compared to a capacitors $1/j\omega C$. The f_{3dB} in this case is $R/2\pi L$. Inductors act like resistors, in that you can add them up in series like resistors, and treat them as you would with resistors in parallel. However, when we consider only impedance, everything functions like a resistor. That makes analyzing our below circuit much nicer.



This can be solved as $Z_2/Z_1 + Z_2$, where $Z_2 = R$, and $Z_1 = j\omega L + 1/j\omega C$. Let me try a bit of math here:

$$\begin{aligned}
Z_1 &= j\omega L + \frac{1}{j\omega C} \\
Z_1 &= \frac{-\omega^2 LC}{j\omega C} + \frac{1}{j\omega C} \\
Z_1 &= \frac{1 - \omega^2 LC}{j\omega C}
\end{aligned} \tag{2.22}$$

The impedance, Z_1 , goes to zero when $\omega^2 LC = 1$. In other words, at some frequency, f_0 , the impedance will be minimized. This is called the resonant frequency, and is found at $f_0 = 1/2\pi\sqrt{LC}$. You can think about what would happen when the inductor and capacitor are in parallel in the circuit above:

$$\begin{aligned}
Z_1 &= j\omega L \parallel \frac{1}{j\omega C} \\
Z_1 &= \frac{j\omega L / j\omega C}{j\omega L + 1/j\omega C} \\
Z_1 &= \frac{j\omega L}{1 - \omega^2 LC}
\end{aligned} \tag{2.23}$$

Now, impedance will go to infinity at the described f_0 —and you can filter out a specific frequency. It is useful to know how this filtering will affect the power dissipated by your circuit. At $\pm\Delta f = R/2\pi L$, the power halves, so one would call the bandwidth of this circuit to be $2\Delta f$. A halved power corresponds to an amplitude decrease of $1/\sqrt{2}$ (since $P = V^2/R$). Thus, at the two sides of the bandwidth, you'd expect to see an amplitude that is about 70% as large as at f_0 .

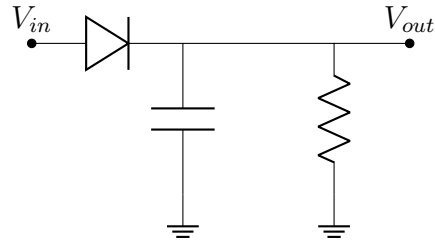
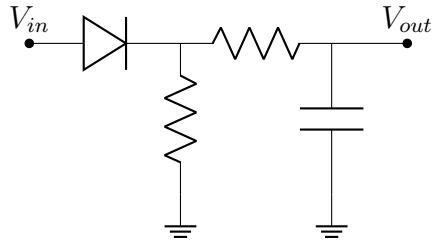
Either or?

So why are capacitors much more widely used than inductors? To start, inductors are usually large and heavy. As it must be a coil of wires, usually wrapped around some magnetically-permeable metal, it doesn't easily fit into circuit boards. Too, inductors will continuously dissipate energy, while capacitors that are charged do not.

2.8 Peak Detection

An interesting application of a low-pass filter is peak detection. There may be times where you are only interested in extremes, and not the little fluctuations in between. For example, perhaps you're interested in neural activity. You probably don't care too much about individual peaks, but instead you want to get a measure of the overall activity. This is one such way to do so⁹:

⁹These two examples are from Tom Hayes' Chapter 3N.

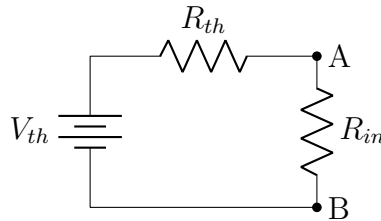


You can conceptually imagine that to create some form of peak detection, you want the RC decay value to be slow relative to the minute fluctuations, but fast relative to the longer term fluctuations you are interested in capturing.

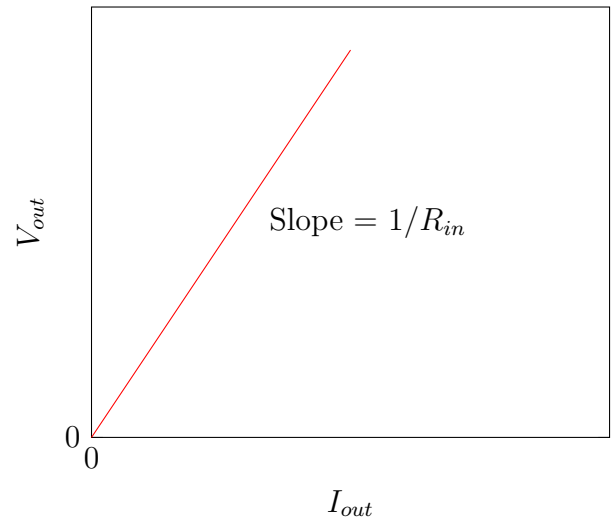
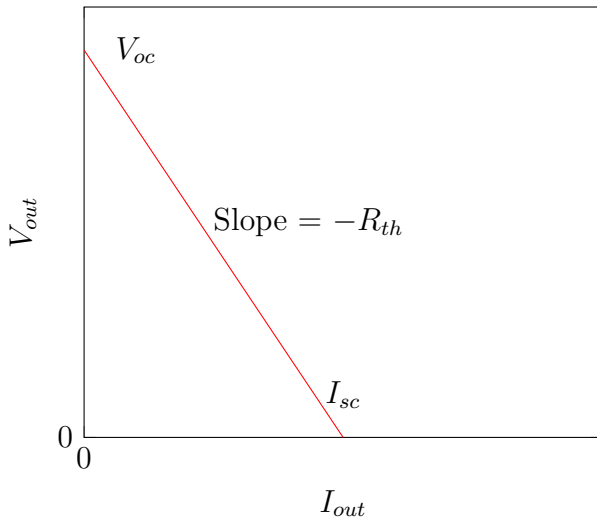
2.9 Input and Output Resistance

Now that we have a better understanding of impedance, let's discuss the idea of input and output resistance again. This concept is actually quite interesting and important, because when you are supplying a voltage to the body (say, in stimulating the spinal cord) you'll see impedance drifts, and phase shifts over time. Therefore, having a strong conceptual understanding of voltage sources & sinks, and input & output resistances is useful in quantifying this.

So for:



We get:



The left graph was presented in an earlier section. The important takeaway is that for a linear system, $R_{th} = -\Delta V_{AB}/\Delta I_A$. For a non-linear system, we can generalize this to include the impedance:

$$Z_{out} = -\frac{dV_{AB}}{dI_A} \quad (2.24)$$

Where V_{AB} is across the voltage source, and I_A is from the voltage source, and when we are varying the load resistance. Then, the input resistance of the load can be defined as:

$$\frac{1}{Z_{in}} = \frac{dI_A}{dV_{AB}} \quad (2.25)$$

For the I_A into the load and the V_{AB} across the load when we are varying the voltage source.

The next section should be diodes/LEDs, but I find those to be just so boring. So I'd rather skip to opamps.

Chapter 3

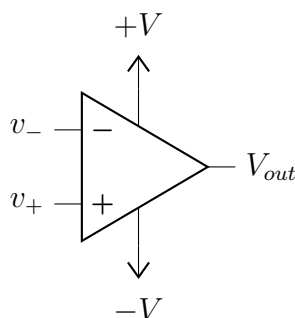
Opamps

Operational amplifiers (opamps) are one of the most ubiquitous tools in electronics, just behind classics like the resistor and capacitor. While they themselves are amazing, making CircuitTikz diagrams for them is a nightmare! So wish me luck in the coming parts!

As there are countless opamp applications, it can become muddled why you'd want a circuit to do such things. Thus, I'll do my best to think of interesting biological applications for the less obvious ones.

3.1 Introduction and Gold

Opamps are active components, in that they can take a circuit's power and increase it. They have the ability to amplify signal, act as a voltage clamp, do addition and subtraction, and even integration and differentiation. Let's discuss:



Inside of an opamp is a large network of transistors. It isn't worth trying to understand all the internals, but it is worth understanding all of the externals. An opamp has two inputs (v_- and v_+), and two power rails ($+V$ and $-V$). In general, an opamp's goal will be to minimize the difference between the two inputs, and it has some range of power to work with in doing so, which is limited by $+V$ and $-V$. It tries to minimize this input through its V_{out} . Therefore, one would often connect the v_- to V_{out} as a form of negative feedback. This will likely make more sense in the later sections. If there is no connection between V_{out} and either of the two inputs, your opamp will oscillate between the two power maximums set by $+V$ and $-V$. As in, if $v_- > v_+$, then $V_{out} = +V$. This is an opamp functioning as a *comparator*, in that it makes the somewhat binary comparison of which input is larger, and outputs either high or low voltage.

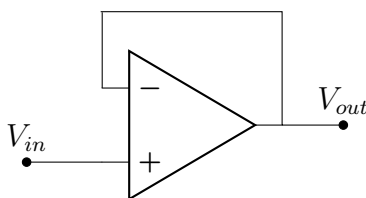
3.1.1 Golden Rules

In adding some form of negative feedback, and keeping your opamp from being saturating (i.e., clamping V_{out} to either of the two power rails)¹⁰, an opamp will adhere to two essential rules:

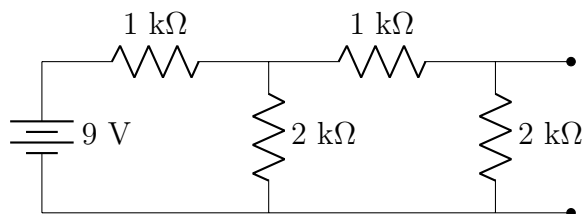
1. V_{out} does whatever needed to ensure $v_+ = v_-$.
2. v_+ and v_- draw no current.

3.2 Simple Opamp Circuits

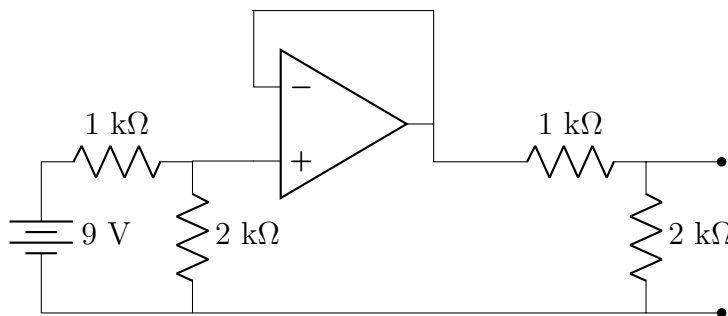
Implicit in rule two is that an opamp has immensely high resistance. That means that the input resistance seen by earlier circuit components is effectively an open circuit ($R = \infty$) for an ideal opamp. The simplest opamp circuit is seen as follows¹¹:



This is called a *follower*, or *buffer*. In such diagrams, usually $-V$ and $+V$ are omitted. Based on our golden rules, v_- should match v_+ , and our circuit shows $v_+ = V_{in}$, so therefore V_{out} will be increased by the opamp until it reaches V_{in} , because v_- is tied to V_{out} . The point being, the circuit follows as $V_{in} = V_{out}$. You might say “so it’s just a wire then?” In many ways, you are correct! But here is a nice application that shows why a follower would be useful:



Recall this circuit from before. The important principle we learned was that because the R_{th} of the first divider was similar to the R_{eq} of the second, you could not treat this as $V_{in} \times \frac{2}{3} \times \frac{2}{3}$. However, if we do the following:

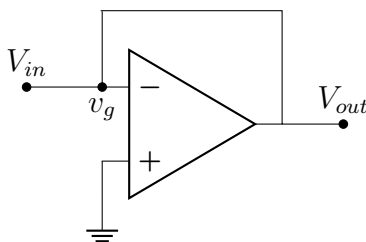


¹⁰These two specifications are sometimes called the 0th rule.

¹¹Get it?

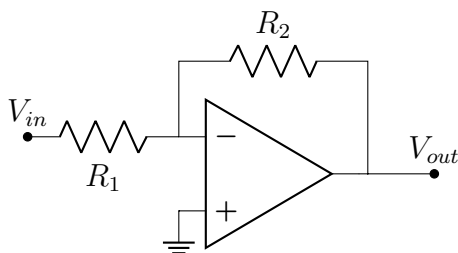
Now, the first voltage divider will “see” an input resistance of the opamp as being infinite. The opamp’s output will be the voltage of the first voltage divider, and apply it to the second voltage divider. As such, we do get $V_{in} \times \frac{2}{3} \times \frac{2}{3}$.

v_- is commonly called the *inverting input*, because one can invert with it. An inverting follower would be seen as follows:



Intuitively, since v_+ is grounded (or, $V = 0V$), to make $v_+ = v_-$, v_- must equal $-V_{in}$, and or, $V_{out} = -V_{in}$. Because of this, this node is sometimes called a *virtual ground*, or v_g .

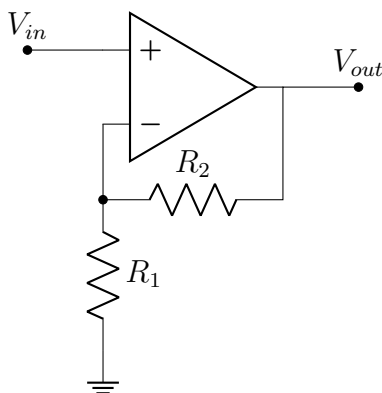
Given some of these ideas, we can imagine some special opamp uses. Like:



This is called an *inverting amplifier*. Sometimes you’ll see circuits like this overcomplicated in explanation. In reality, you should just recognize that the current across R_1 must equal the current across R_2 , since no current flows into v_- . Automatically, this means since $V_{in} = R_1 I$, and $V_{out} = -R_2 I$ (due to direction of flow), you’ll find that:

$$V_{out} = -\frac{R_2}{R_1} V_{in} \quad (3.1)$$

A slightly more complex application is:



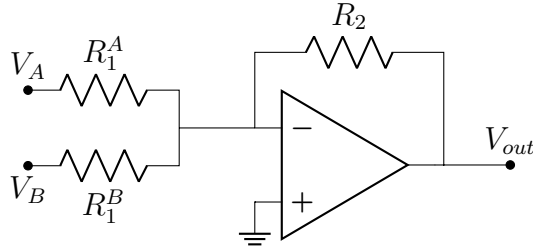
This is called a *non-inverting amplifier*. In this case, you can see that R_1 and R_2 form something of a voltage divider. That is, $V_- = R_1/(R_2 + R_1) \times V_{out}$. Knowing that an opamp always wants to ensure $v_- = v_+$, we can say:

$$\begin{aligned} V_{in} &= \frac{R_1}{R_2 + R_1} V_{out} \\ V_{in} \left(\frac{R_2}{R_1} + 1 \right) &= V_{out} \end{aligned} \quad (3.2)$$

The output resistance of an ideal opamp should be 0. That is, ideally an opamp would be able to drive any voltage irrespective of the current. The input resistance of the inverting amplifier will be whatever value we have for R_1 , while the input resistance for the non-inverting amplifier is ∞ , as it is directly connected to the opamp's v_+ .

Another thing you may wonder is if we can drive an infinite voltage at V_{out} . Recall that we are limited by whatever voltage is provided to the opamp's power rails, shown at the start of this section.

An expansion of the inverting amplifier is the *summing amplifier*:

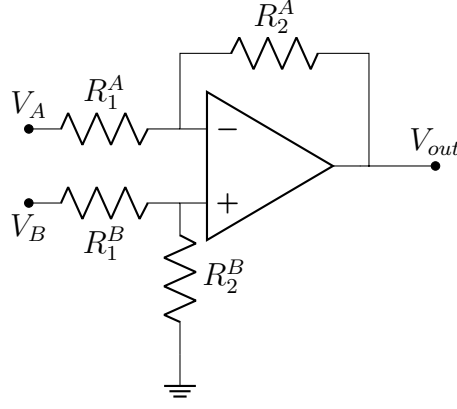


The interpretation is largely the same. Given that all of the currents through individual resistors will sum together through R_2 :

$$\begin{aligned} V_{out} &= -R_2 \left(\frac{1}{R_1^A} V_A + \frac{1}{R_1^B} V_B \right) \\ V_{out} &= -\frac{R_2}{R_1^A} V_A - \frac{R_2}{R_1^B} V_B \end{aligned} \quad (3.3)$$

Perhaps one application would be if you were interested in measuring the overall activity within the brain, and you are not so interested in discriminating individual electrodes in an EEG. Because the voltage changes measured by an EEG are so small, you'll need to amplify it. Thus, you throw them all together into a summing amplifier.

Next is a *differential amplifier* (not to be confused with derivative).

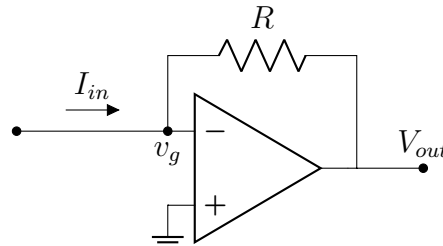


Knowing that $v_- = v_+$, and that $v_- = V_A - I_A R_1^A$ and $v_- = V_{out} + I_A R_2^A$:

$$\begin{aligned}
\frac{V_A - v_-}{R_1^A} &= \frac{v_- - V_{out}}{R_2^A} \\
R_2^A(V_A - v_-) &= R_1^A(v_- - V_{out}) \\
R_2^A V_A + R_1^A V_{out} &= R_1^A v_- + R_2^A v_- \\
\frac{R_2^A}{R_1^A + R_2^A} V_A + \frac{R_1^A}{R_1^A + R_2^A} V_{out} &= v_- \\
v_+ = v_- &= V_B \left(\frac{R_2^B}{R_1^B + R_2^B} \right) \\
\frac{R_2^A}{R_1^A + R_2^A} V_A + \frac{R_1^A}{R_1^A + R_2^A} V_{out} &= V_B \left(\frac{R_2^B}{R_1^B + R_2^B} \right) \\
R_2^A V_A + R_1^A V_{out} &= R_2^B V_B \\
R_1^A V_{out} &= R_2^B V_B - R_2^A V_A \\
V_{out} &= \frac{R_2^B}{R_1^A} V_B - \frac{R_2^A}{R_1^A} V_A
\end{aligned} \tag{3.4}$$

So that if $R_2^A = R_2^B$, you get $V_{out} = \frac{R_2}{R_1}(V_B - V_A)$. An important application of this is most physiological signals. Physiological signals are accompanied by an incredible amount of background noise, so it is useful to subtract an electrode placed on your location of interest with some other reference electrode. For example, if someone sustained damage to their left bicep, and doctors were using EMG recordings to measure recovery, an electrode should be placed on the left bicep and the right bicep. While the left bicep flexes, the right bicep can remain relaxed, and one can subtract the two signals to get the signal specific to the left bicep's flex. Because we are reading muscle depolarization through the skin, the measurable ΔV will be extremely small, hence the need to amplify it.

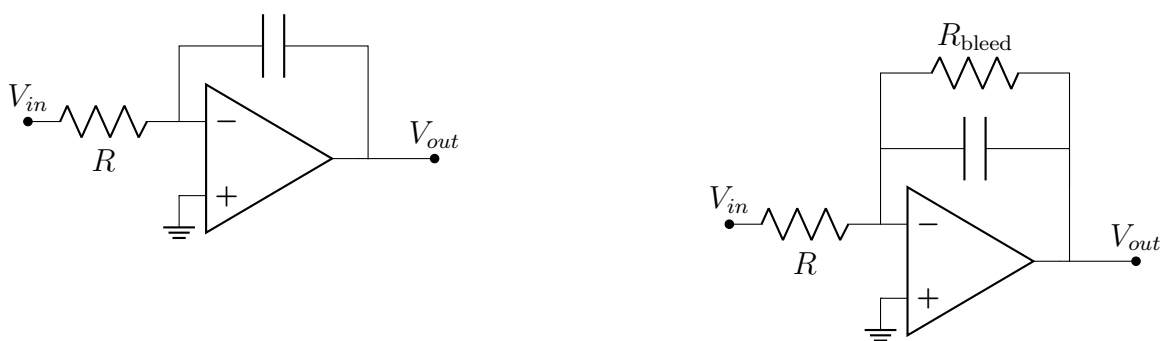
Next we will show the *current-to-voltage amplifier*. V_{out} will simply be $I_{in} \times R$:



Using an opamp is particularly beneficial, in this case, because if your current source is weak, you will not further inhibit it by adding a resistor in its path. Whatever current source you use will essentially drive a short circuit, due to the opamp's virtual ground (v_g)—and current sources love short circuits.

You may ask why you would ever need to convert current to voltage? Or, when would you be able to read current as opposed to voltage? An example from Prof. Ashmanskas is in PET scanners—photons emitted from fluorodeoxyglucose (18F) hit the walls of the PET scanner, and excite atoms enough to release electrons, generating an extremely small current. Really all piezo-electric compounds can be measured in this way. You can imagine one mode of stimulation would be implanting some piezo-electric compound and inducing electron release through low-intensity ultrasound. In testing, you'll need to measure such electron release using a current-to-voltage amplifier.

The next circuits are both integrators.

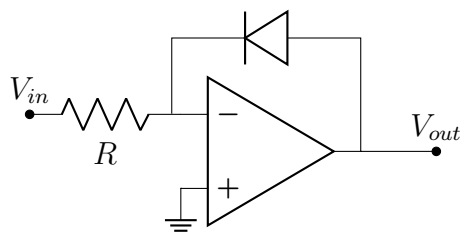


Both function as integrators (and low-pass filters), much like the low-pass filter discussion from long ago. That is, the current through the resistor is the same as through the capacitor, allowing us to use $I = CVdt$ to solve. Usefully, though, there is not a voltage limit as there is with the low-pass filter of the earlier parts. If you recall our opamp Golden Rules from section (3.2) you'll recall that one of the requirements is that there will be feedback. You may then realize that if V_{in} 's average over time is non-zero, there cannot be proper feedback in the left circuit, as the capacitor will block DC. Therefore, the second circuit uses a bleed resistor to allow for feedback when the capacitor is fully charged. This can be a bit dubious, as it is not expressly clear how this will affect your integration, but you can imagine that if your $R_{bleed}C$ value is large, it will drain charge from the capacitor over some long time scale. Intuitively, as the frequency applied to V_{in} increases, the amplification converges to R_{bleed}/R .

Another option is to use a switch to replace R_{bleed} . Therefore, whenever you want to begin integration you can flip the switch to zero the charge on the capacitor. Of course, the capacitor will saturate eventually, but you can “reset” it as desired.

As for applications, one interesting thing you can imagine is using an analog circuit to determine total muscle activity over time. Rather than digitally recording thousands of data points using an EMG and averaging them, you can use an integrator and record one voltage value at the end of your flexion—thus, giving some idea of total muscle output on a relative scale.

The last of this section will be the *logarithmic amplifier*:



I'll not explain the math so much, but you can think about the LED example from the very first section. A diode's current curve is exponential in nature, so the voltage will approach asymptotically toward the diode's diode-drop¹².

Biological applications of this are more obscure, but perhaps you can imagine a scenario where you'd really only care about the lower bounds of some stimulus. For example, if measuring the sub-threshold oscillations of a neuron, you may not want a linear curve—because once the neuron reaches its threshold, the voltage rises dramatically. However, a logarithmic graph of the voltages between hyperpolarization and threshold might be quite useful, and you can configure it so that your circuit approaches its asymptote as the neuron approaches its threshold voltage.

In Summary.

Some of the circuits here are pretty neat. We learned some ways in which analog circuits can perform relatively complex functions, like multiplication, subtraction, addition, integrals and even logs.

3.3 Opamp Imperfections

It is important to understand the slight opamp imperfections that cause them to deviate from being a perfect voltage source, etc. The first two clear deviations from ideality are that the opamp's *input resistance* is not truly infinite, but is something on the order of $10^{10}\Omega$. Secondly, an opamp does not have infinite gain, A , that it can use to drive V_{out} . I.e., $V_{out} = A(v_+ - v_-)$ has some limit in that $A \neq \infty$.

Another difference is a slight offset that will always exist between v_+ and v_- , called the *offset voltage*. In modern opamps, this number might be immeasurably small, but in the canonical LM741 used in most electronics classrooms, it is close to 1mV. This is simply due to difficulty in creating two distinct nodes of exactly the same potential.

As mentioned, the opamp's input resistance cannot be infinite, meaning it will draw some small but non-zero current. This current is called the *bias current*, or I_{bias} , or I_{b+} and I_{b-} for individual inputs. I_{b+} and I_{b-} are slightly different, so I_{bias} typically refers to $1/2(I_{b+} + I_{b-})$. There is also a current due to the offset voltage, which is typically an order of magnitude or two below I_{bias} . I_{bias} for the LM741 is $\approx 100\text{nA}$. The LM741's internal make-up is largely bipolar junction transistors (BJT), while higher-end opamps will use field effect transistors (FET), which allow for many orders of magnitude higher input resistance.

The LM741 is only capable of driving a small current of about 25mA. This is actually a very considerable point to keep in mind. Of course, this means an opamp cannot directly power any meaningfully

¹²I still haven't done a Part on diodes yet, so the term "diode-drop" is not yet explored.

high power devices without the help of some external transistors.

Notably, all transistors have some finite capacitance, so it implies that the inner workings of an opamp may demonstrate some of the same phase shift or filtration we saw in the capacitors section. This is indeed true, and is worth considering at exceptionally high frequencies. Fascinatingly, at such exceptionally high frequencies, where the phase shift extends beyond 180° , the negative feedback switches to positive feedback. This effectively switches your opamp to comparator mode as V_{out} oscillates from its V_+ to V_- . Intentionally, opamp designers include a low-pass filter within it to avoid this, reducing the gain, A , before you can reach 180° . This is called *frequency compensation*, and again is an intentional feature. This is potentially quite interesting, as the small, immensely fast oscillations at physiological levels could theoretically exceed the opamp's 180° . So, it is curious to consider if such situations would cause positive feedback.

Opamps also have a *slew rate* which defines some $\max V_{out}dt$. That is, if the input is a square wave, the V_{out} cannot instantaneously follow it, and there will be some slight slope. For the LM741 it is $\approx 0.5V/\mu s$. The result is related to the internal capacitance and its charge time, making the effect non-linear and giving it some amplitude dependence. Driving a high amplitude and high frequency can therefore introduce considerable distortion.

NOTE: It would maybe be useful to make comments about the *output resistance*. Though, it is not immensely interesting.

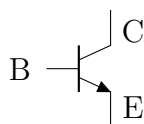
Chapter 4

Transistors

4.0.1 Transistor Overview

The prime purpose of a transistor is to use a small current to control a large one. A straightforward example being using the turning of a key to start a car. Naturally, you wouldn't want a humongous current, capable of powering your car, to be connected to the keyhole—so you use this small current to control the flow of a larger one.

Bipolar junction transistors (BJTs) are 3-terminal devices either composed as NPN or PNP. The three terminals are the emitter (E), base (B), and collector (C). The large current you are interested in controlling flows from the collector to the emitter, and is operable by flow at the base. Though, the current at E will indeed be $I_C + I_B$, but you'd expect I_B to be many orders of magnitude below I_C . The relationship between I_C and I_B is called β , where $I_C = \beta I_B$.

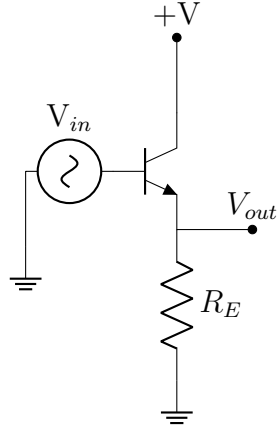


For an NPN transistor, it can either be off, where $I_B = 0$ (in this case, the voltage at the base will be below a diode drop), it can be active, where $I_B \neq 0$ and $I_C \leq \text{max}$, or it can be saturated, where $I_B \neq 0$ and $I_C = \text{max}$. You can probably imagine: active mode is useful if you'd like to make a transistor-based amplifier, while the saturation mode might be more useful in making a switch.

4.1 Transistor Circuits

4.1.1 A Follower

A follower, as with the opamp follower, is useful in building a high-input impedance, low output impedance element in your circuit. Again, this is useful as it will draw minimal current and preserve the voltage at that point in the circuit.



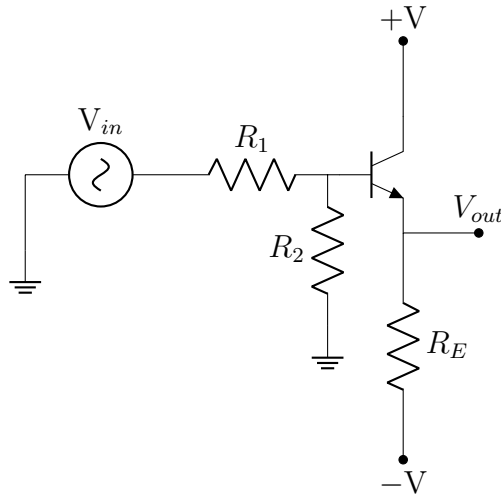
Alrighty, so in active mode, if this functions properly as a follower, we would expect that as V_{in} changes by ΔV , so too would V_{out} . Too, it will function very much like a diode—meaning V_{out} will feature a diode drop and cannot drop below 0. In later circuits, we'll show how to fix this by tying E to some negative voltage, $-V$. Thus, we get that: $\Delta I_B = \Delta I_E / (\beta + 1) = \Delta V / R_E (\beta + 1)$. Since $R_{in} = dV_{in} / dI_{in}$, we get:

$$R_{in} = (\beta + 1)R_E \quad (4.1)$$

Therefore, from the perspective of V_{in} , the load, which would be attached at V_{out} now appears to be much higher. More explicitly, it appears as:

$$R_{in} = (\beta + 1)(R_E || R_{load}) \quad (4.2)$$

Again, this is preferable for the source. As we explored in the very early voltage divider section, if you were to have the following circuit:



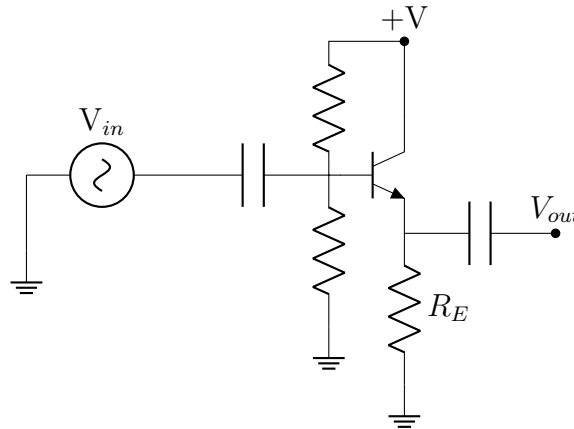
Now we have $R_2 || (\beta + 1)R_E$, which we would expect to be $\approx R_2$. Therefore, the voltage divider acts as it would if there were no load there at all. The output impedance will be that which exists at V_{out} . Since the current at ΔV_{out} varies with ΔV_{in} , and ΔI_{out} varies with $(\beta + 1)\Delta I_B$. So, $\Delta V_{out} = \Delta I_B (R_1 || R_2)$ or $\Delta V_{out} = \Delta I_B R_{th}$. Since $R_{out} = dV_{out} / dI_{out}$, we get:

$$R_{out} = \frac{R_{th}}{\beta + 1} \quad (4.3)$$

Which we expect to be quite small. Therefore, the output resistance is quite small. Since technically R_{load} is again in parallel with R_E , it should actually be:

$$R_{out} = \frac{R_{th}}{\beta + 1} || R_E \quad (4.4)$$

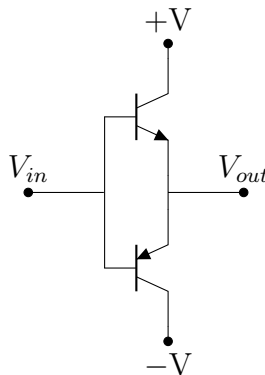
Which again we expect to be $\approx R_{th}/\beta + 1$, and or, a very small value. You could build a more complete BJT follower in this way:



I'll not walk through the entire idea, using explicit values, but you should be able to get the gist. The capacitors are used to remove the DC. The $+V$ adds a DC-offset, so that the oscillations of V_{in} can be all positive, removing the restriction of keeping V_E above 0. The two resistors are used as a voltage divider, stemming from $+V$, allowing us to pick our DC offset. One of the largest takeaways from this is simply that it is much more complex, and annoying, than opamp-based followers. However, it should give insight into what might be within an opamp.

Push-Pull Follower.

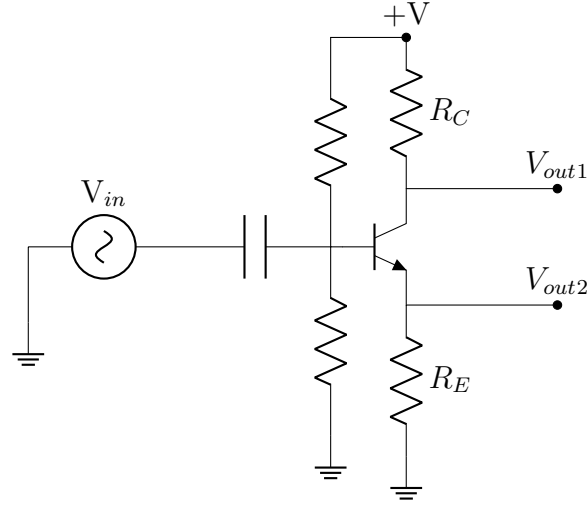
A neater way to avoid some of the drawbacks to the preceeding designs is to use what is called a *push-pull follower*. It takes advantage of using two BJTs. Where the first NPN handles the positive half, and the second, now a PNP, handles the negative half. It is seen as below:



The problem, of course, is that you will still have two diode drops in either direction. This is called *crossover distortion*. An intelligent way to avoid this crossover distortion would be to add some additional diodes around the base of the two transistors connected to a power supply. An easier way, virtually by cheating, would be to use an opamp whose feedback loop connects to the output of the push-pull circuit, allowing the opamp to “pre-compensate” for the two diode drops.

4.1.2 Amplifiers

The first iteration is the common emitter amplifier, seen as follows:



Let’s again analyze solely by glancing at the circuit. We know that the voltage at V_E will be one diode drop (say, 0.6V) below V_B in the active mode. We know that the current through R_E must therefore be $(V_B - 0.6)/R_E$. We know that $I_C \approx I_E$, therefore $I_C = (V_B - 0.6)/R_E$. If $V_B = V_{in}$, this must mean that the voltage at C:

$$V_{out1} = +V - (V_{in} - 0.6) \frac{R_C}{R_E} \quad (4.5)$$

Using a capacitor to remove the DC offset will further make it function like the amplifier you desire. Something small to keep in mind is the limits of R_E . Let’s suppose you were to take $R_E \rightarrow 0$. The truth of your equation is this:

$$\begin{aligned} V_{out1} &= V_{out2} \frac{R_C}{R_E + r_e} \\ V_{out1} &= V_{out2} \frac{R_C}{r_e} \end{aligned} \quad (4.6)$$

Where r_e is the resistance of the diode, set approximately by $25\text{mV}/I_C$. Therefore, your output will experience “barn roof distortion” due to the logarithmic nature of a diode’s IV curve.

4.1.3 Current Sources

Let's take this circuit:



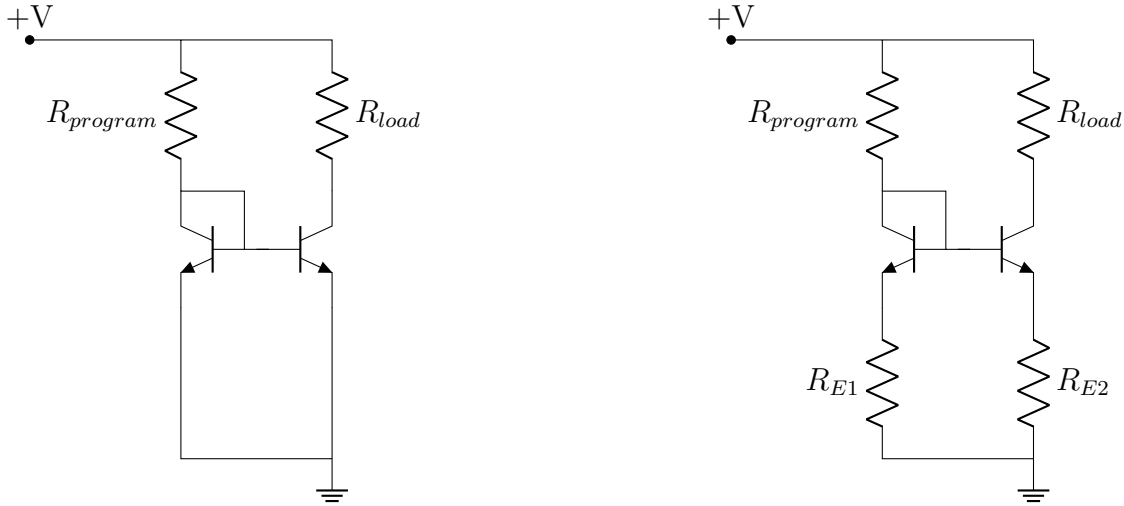
Recall that the current through the collector is set by the emitter. The voltage at the emitter is set by the base. V_E will be one diode drop below the base (for the leftward circuit, that is—for the rightward, it will be one diode drop above). So if the resistance at the emitter, R_E , is 1 k Ω , then we would want V_E to be 2 V, and V_B to be 2.6 V. Note that the transistors input resistance is $\beta(r_e + R_E) \approx 100k\Omega$.

Keeping a small R_E is important here, as the larger that R_E gets, the closer you will be to saturating your R_{load} . Let's try to consider an example. Covered much, much later in this book, we discuss a Courtine lab paper that used electronic dura mater. The load value appeared to vary all the way from 5k Ω to 100k Ω . If you wanted to supply a constant 2mA over this entire impedance range, you would need the following:

$$\begin{aligned}
 V_B &= 2.6\text{V} \\
 R_E &= 1\text{k}\Omega \\
 I_C &= 2\text{mA} \\
 V_C &= +V - R_{load}I_C \\
 V_C &= +V - (100k\Omega \times 1\text{mA})
 \end{aligned}
 \tag{4.7}$$

It looks like you'll need a 100V supply to keep your transistor from saturating. That is... not good!

Current Mirror.



On the left circuit, your $R_{program}$ sets the current via the fact that the voltage drop between $+V$ and ground happens only across $R_{program}$, so the current flowing through the emitter is $+V/R_{program}$. The same current will be pulled through R_{load} . Adding in the R_E on the rightward circuit gives a path to bleed and allows your programmed current to stay flat for longer. However, even in this case, R_{load} cannot exceed $R_{program}$.

So why would you want a current mirror? Here's an example from this video¹³. Amplifiers can be biased using current sources, which allows the biasing current to become very stable. This is important, because as voltage or temperature fluctuates, the current can be maintained. Adding a current source to every amplifier would require too much annoying circuit building, so one way to avoid this is using a current mirror.

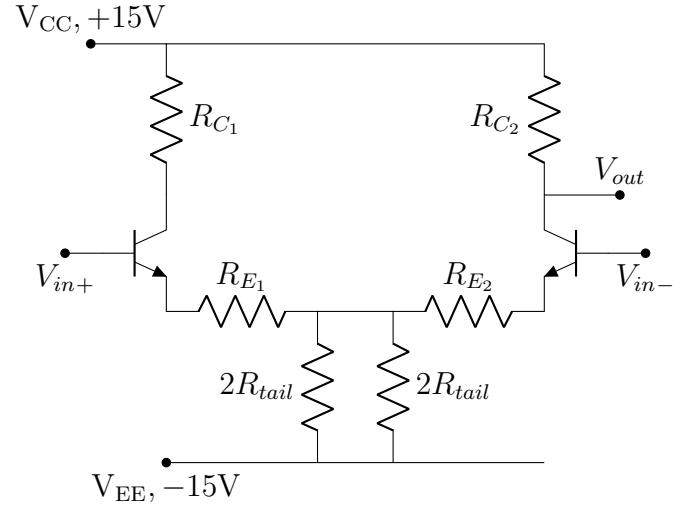
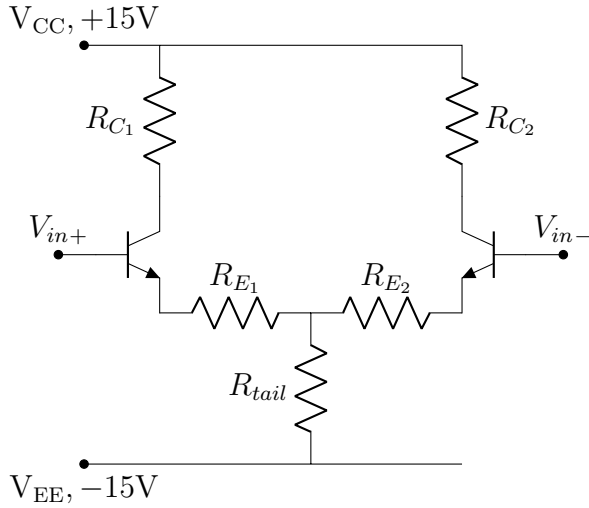
4.1.4 The Components of an OpAmp

Opamps are transistor-based at heart. The key components of an opamp is that it should have a large, ideally infinite differential gain. This means that an opamp can ideally amplify any difference between V_+ and V_- . Conversely, an opamp should ideally have a 0 common mode gain. This means that when $V_+ = V_-$, $V_{out} \approx 0$. Other important components of an opamp include a high current supplied to V_{out} , accomplished by an ideally 0 output resistance. Let's consider how we can accomplish these things.

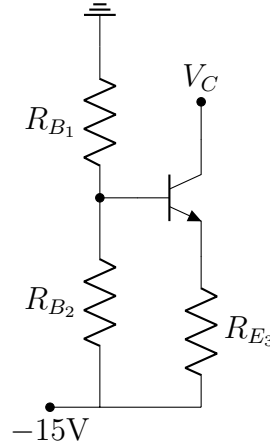
The first step is to generate a circuit with a decent differential gain and a somewhat low common-mode gain. Let's see what we can gather about the below circuit(s).

$$\begin{aligned} A_D &= \frac{R_C}{2(R_E + r_e)} \\ A_{CM} &= -\frac{R_C}{2R_{tail} + R_E + r_e} \end{aligned} \tag{4.8}$$

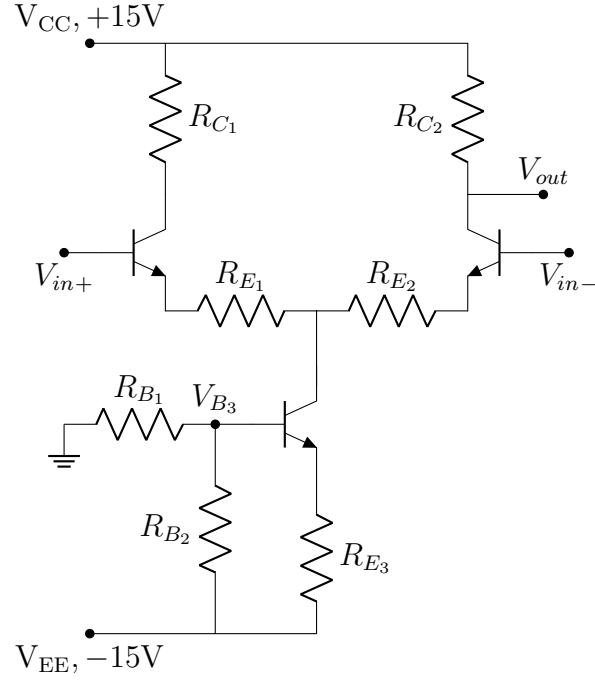
¹³https://www.youtube.com/watch?v=VnJHXQCPIvs&ab_channel=ALLABOUTELECTRONICS



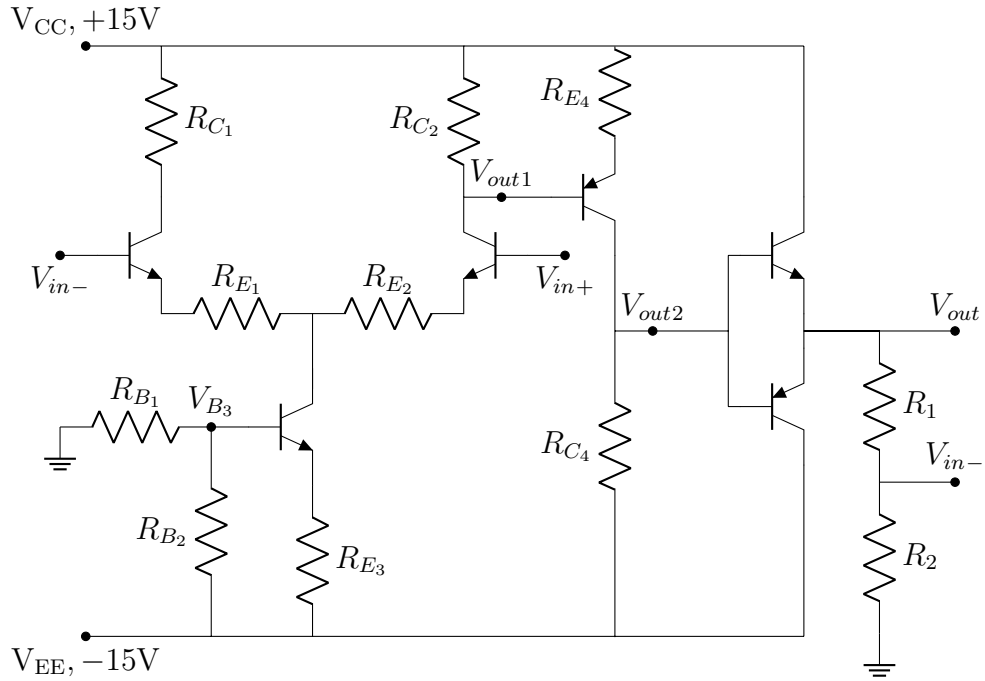
These two circuits are equivalent, but the right one is a bit easier to analyze. Considering equations 4.8, you may want to pick an incredibly large R_{tail} , or better yet, to pick a downward circuit fragment with a very high R_{in} . Let's try:



In the quiescent state, we can easily determine the voltage at the base as $V_B = 15V \times R_{B1} / (R_{B1} + R_{B2})$. Therefore, we can determine the voltage at the emitter as $V_E = V_B - 0.7V$. We can determine the voltage drop across R_{E3} here as $15V - V_E$, and therefore easily determine I_{E3} , and thus I_{C3} , as $R_{E3} / (15V - V_E)$. Let's connect this fragment to our circuit as below:



Because we know the quiescent I_{C3} , we can know that $0.5I_{C3}$ flows through R_{E1} and R_{E2} , allowing us to easily deduce what V_{out} is in the quiescent state. We might be tempted again to take the limit of $R_{E1,2} \rightarrow 0$, but recall that we will introduce distortion this was as r_e becomes the only source of resistance in the system. If we assume the R_{in} into this third transistor fragment is extremely high, on the order of M Ω s, then we can know that the differential gain is extremely high, while the common mode gain is extremely low. Let's add some extra circuit fragments:



We've now added a common emitter amplifier to the output of stage 1 (now called V_{out1}). It will amplify as $A = -R_{C4}/(R_{E4} + r_e)$. However, one consideration is to keep the voltage of V_{out1} low enough so that the transistor does not saturate. We take the output from this (V_{out2}) and connect it to a push-pull circuit—which is helpful in increasing the current supplied by the homemade opamp. However, it

introduces crossover distortion. This crossover distortion is eliminated when feedback is added, with V_{in-} connected to V_{out} as shown above. The whole circuit amplifies as: $(1 + \frac{R_1}{R_2})(V_{in+} - V_{in-}) = V_{out}$.

One slight issue you may encounter is an annoying fuzz on the output. This may be due to unintended high-frequency gain. One way to avoid this is adding a very small capacitor between V_{out1} and V_{out2} . This effectively acts as a high-pass filter, removing it from amplification by the common-emitter amplifier.

Chapter 5

Writing Hardware

5.1 Introduction

Verilog¹⁴ is a language used to describe electronics, and allows you to avoid the physical action of wiring. This is the reason for the designation **writing hardware**. In this way, you can pick your poison: debugging code, or debugging breadboards. Importantly, though, Verilog is capable of computation and writing data files that go beyond circuit descriptions. Thus, it is not a “markdown” language and is Turing Complete¹⁵.

Tools like Field Programmable Gate Arrays (FPGAs) allow for this, as their internal composition is something of an array of transistors, which can be rewired through code in order to meet the demands of the programmer.

5.1.1 Creating Modules

In Verilog, a circuit is called a `module`. Each module is defined between a `module` and `endmodule`, which can be named as shown in the example below. Different ports connect the module to things outside of the module.

```
1 module example1(o, i1, i2);
2 // example1 is the name of our module, and o, i1, and i2 are our ports
3 // it is convention to list outputs first
4
5 output o; // this defines o as an output
6 input i1, i2; // this defines i1 and i2 as inputs
7
8 endmodule
```

Gates are also initialized like modules. The way to do this is with the built in primitives for AND and OR gates (`and` and `or` respectively). For example:

```
1 module example2(o, i1, i2);
2
```

¹⁴A large part of the background information and general syntax comes from the YouTube channel: CompArchIllinois.

¹⁵Or at least, I think it is. I can never remember the exact definition of Turing Complete :)

```

3 output o;
4 input i1, i2;
5 wire wire1, wire2; // this initializes two wires called wire1 and wire2
6
7 or or1(wire1, i1, i2);
8 // this makes an OR gate named or1 with inputs i1 and i2, and output called
  wire1
9 and and1(o, wire1, wire2);
10 // this makes a NOT gate named not1 with input i2, and output called wire2
11 // one of the outputs of the OR gate feeds into the AND gate (via wire1) in
   this example
12
13 endmodule

```

The order in which things are initialized do not matter. It is very important to not reuse wire or other variable names, as Verilog will read these as being connected irrespective of where they are intended to be. As mentioned, the code above uses modules built into Verilog, but you could make your own module in the following way:

```

1 module andgate(output o1, input i1, input i2);
2     assign o1 = i1 & i2;
3     // for OR you would use |, and for XOR you would use ^
4 endmodule;

```

5.1.2 Bus Notation

Bus notation is used to simplify the pins used (in Verilog, this is called a vector). For example, a multiplexer or an adder will have many inputs, which would be inconvenient to initialize individually. Instead, we can use something like this:

```

1 module adder(c, a, b); // a, b, c are 3 bus inputs we will use
2     output [3:0] c; // initializes 4 wires within our c bus
3     input [3:0] a, b; // initializes 4 wires within our a and b buses
4 endmodule

```

Firstly, note that Verilog is 0 indexed, so `[3 : 0]` includes 4 wires. In a circuit schematic, busses are drawn as thicker wires with a slash through them and a number denoting the amount of wires in the bus. If we wanted to call individual wires from our busses into the `andgate` module we declared earlier, we could do it as:

```

1 andgate(c[0], a[0], b[0]);

```

And we can connect busses together, or wires together, using the assign command like before. For example:

```

1 wire wire3;
2 assign wire3 = c[2];
3 assign c[2:0] = a[2:0]; // wire3 will now be connected to bus a[2] through
   bus c[2]

```

5.1.3 Constants and Variables

You can actually explicitly ascribe a bit value to a series of wires as seen below with `wire4`:

```

1 wire [2:0] wire4 = 3;
2 // wire4 now holds 011

```

Verilog allows us to define constants using 3 parameters, defined as their size, method of encoding, and value. For example, `8'hd7` corresponds to a size of 8 bits, hexadecimal encoding, and the value `d7` (equivalently, `11010111`). You can use this in `boolean` comparisons, as below:

```

1 wire wire5;
2 'define CONST1 3'b011; // CONST1 is the name of the constant
3 wire5 = (a[2:0] == CONST1);
4 // This is a tad complicated. The gist is: all of the bit values in a[2:0]
   will be compared to CONST1 in a NXOR style statement. That will then be
   compared to all of the other bits in an AND style statement. So wire4
   will be on only if all wires in correspond to CONST1.
5 // The C++ equivalent would be something like:
6 //     (a[2] == 1'b0) && (a[1] == 1'b1) && (a[0] == 1'b1)
7 // Also, this could be completely wrong. I can't check any of this without
   an actual FPGA in front of me! So who knows!

```

This does bring up a worthwhile point, which is that everything you write in Verilog has a direct circuit component underlying it (I suppose the same is true for any program, but it's more... explicit with Verilog).

5.1.4 Logic

Verilog has two types of logic it can perform—bitwise and logical. The expressions are: The operators are `~` for bit-wise NOT, `!` for logical NOT; `&` for bit-wise AND, `&&` for logical AND; `|` for bit-wise OR, `||` for logical OR; and `^` (bit-wise XOR). As you'd imagine, a bitwise comparison goes bit by bit. For example:

```

1 wire [0:3] a = 0;
2 wire [0:3] b = ~a;
3 wire [0:3] c = !a;

```

Here, `a = 0000`, `b = 1111`, and `c = 0001`. While:

```

1 wire [0:3] a = 1;
2 wire [0:3] b = ~a;
3 wire [0:3] c = !a;

```

Now, `a = 0001`, `b = 1110`, and `c = 0000`.

5.1.5 Adder

Verilog has the ability to make adders itself. For example (from Prof. Ashmanskas):

```
1 module add4bit (output [3:0] s, output cout,  
2     input [3:0] a, input [3:0] b, input cin);  
3     assign {cout,s} = a + b + cin;  
4 endmodule
```

Where each of the inputs (a, b) and outputs (s) is 4 bits wide. Writing {cout,s} is then a 5 bit wide statement.

Part II

Math and Models

All truly strong people are kind.
– Vagabond by Takehiko Inoue

5.2 Perspective

Truly, I find it endlessly fascinating and miraculous that you can quantitatively describe physical or biological phenomena. Of course, it stands to reason, but its shine is not lost on me. I vividly recall being in my Human Physiology class and having our professor pose the question: *what will happen if two action potentials run into one another?* I knew that they'd terminate, so the result was not what drew my intrigue. What was miraculous is that, to answer this question, our professor pulled up MatLab and simulated it before our eyes. Indeed, the action potentials terminated.

Prior to this, I hadn't thought much about quantitative descriptions like this. Qualitatively, and or conceptually, it made sense to me that action potentials cannot propagate past one another. But naturally, not all answers can be intuited. After scrolling around through the amazing Keener and Sneyd *Mathematical Physiology* textbook, I realized the incredible breadth of phenoma that we have modeled. From membrane electrophysiology, enzyme kinetics, to disease spreading, to fluid dynamics of the circulatory system, to the movement of bacterium, to every other little itty-bitty thing you can become fascinated by—someone has build some differential equations for it.

If anyone ever reads this, besides me, I hope you too will be enthralled by both the brilliance and creativity required to describe something as complex as the biochemistry of a neuron in just a few equations.

Chapter 6

Math Essentials

6.1 Linear Algebra

6.1.1 Cross Products, Dot Products, and Gradients

Recall that the cross product is a vector value whose direction is perpendicular to both of the two vectors crossed. The formula is:

$$\vec{A} \times \vec{B} = \|\vec{A}\| \|\vec{B}\| \sin \theta \vec{n} \quad (6.1)$$

Where $\|\vec{A}\|$ is the length of \vec{A} , θ is the angle between the two vectors, and \vec{n} describes the unit vector between \vec{A} and \vec{B} .

The dot product is a scalar value achieved by multiplying the positions of vectors together, such as below:

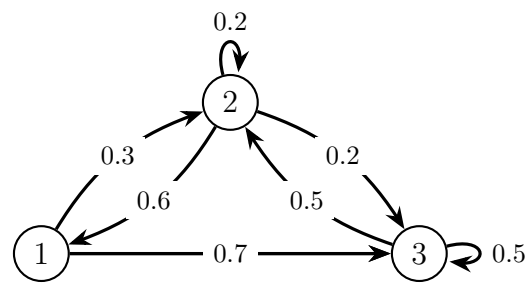
$$A = \begin{bmatrix} a \\ b \end{bmatrix} \cdot \begin{bmatrix} x & y \end{bmatrix} = ax + by \quad (6.2)$$

A gradient, ∇ , describes a derivative vector of a corresponding vector. For example, if vector v_1 exists in 3 dimensions, then:

$$\nabla \cdot \vec{v}_1 = \begin{bmatrix} \frac{\partial}{\partial x} \\ \frac{\partial}{\partial y} \\ \frac{\partial}{\partial z} \end{bmatrix} \cdot \vec{v}_1 \quad (6.3)$$

6.2 Markov-chains

Markov chains are useful in predicting the next state desired.



Chapter 7

Neuron Modeling

It would certainly be worth reviewing the electrophysiology contained in Part **III** before trying this, unless you already have a strong understanding of biochemistry.

7.1 Hodgkin-Huxley

7.1.1 The Main Form

The pair won the nobel prize for this model, which formed the basis of our understanding of action potentials. Beyond neurons, it was used in modeling pacemakers of the heart, and muscle cell depolarizations before better models existed. The basis is simply KCL:

$$C\dot{V} = I - I_{Na} - I_K - I_{Leak} \quad (7.1)$$

Because the equations can be found in nearly any textbook¹⁶ or Wikipedia page, I will focus on some of the conceptual understanding I had issues with at first. The complete equation Hodgkin and Huxley arrived at is as follows:

$$C\dot{V} = I - \bar{g}_{Na}m^3h(V - E_{Na}) - \bar{g}_Kn^4(V - E_K) - \bar{g}_L(V - E_L) \quad (7.2)$$

There are a few main points to make here. Firstly, this model considers only 3 currents. Na and K are self explanatory, but $Leak$ represents the small amount of current that will always occur in cells due to the many routes of charged particles passing through the membrane. It is restorative, in that it pushes the membrane potential back to the resting voltage.

7.1.2 Gating and Conductance

The \bar{g} represent the maximal conductance of these ions. Of course, you may ask, “*shouldn’t conductance be variable, depending on how many channels are open?*” Yes, which is what m , h , and n are

¹⁶Izhikevich, *Dynamical Systems Neuroscience*

for! These three variables are effectively kinetic fits of the opening and closing dynamics of sodium and potassium channels. Again, I will not mention these equations explicitly as they can be found anywhere. Conceptually, there are three things to know:

Firstly, m is an activation curve for sodium, and the power to the 3rd represents that there are three activation gates. h is an inactivation gate for sodium. Potassium has 4 activation gates, n , and no inactivation gate. Gating can be any number of things, for example, h could be a conformational change that occurs in the channel after it has been open for $0.1ms$ that closes it again. Naturally, the gating for every channel will be different. Because the *Leak* current is an ensemble of many channel types, it will not have "gating" per se.

Secondly, m , h , and n all are between 0 and 1 and represent the **proportion of channels open**. For instance, if $n = 1$, then 100% of potassium channels will be open. This is why we multiply by the maximal conductance.

Thirdly, m , h , and n are dependent upon voltage, which affords them a time constant τ . This is the conceptually most difficult part. The experimental explanation may be beneficial in understanding. Hodgkin and Huxley realized that these three gating variables will converge to different values depending on the voltage. This makes sense, because we know potassium channels are voltage gated, we would expect the gating variable n to converge to around 1 as the voltage increases. But, the rate at which channels open and close is different. Therefore, their experiments were done to vary the voltage and determine how long it took the conductance of the channels to converge to some value. Does this make sense? In simplest terms: channels open and close at different rates, and that depends on the voltage.

What is the implication of this? Again, look up the exact equations if you are interested. Otherwise, trust the following: m has a time constant τ_m which is very small compared to τ_h and τ_n . Meaning, sodium channels will open the fastest in response to a voltage increase, causing depolarization of the cell. After some delay, sodium channel inactivation (h) and potassium channel activation (n) will kick in, causing repolarization and then hyperpolarization.

These are all derivatives.

One of the most difficult conceptual understandings I had was that \dot{V} , m , h , and n are all rates that depend on different time constants, which take voltage as their input. So, the derivative of voltage depends on the derivative of m , h , and n , which depend on voltage. The cyclic nature of this makes it strange, but still doable. Use the general form of derivative, $x_{i+2} = x_{i+1} + (x_{i+1} - x_i)/t$, follow the math, and you will survive.

7.2 Fitzhugh-Nagumo Reduction

7.2.1 Why would we simplify this system?

Reduction implies we are reducing the amount of variables. But why would we do this? The system is already incredibly generalized. We only consider two ion channels and are looking at a static neuron. How can we be accurate if we simplify this system any further?

Let's start by doing a simple thought experiment regarding the previous model:

$$C\dot{V} = I - \bar{g}_{Na}m^3h(V - E_{Na}) - \bar{g}_Kn^4(V - E_K) - \bar{g}_L(V - E_L)$$

As mentioned, m , h , and n have their own time constants $\tau_{m,h,n}$. That means you'll need to do at least 6 calculations in order to determine \dot{V} , which, because it is a derivative, has its own time constant τ_v . Thus, the whole equation is 4th dimensional with respect to time and requires at least 7 or so calculations per time step. If you'd like to simulate an action potential for around 10ms with a time step of 0.01ms, that means you'll perform around 7,000 calculations. Which is not so bad!

However, let's say you want to attempt a propagating action potential. Many people would model this on an infinitely long neuron/wire, but for the sake of this thought experiment let's say you're just interested in a 1 cm neuron/wire for 10 ms. To account for this spatial consideration, you'll need to add in another term besides I which receives current input from the previous segment of the neuron. So, this brings us up to at least 8,000 calculations.

You'd probably want to divide up the neuron into segments on the order of 1 μm . This multiplies our 8,000 calculations by an additional 100,000, giving us 800,000,000 to worry about. Still, this is not horrendous. But, this considers a 1D wire. Neurons are 3D dimensional. We are already considering a system that is 4th dimensional with respect to time, and now we desire to consider 3rd dimensional with respect to space. Imagine trying to calculate the flux through a $1000 \times 1000 \times 1000$ resolution box (i.e., perhaps μm^3 with good resolution). The surface area of this box is thus 6×10^6 . Now extend this surface area to include the length of the wire and the area of the soma and dendrites, giving you thousands of millions of points to calculate per time iteration. And, we are still only considering two ion channels. Neurons have dozens and dozens of channels all with different gating kinetics. It does not consider things like lateral inhibition, birufcation, dendritic input, etc. I'll not bother telling you how many calculations we need to perform beyond this point—but it would be large.

7.2.2 How to Reduce

What do we know about the time constants mentioned in the previous section? Roughly speaking, some are fast and some are slow. The upswing of an action potential is on a fast time constant, and the repolarization is on a slow time constant. We also know that the upswing portion is roughly a positive feedback loop, so as voltage increases, so should the derivative of voltage.

This helps us arrive at least at the following:

$$\dot{V} = V \times f(x) \tag{7.3}$$

Simply meaning that the derivative should scale with voltage in some way. We also know that there are at least two “equilibrium points” in a neuron. Meaning, when the neuron is at rest, the \dot{V} will be zero. And, when the neuron reaches the peak of the action potential, the same is true. This will allow us to immediately assume something interesting:

$$\dot{V} = V(V - V_{rest})(V - V_{max}) \tag{7.4}$$

We are already almost there. What we have just done is said that when either $V = V_{rest}$ or $V = V_{max}$, the \dot{V} will not change. These are all on the aforementioned “fast” time scale, and as this is representative of the activation of the action potential, it is effectively a simplification of the sodium channel dynamics. This is also extremely easy to measure experimentally.

On our second time scale, the slow time scale, we have the inactivation/repolarization function. How will this look like? Just as with the first equation, we will want this curve to increase in magnitude with voltage. Because n represented the potassium channel activation in the previous segment, we can use that as our repolarization function here.

$$\dot{n} = V - \gamma n \quad (7.5)$$

What does this say? It says that our repolarization curve \dot{n} will increase with respect to voltage. But, it will also decrease with respect to itself according to some scaling factor γ .

Now we have reduced our function down to two dimensions and can combine terms:

$$\begin{aligned} \dot{V} &= V(V - V_{rest})(V - V_{max}) - n \\ \dot{n} &= V - \gamma n \end{aligned} \quad (7.6)$$

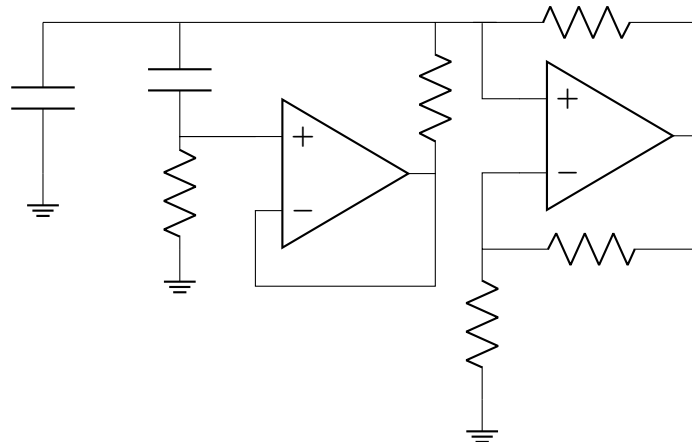
But, we still want voltage to be affected by an injected current, so we can simply add this term back in. And it is also in this equation that we will add our spatial dependence to reach the following:

$$\dot{V} = I_{app} + [V(V - V_{rest})(V - V_{max}) - n] + D \frac{\partial V^2}{\partial x^2} \quad (7.7)$$

D is our spatial dependence, which represents the diffusion of charge around the neuron membrane. And that's it, for now!

Circuits digression.

A lot of the original work done by Fitzhugh and Nagumo used circuit equivalents in order to model neurons. One such example is as follows¹⁷:



¹⁷This circuit is adapted from *Mathematical Physiology*, by James Keener & James Sneyd (1998).

The rightward opamp functions as a Schmitt Trigger, and the entire thing is effectively an opamp oscillator with a second opamp in the middle. The purpose is to simulate an excitable system, like a neuron that is continually firing. Excitable systems are those that fire and have some refractory period before firing again (for example forest fires, or even your toilet).

7.3 Diffusion

Note that in the coming sections, $[f]$ is used to describe the concentration of some molecule f . But, this principal can be applied to anything, including the spreading of voltage across some surface.

7.3.1 Diffusion Equation Derivation

So, let's consider some particle that adheres to the arbitrary function $f(x)$, and has some probability density function of $\Psi(x, t)$ and experiences some noise of W . We can know that, regarding W :

$$\begin{aligned} dW &= 0 \\ dW^2 &= dt \end{aligned} \tag{7.8}$$

By the Itô lemma. And where $dx = \alpha dW$, where α is some function of $k_B T$ and the mobility coefficient, M , of the particle. We can say for an ensemble of particles that:

$$\langle f(x) \rangle(t) = \int \Psi(x, t) f(x) dx \tag{7.9}$$

If we are interested in the change of $f(x)$ over dx , we consider:

$$df = f[x + dx] - f[x] \tag{7.10}$$

And we Taylor Expand around df as:

$$\begin{aligned} df &= f' \alpha dW + \frac{1}{2} f'' \alpha^2 dW^2 + \mathcal{O} dW^3 \\ df &= f' \alpha dW + \frac{1}{2} f'' \alpha^2 dt + \mathcal{O} dt dW \end{aligned} \tag{7.11}$$

If we average over the ensemble, we get:

$$\frac{d\langle f \rangle}{dt} = \frac{1}{2} \langle f'' \rangle \alpha^2 \tag{7.12}$$

This can be solved as:

$$\frac{\partial \Psi}{\partial t} f = \frac{1}{2} \frac{\partial^2 \Psi}{\partial x^2} f \alpha^2 \tag{7.13}$$

And, because f never meant anything anyway, we are saying:

$$\frac{\partial \Psi}{\partial t} = D_c \frac{\partial^2 \Psi}{\partial x^2} \tag{7.14}$$

Another approach.

Let's consider beginning this equation with the Master equation, which describes the probability (still using Ψ) of being at position r at time $t + \Delta t$ for one dimension as:

$$\Psi(r, t + \Delta t) = \Phi \Psi(r - \vec{e}_i, t) + (1 - \Phi) \Psi(r + \vec{e}_i, t) \quad (7.15)$$

Where Φ is the probability of moving left by a distance of \vec{e}_i along your 1-dimensional lattice. In other words, \vec{e}_i is the discrete length that you can travel along this lattice. Do you hate this notation? Me as well.

Let us now try to find the solution to this by Taylor expansion:

$$\begin{aligned} \Psi + \Delta t \frac{\partial \Psi}{\partial t} &= \Phi \left(\Psi - \vec{e}_i \Psi' + \frac{\vec{e}_i^2}{2} \Psi'' \right) + (1 - \Phi) \left(\Psi + \vec{e}_i \Psi' + \frac{\vec{e}_i^2}{2} \Psi'' \right) \\ \Delta t \frac{\partial \Psi}{\partial t} &= -2\Phi \vec{e}_i \Psi' + \vec{e}_i^2 \Psi' + \frac{\vec{e}_i^2}{2} \Psi'' \\ \frac{\partial \Psi}{\partial t} &= \frac{\vec{e}_i(1 - 2\Phi)}{\Delta t} \Psi' + \frac{\vec{e}_i^2}{2\Delta t} \Psi'' \end{aligned} \quad (7.16)$$

Which we can simplify to:

$$\frac{\partial \Psi}{\partial t} = \frac{\vec{e}_i(1 - 2\Phi)}{\Delta t} \frac{\partial \Psi}{\partial x} + D_c \frac{\partial^2 \Psi}{\partial x^2} \quad (7.17)$$

We could assign the value of $\vec{e}_i(1 - 2\Phi)/\Delta t$ to be some constant. But, in general, $\Phi = 0.5$, signifying an equal probability of moving left or right, so this entire term is deleted, giving us the same as we got for equation 7.14.

7.3.2 Forward Euler's

Diffusion is accomplished using some diffusion coefficient (D_c) multiplied by some measure of the proportion in one compartment versus another (often $\partial^2[f]/\partial x^2$). D_c can be tuned however desired. The important bit is the second derivative of $[f]$ with respect to space. This can be done using the general form of a second derivative, as written below:

$$f'' = \frac{f_{x+1} - 2f_x + f_{x-1}}{x^2} \quad (7.18)$$

One may wonder how one would solve for an edge case, as the general form of a second derivative requires three data points. There are some nuances, but in general the solution is simply the first derivative of the non-edge side. That is, since the second derivative is the difference in derivatives, that leaves simply the derivative of one side minus zero. This is like applying a closed end to your surface. You can ponder how to solve for an open end, if that ever arises.

This method has some slight issues in which the $[f]$ can occasionally go negative. The way in which this occurs is stated below (note that now $[f]$ is used instead of f to signify concentration at a value x and time t). We can first describe a simplified version of the problem:

$$\begin{aligned}
[f]_i &= f_0 \exp(-mt) \\
\frac{d[f]}{dt} &= \frac{[f]_{i+1} - [f]_i}{\Delta t} = -m[f]_i \\
[f]_{i+1} &= (1 - m\Delta t)[f]_i = [f]_i - m\Delta t[f]_i \\
[f]_i &= (1 - m\Delta t)[f]_{i-1} = (1 - m\Delta t)^2[f]_{i-2} \\
[f]_i &= (1 - m\Delta t)^i[f]_0
\end{aligned} \tag{7.19}$$

You can see easily, from this, that if Δt is too big, you will abandon the characteristic decay you'd expect from $f_0 \exp(-mt)$, and instead get some diverging oscillatory function. How this applies to our interest in diffusion is described below:

$$\begin{aligned}
\frac{[f]_x^{t+1} - [f]_x^t}{\Delta t} &= \frac{[f]_{x+1}^t - 2[f]_x^t + [f]_{x-1}^t}{x^2} \\
[f]_x^{t+1} - [f]_x^t &= \frac{\Delta t}{x^2} ([f]_{x+1}^t - 2[f]_x^t + [f]_{x-1}^t) \\
[f]_x^{t+1} &= \frac{\Delta t}{x^2} [f]_{x+1}^t + \left(1 - 2\frac{\Delta t}{x^2}\right) [f]_x^t + \frac{\Delta t}{x^2} [f]_{x-1}^t
\end{aligned} \tag{7.20}$$

Therefore, if we want to ensure that the concentration is always positive, we are constrained by:

$$\begin{aligned}
1 - 2\frac{\Delta t}{x^2} &= 0 \\
\Delta t &< \frac{x^2}{2}
\end{aligned} \tag{7.21}$$

The relevance of this being that if one were interested in modeling on a very small Δx , then one would have to use a Δt that is not physiological, and thus waste a great deal of computing power in doing so. This can be avoided explicitly using some other methods, discussed next.

7.3.3 Backward Euler's

This form serves to solve the time-scale dilemma by swapping $[f]_{x+1}$, and can be used with any Δt . Let us consider the same example from above:

$$\begin{aligned}
[f]_i &= f_0 \exp(-mt) \\
\frac{d[f]}{dt} &= \frac{[f]_{i+1} - [f]_i}{\Delta t} = -m[f]_{i+1} \\
[f]_{i+1} - [f]_i &= -m\Delta t[f]_{i+1} \\
[f]_{i+1} &= \frac{1}{1 + m\Delta t} [f]_i
\end{aligned} \tag{7.22}$$

Naturally, there is no longer a concern of the size of Δt . Though, one immediate concern is the difficulty of solving your equation for $[f]_{i+1}$. Getting back to the diffusion interest, we now have:

$$\begin{aligned}\frac{[f]_x^{t+1} - [f]_x^t}{\Delta t} &= \frac{[f]_{x+1}^{t+1} - 2[f]_x^{t+1} + [f]_{x-1}^{t+1}}{x^2} \\ [f]_x^{t+1} - [f]_x^t &= \frac{\Delta t}{x^2} ([f]_{x+1}^{t+1} - 2[f]_x^{t+1} + [f]_{x-1}^{t+1})\end{aligned}\tag{7.23}$$

Which simply replaces the previous $[f]_x^t$ with $[f]_x^{t+1}$. This leaves us with three unknowns (those being $[f]^{t+1}$ at $x-1, x, x+1$). We must use linear algebra to solve by first rewriting the left and right side as vectors and a matrix in the following way:

$$[\vec{f}]^{t+1} = \begin{bmatrix} [f]_0^{t+1} \\ [f]_1^{t+1} \\ \vdots \\ [f]_x^{t+1} \end{bmatrix}; [\vec{f}]^t = \begin{bmatrix} [f]_0^t \\ [f]_1^t \\ \vdots \\ [f]_x^t \end{bmatrix}\tag{7.24}$$

and

$$A = \frac{\Delta t}{x^2} \begin{bmatrix} \dots & \dots & \dots & \dots & \dots \\ 1 & -2 & 1 & & \vdots \\ \vdots & 1 & -2 & 1 & \vdots \\ \vdots & & 1 & -2 & 1 \\ \dots & \dots & \dots & \dots & \dots \end{bmatrix}\tag{7.25}$$

The corners 1, 1 and x, x were intentionally omitted, as what one desires to do with this is dependent on how they would prefer to treat their edges. As described before in the *Forward Euler's* method, one can use instead of the $(1, -2, 1)$ pattern, simply $(\emptyset, -1, 1)$ pattern, which signifies a closed edge. Therefore, together now we get:

$$\begin{aligned}[\vec{f}]^{t+1} - [\vec{f}]^t &= A[\vec{f}]^{t+1} \\ I[\vec{f}]^{t+1} - A[\vec{f}]^{t+1} &= [\vec{f}]^t \\ [\vec{f}]^{t+1} &= (I - A)^{-1}[\vec{f}]^t\end{aligned}\tag{7.26}$$

Where I is the identity matrix.

Remarks.

Forward Euler's is explicit, and will be preferred whenever the differential equations are non-stiff¹⁸. It is the more accurate of the two methods, and can be less computationally intensive if your decay rates are all slow. Backward Euler's is implicit, and can not be used to solve everything, but is doable in most cases. The extra computation required to solve the system of equations more than makes up for potential limitations in your Δt .

Ramblings.

I have this constant wonder if this method can be used to model the spread of voltage over a resistor lattice, by perfecting the D_c value. I am presuming it would work for a sufficiently large lattice, perhaps 100×100 . This would be a good exercise to do sometime in the future.

¹⁸On approximately the same time scale.

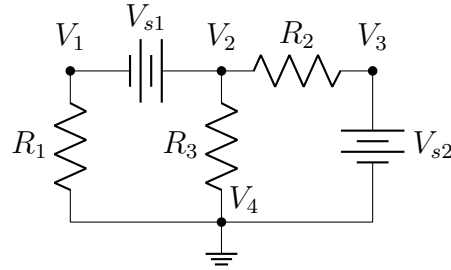
Chapter 8

Modeling Circuits

The idea of this algorithm comes from¹⁹ and is an expansion of what was discussed earlier in the **Electronics** part of this book. Not by coincidence, both of the examples in the earlier section had symmetric matrices. The general way to extract equations from a circuit is in the following pattern:

$$\begin{bmatrix} \mathbf{G} & \mathbf{V} \\ \mathbf{V}^T & \mathbf{Z} \end{bmatrix} \quad (8.1)$$

\mathbf{G} is essentially the way nodes are connected by resistors (represented as conductances). The diagonal represents the total number of resistors connected to a diagonal, and the other bits represents how nodes are connected by resistors. I will use the example provided in the footnote directly to illustrate:



There are 4 nodes, but as mentioned before, Node 4 is grounded, a reference, and thus not included in our calculations. This will mean our matrix \mathbf{G} must be $n \times n$, where n is $N - 1$. Node 1 is connected only to R_1 , resolving the $(0,0)$ ²⁰ position of the matrix to be G_1 . Node 2 is connected to R_2 and R_3 , giving us $(1,1) = G_2 + G_3$. Node 3 to only R_3 , giving us $(2,2) = G_3$. Node 2 and Node 3 are connected via R_2 , meaning the 1,2 and 2,1 positions will have a G_2 , though notably, it will be $-G_2$:

$$\mathbf{G} = \begin{bmatrix} G_1 & 0 & 0 \\ 0 & G_2 + G_3 & -G_2 \\ 0 & -G_2 & G_3 \end{bmatrix} \quad (8.2)$$

There are two voltage sources ($V = 2$), and 3 nodes, meaning the matrix must be $n \times m$, where $n = N - 1$ and $m = V$. You fill the matrix as if the positive terminal of the j^{th} voltage source is connected to the i^{th} node, point $(i,j) = 1$, or $(i,j) = -1$ for the negative terminal. So for the above, since the negative terminal of V_{s1} is connected to Node 1, $(0,0) = -1$, and as the positive terminal connects to Node 2, $(1,0) = 1$. Lastly, as Node 3 connects to the positive terminal of V_{s1} , $(2,1) = 1$.

¹⁹<https://lpsa.swarthmore.edu/Systems/Electrical/mna/MNA3.html>

²⁰You are a computer scientist in addition to a mathematician, so of course our matrices must be 0 indexed.

$$V = \begin{bmatrix} -1 & 0 \\ 1 & 0 \\ 0 & 1 \end{bmatrix} \quad (8.3)$$

$$V^T = \begin{bmatrix} -1 & 1 & 0 \\ 0 & 0 & 1 \end{bmatrix} \quad (8.4)$$

And lastly, Z for zero is an $n \times n$ matrix of zeros where $n = V$:

$$V^T = \begin{bmatrix} 0 & 0 \\ 0 & 0 \end{bmatrix} \quad (8.5)$$

Giving us an $Ax = B$ of:

$$\begin{bmatrix} G_1 & 0 & 0 & -1 & 0 \\ 0 & G_2 + G_3 & -G_2 & 1 & 0 \\ 0 & -G_2 & G_2 & 0 & 1 \\ -1 & 1 & 0 & 0 & 0 \\ 0 & 0 & 1 & 0 & 0 \end{bmatrix} \begin{bmatrix} V_1 \\ V_2 \\ V_3 \\ I_1 \\ I_3 \end{bmatrix} = \begin{bmatrix} 0 \\ 0 \\ 0 \\ V_{s1} \\ V_{s2} \end{bmatrix} \quad (8.6)$$

You may, rightfully, say “*Uh, who cares?*,” since we already know that each row corresponds to a different equation. Well, there are a few reasons. Firstly, doing this algorithmically allows us to avoid accidentally underdetermining our matrix using the ol’ eye-balling it technique. More importantly, though, the algorithmic approach allows us to solve this via code. Once I can write a bit more neatly, I’ll likely upload some snippets here.

Chapter 9

Fluid Mechanics and Cell Motility

9.1 Introduction

The life of small things is hard. Brownian motion reorients *E. coli* a full 90° approximately once per second. The objects which they are trying to chase after and eat, too, undergo Brownian motion. A good question to ask yourself, then, is what do they do to make it worth it?

9.2 Cell Motility

I have an idea. I'm wondering if you can use cell motility models, with a bit of adaptation, and use it to model growth cone motility. I.e., model an ensemble of neurons after injury. The motivation being that the architecture of the neurons after injury is quite important to recovery. This idea, sprouting, is explored in-depth throughout this work, such as in a discussed Courtine review. Similarly, the movement of axons on a single cell level is naturally a form of cell motility.

There have been a number of papers that have gathered the 3D structure of axons after injury—so it is not impossible to verify models^{21,22}.

9.3 Fluid Mechanics

There are two main open questions in the field of fluid mechanics. First, Newton's equations have been used for centuries and, in large part, model the world very well. However, we still haven't determined if these work completely, in all cases. Another open question is the origin of turbulence. Broadly speaking, we can define fluids as something that can be deformed, are continuous, and have no memory of its previous position. Complex fluids, like toothpaste, exhibit both fluid-like behaviors, but also retain their shape when left alone.

Knudsen number is used to define how continuous a fluid is:

$$K_N = \frac{\lambda}{L} \tag{9.1}$$

Knowing a system is continuous allows us to define dynamic, average quantities like $\rho(x; t)$, $p(x; t)$, $\mathbf{u}(x; t)$. Our pressure value, $p(x; t)$, is useful in defining the resistance of a fluid to force. Pressure is isotropic,

²¹<https://www.sciencedirect.com/science/article/pii/S0896627321007753?via%3Dihub>

²²<https://www.sciencedirect.com/science/article/pii/S2211124720308883?via%3Dihub>

meaning it is independent of direction. Defining the velocity, $\mathbf{u}(x;t)$, may be done by quantizing some small segment of the fluid and following its trajectory. This is the Lagrangian description. The trajectory that your quantized box follows is called the *pathline*. Alternatively, the Eulerian description treats the fluid as an ensemble, defining \mathbf{u} everywhere and producing a vector-field like array of streamlines. Conversion between the Lagrangian and Eulerian descriptions is:

$$\frac{Df}{Dt} = \frac{\partial f}{\partial t} + \mathbf{u} \cdot \nabla f \quad (9.2)$$

You can define movement of a fluid with three fundamental flows: translation, rotation (solid body), and extension. Translation and rotation both do not cause any deformation. The streamlines simply move in unison in some direction. Extension causes deformation, and have hyperbolic streamlines. A microfluidic chamber, in which 4 channels come together in a cross, is an example of extension flow. At the intersection, components will be stretched. Deformation like this will lead to friction.

The Reynolds Number.

A large part of this section will come from²³ and²⁴.

The Reynolds number, Re , describes the flow of a fluid and is used to characterize it as turbulent or laminar. Such turbulent or laminar flow is interesting and important in biology. For example, flow in the circulatory system is typically turbulent (unless we are discussing the capillaries). Areas of high turbulence are known to accumulate plaques more frequently. It is calculated as:

$$Re = \frac{\rho LU}{\eta} \quad (9.3)$$

$$Re_\omega = \frac{\rho L^2 \omega}{\eta} \quad (9.4)$$

Where ρ describes the density of the fluid, L describes the characteristic length, U describes the flow speed, and μ describes the fluid's viscosity. It is common to see these variables interchanged with others, such as describing U as v , or η as μ , or others. Another common thing you may see is the replacement of ρ/η with a different constant called the *kinematic viscosity*, usually represented by ν .

The Reynolds number can be interpreted as a ratio of the inertial force to the viscous force. An Re less than 10^3 is considered to be viscous dominated and laminar. An Re greater than 10^4 is considered inertia dominated and turbulent. A more apt description may be that the viscous nature of the fluid holds significantly less weight for something at a high Re —meaning that a blue whale's motion, which swims at an Re of around 10^7 , is dictated nearly purely by inertia, as you would expect. In

²³<https://www.cambridge.org/us/universitypress/subjects/mathematics/fluid-dynamics-and-solid-mechanics/fluid-dynamics-cell-motility?format=HB&isbn=9781107174658>

²⁴<https://pubs.aip.org/aapt/ajp/article-abstract/45/1/3/1043148/Life-at-low-Reynolds-number?redirectedFrom=fulltext>

microbiology, R_e is $\ll 1$, making it highly viscosity dependent.

A nice equation you can find is the following:

$$\frac{\mu^2}{\rho} = F_{tow} \quad (9.5)$$

F_{tow} is the force required to “tow” an object in some liquid when $R_e = 1$. That is, any object with $R_e = 1$ can be towed by this force. The purpose of this is to demonstrate that small R_e is correlated to small forces. Another interpretation of R_e is that if you have an object, like a micro organism, with a very small R_e , you could push it with all your might, and nearly the instant you stop pushing, it will immediately halt. This is, again, because it is completely inertia-independent.

Swimming itself is a cyclic process, usually described as n cycles. Reciprocal swimming is when one’s motion is equal in either the forward or reverse direction, and where one ends up in the same state at the end of the cycle. Interestingly, at high R_e this cycle of swimming is acceptable. The example described in *Life at Low R_e* is a clam who opens its mouth to move and then closes it, shunting it forward and is carried by momentum. Of course, such momentum does not help at low R_e , so a swimmer must have multiple, non-reciprocal movements.

Lizard Digression.

A neat question you can ask is how exactly a large animal, like a lizard, are able to run on water? To do this, we’ll make a number of huge simplifications. First, let’s say the lizard’s foot deflects / indents the water in an approximately cube-like manner with a length R . The density of the fluid is what we’ll call ρ_f . The speed that they’re running we’ll call v , and the frequency of their steps to be ω . The force generated by stepping, also called the Shoke force, is due to the inertia of the fluid, and is summarized as:

$$F_{up} \approx R^3 \rho_f v \omega \quad (9.6)$$

The lizard is fighting the force of gravity pulling it down. If we take the lizard to be approximately cube like, with dimension L and density ρ_l , then:

$$\begin{aligned} F_{down} &\approx L^3 \rho_l g \\ R^3 \rho_f v \omega &\geq L^3 \rho_l g \end{aligned} \quad (9.7)$$

To simplify further, let’s assume $R \approx L$, and that $\omega \approx v/L$. Now we can simplify to:

$$\begin{aligned} \rho_f \frac{v^2}{L} &\geq \rho_l g \\ v &\geq \left(\frac{\rho_l}{\rho_f} g L \right)^{\frac{1}{2}} \end{aligned} \quad (9.8)$$

For the sake of not thinking too hard, you can intuit that body’s have physiological limits. Perhaps theoretically, an elephant can run on water if it moves its legs fast enough. However, you can probably

see that this isn't feasible; muscles have limits. Let's say the physiological constraint conforms to the following equation, where K is a constant describing muscle output:

$$\begin{aligned} Fv &\leq \rho_l L^3 K \\ R^3 \rho_f v^2 \omega &\leq \rho_l L^3 K \\ v &\leq \left(\frac{\rho_l}{\rho_f} L K \right)^{\frac{1}{3}} \end{aligned} \tag{9.9}$$

Therefore, the result you'll see is that to run on water, you are constrained between equation (9.8) and equation (9.9). At some point the result of (9.8) exceeds that of (9.9), making it so the burden of running on water exceeds physiological limits. This example wasn't explained in significant depth, and we made some grand simplifications, but the central theme is the ability to map the real, moving world onto equations and make some statements about what is possible.

9.3.1 Conservation of Mass

Let's discuss a fluid at point x and time t . Its velocity is $\mathbf{u}(x; t)$, and its density $\rho(x; t)$. If we are interested in some space, ω , we can determine the mass of fluid in this space by:

$$\int_{\omega} \rho(x; t) d\omega \tag{9.10}$$

If we are interested in the rate of change of fluid in our space ω , we can determine it by:

$$\int_{\omega} \frac{\partial}{\partial t} \rho(x; t) d\omega \tag{9.11}$$

Knowing that any change in mass of the fluid is due only to fluid flowing in and out of our space ω , we can rewrite this integral in terms of fluid passing the space's boundaries, which we'll call S , and let's define a vector normal to this space as \vec{n} . In other terms:

$$-\int_{S, \partial\omega} \rho \mathbf{u} \cdot \vec{n} dS = \int_{\omega} \nabla x \cdot [\rho \mathbf{u}] d\omega \tag{9.12}$$

The conversion between the two is a result of Gauss' theorem. This also means that, because ω is arbitrary:

$$\frac{\partial}{\partial t} \rho(x; t) = -\nabla x \cdot [\rho(x; t) \mathbf{u}(x; t)] \tag{9.13}$$

This is like saying the total change in density is equal to the change in density and velocity at all points x . Which we can rewrite in a way that is clearer, demonstrating mass is conserved:

$$\frac{\partial \rho}{\partial t} + \nabla \cdot (\rho \mathbf{u}) = 0 \tag{9.14}$$

Where $\partial \rho / \partial t$ is the change in density and $\nabla \cdot (\rho \mathbf{u})$ is the advection term. For an incompressible fluid, where your density is fixed, you are left with:

$$\nabla \cdot \mathbf{u} = 0 \quad (9.15)$$

This, of course, is the first equation in the Navier-Stokes equations, discussed in section **9.3.4**.

9.3.2 Stress Tensor

Conservation of momentum can be solved using the forces applied to the system. This includes body forces ($\mathbf{F}(x; t)\delta V$ for some volume δV) and forces applied to a segment of the surface ($\tau(x; t)\delta S$ for some surface $\vec{n}\delta S$).

Body forces scale with $\mathcal{O}(\mathbf{FL}^3)$, and the canonical example is gravity. Forces applied to the surface include pressure, which scales with $\mathcal{O}(\mathbf{FL}^2)$. The force of friction (or viscosity), just as the friction of two solids, comes in two components: the normal force and the force which opposes movement laterally.

To think about this, consider some arbitrary object with a face. Regardless of the face, it has some normal vector \vec{n} , and let's say this surface has an area A . As mentioned before, body forces scale with $\mathcal{O}(\mathbf{FL}^3)$, while surface with $\mathcal{O}(\mathbf{FL}^2)$. This means that when $\lim_{V \rightarrow 0}$, body forces and surface forces must be equal. So let's think of τ as:

$$\tau(x; t) = \lim_{A \rightarrow 0} \frac{F}{A} \quad (9.16)$$

Let's first think of a cube whose faces are aligned with basis vectors $\{\vec{e}_1, \vec{e}_2, \vec{e}_3\}$. All traction vectors can be summarized using these components such that if we have vector τ acting in the direction e_3 , we can describe it as:

$$\begin{aligned} \tau_{e_3} &= \sigma_{3,1}e_1 + \sigma_{3,2}e_2 + \sigma_{3,3}e_3 \\ \tau_i &= \sigma_{i,j}e_j \end{aligned} \quad (9.17)$$

This works nicely and succinctly when we are discussing a vector τ in the direction of a basis vector. Cauchy describes a more general case for some arbitrary tetrahedron. Forces applied to three of the faces on the tetrahedron can be described using $\{\sigma_{i,1}, \sigma_{i,2}, \sigma_{i,3}\}$, but the fourth face is misaligned with the bases. The 4th face of the tetrahedron has the normal vector \vec{n} , which can be defined as $\vec{n} = \vec{n}_1e_1 + \vec{n}_2e_2 + \vec{n}_3e_3$. A force acting on this face, τ is not aligned with any basis vector, but we can cheat by splitting τ into its components, $\tau = \tau_{n_1} + \tau_{n_2} + \tau_{n_3}$.

I'm going to yada-yada through the proof a little bit, but the gist is that if you take Newton's laws and describe them for each normal, you get something along the lines of:

$$\sum \mathbf{F}_{\mathbf{e}_1} = -\sigma_{1,1}n_1 - \sigma_{2,1}n_2 - \sigma_{3,1}n_3 + \tau_{n_1} + mg = ma \quad (9.18)$$

Since, as mentioned earlier, we are taking the limit as the volume goes to zero, we can say that:

$$\begin{aligned} -\sigma_{1,1}n_1 - \sigma_{2,1}n_2 - \sigma_{3,1}n_3 + \tau_{n_1} + 0 &= 0 \\ \sigma_{1,1}n_1 + \sigma_{2,1}n_2 + \sigma_{3,1}n_3 &= \tau_{n_1} \end{aligned} \quad (9.19)$$

And this holds true for all of the components of τ . This makes it more obvious that σ will be linear and homogenous. We can now write this as:

$$\begin{bmatrix} \tau_{n1} \\ \tau_{n2} \\ \tau_{n3} \end{bmatrix} = \begin{bmatrix} \sigma_{1,1} & \sigma_{2,1} & \sigma_{3,1} \\ \sigma_{1,2} & \sigma_{2,2} & \sigma_{3,2} \\ \sigma_{1,3} & \sigma_{2,3} & \sigma_{3,3} \end{bmatrix} \begin{bmatrix} n1 \\ n2 \\ n3 \end{bmatrix} \quad (9.20)$$

Simplified, this is:

$$\tau_n = \sigma^T n \quad (9.21)$$

Where the transpose of σ multiplied by the normal gives us the force. So in short, to find the force acting on a plane you take some stress tensor and multiply it by the normal of that plane.

One component you may be interested in calculating is the force normal to the plane. Let's call this σ_n . This can be accomplished via a linear projection. From linear algebra, this is:

$$\begin{aligned} \sigma_n &= \text{proj}_n \tau_n = \frac{\tau_n \cdot n}{||n||} \\ \sigma_n &= \tau_n \cdot n \end{aligned} \quad (9.22)$$

Because the length of a unit vector, n , must equal 1. A shear stress, on the other hand, is parallel to the surface of the plane. For now, I'll call this π_n . Because the traction vector, τ_n , is the vector addition of σ_n and π_n . In other words, for either the vector or the scalar:

$$\begin{aligned} \vec{\pi}_n &= \tau_n - \sigma_n n \\ \pi_n &= ||\tau_n - \sigma_n n|| \end{aligned} \quad (9.23)$$

$\tau(x, t)dS$ describes the force exerted on a surface, called a traction. One component will be the normal force. The normal force will always point in the direction opposite of τ , which can be written as $\tau(x, t, -\vec{n}) = -\tau(x, t, \vec{n})$. To characterize this, you need to know the magnitude, direction, and orientation of the surface.

Defining $\tau(x, t)dS$ can be done with $\tau(\vec{n})dS = -\tau(e_1)dS - \tau(e_2)dS... = -[\tau(e_x)dS] \cdot \vec{n}$, where e_x is a surface. Somehow this leads to, via some linear projection, $dS_i = dS\vec{n} \cdot e_i$ and then $\tau = \sigma \cdot \vec{n}$. σ is your Cauchy stress tensor, in units of Pascals, which usually comes in the form of a 3×3 matrix.

This matrix, σ , is inherently symmetric.

9.3.3 Conservation of Momentum

To achieve the hydrodynamical equation of motion, we equate the rate of change of momentum within ω and out of the boundaries with the sum of forces acting on ω and the boundaries. The rate of change of momentum, in this case, is:

$$\int_{\omega} \frac{\partial}{\partial t} [\rho(x; t) \mathbf{u}(x; t)] d\omega \quad (9.24)$$

We can describe the outflow of momentum from the space ω by:

$$\int_{\partial\omega} \rho(x; t) \mathbf{u}(x; t) \mathbf{u}(x; t) \cdot d\mathbf{S} = - \int_{\omega} \nabla x \cdot [\rho \mathbf{u} \mathbf{u}] d\omega \quad (9.25)$$

The sum of forces acting on the fluid within ω are loosely defined with X , where X is the force per unit volume from external forces:

$$\int_{\omega} X(x; t) d\omega \quad (9.26)$$

And the force force experienced, using σ as the stress tensor, is:

$$\int_{\partial\omega} \sigma(x; t) \cdot d\mathbf{S} = \int_{\omega} \nabla x \cdot \sigma d\omega \quad (9.27)$$

These are all combined and simplified into:

$$\frac{\partial}{\partial t} [\rho \mathbf{u}] + \nabla x \cdot [\rho \mathbf{u} \mathbf{u}] = X + \nabla x \cdot \sigma \quad (9.28)$$

We are allowed to make this simplification because ω is a nonexistant, arbitrary space.

$$\begin{aligned} \frac{\partial}{\partial t} \int_{\omega} \rho \mathbf{u} d\omega &= \int_{\omega} \mathbf{F} d\omega + \int_{\partial\omega} \sigma \cdot \vec{n} dS - \int_{\partial\omega} \rho \mathbf{u} (\mathbf{u} \cdot \vec{n}) dS \\ \rho \left[\frac{\partial \mathbf{u}}{\partial t} + \mathbf{u} \cdot \nabla \mathbf{u} \right] &= \rho g + \nabla \cdot \sigma \end{aligned} \quad (9.29)$$

At present, this cannot be solved because we do not know how σ behaves in the system. With an assumption, we can find the constitutive equation for σ :

$$\sigma = -pI + \mu(\nabla \mathbf{u} + {}^T \nabla \mathbf{u}) \quad (9.30)$$

Where $-pI$ is pressure multiplied by an identity matrix, giving us an isotropic term. The second term is viscosity, which was empirically determined by Newton. It was shown that the drag force experienced by an object scales with \mathbf{u} and A , but inversely with h . Thus, we get:

$$\frac{F}{A} = \mu \frac{\mathbf{u}}{h} \quad (9.31)$$

μ is a scaling factor, which is called the dynamic viscosity and has units of Pascal·seconds.

9.3.4 Navier-Stokes Equations

In knowing the velocity vectors at all points in a fluid allows you to describe the movement of the fluid over time. Three key assumptions in this are that the fluid be Newtonian (meaning applying a shear force does not affect it in any way), incompressible, and isothermal. This brings us to:

$$\begin{aligned}\nabla \cdot \mathbf{u} &= 0 \\ \rho \frac{\partial \mathbf{u}}{\partial t} &= -\nabla p + \mu \nabla^2 \mathbf{u} + \mathbf{F}\end{aligned}\tag{9.32}$$

$\nabla \cdot \mathbf{u} = 0$ simply states that the mass is conserved. When describing a 3 dimensional velocity, we'll consider (x, y, z) . Thus:

$$\nabla \cdot \mathbf{u} = \frac{\partial \mathbf{u}}{\partial x} + \frac{\partial \mathbf{u}}{\partial y} + \frac{\partial \mathbf{u}}{\partial z}\tag{9.33}$$

Taking the gradient of \mathbf{u} is used to solve the divergence of the field. A nonzero divergence would describe a source of fluid flowing into the system (or a sink).

The second equation is a rewriting of Newton's second law, $\sum F = ma$. Some would describe it as being a conservation of momentum equation. Let's see how:

$$\begin{aligned}F &= ma/V \\ F &= \rho a \\ F &= \rho \frac{d\mathbf{u}}{dt}\end{aligned}\tag{9.34}$$

Because we are considering individual points, rather than the ensemble, we divide by the volume V , giving us the density. Acceleration can be rewritten as the change in velocity over time, $d\mathbf{u}/dt$. Next we will consider the forces relevant to this system.

$$-\nabla p + \mu \nabla^2 \mathbf{u} + \sum F = \rho \frac{d\mathbf{u}}{dt}\tag{9.35}$$

The ∇p describes one of two internal forces. It accounts for forces due to a change in pressure (recall that $p = F/A$). Again, in a 3D space, $\nabla p = \partial p / \partial x + \dots$, etc. The second term, $\mu \nabla^2 \mathbf{u}$, describes force of friction, and or viscosity.

Lastly, we can summarize all external forces ($\sum F$) within this big \mathbf{F} . We may see gravity as an external force, for example, in which case we may replace \mathbf{F} with ρg . Therefore, the Navier-Stokes equations are essentially the reapplication of fundamental concepts in physics for fluids.

\mathbf{u} we can define, perhaps overly complexly, as:

$$\mathbf{u}(r_s t) = \dot{r}_s + \mathbf{U}(t) + \Omega(t) \times r_s\tag{9.36}$$

Where r_s is defined as any point on the swimmer, and $\dot{r}_s = \partial r_s / \partial t$. $\mathbf{U}(t)$ describes the instantaneous linear velocity, and $\Omega(t)$ the angular.

As it goes, this equation can be made dimensionless as:

$$-\nabla p + \mu \nabla^2 \mathbf{u} + R_e \sum F = R_{ew} \frac{d\mathbf{u}}{dt} \quad (9.37)$$

Given that both R_e and R_{ew} are expected to be tremendously small for micro organisms, we can reduce the equations to the simplified Stokes equations. Importantly, this is simply the same as **removing the inertial terms**:

$$\begin{aligned} \nabla \cdot \mathbf{u} &= 0 \\ \nabla p &= \mu \nabla^2 \mathbf{u} \end{aligned} \quad (9.38)$$

Another slight confusion is that this entire equation seems to be zero. Maybe I am simply bad at math, but if $\nabla \cdot \mathbf{u} = 0$, then how does $\mu \nabla^2 \mathbf{u} \neq 0$?

9.3.5 Propulsion

Presently, I do not understand the theory behind this, but somehow everything that occurs at low R_e is linear. As it goes, force and torque are related by the following equations:

$$\begin{aligned} F &= AU + B\Omega \\ \tau &= CU + D\Omega \end{aligned} \quad (9.39)$$

We can use this to construct *propulsion* matrices like:

$$P = \begin{bmatrix} A & B \\ C & D \end{bmatrix} \quad (9.40)$$

The proof is not shown here but interestingly $B = C$. To think of this matrix, let's consider dropping a cork-screw into a vat of syrup. You probably expect that the cork-screw will turn to some degree, but that there will still be some *slippage*. That is, it sinks at a rate faster than it spins. If something were to sink without spinning at all, you can imagine that the matrix would be completely diagonal, because, given our equation 9.39, that would mean the linear force, F , and the rotational force, τ , are completely decoupled. The propulsion efficiency is defined as (or proportional to) these off diagonal elements squared (i.e., B^2)—evidently, though, this is considered unimportant in the grand scheme of interactors.

Diffusion.

Diffusion coefficients describe how quickly an object moves around in a fluid. The formula, where a is the object's radius, is:

$$D = \frac{k_B T}{6\pi\eta a} \quad (9.41)$$

You may see the denominator rewritten as f , representing the friction coefficient of the object.

Fascinatingly, at very low R_e your movement inherently takes your surrounding environment with you. This actually has quite large consequences, and is called the *added mass phenomenon*. In short, if you move and carry a load of liquid along with you, it is as if you are propelling a much greater mass. It's estimated that:

$$\begin{aligned}\tau_{stir} &= \frac{l}{v_{stir}} \\ \tau_{diff} &= \frac{l^2}{D}\end{aligned}\tag{9.42}$$

Where τ is the time it takes you to move an object some distance l by either stirring or diffusion, and v_{stir} is the velocity of stirring performed. The ratio of such, i.e. lv/D (or LU/D), is called the Péclet number (P_e). Maybe you can recall from earlier that R_e can be written as lv/ν (equivalently LU/ν), so you can see how the Reynolds number and the Péclet number describe systems in a similar way. Stirring is only helpful if $lv/D > 1$, which gives us an indication of how much you can accomplish either by stirring or diffusion. When $P_e \ll 1$, diffusion dominates. For micro swimmers, like bacteria, stirring is virtually useless, and they're better off simply waiting for items to diffuse toward them. Another fascinating realization is that bacteria do not move to reach more nutrients—as we just stated that this would be useless. Instead, they travel to areas of a higher density, where the probability of diffusion is greater²⁵.

9.4 Literature

Here I'll discuss some of the literature surrounding fluid mechanics and neuroscience.

9.4.1 CSF Flow

A large topic is the flow of CSF inside the brain and spinal cord, which has implications in drug delivery and hydrocephalus. Other notable topics include the application of shear stress to neurons, which may activate mechanically gated channels.

Here I'll discuss²⁶. The composition and flow of cerebrospinal fluid (CSF) is both a key diagnostic tool and often at the center of pathologies. For example, measuring CSF composition aids in diagnosis of diseases like Alzheimer's via monitoring amyloid presence²⁷. Similarly, being able to model particle flow in the CSF is helpful in understanding drug delivery. Blockage of CSF flow is responsible for hydrocephalus, which on its face is easy to treat, but is frequently misdiagnosed as Alzheimer's or other neurodegenerative diseases²⁸.

The Sánchez group at UCSD has many papers on modeling CSF flow, so their works are a great resource for further learning. The specific focus of this work is on intracranial pressure (ICP), which can

²⁵Okay—indeed there is something immensely fascinating here. Can the same be true for growth cones? I suppose... yes!

²⁶<https://www.cambridge.org/core/journals/journal-of-fluid-mechanics/article/onedimensional-model-for-the-pulsating-flow-of-cerebrospinal-fluid-in-the-spinal-canal/3710D122EC70FCB29DEF0AB196ADCCD>

²⁷<https://www.youtube.com/watch?v=zCmngDk9VDU>

²⁸<https://www.alz.org/alzheimers-dementia/what-is-dementia/types-of-dementia/normal-pressure-hydrocephalus>

be clinically measured with the surgical implantation of sensors. The goal of this work is to allow for indirect measures, such as MRI, combined with computation to serve in place of invasive procedures. CSF is generated in the brain ventricles, travels through the CNS (including the spinal canal), and eventually exits through arachnoid villi, where it drains into the venous sinus. The venous sinus connects directly to the circulatory system, and thus the spaces housing CSF experience pressure fluctuations with the beats of the heart—they call this ICP pulsations. Many works have modeled the spinal canal and connected spaces as hollow—these simplifications limit the clinical relevance of the models. This work improves upon previous, as it considers the role of arachnoid trabeculae (web-like structures in the arachnoid space, which reduce the pressure).

In initial models, because the spinal canal’s axial distance is significantly longer than its transverse, they use a slender-flow approximation, and state that the velocity and pressure is uniform for a given cross-section. The total volume of CSF is calculated to be 80cm^3 , and with each ICP pulse $\approx 1\text{cm}^3$ of CSF either in or out of the spinal canal, which induces fluctuations in the cross sectional area of the spinal canal (some ΔA). They approximate this change to be about 1mm^2 , and use a linear-elastic model to survey it. These simplifications allow the creation of a one-dimensional model. However, they comment that these initial models fail to capture a “phase lag” between pressure and flow changes that are observed by MRI—they attribute this to the exclusion of trabeculae from the space which would contribute to viscous pressure losses.

Therefore, the bulk of this work focuses on including the viscous pressure loss associated with trabeculae. They introduce a resistance coefficient which is dependent on the viscosity and pulse frequency, $\mathcal{R} = \nu/(k\omega)$, where k is a function of the trabeculae webbing. They also utilize the Womersley number, α , which can be written (using numbers from our class) as $= \sqrt{2\pi R_e St}$, or as $\sqrt{A_0 \omega / \nu}$. An $\alpha \ll 1$ means the frequency of pressure pulses is slow enough that the velocity changes will be in-phase with pressure—whereas an $\alpha \gg 1$ means it will be out of phase by $\approx 90^\circ$ (from Wikipedia²⁹). In fact, they include the pressure loss due to the Stokes layer (Stokes flow induced by the moving boundaries³⁰) but state that this pressure loss is much smaller than is due to trabeculae. Therefore, future models may explore removing this term in order to further simplify.

To verify their model, they compare with actual MRI data from two patients. They vary the resistance coefficient, \mathcal{R} , and show that when $\mathcal{R} = 0$, no phase lag is observed—but one becomes present as \mathcal{R} increases (i.e., the inclusion of trabeculae). Therefore, their updated one-dimensional model is able to account for clinically observed phase lags through the inclusion of increased resistance caused by trabeculae. Some interesting takeaways to me: 1) That you can make a clinically relevant, one-dimensional model at all! I’m surprised you can take the complex, 3D, curvilinear geometry of the spinal canal and reduce it down so much. 2) Learning of the Womersley number, α , is interesting and worth remembering for the future. 3) The fact that they verified the model with clinical data is very supportive. It’s good to see them take it out of just theory and apply it.

²⁹https://en.wikipedia.org/wiki/Womersley_number

³⁰https://en.wikipedia.org/wiki/Stokes_problem

Chapter 10

Machine Learning

Yeah, whatever. I'll do it myself. I always find the cure to fret is learning.

So what is Machine Learning³¹? ML is a subset of AI which looks to find patterns and make predictions about data. ML has a few types:

1. Supervised learning, which uses input data which has an associated, given label.
2. Unsupervised learning, where data does not include labels and instead the learning's goal is to find patterns in the data.
3. Reinforcement learning, where an algorithm learns based on a system of rewards and punishments.

Ratings in learning can be binary, which is called *one-hot encoding* (i.e., you are either happy or not happy, 1 or 0), or there can be *ordinal data*, which has some order (i.e., a spectrum of feelings, say rated 1 to 5). These are qualitative pieces of data, and there can similarly be quantitative discrete or quantitative continuous types of data.

A computer can either predict a class, which is discrete, or can use a regression, to output a continuous value. A model will take a *feature vector* and output a classification.

Calculating Loss.

The first way to calculate loss is called L1 loss. It is simply calculated as:

$$L_1 = \sum (|y_{real} - y_{predicted}|) \quad (10.1)$$

The second way is called L2 loss. The function is quadratic, which increases penalty the further you get from the true value as:

$$L_2 = \sum (y_{real} - y_{predicted})^2 \quad (10.2)$$

Finally, we can calculate binary cross-entropy loss. Without diving in to the formula, it is seen as:

³¹From: https://www.youtube.com/watch?v=i_LwzRVP7bg&t=243s&ab_channel=freeCodeCamp.org

0.99	0.01
0.05	0.95

$$L = -\frac{1}{N} \sum (y_{real} \cdot \log(y_{predicted}) + (1 - y_{real}) \cdot \log(1 - y_{predicted})) \quad (10.3)$$

One could also compute by accuracy.

10.0.1 Models.

KNN.

One model is called K-nearest neighbors (KNN). Suppose you have a set of binary classifications plotted on an X-Y graph. For example, you plot the relation between years spent in school and the money someone earns per year, and your binary classification is whether or not they own a home. You could compute the distance (on the plot) between nearby points. Suppose you take $k = 3$, to find the 3 nearest neighbors. If all of the nearest neighbors to a point is that one owns a home, you'd predict that such a point is also a home owner. If it is ambiguous, you'd predict via the minimum distance between each class and that point.

Naive Bayes.

Naive Bayes depends on conditional probability. So, recall that Bayes theorem goes as:

$$P(A|B) = \frac{P(B|A) \cdot P(A)}{P(B)} \quad (10.4)$$

Where this is the probability of A given B . Therefore, suppose the probability of getting a false positive is 0.05. Suppose the probability of getting a false negative is 0.01. And suppose the probability of having the disease at all is 0.1. Now, ask yourself: what is the probability of having the disease, given that you've tested positive?

We filled in 0.99 and 0.95 simply by knowing that they should sum to 1. That is, the probability that you test either positive or negative most definitely = 1. Now:

$$P(A|B) = \frac{0.99 \cdot 0.1}{0.99 \cdot 0.1 + 0.05 \cdot 0.9} = 0.6875 \quad (10.5)$$

We can use this for classifications. See below:

$$P(C_k|x) = \frac{P(x|C_k) \cdot P(C_k)}{P(x)} \quad (10.6)$$

This essentially asks: what is the probability of x fitting into some category C_k ? $P(C_k|x)$ is considered the posterior. x is the feature vector. $P(x|C_k)$ is the likelihood. $P(C_k)$ is the prior. And finally, $P(x)$ is the evidence.

$$\begin{aligned}
P(C_k|x_1, x_2, \dots, x_n) &= \frac{P(x_1, x_2, \dots, x_n|C_k) \cdot P(C_k)}{P(x_1, x_2, \dots, x_n)} \\
P(C_k|x_1, x_2, \dots, x_n) &\propto P(x_1, x_2, \dots, x_n|C_k) \cdot P(C_k) \\
P(C_k|x_1, x_2, \dots, x_n) &\propto P(x_1|C_k) \cdot P(x_2|C_k) \cdot \dots \cdot P(x_n|C_k) \\
P(C_k|x_1, x_2, \dots, x_n) &\propto P(C_k) \prod_{i=1}^n P(x_i|C_k)
\end{aligned} \tag{10.7}$$

We removed the denominator because $P(x_1, x_2, \dots, x_n)$ is the same for all classes, so it provides no class-specific info and thus can be neglected. The second assumption that we make is that all probabilities are independent, allowing us to multiply everything together.

We use a \hat{y} as an *argmax*. I.e., we maximize $P(C_k) \prod_{i=1}^n P(x_i|C_k)$. This is also called a Maximum A Posteriori (MAP).

Part III

Physiology

Preoccupied with a single leaf, you won't see the tree. Preoccupied with a single tree, you'll miss the entire forest.

– Vagabond by Takehiko Inoue

10.1 Perspective

Chapter 11

Biochemistry

To be able to interface with the electrophysiology of neurons, one must fully understand it.

11.1 Membranes, Ions, and Potentials

This will be a general overview of some of the electrophysiology of neurons. This should probably precede the math and models section, but here we are anyway.

Of course, the ion composition of cells varies a bit, but a good enough approximation is as follows:

$$\begin{aligned}[\text{Na}^+]_i &= 15\text{mM}, [\text{Na}^+]_e = 150\text{mM} \\ [\text{K}^+]_i &= 120\text{mM}, [\text{K}^+]_e = 5\text{mM} \\ [\text{Ca}^{2+}]_i &= 100\text{nM}, [\text{Ca}^{2+}]_e = 2.5\text{mM} \\ [\text{Cl}^-]_i &= 15\text{mM}, [\text{Cl}^-]_e = 120\text{mM}\end{aligned}$$

Where $[\text{X}^+]_i$ and $[\text{X}^+]_e$ refer to the intracellular and extracellular concentrations respectively. Building up a strong intuition for electrophysiology is quite important to approaching the field. Some of the absolutely key facts to recall include:

1. **The intracellular and extracellular spaces are electro-neutral.** If this weren't the case, cell membranes would be under constant force. This means the sum of positive and negative ions must be equal between the intracellular and extracellular spaces.
2. **$[\text{Na}^+]$ and $[\text{Cl}^-]$ are high outside, $[\text{K}^+]$ is high inside.** This will tell you which directions the ions flow during an action potential—when the gates open, Na^+ wants to enter, K^+ wants to exit³². In other words, $[\text{Na}^+]_i < [\text{Na}^+]_e$, $[\text{K}^+]_i > [\text{K}^+]_e$.
3. **The concentration of ions is approximately static.** The amount of ions that actually flow in an action potential and or through ion channels is quite small relative to the total amount.
4. **Intracellular Ca^{2+} is extremely regulated, and its concentration is small (around 100nM).** Ca^{2+} is the ion responsible for most cellular processes, so its tight regulation is essential. In other words, $[\text{Ca}^{2+}]_i \ll [\text{Ca}^{2+}]_e$.

³²A slight nuance is that this does not preclude ions from flowing against their gradient. It can certainly still happen, but the net movement will be out if channels are open in either direction.

Expanding on the calcium regulation, much of the free $[\text{Ca}^{2+}]_i$ is stored within the endoplasmic reticulum (ER), whose concentration will be many orders of magnitude higher than the cytosol. This is important for cells like myocytes who require a large influx of calcium to contract. Rather than attaining all of this Ca^{2+} from the extracellular space, the cells can use Ca^{2+} -induced- Ca^{2+} -release in order to drive the opening of the ER.

Ramblings.

As a complete aside, it is hypothesized that our cells control ions in this way because we originate from the ocean. As the ocean is salty, cells learned how to pump out as much Na^+ as possible, and based their electrophysiology off of this potential. When evolution allowed us to exit the ocean, we maintained this machinery and keep sodium in the extracellular space.

Direction of Flow.

Knowing the general concentrations of ions is a very important way to intuit ion behavior under different conditions. However, the Nernst Potential offers a way to quantify it as:

$$E_X = \frac{RT}{zF} \ln \frac{[X]_e}{[X]_i} \quad (11.1)$$

Where z is the charge of the ion. This allows you to solve the electromotive force, E , for your ion of interest. Knowing the E values for your ions allows you to determine the overall membrane potential using the Goldman–Hodgkin–Katz flux equation:

$$v = \frac{g_{n_1}E_{n_1} + g_{n_2}E_{n_2} + \dots + g_{n_k}E_{n_k}}{g_{n_1} + g_{n_2} + \dots + g_{n_k}} \quad (11.2)$$

The GHK formula is essentially like taking a weighted average of each ion's (n_i) membrane potential, giving us the total membrane voltage. The conductance, g , is the opposite of resistance (covered in more depth at section 7.1.2). In this case, you can think of conductance as being a measure of the membrane's permeability to an ion. That is, a neuron with a lot of Na^+ channels will have a very high total sodium conductance. Conductance is measured in terms of its maximum, meaning that although sodium channels will open and close, the value g_{Na} refers to when all of them are open. When calculating membrane voltage, generally we only use sodium and potassium (though, the GHK formula technically requests using all charged molecules). The reason being because the conductance of all of the other ions is essentially negligible in comparison.

In most cases, the GHK equation is simplified to only include Na^+ and K^+ . The reason is because these two ions have the highest conductances, by far, making them hold the most weight. For example, even though cells may contain HCO_3^- , there aren't tons and tons of ion channels for it like there are for sodium and potassium—thus it does not contribute to v to nearly the same degree. If this concept is confusing, simply consider $V = IR$. If there is no current, there is no voltage. Therefore, we can use the equation below as a good enough approximation of the resting membrane potential:

$$v = \frac{g_{\text{Na}}E_{\text{Na}} + g_{\text{K}}E_{\text{K}}}{g_{\text{Na}} + g_{\text{K}}} \quad (11.3)$$

Now, let's assume a membrane is at rest around -55mV and that the sodium concentrations are what we listed above (150mM and 15mM). We can use the Nernst equation as follows:

$$E_{Na} = \frac{(8.314)(310.15)}{(96,485)(1)} \ln \frac{150}{15} \rightarrow 0.062V \quad (11.4)$$

Because 0.062V (62mV) > the resting -55mV, we can assume Na⁺ will (on average) flow into the cell if sodium channels open. However, if the cell were to massively depolarize all the way to 100mV, we would actually expect Na⁺ to leave the cell, despite its gradient seemingly telling you otherwise. This is, of course, because ions will be subject to both their chemical and electrical gradients.

11.1.1 Action Potentials

Overview.

When considering an action potential, likely you'll want to focus on the flux of Na⁺, K⁺, and Ca²⁺. The standard description is that some kind of stimuli causes an influx of positive ions into the neuron's dendrites or soma, which leads to opening of voltage gated sodium channels in the initial segment of the axon. Sodium flows inward, which causes this segment of the axon to greatly depolarize (causing it to shoot up from $\approx -55\text{mV}$ to $\approx +20\text{mV}$). When the membrane reaches these more positive voltages, voltage gated calcium channels will begin to open and sodium channels will begin to close. More slowly (i.e., delayed in respect to sodium channel opening) in the depolarization process, potassium channels will open which allow for the efflux of potassium ions, causing the membrane to repolarize. Similarly, the depolarization will cause, the next set of sodium channels further along the axon to open, causing the depolarization to propagate down the axon. After the action potential is complete, active transport can somewhat quickly restore the ionic composition to exactly what it was before.

A Common Misconception.

The concentration of ions really does not change during an action potential. It is only a negligibly small amount of ions that are required to change the membrane voltage of the neuron. So, for example, [Na⁺]_e really only goes from 120mM to 119.99...mM during an action potential. Therefore, the membrane potentials that you calculate here are roughly true at any point in an action potential. What changes is the membrane voltage of the neuron, causing channels to open and close, which is what leads to the characteristic peaking of an action potential.

This idea is quite important. Many assume that ions flowing in and out substantially impacts their concentrations, and that is what leads to the in and outflowing of ions. It is often said that ion channels always pass ions "with their concentration gradient." While "transporters" pass ions or molecules against their gradient. But this is not true! Firstly, you can imagine that if channels are unidirectional, there will always be some stochastic passage against a concentration gradient. But more explicitly, many channels solely exist to passively pass ions against this gradient. For example: there are many "inward rectifying potassium channels," meaning they pass potassium ions into the cell (a famous example being the Kir family of channels). Importantly, the concentration of K⁺ outside of the cell will *never* exceed the concentration inside the cell. Therefore, any and all inward pointing K⁺ channels will inherently be against the chemical concentration gradient.

You may be slightly puzzled about why such a small concentration of ions is able to generate an action potential. This is because the voltage generated is hyper-localized to the membrane. The lipid composition of the membrane is also very strictly controlled. The hydrophobic heads of the lipids on the outside monolayer of the membrane (thus, those facing the extracellular space) are most often neutral in charge—still polar, though. Those on the inner monolayer (the cytoplasmic side) have a higher proportion of negatively charged heads. This helps create a partial membrane voltage and is incredibly important for ion behavior, as well as how transmembrane proteins orient themselves in the membrane.

Let's motivate this a little bit: the capacitance of a cell (C_m) is around $1\mu\text{F}/\text{cm}^2$, shown here³³. If the radius of the cell is $10\mu\text{m}$. Given that the voltage swings by around 100mV during an action potential, we can determine that:

$$\begin{aligned}C_{total} &= C_m \times 4\pi r^2 \\q &= C_{total}\Delta V \\q &= 1.3 \times 10^{-12}\text{C}\end{aligned}\tag{11.5}$$

Dividing this number by Faraday's constant, F , gives you the moles of charge, m . You can divide the moles by the volume to approximate ΔC (i.e., the change in total charge):

$$\Delta C = \frac{m}{4\pi r^3/3} \rightarrow 3.1 \times 10^{-7}\text{mM}\tag{11.6}$$

Don't forget to convert the volume into units of liters.

$3.1 \times 10^{-7}\text{mM}$ is a very small number, many orders of magnitude below the concentrations of either sodium or potassium. Therefore, in theory, to generate an action potential you'd require a nearly 0% change in ion concentration. However, what this actually describes is the *net* movement. That is, if the concentration of sodium inside the cell increases by x when sodium channels open, the concentration of K^+ must decrease by no more than $x - 3.1 \times 10^{-7}\text{mM}$ to depolarization the cell by 100mV . Thus, by this logic, x can be nearly any value—and perhaps the change in sodium and potassium is actually quite large? To verify that the general idea of this exercise is true, I simulated an action potential using the Hodgkin-Huxley model to find some approximations of ion currents, and found that the sodium concentration changes by $\approx 0.002\text{mM}$. This is only a small fraction of a percentage of the total concentration, so the principle holds.

11.2 Ion Channels

This section will be filled in better throughout the semester, through more Biochem courses.

11.2.1 Voltage Gated Channels

Voltage Sensing.

You may ask yourself "how does an ion channel know when the voltage is positive or negative?" Structure informs us of almost every puzzle in biology, and this case is no different! Let us consider

³³<https://pubmed.ncbi.nlm.nih.gov/19571202/>

one potassium channel called KvAP. KvAP is hypothesized to be voltage gated due to the presence arginine side chains (as positively charged amino acid)³⁴. Because of the positive charge on arginine, you can imagine that if the outer membrane voltage becomes especially negative, it will pull the arginines outward, almost like opening the lid of the channel.

Some notes:

To clean up later. 1) How membrane capacitance is measured³⁵. Currents are often corrected for by capacitance in order to account for changes in conductance (i.e., channel expression). 2) Gating current refers to the current through a ion channel induced in the channel's opening (and or, while conformational changes are occurring). This sort of thing is frequently measured with channel inhibitors, therefore allowing current through only during these "phase changes." For example, one could: administer tetrodotoxin, and perform a voltage step from $\approx -75\text{mV}$ to 0mV , thus capturing the opening of sodium channels. Two currents will be seen, the capacitance current and the gating current. One can determine the capacitance current of the membrane by performing a voltage step from $\approx -75\text{mV}$ to -100mV . Thus, no voltage gated channels will be opened, but you'd see a current induced by the membrane's capacitance.

11.3 Current Literature

Octopus Sensory Receptors.

Chemotactile receptors (CR) allow cephalopods to taste via touching³⁶. The key question addressed by this paper is how ion channels diverge and become specific to certain functions.

To this point, quite a bit is known about nicotinic acetylcholine receptors in the context of humans. This includes their basic function in neuromuscular junctions, structural information, where acetylcholine binds, etc. However, not much is known about octopus chemotactile receptors, nor how they arose.

Many molecules remain insoluble in the ocean, thereby requiring physical contact to sense them. This diverges from how terrestrial species detect airborne chemicals. It was known that CRs were evolutionarily related to mammalian nicotinic receptors and are both members of the cys loop family of channels, which have a large extracellular domain and underlie fast transmission. Under disruptive selection, signified by the ratio of nonsynonymous to synonymous mutations, these receptors diverge and become specialized for different molecules. Those presented in this paper have highly hydrophobic binding pockets, making them specialized for analyzing greasy materials, namely terpenes. This paper focused specifically on chemotactile receptor for terpenes 1 (CRT1) (which was the best characterized CR to this point) in order to compare it with the $\alpha 7$ nicotinic receptor (which it shared the most sequence homology to).

Their paper used two primary routes of investigation: structural studies and electrochemical studies. Using cryo-EM, it was found that CRT1 has a symmetric, homopentameric structure, (similar to $\alpha 7$ receptors). Interestingly, in both CRT1 and $\alpha 7$ are glutamate residues which are key to their calcium

³⁴<https://www.ncbi.nlm.nih.gov/pmc/articles/PMC1253646/>

³⁵<https://pubmed.ncbi.nlm.nih.gov/21713564/>

³⁶<https://www.nature.com/articles/s41586-023-05822-1>

permeability's, but not their permeability of other ions. Naturally, upon identifying such conserved features, they looked to find different sites in order to address how CRT1 became specialized for ocean life. Before doing so, they applied different terpenes and found that the channel was consistently activated, but not when ACh was applied. Conversely, standard $\alpha 7$ receptors were activated by ACh but none of the terpenes. To identify the binding site of the terpenes, they tested costunolide.

Amazingly, upon structural analysis they found the channel was open but no costunolide was bound—in fact, the detergent they used to extract and purify the protein was bound, called diosgenin. As such, they suspected similar oily compounds could tightly bind to CRT1. This is the same site that ACh would bind to the $\alpha 7$ channel. The binding sites differ in that one loop, the C-loop, is shorter in CRT1, and is missing aromatic and cystine residues. Such residues are needed for ACh binding, and their absence makes the binding site flatter and more hydrophobic.

Given this surprising result with diosgenin, they tested other oily compounds and too found strong responses. In amputated octopus limbs, nerve responses were generated when in contact with such compounds. Octopus limbs have a high degree of autonomy, and react strongly to stimuli even after amputation, including moving physically away from such stimuli.

Bacteria Deliver Channels to Plants.

Bacteria use a type III secretion system, meaning it allows them to insert bacterial proteins into their host. One well conserved effector family is called AvrE, and is associated with 'water soaking' and increased pathogenesis. Water soaking refers to dark, sunken spots often seen on plants where bacteria are multiplying. AvrE family proteins have been challenging to study due to their size and high toxicity—as well as limited sequence similarity to other known proteins.

This work identified AvrE proteins, namely the DspE channel, as folding into a β -barrel, which has a porin-like structure via AlphaFold2 analysis, which was verified through cryo-EM. Prior to this work, nothing was known beyond that these proteins are likely membrane bound. Therefore, their hydrophilic interior and hydrophobic exteriors gave the first indication of pore formation at all.

They determined the channels are permeable to ions and generate currents in either direction, with a reversal potential around -25mV . Notably, canonical inhibitors did not block the channel's permeability, and replacing the extracellular ion compositions did not alter the current noticeably. The reversal potential was mildly affected when Cl^- was removed, suggesting a potential selectivity for anions.

In doing their anion experiments, they noticed oocytes swelling. Expression of AvrE proteins in *Xenopus* oocytes allows for water permeability and oocyte thus swelling, as evidenced by altering the solution's osmolarity. Because the ion's pore is so large (15\AA), it seemed plausible that the channel would be permeable to other molecules larger than water. Indeed, dyes like fluorescein, but not large proteins like GFP, were able to pass through it.

In mutations deleting a large amount of the β -barrel, currents are abolished. Deletion of leucine residues around the base of the channel similarly abolish conductance. Because surface biotinylation did not detect the protein, it is suspected that these residues are necessary for membrane inclusion. Moving forward, they looked for object that might be able to fit into this wide pore. They specifically selected polyamidoamine dendrimers (PAMAM), because their characteristic length can be altered. Indeed, PAMAM G1, which has a length of $\approx 22\text{\AA}$, inhibited DspE 71% and AvrE 93%, as evidenced

by limited membrane current. Baseline swelling was also inhibited, as well as fluorescein uptake.

Inhibition of AvrE was associated with decreased virulence in plants.

Using FRET for VRACs

Here we discuss³⁷. The suprachiasmatic nucleus (SCN), a bilateral nucleus in the hypothalamus, is responsible for maintaining the circadian rhythm. It is known that the SCN produces changes in repeat firing that varies with the time of day. It is thought that subthreshold, leak currents are responsible for changes in firing rate. Research has been done on increased K^+ conductance, but this paper postulates a greater role of subthreshold Na^+ conductance. This role of Na^+ was proposed first in *Drosophila*, so this work helps to verify conservation in mammals. They determined that sodium conductance has a greater role in the daytime than night, and that their affect depends on K^+ currents and their affect on the input resistance of the membrane.

The authors focused on three different neuron-types—NMS, GRP, and VIP-expressing cells. VIP-labeled cells were recorded from via removal and slicing either during the day or night. VIP cells were found to fire more frequently during the day than night, and their R_{in} was higher during the day than night. The depolarization (ΔV) associated with action potentials was similar at night than during the day, though. Interestingly, they found that sodium currents associated with leak channels (i.e., in the presence of TTX) was variable, but consistent across day and night. Though, when Na^+ is removed and replaced with NMDG⁺, the resting membrane voltage was much more hyperpolarized, and this effect was observed to be stronger during the day than night. This led them to conclude Na^+ leak channels are particularly useful in maintaining day time resting membrane voltages³⁸.

In comparing NMS+ and GRP+ cells in the same tests, they found that NMS+ cells show higher firing rate, higher input resistance, and higher resting membrane potential during the day than night. This was not so for GRP+ cells. Na^+ current density was shown to be similar in both the day and night for NMS+ and GRP+ cells, however removing Na^+ current demonstrated a greater hyperpolarizing shift in the daytime than nighttime for both cell types. This, to them, suggested that Na^+ leak currents too maintain a higher resting voltage during the day than night across these cells types.

Ryanodine in Chemobrain

Here we discuss³⁹. Chemotherapy can lead to something called “chemobrain”—a cognitive dysfunction in cancer treatment that is currently not understood. PET and MRI scans have shown structural and functional changes in the brain associated with prolonged treatment. This work determined that improper modifications to RyR2 channels leads to leakiness, thereby inducing dysfunction in metabolic signaling paths, leading to cognitive decline.

RyR channels are the largest known ion channels—on the order of 5,000 amino acids! RyR channels have 3 isoforms, with RyR2 being the most common in the brain. Using a mouse breast cancer model, their initial tests showed that treatment with doxorubicin leads to increased RyR channel opening time and open probability from signal unit recordings. They developed an orally admissible drug called S107 that is said to stabilize RyR channels. Use of this drug in conjunction with doxorubicin

³⁷<https://pubmed.ncbi.nlm.nih.gov/37339878/>

³⁸Is this surprising, or is this something you learn in introductory neuroscience? That’s the question.

³⁹<https://pubmed.ncbi.nlm.nih.gov/37756377/>

results in WT levels of openness. Via PET scans, they determined a reduction in glucose metabolism in doxorubicin treated mice, which was recovered in S107 treated mice. However, it's worth noting that these phenotypes seem quite weak (i.e., on the order of a couple percent difference). Similar effects were observed with a second chemotherapeutic treatment course called MTX + 5-FU.

RyR immunoprecipitated from whole brain lysates were compared for post-translational modifications. In order of their Figure, RyR2 shows increased phosphorylation, oxidation, nitrosylation, and decreased calstabin-2 binding. Calstabin binding is known to stabilize RyR channel structure, and treatment of with S107 recovered this binding, but none of the other post-translational modifications. Through behavioral tests, like the Morris water maze, they found clear cognitive impairments in doxorubicin treated mice that were rescued with S107. In the novel object discrimination test, S107 actually seemed to improve scores above WT.

11.3.1 Piezo

Piezo channels are near and dear to my heart, as we study them extensively. Piezo channels have been implicated in nearly every cell of various organisms. There's no shortage of mechanisms hinging on Piezo channels, including neuron regeneration. Here, I'll discuss some current literature pertaining to Piezo channels.

Piezo in B Cells.

Adding yet another function to Piezo, they play a crucial role in B cell responses⁴⁰. B cells are activated when antigens bind to B cell receptors (BCRs), primarily through surface expression via antigen-presenting cells (APCs). This induces BCR clustering, phosphorylation, and formation of a signalosome. Importantly, such responses involve significant membrane and matrix reorganization. This is marked by the formation of an "immune synapse," where BCRs cluster with other important membrane proteins at the interface of the APC. Because B cells seem preferentially activated by antigens on the surface of cells, rather than soluble antigens, it is plausible that some physical interaction is beneficial to B cell activation.

Some background work showed B cells express Piezo1 mRNA, but not Piezo2 mRNA. To explore a potential Piezo1 role, they first physically poked B cells using a micropipette and saw, via a calcium indicator, that Ca^{2+} influx occurs. In administering the Piezo1 inhibitor GsMTx4, such Ca^{2+} influx was abolished. They also imaged B cells laid out on a glass sheet. When flattening out on the glass, calcium influx occurred. To test if this was Piezo-dependent, they applied oligomerization-blocker 1 (OB1), which is said to block Piezo channels. In this case, again calcium influx and cell flattening was decreased. It's not clear to me why they used two different Piezo blockers for these experiments. Using an interesting tool called Flipper-TR, they were able to fluorescently measure membrane tension, and found that indeed tension increases when B cells flatten on glass.

To test if Piezo is required for B cell response, they bound anti-Ig to a polymer substrate and found that BCRs cluster around the interface between the substrate and the B cell. This clustering was abolished in the presence of the OB1 Piezo inhibitor. This same result was observed when using RNAi knockdown of Piezo channels.

⁴⁰<https://www.science.org/doi/10.1126/scisignal.abq5096>

Chapter 12

Muscles

A few things: First, as it turns out, there is some incorrect info in the Silverthorn book [i.e., Dr. Delp comments that skeletal muscles have a force-stretch graph similar to cardiac muscle], especially pertaining to muscle physics. Second, it would be wise to include some more cardiac info since loss of MAP is a key cause of death after SCI.

A large part of this information comes from Dee Silverthorn's *Human Physiology* textbook—arguably the best textbook of all time.

12.1 Skeletal Muscle

12.1.1 A Cellular Level

Structure.

Skeletal muscles are composed of muscle fibers, which are composed of myofibrils. Muscles use a silly nomenclature, in which “sarco” is added to words. For example, the whole structure sits within the sarcoplasm (cytoplasm), fibers are intertwined with the the sarcoplasmic reticulum (equivalent to endoplasmic reticulum) and surrounded by the sarcolemma (equivalent to the cell membrane). An individual myofibril is made up of overlapping actin and myosin segments, held together, to some degree, by titin. The myosin heads are the canonical structure you imagine, which bud off of the end of a chain like leaves on a branch and bind to actin. Undeniably, the most uninteresting part of muscle physiology is as follows: The “centerline” of the myosin networks is called the M line, while the “centerline” of the actin network is called a Z disk. Titin branches off from the Z disks to bind to the ends of myosin chains, providing both some elasticity and support for myosin. Actin chains are centered around a line of nebulin, which too provides structural support and organization. The I band is considered to be the unbound part of the actin structure, centered around the Z disks. The H zone is the unbound part of the myosin structure, centered around the M line. The A band is the entire length of the myosin fibers, thereby encapsulating both the bound part of the actin-myosin complex and the H zone, meaning it too is centered around the M line. Therefore, when contraction occurs, the size of the H zone and I band decreases, while the size of the A band stays the same.

Contraction-relaxation.

Myosin heads desire to bind to actin, but are blocked by tropomyosin. Ca^{2+} can bind to troponin, bound to tropomyosin, to cause conformational changes resulting in the exposure of the actin to the

myosin heads. In doing so, binding can occur, followed by myosin's power stroke. The energy for the stroke comes from hydrolyzing ATP, which had already occurred by the time myosin attached to the actin. The powerstroke allows the release of the ADP and P_i . ATP then can bind to the empty active site of myosin, which causes the release of the head and prepares it for another cycle. Notably, when ATP does not bind to myosin, the muscle will be stuck in the rigor state.

In skeletal muscles, the source of Ca^{2+} is a combination of the extracellular Ca^{2+} flowing inward, and further release from the sarcoplasmic reticulum. The story goes as follows: a motor neuron releases acetylcholine onto the motor end plate (an area which has a high density of sodium channels). This causes a depolarization, which propagates down the muscle fiber. Structures called T-tubules sink lower into the tissue, allowing for more direct access to the inner processes (visually, these look similar to gyri in the brain or the crypts of the intestinal wall). The T-tubules are lined with dihydropyridine (DHP) channels, an L-type VGCC (specifically $Ca_v1.1$). DHP and ryanodine receptors (RyR) can be mechanically coupled, where influx of Ca^{2+} through DHP mechanically opens RyR channels of the sarcoplasmic reticulum (a large store of Ca^{2+}). The free calcium is lowered through things like active pumping out of the sarcoplasm.

A steady supply of ATP is needed to maintain pumping, and it is said that at any given time, there is 8 or so twitches worth of ATP within the muscle fiber. Therefore, frequent production and alternate stores are required for continuous movement. One such storage is phosphocreatine, whose phosphate group can be quickly transferred to ADP through creatine kinase. Muscles therefore contain high levels of this enzyme, and **testing for it in the bloodstream can be a good proxy for muscle damage**.

Notably, it is very difficult to fully deplete a muscle of its ATP. Other forms of fatigue begin before this can possibly occur, which include CNS or PNS feedback. An example of this may be that acetylcholine is not synthesized fast enough to continually stimulate muscle fibers. Continual stimulation of muscle fibers, beyond what is allowable under normal conditions, **will fully deplete ATP levels and therefore cause damage to muscles**. Another consideration is the continuous use of ATP may result in P_i buildup in the sarcoplasm, making release of $ADP + P_i$ from myosin less likely to occur. Too, this opens the possibility of calcium phosphate forming, which can be quite damaging if it crystallizes further. There are also ion concentration changes to consider, and continued stimulation can result in tetanus.

12.1.2 Disorders Digression

There are many ways one can lose control of their muscles. Nerve damage, for example, will halt the release of acetylcholine onto the motor plate. In a similar manner, botulism is a result of the botulinum toxin blocking release of acetylcholine, resembling the effect of nerve damage. In McArdle's disease, muscles simply cannot convert glycogen to glucose-6-phosphate, causing the energy supply to be limited.

Muscular Dystrophy.

Muscular dystrophy is an umbrella term⁴¹. There are more than 30 types, and in modern times the lines between muscular dystrophy and other disorders is more blurred. Duchenne muscular dystrophy (DMD) is the canonical type, which presents in children. Early signs include weakness in the shoulders

⁴¹https://www.youtube.com/watch?v=S6gPsYVmIEI&ab_channel=MayoClinic

or hips—i.e., the larger muscles. In DMD, the protein dystrophin is absent, which would normally attach actin to the cell membrane. This can result in membrane permeability, calcium influx, and thus activation of digestive enzymes that breakdown muscle fibers.

Treatment of muscular dystrophy is centered on symptom management. For DMD, steroid usage seems to help. It is thought that muscle breakdown leads to immune responses, which can be aided by steroids. But, there is no cure, and eventually these steroids become less effective.

Multiple Sclerosis.

Multiple sclerosis (MS) is a CNS disorder, thought to be autoimmune in origin, and resulting in degradation of the myelin. It can be identified by plaques, and or, scar-looking lesions in the brain.

MS is rapidly developing. Over the course of days or weeks, one might slowly find numbness in a limb. Some light, tingling feeling is a typical first symptom. A clinician would follow-up with an MRI of the brain and spinal cord, looking for lesions within the myelin. The scarred regions are characterized in 4 ways: (1) an *active lesion*, which is acute and marked by inflammation and continual de- and remyelination, (2) an *inactive lesion*, which is chronic and marked by demyelination and limited inflammation, (3) a *mixed lesion*, where the center is primarily demyelinated, but the borders include microglia aiding in remyelination, and (4) a *remyelinated lesion* where a significant degree of healing has occurred.

The furthest downstream causes are classified as (1) a reduction in myelin during the active lesion, (2) total oligodendrocyte loss during the mixed and inactive lesions, and (3) poor differentiation of progenitor cells into remyelinating oligodendrocytes.

12.2 Smooth Muscle

Smooth muscle is much more variable than skeletal, differing by location, contraction pattern, required inputs, and structure.

12.2.1 A Cellular Level

Structure.

Smooth muscle is not considered to have sarcomeres, despite it having the same basic structural components of skeletal muscles. Smooth muscle contains much more actin than does skeletal muscle, and notably does not contain troponin like skeletal muscle does. Smooth muscle networks are connected through intermediate filaments, which usually attach to dense bodies within the cytoplasm. Actin also attaches to dense bodies, maintaining the actin-myosin network within the cell as well. Smooth muscles do not have T-tubules like skeletal muscles. A comparable structure may be caveolae, which do indent into the membrane and seem spatially associated with the sarcoplasmic reticulum. The autonomic nervous system stimulates fibers through neurotransmitter release from varicosities, or bulbous stores of the chemical. The neurons may innervate the muscle fibers, allowing multiple muscle cells to be stimulated at once, or they may be released to a few fibers, which are connected through gap junctions and stimulate the nearby ones, causing a propagating wave to stimulate others. The first case describes a multi-subunit muscle, and the second a single subunit.

Contraction-Relaxation.

Initiation of contraction begins the same as skeletal muscle, in that calcium enters and the concentration is further driven up by sarcoplasmic calcium release. Though, in this case Ca^{2+} may enter either through gap junctions or membrane ion channels. As such, there are many more modes of entry than in skeletal muscle. For example, voltage-gated Ca^{2+} channels may open, but there are also ligand gated channels or stretch-activated channels, adding extra layers of possible regulation. Intracellular differences arise beginning from release from the SR. Firstly, it is no longer a mechanically gated RyR channel which allows its release. The release mechanism is now Ca^{2+} activated RyR release (commonly called Ca^{2+} -induced- Ca^{2+} -release (CICR)), and the IP_3 path. GPCRs activate phospholipase C, driving IP_3 production which binds to SR channels and causes them to open. The IP_3 path is usually considered the greatest way to drive up intracellular Ca^{2+} (or at least, that is what computational biologists seem to think). When Ca^{2+} is available, it binds to calmodulin (CaM), which then binds to the myosin light chain kinase (MLCK). MLCK phosphorylates myosin to increase myosin ATPase activity. Importantly, once contraction occurs, it stays stiff until released by a different mechanism. Because after contraction, no work is being done in the stiff state, smooth muscle is able to stay contracted for long periods. This explains why sphincters in the body are able to stay closed all the time, while one's bicep fatigues after carrying groceries for just a little while. Relaxation begins when Ca^{2+} is either pumped out of the cell through a Ca^{2+} ATPase pump, or sodium transporter. This causes CaM to unbind, myosin light chain phosphatase (MLCP) to dephosphorylate myosin, and the myosin heads to release from actin. Interestingly, diacylglycerol (DAG), another product of the IP_3 path, inhibits MLCP and thereby enhances muscle contraction.

The calcium stored in the SR is maintained in a number of ways. One example being the protein STIM1 responding to lower Ca^{2+} levels within it, moving toward the cell membrane, and activating store operated Ca^{2+} channels, such as Orai1.

12.3 Cardiac Muscle

12.3.1 A Cellular Level

Structure.

Cardiac cells contain sarcomeres, but the fibers themselves are smaller and often mono-nucleated. Cell edges are called *intercalated disks*, held together by desmosomes and permeated by gap junctions. The role of gap junctions is obvious but essential, and key to the rhythmic firing of the heart. Despite not requiring nervous system input, cardiac muscles have large T-tubules, and a significant amount of mitochondria.

Contraction-Relaxation.

Initiation of cardiac muscle contraction requires extracellular calcium, and generation can be graded. The entrance of Ca^{2+} powers the opening of non-mechanical RyR channels, as a method of CICR. Because of this, the sarcoplasmic reticulum is smaller in the myocardium, because some of the Ca^{2+} required for contraction comes from extracellular entry in about a 10:1 ratio of sarcoplasmic reticulum:extracellular origin. Ca^{2+} is removed using the Na^+ - Ca^{2+} exchanger (NCX).

The electrophysiological profile is marked by Na^+ entry but maintained by Ca^{2+} in a plateau phase.

The fall occurs via K^+ entry. The refractory period is long due to this plateau phase, which prevents Na^+ channels from resetting.

Pacemakers.

Hyperpolarization cyclic nucleotide (HCN) gated channels induce an inward hyperpolarization (I_h , or I_f) current. Within the hyperpolarization range, HCN channels open and cause steady depolarization rhythmically. HCN channels are typically permeable to multiple cations, and in this case Na^+ is the biggest player. When the membrane potential is high enough, VGCCs will open and cause depolarization required to propagate the signal between myocytes. At peak, slow opening K^+ channels open and repolarize the membrane. Notably, voltage gated Na channels do not play a role in myocyte depolarization.

Expectedly, as β -blockers will inhibit a rise in cAMP, HCN channels will be less active. This decreases heart rate, among other things.

Chapter 13

Sensory Processing

Somatic senses are picked up by receptors on *primary sensory neurons*, whose cell bodies reside in the dorsal root ganglia and project to CNS interneurons. Such interneurons are considered *secondary sensory neurons* and their location depends on function. Fast traveling senses, like proprioception, are sent to the medulla before reaching interneurons (cross the body's midline in the brain), while slower traveling senses, like temperature, synapse onto interneurons upon entering the spinal cord (immediately crossing the midline). Neurons of the thalamus are considered *tertiary sensory neurons* and project to the somatosensory cortex.

Convergence and Lateral Inhibition.

Sensory neurons have some range of stimuli that will activate it. The easiest examples are touch receptors. That is, individual sensory neurons cover some range on your skin. However, many primary sensory neurons may converge onto a single secondary sensory neuron. Therefore, when multiple stimuli are initiated within this range, it is perceived as one touch (because only a single downstream neuron, the secondary sensory neuron, is activated by it, despite their being multiple signals inputted). A high degree of convergence (i.e., many primary neurons synapsing onto a single secondary neuron) means there is a wide receptive field.

Lateral inhibition is when a sensory neuron becomes activated (usually a secondary sensory neuron) and inhibits the surrounding neurons from transmitting signals. That is, imagine a pin prick: the neurons at the center of the pin prick inhibit the response of the surrounding neurons, thereby allowing your body to precisely locate this fine stimuli. This helps discriminate between stimuli even better, as well as in precise perception and edge detection of stimuli.

Adaptation and Frequency Encoding.

Adaptation refers to how a signal alters in response to a stimuli. Tonic and phasic receptors differ in how they respond to stimuli. Tonic sensory neurons are those that continually fire in response to some stimuli. Phasic are those that respond when the stimuli changes (a phase change). Phasic receptors are therefore considered fast adapting.

Frequency coding is the conversion of some graded potential into some corresponding frequency of action potential firing. That is, a long, strong stimuli manifests as many action potentials, resulting in heightened neurotransmitter release. Conversely, a quick, weak stimuli may not initiate an action

potential at all, and if it does it will be only one, resulting in minimal neurotransmitter release. In a sense, this helps digitize neural signals (i.e., they become binary 1s or 0s by neurons either firing or not firing).

13.1 Various Senses

13.1.1 Touch

13.1.2 Temperature

13.1.3 Pain

Nociceptive neurons respond to a variety of stimuli that can cause damage to cells. Afferent pain signals are carried either by myelinated $A\delta$ and unmyelinated C fibers. $A\delta$ carried pain is faster and perceived as sharp, local pain. C fiber carried pain is less sharp and less localized.

Transient receptor potential (TRP) channels are the most canonical class of ion channels, and are responsible for a great deal of pain sensation. Vanilloid ($TRPV_1$) channels respond to heat, while TRPM8 respond to cold. An immediate response to cell damage is lysing, causing marked increase in K^+ in the surrounding areas. Other released chemicals include histamine and prostaglandins. Upon activation, nociceptive neurons can trigger two responses. The first being reflexes that are integrated at the spinal cord, and the second being somatosensory cortex integration⁴².

As an aside, the idea of referred pain is: pain is perceived as being from different body parts because they share the same neural paths, but does not necessarily originate from that part of the body. The canonical example is a heart attack perceived as pain in the left arm.

13.1.4 Olfaction

Information is transmitted directly from the olfactory epithelium to your brain. This occurs first through the olfactory bulb (where secondary sensory neurons are present), to the olfactory tract, and to the olfactory cortex.

Primary olfactory neurons contain GPCRs (one type per neuron). In total there are ≈ 350 olfactory GPCRs (350 per parent, which theoretically means up to 700 total, if you assume mutations cause functional divergence). As you should know, GPCRs use secondary messengers like cAMP. cAMP can be used to open ion channels and thus allow for depolarization. Different primary sensory neurons, which express the same GPCR, synapse onto the same secondary sensory neuron in the olfactory bulb. The way that different chemicals bind to different GPCRs generates different arrangements of neuron firing, so they can be combinatorically encoded.

13.1.5 Ears in Hearing and More

The Auditory Path.

The outside of the ear is called the pinna, and is helpful in capturing sound. Sound travels down the ear canal until it reaches the eardrum (tympanic membrane). Beyond the tympanic membrane

⁴²This ended up being much less interesting to write than I thought it would be.

is considered the middle ear, where the malleus (hammer) vibrates the incus (anvil), which then vibrates the stapes (stirrup). These three bones, called ossicles, help amplify sound / vibrations. This middle ear area is connected to the throat through the Eustachian tube (which allows pressure to be maintained between the spaces of the ear). The stapes is connected to the oval window, which marks the beginning of the inner ear and or cochlea.

The cochlea has 3 layers: the vestibular duct, the cochlear duct, and the tympanic duct. The oval window interfaces with the vestibular duct. Vibrations propagate through the cochlea and cause movement in the basilar membrane (between the cochlear and tympanic ducts). The vibrations are dissipated through the tympanic duct, which connects to the round window. A key component of this system is that the cochlear duct houses endolymph, while the other two house perilymph. Perilymph is standard, and has a composition similar to most interstitial / extracellular fluid. Endolymph's composition is more similar to the intracellular fluid. Finally, at the apex of the cochlea is what's called the helicotrema. On a microscale, the cochlear duct houses the organ of corti, which is where the cells that detect sound are housed. Between the tectorial (top) and the basilar (bottom) membranes are layers of hair cells which are used to sense sound by the movement of such membranes.

Sound travels down the ear canal, vibrate the tympanic membrane, and moves the ossicles. The ossicles amplify sound onto the oval window, which transmits it into the cochlea and activate hair cells. Inner hair cells, of which there are $\approx 3,500$, transmit information to the brain by depolarizing nearby sensory neurons. Outer hair cells are helpful in amplifying the response of inner hair cells by physically magnifying the membrane displacement. There are 3 rows of outer hair cells, and there is $\approx 3,500$ outer hair cells per row too—so there's about $3\times$ as many outer haircells as there are inner.

As the basilar membrane moves up or down, hair cells move and deflect. Because they're tied to the tectorial membrane above, their movement causes pulling on the tips of hair cells, which opens mechanically gated ion channels. When deflected in a way that increases the angle between the stereocilia and the cells (i.e., generating more force on the mechanically gated channels), they open and cause the cell to depolarize. Conversely, when the angle lessens (lessening the force on mechanically gated channels), they hyperpolarize. Stereocilia are linked together via tip-links, allowing for the pulling of one to pull, and thereby open, many others. Recall that the endolymph is high in potassium, so it is potassium that enters and causes depolarization.

We can hear a range from about 20 to 20,000Hz, depending on where the vibrations occur in our ear. This is called tonotopic arrangement⁴³. The innermost segment of the cochlea (near the apex / helicotrema) senses longer wavelengths, while the outermost part senses higher frequencies. The basilar membrane is also much thinner and wider closer toward the helicotrema, while it is much thicker and narrower closer to the entrance. This allows certain frequencies to preferentially excited different segments along the cochlea, and is key to our perception of sound. Note that this scale is not linear—it is logarithmic (think of decibels).

Balance and Such.

recall that it is indeed endolymph in this system, as it connects directly to the cochlear duct. They detect rotational acceleration (form equals function) via ampulae, which contain cristae, which contain

⁴³There's a super great lecture by Dr. Ian Shipsey. He went deaf, got a cochlear implant, and had his hearing restored. He discusses the science and limitations of cochlear implants. Link: https://www.youtube.com/watch?v=aecxK2gFBRY&ab_channel=OxfordUniversityPhysicsSociety

cupula. They detect rotational acceleration via deflection of the cupula, which contains hair cells and thus deflect and respond similar to inner / out cells.

The utricle and saccule contain macula, which detect linear acceleration and gravity. They do so via these little crystal structures called otoliths, which are slightly denser than the endolymph and move around in response to motion. Their sinking or deflection of the membrane is particularly helpful in detecting things like gravity.

Many years ago, NASA sought out deaf employees for their early space programs—specifically looking for those with damaged vestibular systems. Those selected were typically deaf from childhood spinal meningitis, which left their hair cells damaged. Therefore, the hair cells in the vestibular systems made them incapable of feeling motion sickness. This allowed scientists to test the effects of high g on their bodies, without them feeling sick. They are colloquially known as the Deaf 11.

13.1.6 Vision

The cornea is the outermost layer, the pupil changes in size to let in more or less light, the iris is the muscle which opens and closes the pupil, the lens is adjusted in order to focus light onto the back of the eye, the retina is at the back of the eye and where light rays hit, the macula / fovea is where the highest density of cones are. The aqueous humor is a fluid surrounding the lens, and which provides nutrients to the lens (because the lens does not have any blood vessels).

The right visual field of both eyes going to the left visual cortex, and the opposite for the left visual field. This information is transmitted down the optic nerves, intersects at the optic chiasm, continues down the optic tracts, is trafficked through the lateral geniculate nucleus [probably don't need to know that] of the thalamus, and onto the visual cortex in the occipital lobe.

As briefly mentioned earlier, the macula is the central region where cones are, and at the center of that is the fovea. Rods are more densely populated in the outer regions of the retina. Where the optic nerve leaves the retina, there is a blind spot. This is intuitive, because there cannot be rods / cones right at the “exit” of the eye (recall that the photoreceptors are technically beneath the nerves). At the kind of “base” of the retina, i.e., the innermost layer, is the pigment epithelium. This is useful in absorbing light to prevent scattering and in providing nutrients to the photoreceptors. The next layer is the photoreceptors, i.e., the rods and cones (which differ in both structure and function—rods literally look like rods, and cones literally look like cones). Photoreceptors transmit to interneurons (bipolar cells), which then transmit to retinal ganglion cells. Such transmission is under considerable control by horizontal cells (which are at the synaptic junction between photoreceptors and bipolar cells) and amacrine cells (at the junction between bipolar and retinal ganglia). Such cells are helpful in lateral inhibition.

To understand how photoreceptors operate, first consider rods at rest: cyclic guanine monophosphate (cGMP) levels are high. cGMP binds to cyclic-nucleotide gated (CNG) channels, allowing for influx of positive ions, maintaining a relatively high membrane potential. This leads to the tonic release of neurotransmitters. The structure used to sense light is called rhodopsin, a GPCR in the photoreceptor membrane. It is composed of opsin, a protein, and retinal, a compound derived from Vitamin A. Retinal is able to change conformations (from *cis* to *trans*) upon being hit by light, which alters opsin's structure too. When “activated by light,” opsin decreases production of cGMP through the g-protein

transducin. The key oddity here is that neurotransmitters are released in the absence of light, but not when light is present. The difference between rods and cones, in this regard, is that cones express different proteins (pigments) other than rhodopsin that respond preferentially to different wavelengths of light.

Humans can detect a very small amount of photons and so too can we in bright light. This is achieved in a number of ways, including that the pupil can adapt (let in more or less light), we can rely more so on cones (high light levels) or on rods (low light levels). Rods in particular can converge on a single retinal ganglion, which is helpful in “amplifying” the response to a light stimuli. Further aiding in our visual perception is on and off center retinal ganglia, two modes of detecting light (or the absence of it). On center describes when light levels are high at some central point, so on center ganglia are active, while off center are inhibited. Off center describes when surrounding light levels are high, but not necessarily at the center. Thus, on center ganglia are inhibited, while off center ganglia are active. The difference lies in how they respond to the neurotransmitter released by photoreceptors (glutamate). Because photoreceptors are depolarized in the absence of light, these off center ganglia fire in response to glutamate, while on center ganglia are inhibited by glutamate. Thus, when a photoreceptor becomes hyperpolarized in the presence of light, on center ganglia can be active due to loss of glutamate, and off center become inactive for the same reason. Off center cells are, in a sense, detecting darkness, and or the lack of stimuli. For example, walking through a doorway into a dark room from a well lit room. You can clearly detect that the upcoming room is dark, because off center ganglia are active.

Chapter 14

The Central Nervous System

The Meninges.

The layers of the meninges are: the dura mater, the subdural space, the arachnoid membrane, the subarachnoid space, and the pia mater, which all sits beneath the skull. The dura mater is the thickest of the three. The subarachnoid space has a spongy texture and houses the flowing cerebrospinal fluid. The bottom layer, and the thinnest, is the pia mater. The pia mater is surprisingly tough—if you’ve ever done brain dissections before, it feels similar to a thin film around the brain. A key role of the meninges is to cushion the brain.

READ THIS: https://journals.lww.com/onsonline/fulltext/2016/06000/anatomy_of_the_spinal_meninges.10.aspx

14.1 Spinal Cord General Structure

A cross section of the spinal cord would reveal meninges just like the brain and skull; an outer layer of dura, then arachnoid, and finally pia mater. Too, there is an outer layer of white matter followed by a grey matter interior, which is centered around a “central canal.” The spinal cord has 33 vertebrae, beginning with cervical (C₁ to C₇), then thoracic (T₁ to T₁₂), then lumbar (L₁ to L₅), then sacral (S₁ to S₅), and finally one coccyx (Co₁ to Co₄). The sacral, and especially the coccygeal, vertebrae are fused, so you may see them depicted as a single unit. Adding slightly to the confusion is that there are only 31 pairs of spinal nerves. These are C₁ - C₈, T₁ - T₁₂, L₁ - L₅, S₁ - S₅, and Co₁. **Note: The difference in the nerve location and vertebrae labels is actually quite important, as it is not always that a fracture at some vertebrae leads to nerve damage at the same site**—this is expanded on in later chapters. The spinal nerves exit the spinal cord on either side, i.e., either dorsal or ventral roots. Dorsal entry neurons carry sensory information to the CNS, while ventral exit zones carry information from the CNS to the muscles. Though, importantly, their axons can not necessarily be found on either side, this will depend on where crossing over occurs. The section of grey matter which connects to the dorsal root is called the dorsal horn, and the same is true for the ventral horn. The lateral horn is in between the dorsal and ventral horns.

Note to self: It might be fun to add a more detailed breakdown at some point, such as the general arrangement of all the nuclei in the spinal cord.

Another note to self: It would be good to integrate more clinical outcomes into this. For example, what happens in the case of SCI at various vertebrae, or in vagotomy, etc.

14.2 Autonomic Nervous System

Pathways of the autonomic nervous system require two neurons, one that originates in the CNS and terminates at a ganglion, and a post-ganglionic neuron which terminates at the tissue of interest. While the circuit is often considered to have only two neurons, in fact many pre-ganglionic neurons synapse onto many post-ganglionic neurons, which means one neuron can affect many target tissues. Adding to this is the mode of release. The connection between neuron and target tissue is called the *neuroeffector junction*. At this junction, transmitters are secreted indirectly from bulbous varicosities into the interstitial space, meaning neurotransmitters can diffuse over a larger area. Fascinatingly, these neurotransmitters are actually often synthesized within the axon / varicosities of neurons.

14.2.1 Sympathetic Nervous System

Pre-ganglionic neurons of the sympathetic nervous system originate in the hypothalamus or reticular formation and extend down to the mid-sections of the spinal cord, from neuron pairs T₁ to L₂. Sympathetic ganglia are directly beside the spinal cord in a long chain (often called the sympathetic chain). Generally speaking, neurons closer to the T₁ section correspond to organs higher in the body, such as the heart or lungs, while neurons closer to the L₂ section corresponds to those lower in the body, like one's reproductive organs⁴⁴.

Pre-ganglionic neurons release acetylcholine onto nicotinic receptors, and post-ganglionic neurons release norepinephrine onto adrenergic receptors. As all adrenergic receptors are GPCRs, their cellular response will be slower than ion channel transmission and occur at the protein-level primarily. Too, they will occur through secondary messenger, for example through the IP₃ path or cAMP. Norepinephrine is a tyrosine derivative and, like other catecholamines, can be broken down either by monoamine oxidase (MOA) in the neuron's mitochondria, requiring re-uptake, or in the liver by catechol-o-methyltransferase (COMT).

Dysregulation of the sympathetic nervous system most often manifests as cardiovascular pathologies, such as low blood pressure. Though, incontinence or impotence may also occur. On a cellular level, a process called *denervation hypersensitivity* may also occur, where in response to decreased sympathetic neurotransmitters, the body increases expression adrenergic receptors. This is easily measured as increased response from small doses of norepinephrine.

Adrenal Medulla Digression.

It's worth noting that the adrenal medulla secretes epinephrine in a hormone-like manner. However, the adrenal medulla is often considered a collection of pre-ganglionic neurons, meaning epinephrine acts globally like a hormone, but is also a neurotransmitter.

Let us look at the different adrenergic receptors⁴⁵:

⁴⁴Memorizing which nerves respond to which segments is likely not a good use of your time at this stage..., although it might have some clinical use to know which organs may be affected after SCI.

⁴⁵This is ripped directly from Silverthorn.

Adrenergic Receptors			
Receptor	Location	Sensitivity	Effect
α_1	Most tissues	NE > E	Increase Ca^{2+}
α_2	Gut and pancreas	NE > E	Decrease cAMP
β_1	Heart and kidney	NE = E	Increase cAMP
β_2	Select smooth muscle	NE < E	Increase cAMP
β_3	Adipose	NE > E	Increase cAMP

14.2.2 Parasympathetic Nervous System

Parasympathetic neurons originate from the uppermost and lowermost sections of the spinal cord, either leaving directly from the cranial nerves or from the S₂ to S₄ nerves. Ganglia in the parasympathetic nervous system are close to the target tissue, meaning post-ganglionic neurons are very short compared to the pre-ganglionic ones. One of the key paths being from the vagus nerve (a cranial nerve), which carries the majority of parasympathetic signals to organs including the heart, lungs, liver, stomach, intestines, and pancreas. Like the sympathetic nervous system, pre-ganglionic neurons release acetylcholine onto nicotinic receptors. Notably, parasympathetic post-ganglionic neurons also secrete acetylcholine, but onto muscarinic receptors instead.

Cholinergic Receptors		
Receptor	Location	Effect
N _N	Postganglionic neurons	Opens cation channels
N _M	Skeletal muscle	Opens cation channels
M ₁ , M ₃ , M ₅	Target tissues	Increase Ca^{2+}
M ₂ , M ₄	Target tissues	Decrease cAMP, open K ⁺ channels

Exceptions.

There are some exceptions to these rules, such as some sympathetic postganglionic neurons that terminate on sweat glands secrete norepinephrine rather than acetylcholine. These are called “sympathetic cholinergic neurons.” There are also neurons which secrete none of these, are called “nonadrenergic, noncholinergic neurons.” There are also neurons which secrete multiple types of neurotransmitters.

14.3 Somatic Nervous System

The somatic motor division is exclusively excitatory, and neurons project from the CNS all the way to muscles. Inhibition can occur at the neuronal level (i.e., motor neurons are inhibited) but not at the muscle level. Cell bodies of motor neurons are either within the ventral horn of the spinal cord or within the brain. Close to the muscle itself, the axons branch and connect to the muscle at the neuromuscular junction (NMJ), which includes both the target muscle and Schwann cell projections. The “synapse” equivalent is called the *motor end plate*, which is an area on the muscle with a high density of nicotinic receptors. The ECM contains acetylcholinesterase, responsible for breaking down acetylcholine. Notably, the nicotinic receptors on muscle cells are considered N_M, a slightly different

version than is found on neurons (N_N). This difference has proven to be curical in examples such as α -bungarotoxin, which binds only to N_M ⁴⁶.

14.4 Acetylcholine, Nicotinic Receptors, and Muscarinic Receptors

Acetylcholine (which I'll call ACh for this section) is unquestionably one of the most important molecules in the body. It is sythesized from choline (a hydroxyl azanium) and acetyl-CoA. Typical usage goes as follows: ACh is released from vesicles and binds to cholinergic receptors. Upon unbinding, acetylcholinesterase (AChE) breaks it down into acetate and choline. Choline is brought back into the pre-synaptic neuron through sodium cotransporters so that it may be reused. It is then re-combined with acetyl-CoA and repackaged and vesicles.

Funnily enough, nicotinic receptors (nAChRs) have been described as the most well understood membrane receptor⁴⁷. Nicotinic receptors are fast opening non-specific cationic channels. They are expressed throughout much of the major structures in the brain, peripheral nervous system, and skeletal muscle. As such, drugs targeting these receptors are of considerable interest in many neurological disorders. The binding site for ACh is composed of aromatic amino acids, namely W and Y. This paper describes continual exposure to drugs treating nAChRs as causing their eventual desensitization, while exposure to nicotine increases their expression greatly.

Both of these are of key interest in treating Alzheimer's disease, as loss of cholinergic synapses is one of its features (including significant reduction of both muscarinic and nicotinic receptors). Interestingly, Alzheimer's shows varying loss of nicotinic receptor subtypes across the brain. There is no shortage of drugs currently in development for reversing this.

Myasthena Gravis Digression.

Myasthena Gravis, an autoimmune disorder, is an example of an actylcholine dysregulation caused muscle disorder. As a digression within a digression, autoimmune disorders most often target endocrine organs, and the belief is that they are to protect against mutations causing hypersecretion⁴⁸. Upon first glance, you may think that Myasthena Gravis evades this generality, but in fact it does not, as it is well associated with patients that dually have a thymoma (tumor of the thymus). Immune cells begin attacking cells with ACh recepetors, tagging them with antibodies. Therefore, Myasthena Gravis presents itself usually in the weaker muscles, such as those that control the eyes, as they have less ACh receptors and therefore a diminished response to signals. Thus, patients may have drooped eyelids (ptosis), double vision (diplopia), or trouble following moving objects with their eyes. The disease worsens with increased activity, as this causes more antibodies to be released onto ACh receptors—but improves on rest. Fascinatingly, men and women “get” the disease at different times (women typically under 40, while men over 60).

Antibodies may also target other genes (such as MUSK or LRP4) which are involved in ACh receptor localization, or other forms of regulation.

⁴⁶Dee Silverthorn quite possibly wrote the greatest textbook known to humanity, didn't she?

⁴⁷<https://www.nature.com/articles/nrd2927>

⁴⁸[https://www.cell.com/immunity/pdf/S1074-7613\(20\)30180-1.pdf](https://www.cell.com/immunity/pdf/S1074-7613(20)30180-1.pdf)

14.5 Cerebrospinal Fluid

14.5.1 Structure Overview

Cerebrospinal fluid is derived from the choroid plexus, which exists in two main places in the brain (toward the center of the brain in and in the brainstem) along the ventricles. The ventricles, importantly, is derived from the hollow space of the neural tube. The choroid plexus is derived from ependymal cells. It is composed primarily of transport epithelium with many capillaries, which should be unsurprising since a key role it has is to transport ions, which draws out fluid into in the brain / spinal cord. After being secreted into ventricles, cerebrospinal fluid (CSF) flows into the subarachnoid space and eventually out of the arachnoid villi into the venous sinus. CSF is composed similar to the extracellular space. When CSF flow is obstructed, it can cause hydrocephalus.

When patients have hydrocephalus, the surgical intervention is fairly simple: you take a tube and connect it from the brain ventricles into the stomach to help drain the CSF. Interestingly, hydrocephalus is becoming a growing interest in neuroscience because there is some evidence that hydrocephalus can present like a neurodegenerative disease in older patients. I.e., it can cause people to have fading memory or general cognitive decline—so it is hypothesized that some patients may be misdiagnosed as having diseases like Alzheimer’s when in reality they have hydrocephalus.

14.5.2 CSF Contacting Cells

This topic may appear niche, but it is indeed of considerable interest! To start, epidural electrical stimulation (EES), which is covered in considerable detail later, does not stimulate specific neurons but rather depolarizes the entire CSF. Therefore, the cells in direct contact with the CSF may be the key modulators in restoration and regeneration.

To begin, let us discuss this paper⁴⁹. CSF contacting neurons (CSF-cNs) are described as being chemosensitive, mechanosensitive, and may even act as stem cells. As mechanosensors, they inhibit motor neurons (i.e., in normal walking they are used to prevent over-compression of the spinal cord). Canonically, they are ciliated and function in tandem with the Reissner fiber to sense spinal curvature. The Reissner fiber is a protein fiber that extends along the spinal cord, and its breakdown is a known cause of scoliosis in model organisms⁵⁰. CSF-cNs cells modulate excitatory interneurons and reticulospinal neurons. Because of their location, CSF-cNs cells are very difficult to study. They are seated in the ependymal layer of the central canal. The Review cited above discusses their investigation primarily in zebrafish. An important advancement in their study was in discovering the marker polycystic kidney disease 2-like 1 (PDK2L1), which labels all CSF-cNs.

Given their hair-like structures that extend into the apical side of the central canal, their discoverers compared them to hair cells of the ear (though, these hairs are disordered, unlike inner or outer cells). Interestingly, though, these cells are GABAergic, and thus inhibit rather than excite. In spinal curvature tests, to the surprise of the experimenters, only those that were on the concaved side of the spinal cord responded, meaning they response to compression. Restated, those cells on the left side of the body respond to bending of the spinal cord toward the left side.

⁴⁹<https://www.nature.com/articles/s41583-023-00723-8>

⁵⁰Very interestingly, no studies have been done to show the existence or lack of a Reissner fiber in humans.

Remarkably: PDK2L1 is an ion channel with a quite high conductance (hundreds of pS) and the high membrane resistance of CSF-cNs neurons (on the order of GΩ)... the opening of a single PDK2L1 is able to depolarize a cell! It was demonstrated that mechanical force opens PDK2L1 channels, and that in the absence of such channels, CSF-cNs do not respond. Another responder to mechanical force seems to be acid-sensing ion channels (ASICs), which is indirectly affected when an ASICs modulator is altered by force. An unanswered question was what PDK2L1 is actually responding to, as the response did not correlate with the calculated CSF flow. Instead, evidence suggests it is coupled to the Reissner fiber. Structural analysis revealed vesicles on both the apical and basolateral sides, suggesting they can secrete both neurotransmitters, namely GABA, onto neurons or peptides into the CSF. Notably, after SCI it is said that CSF-cNs secrete monoamines. While neurotransmitter containing vesicles have been shown to release after a single depolarization, the root of apically released vesicles is not known.

CSF-cNs-connected neurons ascend ipsilaterally a couple hundred microns. Those that are particularly rostral may connect directly to the midbrain. Driving CSF-cNs also modulate activation of the central pattern generator, suggesting neural connection there as well. Their connection to V2a spinal interneurons is not especially conclusive yet, but is quite a promising possibility. Similar connections have been shown with reticulospinal neurons and propriospinal neurons.

Fascinatingly, despite CSF-cNs being inhibitory, optogenetic stimulation of them can lead to locomotion in zebrafish—indicating they have a multiplexed role. This data seems quite contradictory and unclear, as contrastingly, somatostatin expressing cells (specifically Sst1.1) are said to synapse onto excitatory interneurons and inhibit them. Sst knockout zebrafish exhibited longer durations of spontaneous locomotion. Their ability to promote locomotion seems much less supported than their ability to inhibit it.

As a lasting note, CSF-cNs show characteristics of immature neurons, and indeed seem to be able to differentiate into astrocytes or oligodendrocytes. Similarly, they seem to be able to recover after injury, and this was shown in a SCI model with EES.

14.6 Myelin in Health and Regeneration

Here we'll discuss the role of microglia in regulating myelin⁵¹. Microglia are the macrophages of the CNS, and are derived from erythromyeloid progenitor cells. During embryogenesis, they enter the CNS. Notably, they have a long lifespan in non-pathogenic environments. Microglia respond to CNS damage via receptors for damage-associated molecular patterns (DAMPs) or pathogen-associated molecular patterns (PAMPs) and proliferate. Interestingly, microglia phagocytose oligodendrocyte progenitor cells before they mature, preventing myelination during development which helps “organize” myelin wraps depending on neural activity. After injury, microglia are activated to clear debris and force an environment in which oligodendrocyte progenitors can migrate and re-wrap neurons. Perhaps more fascinatingly, upon aging, microglia lose the ability to prune myelin sheaths, resulting in hypermyelination that in turn becomes degenerative.

Discussing such matters in the context of degenerative diseases is some of the most helpful. For example, multiple sclerosis is touched on a bit in section 12.1.2, and Alzheimer's is discussed in depth in the

⁵¹<https://www.nature.com/articles/s41577-023-00907-4>

Addendum (Part **VII**, which is supposed to be a secret). Of course, in MS the topic of myelin is core, but demyelination is a common feature of many degenerative diseases, including AD. Fascinatingly, changes in the myelin / white matter structures can be seen decades before AD symptoms arise. Such regions are called white matter hyperintensities (WMHs) and can be seen by MRI—and splotches in the parietal lobe are especially predictive of AD. Though, it is presently unclear if axonal changes precede such myelin changes.

14.6.1 Initiation of Demyelination

The factors leading to demyelination are largely unknown. In the case of MS, it is thought to be an immune response which triggers myelin degradation. However, it is also hypothesized that transcriptional profile alterations lead to oligodendrocyte instability, perhaps predisposing them to degradation. Similarly, hypermyelination precedes demyelination in many cases, and is thought to be triggered by an autophagy pathway⁵². In a mouse AD model, preceding a period of degeneration was months of oligodendrocyte growth, in which myelin sheaths were thicker than wildtype neurons. Follow-up work showed both de- and remyelination occur throughout the pathology's progression, but in the end demyelination prevails. Inhibiting demyelination via promoting oligodendrogenesis through inhibition of oligodendrocyte muscarinic receptor 1s seem to improve the cognitive impairments associated with AD. If interested, muscarinic receptors are discussed throughout section **14.2**. These authors suggest monitoring lipid profiles as an early diagnostic tool of AD.

14.7 Central Pattern Generation

Defining the central pattern generator is still somewhat contested. Computational models have been used to explore its existence⁵³, and for now we should take a few unifying assumptions: **(1)** the central pattern generator exists and is used to generate rhythmic moving, such as walking, **(2)** in many cases it is initiated by the CNS, but aside from that is largely devoid from CNS input, and **(3)** the CNS can work in tandem to compute integrated moving that requires coordination and balance.

⁵²This is actually interesting. I wonder if this is linked to the broad endocrinology hypothesis regarding quickly growing cells

⁵³<https://www.nature.com/articles/s41598-021-91714-1>

Part IV

Spinal Cord Injury

Maybe it sounds like I'm just spouting moral platitudes. But from a vagabond like me, it's not that. I can't begin to tell you how lonely I feel when I come across a beautiful view, then suddenly realize there's no one to enjoy it with me.

– Musashi by Eiji Yoshikawa

Chapter 15

The Injury Itself

Spinal cord injury is composed of the primary injury, prototypically, but not restrictively, due to some kind of high impact action. This is usually unpredictable and highly variable. Secondary injury, resulting from inflammation, oxidative stress, and other biological responses is much more predictable and potentially lends itself better to therapeutic intervention.

The lesion's composition is categorized in three ways: **(1)** the non-neural core, **(2)** the astrocytic scar around the core, and **(3)** the spare reactive neural tissue. In the mix of immune cell influx and scar formation, no neural cells can survive at the center of the lesion. On a neuronal level, the rostral end retracts in a process of Wallerian degeneration. The caudal end dies away. Growth from the cell body is limited both by the damaged cell's biochemistry and by the physical barriers which now present themselves in front of the axons. The physical barriers that immediately succeed injury are often called damaged axon-glia complexes (AGCs). Discussed further later, immune cell influx causes astrocytes to form a scar, meant to save the spare surrounding neural tissue, which is composed of both glia and neurons.

The traditional aim of treatment is to bridge the corticospinal tract with distant neurons through a therapeutic combination of inhibiting anti-regenerative and promoting regenerative factors. As I have commented many times, getting neurons to regenerate alone is insufficient in many cases, as reformation of the correct synapses will not necessarily follow. Forcing axon regeneration alone is, incidentally, not too hard—one can pump neurons full of metabolites or simply implant stem cells. The issue being that they do not know where to grow to. One possible route to solving this is remodeling neural circuits using interneurons to bridge these connections. There are also attempts to use biomaterials to simulate a pro-regenerative environment, hopefully enhancing plasticity of the circuits.

15.1 Cell Specific Responses

The discussion, for the moment, will mostly use information gathered from⁵⁴.

15.1.1 Immune Response

As SCI breaks the spine-blood barrier, influx of immune cells can cause further damage. Evidently, the nature of the immune response being helpful or harmful is still largely contested.

⁵⁴<https://www.nature.com/articles/s41392-023-01477-6>

Neutrophils.

Neutrophils compose part of the immediate response to injury, which are recruited by cytokines and chemokines secreted by cells damaged in the primary injury. They essentially initiate the secondary injury, and reach their peak around 1 DPI. Like most cells, the role of neutrophils cannot be characterized as solely pro- or anti-regenerative. While a high influx of neutrophils is associated with poor patient outcomes, so too are neutrophils associated with guiding macrophages to damaged tissue, suggestive of better recovery.

Microglia.

In mouse SCI models, it seems that there are two peaks of microglial activity. The time course is remarkably long and disparate, reported 7 DPI and 60 DPI. Microglia can either promote inflammation, thereby worsening the secondary injury (called the M1 phenotype) or decrease inflammation, and promote repair (called M2). It is likely that this response depends on the subtype of microglia, which varies depending on the environment. Regardless, it is true that the earlier one treats SCI, the more likely one is to avoid negative microglial effects. Fascinatingly, in a neonatal setting microglia are able to heal SCI almost entirely through their role secreting fibrinogen, which is able to connect damaged axons back together.

Macrophages.

Macrophages are considered to be the dominant immune cell located around the injury site. Microglia, conversely, are scattered around the borders of the injury. Depending on the type of glial scar that is formed, different types of macrophages have been found. Macrophages mediate the corraling⁵⁵ of cells around the injury site. The phagocytotic abilities of macrophages are of key importance, as loose fragments of cells must be removed, and microglia are incapable of keeping up such a high demand for removal. As a large part of this includes the destroyed myelin of oligodendrocytes, macrophages uptake great amounts of lipids. This can result in the formation of lipid droplets, which causes macrophages to become “foamy.” This foamy phenotype impairs further repair.

Lymphocytes.

The adaptive immunity is fairly universally regarded as harmful to regeneration (with some exceptions, of course). T cells further break down the spine-blood barrier and increase immune cell invasion. Evidently, T cell entry is also a major source of neuropathic pain in SCI patients. In general, it seems established that the overall immune response after injury impairs further regeneration, and a good example of this can be found here⁵⁶. **NOTE: It would be good to read this entire article.**

15.1.2 Neural Response

Apoptosis of neurons initiates at around 4 h AI, but peaks at only 8 h AI⁵⁷.

⁵⁵Corraling is a term used to describe the formation of a barrier around the injury, preventing further injury. It is composed astrocytes, and other cells, and is important in repair.

⁵⁶<https://www.science.org/doi/full/10.1126/science.abd5926>

⁵⁷It is worth noting that these times are likely quite inaccurate, or very injury-type specific. But, they do give a good indication of the approximate timeframe—such as that the majority of this apoptosis occurs within the first day or so after injury.

Interneurons.

Fascinatingly, it was shown that the ability of neonatal mice to fully recover from SCI was due, in part, to interneurons maintaining excitatory conditions. In adult mice, these interneurons switch to inhibitory after SCI, which dampens signals to motor neurons. A paper investigating this can be found here⁵⁸. One must wonder, can you electronically mimic the excitatory interneurons in fully grown mice? Similar approaches have been done therapeutically, such as with potassium-chloride cotransporter-2 (KCC2) agonist CLP290⁵⁹ which seems to dampen the overexcited, inhibitory interneurons. Perhaps one could simply use something like DBS (or in this case, DSS?) on these interneurons.

Astrocytes.

Astrocytes, being the dominant supportive cell, plays an essential role in SCI. After injury, astrocytes form a physical barrier that is supposedly intended to limit the secondary injury. The old perspective was that astrocytes, like the fibrotic scar, impair recovery as a physical barrier. It is now more accepted that the astrocytic scar (or border) is a necessary mechanism of limiting inflammation. This occurs after astrocytes become activated, and are helpful in the initial stages but later form a glial scar, impairing regeneration. Astrocytes may either be activated by inflammation, causing them to be neurotoxic (called A1 cells) or by ischemia, causing them to be neuroprotective (A2 cells). The first transformation occurring through the NF- κ B path, and the second through STAT3. Microglia are said to be the greatest contributor to activating astrocytes through release of signaling molecules. Another important factor is type 1 collagen upregulation, which results in astrocytic adhesion through cadherin, causing activation and eventual scar formation.

The astrocyte scar is surprisingly thin, only a few layers of cells. Though, its importance is not to be underestimated. When ablated, mice with SCI were worse off by almost every metric. A cornerstone paper on the topic seems to be here⁶⁰. While scar tissue is primarily astrocytic in origin, it is worth mentioning that pericyte derived scar tissue (sometimes called the fibrotic scar) too play a role. Their positive roles include boosting tissue integrity, but so too do they seem to block axon regeneration as a physical barrier.

Oligodendrocytes.

Oligodendrocytes reportedly begin apoptosis around 1 DPI and it peaks around 8 DPI. Oligodendrocyte precursor cells (OPCs) may differentiate into oligodendrocytes or Schwann cells after SCI. OPCs have been shown to remyelinate neurons after SCI, but fascinatingly, it has been shown that locomotor recovery after SCI does not necessarily require remyelination by oligodendrocytes⁶¹. Though, plenty of other research suggests it is required—so it is likely context dependent.

15.1.3 IL-12 Sensing Neurons Promote Neuroprotection

Here I'll comment on this article⁶², which does not directly describe spinal cord injury, but still broadly covers neural damage, inflammation, and the immune response.

⁵⁸<https://www.nature.com/articles/s41593-022-01067-9>

⁵⁹<https://www.sciencedirect.com/science/article/pii/S009286741830730X>

⁶⁰<https://www.nature.com/articles/nature17623>

⁶¹<https://www.nature.com/articles/s41467-018-05473-1>

⁶²<https://www.nature.com/articles/s41593-023-01435-z>

Multiple sclerosis (commented on in section **12.1.2**) is characterized by inflammatory lesions, induced by type-1 immune response. The type-1 immune response is typically responsible for protection against bacterial or viral infections. Interleukin-12 (IL-12) is a necessary activator of type-1 immunity. With IL-23, a complex relationship is formed resulting in the regulation of inflammation. Though, in the CNS, IL-12 has been known to reduce inflammation and protect against worsening MS. The protective benefits of IL-12 is the topic of this work.

Using the *CMV* promoter, driving *Cre* expression in all tissues, this group generated global knock-down of the IL-12R subunit B2, dubbed *Il12rb2^{del/del}*. Such mice were shown to be susceptible to autoimmune encephalomyelitis. They postulated that this was due to altered T cell activity, since T cells are the primary respondents in autoimmune encephalomyelitis. However, after generating T cell-specific knockdowns—they found that the mice were still susceptible to the disease. The same was true for NK cell-specific knockdown.

In order to determine which cells express the IL-12 receptor, they used both immunostaining for β -gal in *Il12rb2^{LacZ/LacZ}* mouse lines, as well as RNAscope to detect *Il12rb2* mRNA. They identified the IL-12 receptor (IL-12R) as being expressed in natural killer (NK) and T cells, in addition to oligodendrocytes and neurons. Specifically, they found expression in NeuN-positive and *Rbfox3/Map2*-positive cells (neurons) and myelin forming and mature oligodendrocytes. They verified this expression profile in deceased patients who had multiple sclerosis. Ablation of IL-12R in neurons and glia by *Nestin^{Cre}* worsened the response to experimentally induced encephalomyelitis. This phenotype was marked by increased CD4⁺ T cell infiltration into the CNS and accompanying microglial activation. Finally, they demonstrated neurons are the key actors by performing glia-specific knockdown, and demonstrating a lack of inflammation.

To understand the transcriptional response to IL-12, they performed RNAseq showed that IL-12R induced a strong response particularly in granule cells, excitatory neurons, cholinergic neurons, microglia, molecular layer interneurons (MLIs), and MOL1 and MOL2. Particularly in granule cells, responses include increased expression of genes involved in neuroprotection and decreased transcription of genes involved in immune cell recruitment. In short, they revealed a novel role of IL-12 in neurons, rather than immune cells, which mediates a neuroprotective response.

Chapter 16

In The Clinic & Therapeutic Approaches

16.1 Clinical Presentation

Death rates from SCI are still as high as 20% in some countries. There is a strong age dependence to this, as the probability of walking again after SCI in those older than 50 is much lower than those under.

Diagnosing Injury.

Immediate diagnosis is done through scanning, such as X-ray or CT scans, combined with general neurological exams, including voluntary or involuntary motor control tests. An alternative technique in neural evaluation, if the patient is not responsive, is electrophysiological recordings (either through EEG or EMG). X-rays are often used to immediately see large fractures, and follow-up CT scans for investigating the more possible hairline fractures. CT angiography may be used to investigate vascular destruction. More soft-tissue damage follow-up is done through MRIs. Interestingly, a trade-off exists in an MRI vs. immediate surgery. An MRI may be used to detect non-obvious issues, like disc herniations away from the primary injury site—which, if not fixed, will cause further degeneration. However, doing an MRI delays one's ability to decompress the spine.

Classifying Injury.

You will often hear injuries as being complete or incomplete. Another helpful distinction is discomplete, where the injury is considered clinically complete, but one can still observe connections through electrophysiology. The main method of classifying injury and tracking progress of patients is called the American Spinal Injury Association (ASIA) impairment scale. ASIA scores are broken into the following categories:

1. Grade A: Complete impairment, where there is no motor or sensory information being transmitted below the injury site⁶³.
2. Grade B: Incomplete impairment, where there is no motor information being transmitted, but some sensory information is preserved.
3. Grade C: There is some motor activity preserved, but more than half of the key muscles are too weak to move against gravity (Grade 3 muscles).

⁶³It is not clear to me if this is measured by EMG or movement.

4. Grade D: A fair amount of motor activity is preserved, where at least half of the key muscles are above muscle Grade 3.
5. Grade E: There is no impairment at all!

The most common and complete method of classification is the International Standards for Neurological Classification of Spinal Cord Injury (ISNCSCI). The ISNCSCI uses the ASIA impairment scale, with ASIA motor and sensory scores. It is recommended that assessment be performed immediately upon hospital admission⁶⁴, with follow-ups in the future to assess improvement. Another important metric is quality of life (QOL) assessment.

Importantly, the injury site is often designated by the vertebrae that was fractured, but symptoms are due to the nerve pair that is damaged, which may be at a different location than the primary site of bone damage⁶⁵. This discrepancy seems to be exacerbated the more caudal you go. Injury in the cervical portions can lead to severe bradycardia and hypotension, due to dysregulation of brain-heart communication, particularly regarding baroreceptor feedback. Too, damage to the vagus nerve can occur here, leading to dysregulation of most organs. Injury in the thoracic part may have widespread affects on the symathetic nervous system due to damage both of the spinal cord nerves and the nearby ganglia. Interestingly, an unconsidered byproduct of lower thoracic SCI is damage to motor signals to the legs. The main focus of such being that one loses their ability to walk, but accompanying this is reduced venous return, as veins rely on muscle movement to get blood back to the heart. Dampening of CNS-cardiovascular system communication seems to be one of the primary indicators of poor prognosis.

In evaluating the severity of the injury, a *spinal shock*, marked by temporary paralysis, may muddy the waters. While one may temporarily lose their reflexes, it can sometimes be regained soon later. However, the ability to define this state, and its duration, remains problematic. *Neurogenic shock* manifests similarly, but the cause is hypotension after SCI. This may be caused by hypovolaemia from blood loss, or pooling of blood due to reduced venous return. This occurs most often in SCI above T₆, as it is these sympathetic nervous which maintain vascular tone.

A few named pathologies exist, such as Central Cord Syndrome. This is the most common incomplete SCI. Often, this occurs in elderly patients who fall and already had some form of spondylosis⁶⁶. It is marked by more damage to upper extremities and possible incontinence. Brown-Séquard Syndrome occurs from penetrating SCI, such as a stab wound. It is usually characterized by sensory loss.

16.2 Auxiliary Management

Haemodynamics.

A steady blood supply to the damaged spinal cord is an essential component of treatment. Tool, system hypotension is a common symptom both from nerve damage and the surgery itself.

⁶⁴This is interesting, as in other sections I have detailed that various forms of shock can cause misunderstanding in the initial phases of hospital stay.

⁶⁵<https://www.nature.com/articles/nrdp201718>

⁶⁶Weathering of the vertebrae.

Methylprednisolone sodium succinate.

Evidently, this is controversial! Methylprednisolone sodium succinate (MPSS) has the traditional role of reducing inflammation. The controversy is due to mixed results. Some large clinical trials showed no benefit, while others suggest there was a considerable improvement in ASIA scores, particularly if administered within 8h of injury. The adverse side effects seemed to be minimal, so many surgeons routinely administered it. Follow-up investigations suggest that negative effects are more consistent than previously thought, so the updated guidelines are not to administer MPSS.

16.3 Treatments

This section will cover some of the basic, in a broad overview manner. Complex research, such as the discussion of stem cells and the research surrounding them, will be covered in chapter **21**.

16.3.1 Electrical Stimulation

This will, of course, be covered in excruciating detail in later sections (and or, Parts, like Part **V**). Fascinatingly, electrical stimulation has been used in conjunction with physical therapy in the past with good results⁶⁷. The reasons may be that this promotes stem cell differentiation⁶⁸, or disrupts inhibitory interneuron signaling. The optimal electrical application for differentiation has been explored extensively⁶⁹. One may wonder if the benefits of BSI are in the interface itself, or simply the stimulation. Combining stem cell implantation and electronics is, likely, the future.

A slightly different rose by the same name is functional electrical stimulation (FES). Many trials have shown improvement in patients treated with either external stimulation or internal stimulation.

Light.

Light stimulation feels like a footnote in the electrical modulation story, to me. Though, if one wanted to control different neurons or enzymes on an alternate time course, optogenetic activation may be an option. The obvious issue being that one does not have genetic access to patients, and therefore would need to design (likely very complicated) targeted therapeutics.

Sound.

Another footnote is ultrasound simulation. In this case, it will be low intensity focused ultrasound. Some approaches have seen altered gene expression, but perhaps a more promising one is modulating mechanosensitive channels as was shown here⁷⁰. Notably, this paper found that many mechanically activated channels are affected in ultrasound, including Piezo, and many of the Trp family proteins.

Magnetics.

I would be extremely curious to know if the magnetic field itself has any unique properties beyond its manipulation of the electric field. Still, too, the story is the same. Some seem to enhance channel

⁶⁷<https://www.nejm.org/doi/pdf/10.1056/NEJMoA1803588?articleTools=true>

⁶⁸<https://www.mdpi.com/2073-4409/11/5/846>

⁶⁹<https://www.frontiersin.org/articles/10.3389/fbioe.2021.591838/full>

⁷⁰<https://www.nature.com/articles/s41467-022-28040-1>

activation, while others expression. Interestingly, transcranial magnetic stimulation (TMS) has been used as a treatment with some success. Incomplete spinal cord injury has seen improvements from TMS.

16.3.2 Biomaterials

The overall goal in the use of biomaterials is to block a worsened immune response, scar formation, and promote neuron activity. Adding promise to stem cell implantation is the use of biomaterials that enhance proper network reformation⁷¹. Theoretically, a perfect biomaterial could be a substrate preferable for neuron growth, contain molecules that inhibit the immune response, neurotrophic factors that enhance stem cell differentiation and recruitment, and ion channel agonists. Notably, to date there have been no major publications where a “cocktail” like this has been successful. These sorts of things are usually made from hydrogels, collagens, or select inorganic fibers.

An open question is how one could leverage biomaterials to help clear damaged parts of neurons/cells that would normally be cleared by phagocytosis. Perhaps, one could add materials that are easily oxygenated to dampen the blow of ROS.

To date, implantation of biomaterials have been relatively lackluster in treating patients. While some regeneration scaffolds have proven to improve some neurological function, no patient has regained motor function.

16.3.3 Drug Treatment

Drug treatment primarily follows the same paths, being reduction of inflammation and neuroprotection. Methylprednisolone (MP) is the only drug approved to treat SCI and works through reducing inflammation. Notably, some side effects have been observed and therefore MP has fallen out of favor for treatment.

16.3.4 Surgery

I think you’ll find that there is a disappointing lack of options—signaling the primitive nature of neurosurgery!

Decompression.

Anyway, surgical intervention aims to restabilize the spinal cord as quickly as possible, particularly through decompression. This begins with re-aligning the spine, usually with some kind of hardware to hold bone in place. Early surgery seems indicative of shorter ICU stays and better neurological recovery. The first day or so post SCI is the critical time. Interestingly, even after decompression, the pressure within the spine remains high due to fluid build-up within the dura matter. This makes blood reperfusion more difficult, leading to more problems.

⁷¹<https://pubs.rsc.org/en/content/articlepdf/2022/bm/d1bm01744f>

Dura Matter Manipulation.

While durotomy is often a complication of surgery due to progressive CSF leakage after operation, in this case it can be helpful to lessen spinal pressure, which there evidently is a long tradition of⁷². Duroplasty is a more modern and sophisticated alternative, and can allow opening of the dura matter without as much risk⁷³.

Myelotomy.

Incision directly into the spinal cord itself, myelotomy, has also been done with some success. The belief is that it helps drain some of the harmful dying tissue. There seems to be time dependence in this, where if performed too late after injury it will simply reinvigorate inflammation.

16.3.5 Rehabilitation

As you would intuit, exercise is the most common technique, as it preserves muscle mass and promotes circuit reorganization. Another rehabilitative technique is pumping in a significant amount of oxygen, as ischemia occurs after injury. BSIs have also become more popular. Fascinatingly, decoding of handwriting has been used to generate text⁷⁴. Though, these seem to require deep access to the brain.

16.4 Complications After SCI

The multiplexed complications of SCI are, in reality, unending, as any combination of nerve damage can result in any combination of bodily dysfunction. We can discuss some of the standouts below, but note that this covers just a fraction of a fraction.

Syringomyelia.

Syringomyelia, a cyst forming within the spinal cord, is relatively rare. The fluid filled sac can be large and span far beyond the injury site itself. The symptoms of which may not show for months-years later, and progressively worsen. Cystic cavities are not uncommon, but syringomyelia differs in its size and reach. Symptomatic patients usually undergo a second decompressive surgery, or attempts to connect this cystic space to a drainage site.

Neuropathic Arthropathy.

After SCI, a patient may become numbed, leading to unnoticed injuries. One such result of this is arthropathy (a joint disease). Over time, a patient's joints may slowly degrade, leading to deformity—which may not present for over a decade after injury.

Spasticity.

Spasticity is a common side effect of chronic SCI. Spasticity can lead to further complications, such as microfractures.

⁷²<https://www.sciencedirect.com/science/article/pii/S002013388901325>

⁷³<https://www.liebertpub.com/doi/full/10.1089/neu.2014.3668>

⁷⁴<https://www.nature.com/articles/s41586-021-03506-2>

Cardiovascular.

As mentioned in previous sections, often the clearest symptom of SCI is in significant changes to the cardiovascular system do to sympathetic nervous system impairment. This manifests often as systemic hypotension. In most cases, this seems to resolve itself within a matter of months.

Autonomic Dysreflexia.

This condition is an immediate response to *secondary* injury, and most often presents when the SCI is above T₆, and some other injury occurs in some peripheral organ, which causes a sympathetic spinal reflex. For example, injury to the gut may cause vasoconstriction to be overstimulated in the absence of spinal cord feedback. Too, it can result in overcompensation by the parasympathetic nervous system, leading to a swift drop in blood pressure. Notably, this can occur either in the acute or chronic stages of SCI. It is most often resolved via resolving this secondary injury.

Respiratory.

Damage to nerves innervating respiratory muscles, such as the phrenic nerve which controls the diaphragm, can lead to long term reduced lung capacity. Damage to the respiratory system also has big consequences on the effectiveness of rehabilitation. It is said that respiratory complications are one of the leading causes of death after chronic SCI.

Genitourinary and Gastrointestinal.

Dysregulation of the urinary or digestive systems is often the largest psychological consequence of SCI (barring, of course, large locomotor deficits). Quality of life is greatly impacted by this complication.

Neurogenic Heterotopic Ossification.

Ectopic bone formation can occur on the larger joints⁷⁵. It is not known the exact cause, but physical therapy tends to be the best mitigator.

⁷⁵Funnily enough, this review sites that 10-53% of people with chronic SCI form ectopic bone. Only a 43% margin.

Chapter 17

Approaches to Researching SCI

The first ever modeling and examination of traumatic spinal cord injury dates back to over 100 years ago. Dr. Alfred Allen, at the University of Pennsylvania, devised dog models of spinal cord injury and performed their accompany histological investigations⁷⁶. I believe firms in finding the fundamental source, and appreciating where leaves meet branches, branches meet the trunk, and the trunk meets its roots (section 22.1).

NOTE: It would be good to include some of the other approaches to researching neural regeneration in general—such sciatic nerve crush, optic nerve crush, *Drosophila* axon injury, etc.

17.1 SCI Injury Models

The bulk of this information comes from⁷⁷, and focuses on injuries applied to mice—but similar principles can be done in other mammals. Interestingly, most SCI models focus on thoracic level injury, while in humans cervical is more common.

Contusion.

Contusion is the quick application of a force. Models include dropping a weight on the spinal cord or using an air-gun. One such is called the *NYU (MASCIS) impactor*, where a piece of the bone is removed (laminectomy) and a weight is dropped directly onto the exposed nerves. Severity can be adjusted by the height from which the item was dropped. The most recent iteration is the *MASCIS III*, where an electromagnetic weight is dropped at the push of a button and includes digital measuring to ensure replication. One concern is that the weight dropping may bounce, causing multiple impacts.

Another option is called the *infinite horizon (IH) impactor*. Rather than dropping a weight, a machine applies a set force. A laminectomy is still required⁷⁸, but one can avoid the bounce effect. The *Ohio State University (OSU) impactor* is essentially the same, but uses an electromagnetic force applier. A more recent development is in the air gun. This requires drilling through the vertebrae, exposing the dura, where air pressure will be applied.

⁷⁶<https://jamanetwork.com/journals/jama/article-abstract/448138>

⁷⁷<https://www.nature.com/articles/sc201491>

⁷⁸I suppose repeatability is considered paramount, but I find that these extensive controls may impede investigation. At a certain point, one must wonder if this is an SCI or an axotomy model.

Compression.

Compression occurs over a longer time frame. One interesting application of such models is in first applying contusion, followed by a compression model. This replicates the effects of increased pressure within the spinal cord after SCI, which occurs particularly in the absence of decompression surgery.

A common method is using an aneurysm clip and applying it to an exposed section of the spine, clamping down with some force for a few minutes. The force applied is in the range of 20-50g⁷⁹. An interesting drawback is the velocity of the clip's closing is variable. In the right usage, it can be used to cut off blood supply to simulate ischemia and reperfusion after SCI. Another option is to insert a balloon on a catheter down the spinal cord and inflating it. Another method is called SC-STRAPPER⁸⁰. A string is inserted and wrapped around the spinal cord, and its benefits are that it is relatively noninvasive, and compression is applied to the entire circumference of the spinal cord.

Distraction.

Distraction is done by stretching the spine. This is more commonly done in larger animals, and is difficult to develop a reproducible model. The Harrington distractor requires laminectomy and the addition of hooks to the upper and lower sides of the removed vertebrae. Motor steps are then applied to pull the spinal cord apart. However, as this occurs slowly and is variable in application, it has drawbacks. The UBC multimechanism device uses a wedge applied between the vertebrae to abruptly apply force. Interestingly, their device can also be used to induce contusion or slipped disc injuries—so learning it provides you with considerable versatility, particularly if dislocated vertebrae is your area of study. The singular wedge applies unidirectional injury, and so the UTA distractor aims to improve this by using clips attached externally (i.e., without laminectomy) and pull apart by a motor.

Transection.

Transection requires surgical severing of the spinal cord. Transection models may target the ventral, dorsal, or subsections of the spinal cord. Such models are most useful for studying regeneration, as clean transections are rare clinical pathologies. Interestingly, some animals have impressive, natural recovery of locomotion due to spinal cord circuitry post SCI (i.e., more robust central pattern generation or spinal reflex systems). Therefore, it is often that one must re-transect after locomotor recovery.

17.2 The Basso Scale

The Basso scale⁸¹ has a few variations, such as the Basso, Beattie, Bresnahan (BBB) scale. It is a mode of characterizing injury after SCI in mouse models, specifically in the hindlimbs. You will often see Basso scale comparisons between treatment groups, or as a means to track recovery over time after SCI. The scale is as follows (directly from the paper):

- Rating 0: No ankle movement.
- Rating 1: Slight ankle movement.

⁷⁹Perhaps I am naive, but this seems remarkably small to me. When you consider that human SCI may result from a car accident, a few grams seems inconsequential.

⁸⁰Take a look at Fig. 1: <https://www.sciencedirect.com/science/article/pii/S0165027008000368>

⁸¹<https://pubmed.ncbi.nlm.nih.gov/16689667/>

- Rating 2: Extensive ankle movement.
- Rating 3: Plantar placing of the paw, without stepping, OR consistent or frequent dorsal stepping (without plantar stepping).
- Rating 4: Occasional plantar stepping.
- Rating 5: Frequent or consistent plantar stepping, without coordination, OR some coordination with paws rotated at contact and lift off.
- Rating 6: Frequent or consistent plantar stepping, some coordination, and parallel paws at contact, OR mostly coordinated, paws rotated at contact and lift off.
- Rating 7: Frequent or consistent plantar stepping, mostly coordinated, parallel paws at contact, rotated at lift off, OR mostly coordinated with, parallel at contact and lift off, severe trunk instability.
- Rating 8: Frequent or consistent plantar stepping, mostly coordinated, parallel paws at contact and lift off, mild instability, OR mostly coordinated with paws rotated at contact and lift off, normal trunk stability, and tail up or down.
- Rating 9: Frequent or consistent plantar stepping, mostly coordinated, parallel paws, normal trunk stability, and tail always up.

Slight is defined as less than half joint excursion. *Extensive* is defined as more than half joint excursion. *Plantar stepping* is defined as placing both the thumb and the last toe touching the ground. *Consistent* is defined as without missing more than 5 steps. *Frequent* is defined as more than half the time. *Occasional* is defined as less than half the time moving forward. *Coordination* is defined as proper alternations between feet, and hindlimb and forelimb movements occurring at proper times, and the mouse must move at a consistent, non-slow pace. Some coordination meaning less than half the movements are coordinated, while most is more than half. *Severe trunk instability* is defined as an extreme waddle and collapsing during the test.

It is almost certain that I misworded some of those (as in accidentally wrote most instead of some a few times). But, I think you get the overall gist! Essentially, above 5 seems to have some degree of uncoordinated walking. Around 7-9 seem to have regained functional walking.

17.3 Traumatic and Nontraumatic SCI

Here we'll focus on neuroimaging and the information from⁸². A large focus of this review is the parallels between traumatic SCI and neurodegenerative diseases like degenerative cervical myelopathy (DCM). Traumatic spinal cord injury (tSCI) refers to impact or immediate stress applied to the spinal cord, while nontraumatic occurs over long periods through continuous compression or other. DCM is the most common example of nontraumatic SCI, and can occur through things like disc bulging. Naturally, months or years may go by without symptoms while degeneration is underway.

Animal models indicate considerable overlap in traumatic and nontraumatic SCI, but verification of these processes in humans is harder because metal implants immediately into tSCI patients makes

⁸²<https://www.nature.com/articles/s41582-019-0270-5>

MRIs impossible. Conventional MRI, too, is often not powerful enough to analyze microstructural changes, like demyelination, that are canonical to degeneration. A better method is diffusion tensor imaging (DTI), which captures the diffusion of water through the tissue. It relies on the assumption that water diffuses along the white matter tracts. Core to the benefit of DTI and improved imaging techniques is identifying markers which can inform our understanding of improved recovery after SCI treatment. For example, clinical trials can be better motivated by quantifiable, noninvasive metrics like DTI.

Quantifying DTI.

DTI is devised 3 eigenvectors, let's call them: $\vec{V}_a, \vec{V}_{r1}, \vec{V}_{r2}$. You would expect \vec{V}_a to be the longest of the three as it runs axially, and or with the axons. Its eigenvalue, let's call it λ_a , corresponds to the diffusivity in the axial direction (parallel to the myelin tracts). The average of λ_{r1} and λ_{r2} describes the radial diffusivity, and or that which is perpendicular to the myelin tracts. The average of all 3 eigenvalues is the mean diffusivity. A scenario when $\lambda_a \neq 0$ and $\lambda_{r1} = \lambda_{r2} = 0$ would be described as an *anisotropic* diffusivity, because there is complete directional dependence of diffusion. $\lambda_a = \lambda_{r1} = \lambda_{r2}$ would be *isotropic*, because there is no directional dependence. The idea is that the diffusion of water gives some key insights into the microstructure of the injury, as things like ECM proteins and membrane composition will have some affect on such water diffusion. The axons themselves are naturally the largest contributor to this directional dependence, and you can imagine that in their absence water is much more likely to diffuse in all sorts of directions. The degree of anisotropy is a strong way to measure degeneration, then. There are some limitations, of course, as diffusion is only a proxy for degeneration. Ulterior factors, like inflammation, may too limit diffusion and obscure the contribution by degeneration or demyelination. Similarly, DTI is not as effective at imaging lower spinal cord segments, and is primarily used in cervical injury models.

DTI in Degeneration and SCI.

Of considerable study is the parallels between SCI's secondary injury and degenerative diseases. After tSCI, retrograde and anterograde SCI initiate. Interestingly, in the first 2 years following SCI, tissue volume decreased by $\approx 14\%$, and $\approx 30\%$ in 5 years. Such a decrease was greater in the grey than in the white matter, which is similarly observed in DCM. Interestingly, no difference in diffusivity within the grey matter is observed after SCI, but it is believed this may be due to volume effects in the region.

Without going into the great detail on the vector changes associated with DCM and tSCI, the two show similar decreases in anisotropy. Notably, DTI is able to resolve changes in asymptomatic DCM patients, making it a possibly useful tool in predicting worsening or improving outcomes of SCI that are not detected functionally. Remotely increased radial diffusivity was observed in both tSCI and DCM, suggesting that the local injury site / stenosis can have distant effects in both. However, DCM showed increased axial diffusivity above and below the site of stenosis, differing from tSCI. The authors suggest that this may be because compression at these sites increased cell density and decreased the extracellular space available for diffusion. Notably, though, the increase in radial diffusivity significantly outweighed axial increase, so it is still believed that demyelination is the dominant process in spinal stenosis.

Really, the takeaway from this is that cell death patterns in tSCI and degenerative diseases like DCM are comparable, but better investigations and imaging techniques will be needed to fully resolve this.

Chapter 18

Broad Coverage of Axonal Regeneration

Let's discuss⁸³ and⁸⁴. During development, axons are guided by their growth cones to achieve functional connections at distant targets. A quintessential barrier to recovery after spinal cord injury is the central nervous system's inability to regain such functional connections. In general, neuron regeneration (or neuroregeneration) refers to axonal regeneration of an injured neuron. However, *sprouting* is another form of regeneration in which uninjured neurons may grow to replace the damaged synapses. Similarly, the use of stem cells can too be considered a form of regeneration.

While the CNS is relatively un-plastic after injury, some endogenous plasticity after spinal cord injury can and does occur, but in large part results in spasticity and neuropathic pain after SCI. An in-depth discussion on circuit reorganization is covered later (chapter 20)—so for the moment, let's consider endogenous plasticity to be negligible or harmful after spinal cord injury.

18.1 Intrinsic Factors

Growth Cone Manipulation.

The physical interactions and the cell matrix, which typically relate to growth cone extension, are very important in growth. Deletion of non-muscle myosin II has shown enhanced growth. Deletion of profilin 1, which binds to actin and is thought to enhance its polymerization and use in filopodia, halts regeneration. Stabilizing the growth cone, or trending microtubule dynamics toward polymerization, is key to axonal extension. Doublecortin-like kinases (DCLKs) promote regeneration and are thought to modulate microtubule dynamics. Epothilone B and D are microtubule stabilizers, which have been shown to promote recovery after SCI. Epothilone B is also an anti-cancer drug as it inhibits mitosis, and similarly seemed to reduce glial scarring likely by inhibiting glial mitosis. Other similar, anti-cancer microtubule stabilizing drugs, like taxol, have shown similar outcomes. Importantly, other studies have called these findings into question, and some have shown quite negative outcomes in their usage. Similarly, it is unclear if their benefit is neuronal in origin or if their role in scar formation is sufficient to drive recovery. However, given that they are already used in cancer treatment entices researchers to find a use for them in treating SCI. To this point, though, their conclusive function is unclear.

⁸³<https://www.nature.com/articles/s41582-019-0280-3>

⁸⁴<https://www.nature.com/articles/s41580-022-00562-y>

Anterograde transport, including integrins and their RAB carriers, are shown to support regeneration by supplying the growth cone with necessities. However, selective transport is an essential focus, as RABs are likely to bring both pro and anti-regenerative factors to this site.

RhoA GTPase, a protein localized to the growth cone and functions in microtubule activity through Rho kinase (ROCK), has also been studied in an attempt to maintain the growth cone. Inhibition of RhoA or ROCK has promoted regeneration—specifically in acute SCI. If it is helpful in treating chronic SCI remains unclear.

Promising Proteins.

Target of rapamycin (mTOR) is all too familiar now, as it has been identified as an active translator in the axon and growth cone. mTOR phosphorylates 4EBP1, thereby inhibiting it, preventing it from repressing translation. Phosphatase and tensin homologue (PTEN) is a negative regulator of mTOR. PTEN is likely the most famous regeneration blocker—and for good reason! Inhibition of PTEN even a year after SCI has been shown to promote enhanced recovery. Though, the regeneration is still typically insufficient for meaningful and complete functional recovery. Currently, developing therapeutics against PTEN are marred by worries that it will produce malignancies within the tissues, as PTEN is also an essential tumor suppressor. Interestingly, PTEN inhibition alone strikes somewhat variable results. Co-inhibition of PTEN with suppressor of cytokine signaling 3 (SOCS3) (mentioned in the next section) provided more consistent, enhanced growth—especially in the critical corticospinal tract.

Other proteins, like KCC2 (**20.1.1**), are discussed in-depth in other sections.

Transcriptional Possibilities.

Many transcription factors can be used to boost regeneration. One such is the cAMP-responsive element-binding protein (CREB) is necessary for axon growth in development. CREB activation by TTK21 promotes recovery after SCI. Another is signal transducer and activator of transcription (STAT3). Determining the biochemical barriers to CREB or STAT3 activation has been done through investigating histone deacetylases (HDACs) and DNA methyltransferases. It was shown that in peripheral nerves, where regeneration occurs naturally, histones were acetylated at specific, pro-regenerative sites. TTK21's activation of CREB is done through CREB-binding protein (CBP) acetyltransferase.

Fascinatingly, constitutive STAT3 activation is insufficient to promote regeneration. The reason being SOCS3 is a negative regulator of the JAK-STAT transcriptional pathway. While STAT3 may be activated by therapeutics or intrinsic growth factors, SOCS3 knockdown is required to attain its benefits. Another key family of transcription factors within this umbrella are Krüppel-like factors (KLFs). Many members of the KLF family have been found to block neurite outgrowth, with KLF4 being the strongest. Conversely, overexpression of other KLFs, like KLF6, enhance regeneration. Co-Knockdown of KLF4 and SOCS3 further promoted growth. KLF4 is thought to bind with phosphorylated STAT3 and inhibit it, while KLF6 seems to further activate it.

Minors related is the discovery of the dual leucine zipper-bearing kinase (DLK). DLK is necessary for retrograde transport of STAT3, suggesting it is used in injury signaling. Interestingly, evidence for the DLK pathway's injury response in glia has emerged. In this case, DLK knockout worsens the injury site as astrocytes do not properly respond. The same can be said for SOCS3-STAT3 and PTEN-mTOR, demonstrating a correlation between the intrinsic factors dictating neuronal and glial

injury responses.

18.2 Extrinsic Factors

Growth Factors.

A canonical problem is the lack of growth factors that normally guide axonal growth in development. Such canonical examples include nerve growth factor (NGF), brain-derived neurotrophic factor (BDNF), neurotrophin 3 (NT3), and glia-derived neurotrophic factor (GDNF). Naturally, growth factors have different, neuron subtype-specific effects. NGF modulates nociceptive neurons, NT3 and GDNF modulates corticospinal neurons, BDNF modulates corticospinal and reticulospinal neurons, etc. Notably, matured neurons may not be receptive to such growth factors, and one mode of treatment includes supplementing both the growth factors and their accompanying receptors. Other options exist, such as in sensitizing the neurons to growth factors therapeutically.

A key finding in this department is that the insulin-like growth factor 1 (IGF1) promotes regeneration. This may be partly due to its ability to promote mTOR activity, but the many potential outcomes of IGF1 overexpression are unknown. IGF1 injection has been used to treat autism in the past with relatively safe and promising outcomes, however the fear of tumor production remains a barrier to its use in treating SCI.

Growth Cone Navigation.

The cell-specific responses surrounding neurons is covered in-depth in section 15.1. Many of the modifiers exist in the ECM, such as secretion of collagen protein (Cthrc1), a pro-regenerative protein⁸⁵. Conversely, WNT signaling molecules accumulate around the injury site and repels axon regeneration and sprouting.

Other non-neuronal cells, like astrocytes and fibroblasts, secrete chondroitin sulfate proteoglycans (CSPGs). CSPGs are composed of a protein core with chondroitin sulfate sugar exteriors, whose inherent variability makes their study difficult. After injury, CSPGs too accumulate around the injury site and limit growth. They can do so through the protein tyrosine phosphatase σ (PTP σ) receptor or Nogo, which may trigger RhoA.

Administration of chondroitinase ABC (ChABC) has been shown to promote plasticity and growth by degrading CSPGs. ChABC administration in non-human primates promoted hand dexterity recovery without negative side effects. ChABC has poor stability and is difficult to produce in large quantities, making its clinical applications somewhat limited. Too, there is some evidence of their benefit, such as through perineuronal nets which may provide a supportive structure to neurons in the grey matter.

Myelin Inhibition.

Interestingly, many myelin-associated proteins are inhibitory, called myelin-associated inhibitory (MAI) proteins. These proteins bind to the Nogo receptor complex, and blocking this interaction, such as by NogoA antibodies, promotes growth, especially in the acute phase. Examples include myelin-

⁸⁵[https://www.cell.com/developmental-cell/pdf/S1534-5807\(20\)30984-9.pdf](https://www.cell.com/developmental-cell/pdf/S1534-5807(20)30984-9.pdf)

associated glycoprotein (MAG) and oligodendrocyte myelin glycoprotein (OMGP), which both utilize a NOGO to RhoA-ROCK pathway to inhibit regeneration.

18.3 Recovery of Walking via Target Reconnection

A new paper from Anderson and Courtine labs⁸⁶. Something commented in many places throughout this work is that functional recovery requires more than getting neurons to regenerate—it also requires getting them to regenerate in the right direction and make the right connections. That is a prime focus of this work. Commented in a later section (section 24.0.3) the Courtine lab characterized the cells responsible for stimulation-induced recovery after SCI. Briefly, this work found that a set of interneurons were able to relay signals past the injury site and down to the lumbar spinal cord, where walking-initiating neurons are. Interestingly, these neurons are not required for walking in the absence of injury. This paper is a partial follow-up to this work.

First, to better characterize neurons projecting to the lumbar spinal cord, they injected an AAV containing GFP into the lumbar region, which was then expressed in neurons projecting there. They identified cells they call $SC^{Vsx2::Hoxa7::Zfhx3 \rightarrow lumbar}$. The first part describes their transcriptional profile, and the arrow to lumbar means they project to the lumbar spinal cord. Mice that exhibited recovery after spinal cord injury showed marked transcriptional changes in such cells, including up-regulation of genes involved in dendritic connections and synaptic growth.

To “ablate” these cells, they used $Vsx2^{Cre}$, which blocked differentiation into this cell type. They found that there was a marked decrease in projections to the lumbar spinal cord, taking this to mean these neuron make up a significant portion of the axonal density there. They also found that $Vsx2$ expressing cells connect to many places in the spinal cord, including forming short and long projections. Those that project specifically to the lumbar region are marked by expression of $Zfhx3$. They used similar methods to identify cells of the ventral gigantocellular nucleus (vGi) as projecting to these $SC^{Vsx2::Hoxa7::Zfhx3 \rightarrow lumbar}$ neurons.

With this better understanding of the neurons, they employed the following plan:

1. Reactivate the intrinsic growth capacity of neurons using growth factors like insulin-like growth factor 1.
2. Restore a favorable growth substrate using fibroblast and epidermal growth factors.
3. Guide the axons back to their desired targets using favorable biomaterials infused with growth factors and attractive agents.

This indeed allowed for growth of these neurons beyond the injury site. However, this did not allow for functional recovery. Thus, they concluded that functional recovery can only be achieved via meaningful connection re-formation. Instead, they tried replacing biomaterials with lentiviruses driving expression of growth factors, which indeed allowed for functional recovery. Via their previously mentioned AAV method, transcriptional and immunohistochemical classification, they verified that this was indeed due to $Vsx2$ neuron growth. They verified that motor neurons had regained CNS control via stimulating neurons of the vGi and identifying corresponding leg movements. They verified, via expression of toxin receptors and corresponding toxin administration in $Vsx2$ neurons, that these neurons are required for recovery.

⁸⁶<https://www.science.org/doi/10.1126/science.adi6412>

18.4 Neuronal Excitability and Regeneration

This is quite a difficult topic to cover. There is almost no end to the amount of conflicting information. Presumably, this is because neuronal activity dictates many, many underlying processes. There is a growing hypothesis, put forth largely by the Bradke group, that neuron activity is largely anti-regenerative. The basic principle is that being in "growth mode" or being in "active mode" are somewhat mutually exclusive. Further, other works have found that ablating individual synapses, but maintaining some, limits growth. Conversely, eliminating all synapses evokes a more strong regeneration response. The idea here is that a neuron may attempt to preserve its remaining function by not entering a so-called regeneration mode. The implications of this are not straightforward, as naturally many forms of CNS nerve damage, namely SCI, result in complete axonal severing—yet, of course, such neurons do not regenerate properly. On the other hand, axonal sprouting can and does occur from non-injured neurons. Thus, in my eyes, the whole theory is a bit confusing and may well be subtype-specific.

Furthermore, inhibition of certain calcium channel components, like the $\alpha 2\delta 2$ subunit of voltage gated calcium channels, promote axon regeneration. This subunit mediates influx through N and P/Q-type channels. Thus, it's thought that these channels may underlie activity-dependent halted regeneration. One method of inhibiting neuron activity is through pregabalin, which limits spasms. Further evidence by administration of gabapentinoids enhancing regeneration shows promise in using anti-convulsants to treat SCI. This work fits into the larger hypothesis of neuronal activity limiting axon regeneration. Further work demonstrates that active vesicle machinery, like the protein Munc13, limit axon regeneration.

However, a strange wrinkle arises when considering the Bradke group's work on L-type calcium channels. They found that L-type channels also inhibit axon regeneration in mouse DRG neurons in a work from 2010⁸⁷. Our lab, on the other hand, found that L-type VGCCs are necessary and sufficient for axon regeneration in the *Drosophila* PNS. My hypothesis would be that such channels may be mediating local influx in DRG neurons, whereas it is global in *Drosophila* PNS neurons. There also may be differences in timing and frequency of firing. Unfortunately, the Bradke group did not follow-up on this work, and therefore we have very little to analyze regarding it. The skeptic in me also wonders if they didn't do follow-up work because their results were conflicting, and or, because a phenotype was difficult to nail down. Regardless, the conflict warrants further study.

⁸⁷<https://pubmed.ncbi.nlm.nih.gov/20579880/>

Chapter 19

Metabolism of Neurons

19.1 Programming Mitochondrial Maintenance

This is one of my favorite Reviews ever, so I am pleased to write about it⁸⁸! A key component of this work is discussing the unique structural features of neurons that lead to trouble trafficking mitochondria and meeting injury needs after injury or in degeneration. An incredible amount of energy is consumed by the brain (20% of total body consumption), and approximately 1,000,000 molecules of ATP are used per action potential in an effort to restore ionic concentrations alone. Around 20,000 molecules of ATP are used per synaptic vesicle recycles, and its predicted that the concentration of ATP in the presynaptic terminal is around 2mM.

19.1.1 Mitochondrial Generation and Degredation

Notably, mitochondria are not spontaneously generated, but rather undergo fission to create more—which primarily occurs in the soma where such machinery is located. Thus, irrespective of how much mitochondria are present, the key is that it must be properly trafficked. Amazingly, it can take days for mitochondria to reach the tip of an axon. Late endosomes carrying RNA granules and ribosomes may dock on mobile mitochondria and serve as sites for mitochondrial protein synthesis. Peroxisome proliferator-activated receptor- γ coactivator (PGC)-1 α is a key transcription coactivator of nuclear-encoded mitochondrial genes. ALS and Parkinson's disease models both show decreased distal translation of mitochondrial proteins and build-up of the corresponding mRNA, suggesting the energy demands are not met in these diseases.

Mitochondrial fission is mediated by dynamin-related protein 1 (DRP1), a cytosolic GTPase. DRP1 acts with mitochondrial adaptors, including fission protein 1 (FIS1), mitochondrial fission factor (MFF), and mitochondrial dynamics proteins (MiD), to induce fission. While larger mitochondria are better at energy production, smaller mitochondria are more easily trafficked to distant sites. Notably, fission can lead either to biogenesis or to mitophagy, depending on where the fission occurs and which adaptors mediate it. FIS1 specifically tends more toward mitophagy, while MFF more toward biogenesis.

Mitochondrial fusion is mediated by factors like optic atrophy 1 (OPA1) and mitofusion 1 and 2 (MFN1 and MFN2). Both are GTPases and aid in inner membrane and outer membrane fusion respectively. Fusion is useful in limiting mitochondrial stress, as combining the contents of two dilutes

⁸⁸<https://www.sciencedirect.com/science/article/pii/S0896627322002513>

harmful agents and aids in the increased production of energy. Mutations in OPA1 are commonly linked to Parkinson's disease.

Fixing damaged components of the mitochondria may occur through proteases lining the inner membrane. Alternatively, mitochondria frequently bud off vesicles, called mitochondrial-derived vesicles (MDVs), that contain damaged proteins or reactive oxygen species. Such budding is achieved through mitochondrial Rho GTPase (MIRO) and DRP1, and are then targeted to lysosomes. PTEN-induced kinase 1 (PINK1) is also able to enhance degradation through mitophagy, along with Parkin (PARK2). Such pathways are dysfunctional in Parkinson's disease as well. PINK1, on the outer membrane, recruits Parkin, which recruits degradative machinery. Interestingly, axonal mitophagy is incredibly rare. Typically, mitophagy occurs only after a damaged mitochondrion is trafficked to the soma, and in the case of Parkin or PINK1 mutations, damaged mitochondria build up in the soma rather than the axon.

19.1.2 Mitochondrial Trafficking

Trafficking is necessary for both the removal of damaged mitochondria and the addition of them to energy depleted sites. The speed of trafficking is quite variable, and is capable of both stalling and changing directions. Such movement occurs along the polarized microtubules within axons, especially by motor proteins like the kinesin-1 family (KIF5) for anterograde and dynein for retrograde transport. On the outer membrane, the MIRO-trafficking kinesin-binding proteins (TRAK) complex connects to KIF5 motors. It seems that there is some functional redundancy in the MIRO-TRAK complex with other outer membrane proteins, but in large part it seems to be a strong regulator of mitochondrial placement.

In the case of injury, movement of the mitochondria to the damage site is a key component of repair. One way to enhance promote movement is by deleting syntaphilin (SNPH), a mitochondrial anchoring protein. SNPH is capable of competing with the MIRO-TRAK complex's binding with KIF5. It is thought that p21-activated kinase 5 (PAK5) inhibits SNPH by phosphorylating it, enhancing mitochondrial mobility. Overexpression of MIRO1 was found to increase mitochondrial trafficking to the distal axon segments, leading to larger growth cones. MIRO1 is mediated by neuronal activity, as Ca^{2+} influx binds with MIRO and disrupts complex formation. Though, this blocking seems transient and seems to require the presence of SNPH. This mechanism seems particularly important for halting mitochondrial movement around the Nodes of Ranvier, where a higher energy demand exists to restore membrane potential.

Mitochondrial trafficking is adaptable. For example, high concentrations of glucose are capable of arresting its movement through glycosylation of TRAK. Guidance of mitochondria through the complex branches of an axon require such intracellular cues, some of which are discussed in the next section.

19.1.3 Response to Stress

Stress induced AMP-activated protein kinase (AMPK) phosphorylates PGC-1 α to upregulate mitochondrial RNA. ATP depletion has been shown to activate the AMPK-PAK3 stress pathway, which uses myosin 6 to recruit mitochondria and SNPH to anchor it to surrounding F-actin. Therefore, exceptionally active synapses may experience mitochondrial buildup proportional to their firing. As it goes, stress induced anterograde trafficking in a highly branched axon may result in mitochondrial build-up at the branch sites, which is achieved too by SNPH. Parallely, AMPK is capable of

blocking retrograde transport of mitochondria, resulting in their accumulation at distal, stressed sites. Counteractive to trafficking, reactive oxygen species may result in increasing intracellular Ca^{2+} , which arrests mitochondrial movement. As mitochondria are one of the main sources of such species, this can become a self-fulfilling prophecy of positive feedback.

Neuronal Degeneration.

Most neurodegenerative diseases are accompanied by mitochondrial dysfunction. Build up of protein aggregates, for example, hinder trafficking. Too, mtDNA mutations can regularly cause neurodevelopmental impairments.

PINK1/Parkin, while traditionally known for its role in Parkinson's, defines many mitochondria-related pathologies. Its function is thought to be in degrading MIRO through ubiquitination, causing local mitochondrial arrest and eventual mitophagy. Conversely, a mechanism of remobilization where mitochondrial vesicles containing SNPH are released with the idea of enhancing retrograde transport after stress. This mechanism is activated in pre-symptomatic ALS models and Alzheimer's disease. It seems that early disease causes mitophagy primarily in the soma, while later and/or higher levels of stress may induce it within the axon. The site of mitochondrial degradation is therefore an indicator of disease progression.

19.1.4 Neuronal Injury and Regeneration

While degeneration is progressive and slow acting, injury is acute. Repair is inherently a highly energy intense process. The injury itself can cause mitochondrial structural damage, furthering the energy crisis. Preserving mitochondrial function is a mode of limiting Wallerian degeneration after injury. Axotomy quickly depolarizes mitochondria, and inhibiting SNPH serves as an important way to remobilize and restore their function. In certain injuries, the AKT path becomes activated which promotes PAK5 (mentioned above as inhibiting SNPH), serving as an energy-boosting mode of neuronal repair. Another such method is via ARMCX1, a protein that mobilizes mitochondria through MIRO1. Histone deacetylase 6 (HDAC6) is known to deacetylate the MIRO1 encoding gene, leading to lessened mobility. Conversely, hypoxia inducible factor 1 α (HIF-1 α) activates hypoxia upregulated mitochondrial movement regulator (HUMMR), which promotes MIRO1/2.

After injury resulting in limited blood supply, such as in a stroke, metabolism occurs through glycolysis, resulting in increased lactate production. However, after the blood supply is regained, reperfusion injury can overload the system with oxygen, resulting in production of reactive oxygen species, thereby further harming mitochondria.

Delivery of mitochondria to damaged neurons through vesicles or tunneling nanotubes (TNTs) is thought to be one mode of enhancing recovery. It has been shown that neural stem cells are capable of transferring mitochondria to damaged cells, and microglia use TNT to do so. Mitochondrial transplantation has been done, however the efficacy of such is heavily debated. Though, it is well supported that complex networks of metabolite shuttles exist in the nervous system. The astrocyte-neuron lactate shuttle (ANLS) is a prime example, thought to allow astrocytes to fuel neural oxidative phosphorylation. Glial regulation of neuronal metabolism too occurs, such as through release of sirtuin 2 (SIRT2) which promotes metabolism in neurons.

Chapter 20

Circuit Reorganization and Plasticity

We will cover circuit reorganization in considerable depth, not necessarily in the context of spinal cord injury, in this section.

20.1 Reorganization After Injury

Circuit reorganization naturally and with neuromodulation is covered in-depth here⁸⁹. Part of this paper is framed on the fact that spinal cord circuits are much more complex than previously thought. That is, some computation is done at the level of the spinal cord. Too, the paper attempts to motivate investigating the specific neurons involved in recovery, and that previous investigations have not used the resolution necessary to investigate such matters. One constraint on the field is that, while the brain's cellular profile has been extensively investigated, detailed profiling of spinal cord cells is less explored—particularly in the injury condition.

Circuit reorganization can occur in many ways, both above and below the injury site. Examples seen in our own lab include damage to axons causing retraction and thus sprouting of the axon in seemingly random directions far above the injury site. Too, below the injury site, axons that once filled this space will fade away, and uninjured axons may grow into this now empty space. Interestingly, growth into this empty space has been shown to augment hand function after recovery⁹⁰.

Of course, when damaged neurons regrow in their previous locations it can cause functional recovery. However, fascinatingly, even when all corticospinal tract neurons are damaged, motor cortex signals can be sent through alternative, surviving paths. Here are two brainstem examples: (1) After SCI, cortical neurons can synapse onto the reticular formation and recover walking. (2) Activation of the mesencephalic locomotor region (MLR) after SCI can recover walking. This region is evolutionarily ancient and unable to generate walking on its own, but is able to recruit reticulospinal neurons and generate walking.

In a similar vein, otherwise non-essential neurons, like propriospinal neurons in the cervical region, can be reprogrammed to improve hand dexterity. While one may think that information must be conveyed directly from the motor cortex to the muscles on interest, in this case propriospinal neurons relay information past the injury site. KCC2 downregulation leads to inhibition of such circuits. This

⁸⁹<https://www.nature.com/articles/s41593-022-01196-1>

⁹⁰This is all very interesting when it comes to BSMTs—as one usually focuses on or around the injury site, or the dorsal root exit zones that generate walking. This suggests many sites along the spinal cord may be worth stimulating.

is expanded on in a later section. Much remains unknown about such neurons, what allows them to transmit beyond the injury site, and what recruits them to do so.

Rehabilitation proves to consistently aid circuit reformation, but lack of care causes poor reorganization that can worsen pathologies. Notably, when supraspinal⁹¹ connections are severed, motor control relies on sensory signals only. One example being *V2a* neurons discussed in a previous section. Another similar set of neurons includes *dI3* neurons⁹², another set of interneurons. While these aid in recovery, many changes are harmful to it. As a general trend, it appears that generally less activity, due to injury conditions like hypoxia, immune cells, etc. leads to greatly increased sensitivity of receptors and ion channels alike. Below the injury site often sees large increases in excitatory synapses. This combination leads to abnormal reflex responses, spasms, neuropathic pain, etc.

Effects of Neuromodulation.

Again, neuromodulation is covered in considerable depth in Part V. Both activity and artificial stimulation of the motor cortex promote regrowth of the corticospinal tract. This can be done non-invasively. Timing this with spinal cord stimulation enhances connections. There are a couple of paper's exploring this in depth in NHP⁹³, and in humans⁹⁴. **It would be good to look through these papers in the future.** Fascinatingly, indirect neuromodulation, such as through the vagus nerve, too has been shown to enhance response to rehabilitation. Too, deep brain stimulation has been done on the MLR⁹⁵, and when positive yielded results comparable to stimulating the motor cortex⁹⁶. Though, the MLR's region is less clearly defined, and results were more variable.

Stimulating the spinal cord is primarily done at the dorsal root entry zones or through EES. It is thought that low-frequency EES works through proprioceptive afferents, which help circuit reorganization. Damage to the sympathetic nervous system is an essential problem to solve, as it can lead to life threatening drops in blood pressure. One such way to do so is in stimulating the low thoracic spinal cord's pre-ganglionic sympathetic neurons, causing release of norepinephrine and thereby constrict vessels. Similarly, EES can restore the sympathetic response via large afferents recruiting sympathetic neurons.

Effects of Biological Manipulation.

Biological strategies seem most successful when attempting to enhance the projectome of surviving supraspinal neurons. One such way to do this is through removing damaged tissue and grafting in more malleable, healthy tissue. As part of this, physicians may attempt to ablate the fibrotic scar. Interestingly, partial ablation, and not complete ablation, has shown symptom improvement after SCI.

Pharmacological promotion of axon regeneration has inherent limitations. Such investigations into axon regeneration is covered in better depth in chapter 18. For example, the canonical player PTEN (discussed in other sections) has shown robust regeneration, capable of penetrating the astrocytic border, but only in certain neuronal populations. Too, even in this case neurons abruptly halt when

⁹¹Supra meaning "above" the spine, i.e., brain-to-spine neurons.

⁹²<https://elifesciences.org/articles/21715>

⁹³[https://www.cell.com/neuron/pdf/S0896-6273\(13\)00762-9.pdf](https://www.cell.com/neuron/pdf/S0896-6273(13)00762-9.pdf)

⁹⁴<https://www.pnas.org/doi/abs/10.1073/pnas.1505383112>

⁹⁵Another example of DBS promoting rather than inhibiting—kind of interesting.

⁹⁶It would be nice to build a patient profile of those who may benefit the most from motor cortex vs. MLR vs. vagus nerve etc. stimulation.

reaching the fibrotic scar. Somehow, one must induce global, or brilliantly targeted, growth to achieve true functional recovery.

Another application commented in earlier sections is the conversion of inhibitory neurons into excitatory, or the deletion of inhibitory neurons. One way to do so is via chondroitinase (ChABC) which dissolves glycosaminoglycan side chains of chondroitin sulfate proteoglycans (CSPGs). CSPGs are known for their role in stem cell differentiation, and bookend the periods of neurogenesis. Another such attempt is in inhibiting nogo receptor reticulon 4 (RTN4).

Reversion to a state of biological development too is another core route of investigation⁹⁷. As proprioceptive neurons have been found to be possible relay neurons, these researchers targeted such neurons and were able to achieve growth across the injury site. This required the use of growth factors applied to the neurons, fibroblasts, and attracted molecules downstream of the injury site. Release was done in a spatially and temporally controlled manner. Fascinatingly, **no functional recovery was found**. Therefore, while neurons were able to bridge this gap, they were unable to form useful synapses. Authors postulate this may be due to inactivity or lack of myelin, among other things. In a similar vein, the grafting of stem cells is often successful in allowing for axonal growth across the injury site, but retains the inability to restore function.

20.1.1 Interneurons and KCC2

This is from the paper⁹⁸, but it seems KCC2 is an interesting topic of research in a couple different pathologies, such as in minimizing neuropathic pain, and downregulation increases spasticity after SCI. Some of the background for this paper is in better understanding how spinal cord stimulation leads to regain of function, with one hypothesis being that it helps reawaken “dormant” circuits.

To investigate, they used staggered, lateral hemisections performed at the T₇ and T₁₀ sites. This injury meant all neurons would be severed, except those crossing the midline between T₇ and T₁₀. They verified near complete paralysis after injury, and used this to conclude that while some neurons were spared, they must be “dormant” and/or unable to recover function. They performed a mini-screen of drugs known to modulate neural activity, and landed on CLP290 as the only one showing a phenotype. CLP290 is known to activate KCC2, among other things. They determined that CLP290’s function required some preserved axons—as in their complete lesion tests, no functional recovery was found. They further verified this by determining no enhanced regrowth was found due to CLP290 in their hemisection model. To determine if CLP290’s function was through KCC2, they tried a KCC2 overexpression line and verified similar functional recoveries.

They then used the Cre-Lox system to verify that KCC2’s expression specifically in inhibitory interneurons (driven by Vgat-Cre) leads to recovery. They presumed these neurons interact with / enhance the ability of propriospinal neurons to transmit information, and to resolve the spatial component, they tried local injection of AAV-KCC2 in the lumbar segments and did not find recovery. They believe it is specifically interneurons within the relay site between the two lesions that are required for repair. Their explanation being that when administering systemically, the blood-brain-barrier is compromised only at the lesion site.

⁹⁷<https://www.nature.com/articles/s41586-018-0467-6>

⁹⁸<https://www.sciencedirect.com/science/article/pii/S009286741830730X>

In development, intracellular Cl^- is high. During this period, Cl^- channel opening is excitatory, rather than inhibitory in fully-developed cells. KCC2 upregulation is important in removing this Cl^- , converting Cl^- channel opening into being inhibitory. They believe activating KCC2 helps restore a more physiological state. They also did work to inhibit inhibitory interneurons, and excite excitatory interneurons, and determined that only the former was beneficial in achieving recovery after SCI.

20.2 Non-coding RNA in Rewiring and Plasticity

Background.

Non-coding RNAs (ncRNAs) have been studied quite a bit in recent years⁹⁹. ncRNAs are classified as small (less than 100 nt) or long (above 500 nt), and among the small ncRNAs are microRNAs (miRNAs) of $\approx 20\text{nt}$. They are typically produced through canonical means and play a role in post-transcriptional regulation within the cytoplasm.

As for miRNAs, gene silencing occurs by binding to a complementary untranslated region of an mRNA. This region is sometimes called a *seed region*. From here, a miRNA-induced silencing complex (miRISC) forms. Then, some of the standard RNA degradation mechanisms can occur like decapping. Some of the relevant long ncRNAs include long intergenic RNAs (lincRNAs), which are linear, circular RNAs (circRNAs), and antisense (AS) RNAs. CircRNAs are produced but noncanonical means, and generally seem to function in tandem with miRNA in some manner, and or, they regulate miRNAs. AS RNAs are born of the opposite DNA strand, most often modulate this specific locus, and may be thousands of nt long. They are particularly relevant in early development. ncRNAs work in a symphonious way, usually involving multiple types coordinating together. This Review makes it a point to state that recent data has been overwhelming, due to advancements in technology. Therefore, it remains difficult to stay up to date or understand the complexities as new functions continuously emerge.

Regulation of Local Growth.

Local translation was first determined to be mediated through miRNAs in the case of miR-9's ability to decrease the expression of microtubule protein MAP1B via the brain-derived neurotrophic factor (BDNF) path within growing axons. Similarly, BDNF increased presence of miR-132, leading to increased axonal branching. In *Xenopus*, miR-182 was shown to be necessary for axon targeting via multiple modes of tubulin and actin regulations and their usage in the growth cone's guidance.

In the dendrites, miR-9 has also been implicated. miR-9 is under a negative feedback loop, in which the repressor element 1 (RE-1) silencing transcription (REST) factor is activated by miR-9, which in turn decreases its expression. miR-9 downregulated the actin regulator Diap1, inhibiting further growth. In short, miR-9 inhibits growth of both dendrites and axons.

In mice, loss of miR-101 led to increased network excitability and impaired memory through increased expression of Na-K-Cl cotransporter 1 (NKCC1) and increased synaptogenesis, thought to be mediated through *Kif1a* and *Ank2*. Fascinatingly, miR-101 acute loss did not lead to such a result, but rather only when lost in development. The lincRNA ALAE was the first example of an lncRNA that

⁹⁹[https://www.cell.com/neuron/fulltext/S0896-6273\(23\)00341-0](https://www.cell.com/neuron/fulltext/S0896-6273(23)00341-0)

locally regulates mRNA translation during growth by blocking the function of RNA-binding protein, and therefore allowing GAP43 synthesis, causing axons to grow¹⁰⁰.

Circuit Remodeling.

In general, it appears that miRNA expression is bad for remodeling, and long-term potentiation (LTP) specifically. miR-134 expression was found to inhibit long-term potentiation through inhibition of CREB1. Under physiological conditions, SIRT1 inhibits miR-134 expression. miR-26a and miR-384 also inhibit LTP by different means. Many such other examples exist¹⁰¹.

Interestingly, miR-153 was upregulated in the dentate gyrus during LTP. It seems to be required for exocytosis, suggesting it has a role in excitatory coupling. miR-218 and miR-137 were also named as promoting LTP. I think that's about all that's worth saying, for now.

20.3 Synaptic Pruning

20.3.1 Ube3a E3 Ligase Promotes Pruning in Flies

In general, it is rare for a purely fly paper to make it into the big journals like Science and Nature. Papers that include fly work typically use the later figures to validate their work in higher organisms, like mice—but this paper didn't, and is still in the current issue of Science¹⁰². The topic of synaptic and dendritic pruning is of considerable interest, as it has been implicated in a number of neurodevelopmental diseases. For example, in autism spectrum disorders, synaptic pruning occurs improperly. Flies have long been used as a model to study dendritic pruning, because as they go through metamorphosis (from larva to adult fly), a significant amount of dendrites are pruned and connections are remade. The study of synaptic pruning is more novel, and that's what this paper focuses on.

They investigate using fly class IV dendrite arborization (C4da) neurons, a group of sensory neurons. They identify the ubiquitin ligase Ube3a as being specific to C4da neurons and in presynaptic, but not dendritic, pruning. In Ube3a mutants, or RNAi knockdown, a significant amount of synapses are maintained through metamorphosis. They can visualize this with a marker called brunchpilot (Brp) which marks synapses. They found that Ube3a undergoes anterograde transport toward the synapses with the help of the kinesin motor. They found a missense mutation in Ube3a that was conserved between flies and humans with Angelman disease—a disease where low Ube3a dosage disrupts pruning. This mutation disrupted Ube3a localization but not expression. Naturally, they wanted to test Ube3a's role in degrading proteins. Among its previously established targets is the bone morphogenetic protein (BMP) receptor Thickvein (Tkv). Overexpression of Tkv induced similar defects as seen in Ube3a mutants. Therefore, their hypothesis is that Ube3a activation in metamorphosis downregulates signaling pathways like Tkv, which overall lead to synaptic pruning.

One of the ways this paper shines is in investigating a mutation conserved between humans and flies, which helps provide new insight into Ube3a. However, the paper would be significantly strengthened

¹⁰⁰I think part of the issue with this kind of paper is it is almost purposeless trying actually learn this. It is simply letters followed by numbers doing things redundantly.

¹⁰¹I hate to kind of “yada-yada” through this, but again, it's just miR-*xxx* does different, harmful things.

¹⁰²<https://www.science.org/doi/10.1126/science.ade8978>

if they had mouse work or human cell cultures to support their findings.

Chapter 21

Stem Cell and Tissue Engineering

In this section we'll discuss a few labs in much depth, such as the Tuszynski lab at UCSD and the Cullen lab at UPenn—some of the pioneers in three dimensional tissue engineering. My understanding is that most researchers would agree stem cells alone are likely to be insufficient to attain functional recovery after SCI. Even the most staunch supporters would agree an integrated approach, combining neuromodulation and rehabilitation, is certain to be better. The ependyma is a source of stem cells, which contributes to glial scar formation after SCI. Connexin (gap junction) signaling between ependymal cells is a factor involved in their differentiation, notable because it opens up the possibility of manipulation through epidural electrical stimulation, discussed in chapter 24.

Injections of both oligodendrocyte progenitor cells and spinal-cord derived neural stem cells have been grafted into patients without complications, demonstrating promise.

21.1 Cell Transplantation Therapy

In this section, we'll primarily cover¹⁰³. The majority of implantation investigation focuses on neural stem and progenitor cells (NSPCs, or NPCs), Schwann cells, oligodendrocyte precursor cells (OPCs), olfactory ensheathing cells (OECs), and mesenchymal stem cells (MSCs). NSPCs are multipotent progenitor cells and are able to differentiate into neurons and glia alike.

Naturally, one of the primary benefits of grafting stem cells is that they may replace damaged neurons and form new functional connections. Alternatively, they can form relay stations where endogenous axons synapse onto the newly grafted cells. The physical addition of cells itself plays the role of giving neurons something to synapse and grow onto. If, for example, a neuron was capable of growing, the unideal milieu, such as open cavities filled with interstitial fluid, do not provide anything to grow on. This is sometimes called a *bridge*, especially when it allows neurons to grow rostrally to caudally. Through production of ECM proteins like laminin and collagen, a new, more favorable environment can form. However, such bridges still have great limitations, causing heterogeneous regrowth due both to the neurons' inherent abilities and because the graft may be dissimilar from certain axon's needs.

It is also thought that many such implanted cells allow for neuroprotection after SCI. This will be commented on a bit later, but one issue with this is neuroprotection is strongest when the implantation is done in the acute phase. Implantation after the first day sparsely shows protection. Yet,

¹⁰³<https://www.nature.com/articles/nn.4541>

implantation is normally done at 1-2 weeks after injury, because when done in the acute phase, the graft tissue is more prone to dying. This creates a slight Catch 22, where to maximize protection one must implant early, thereby sacrificing the graft and limiting the other potential benefits. The proposed mechanisms include protecting oligodendrocytes via healthy signaling, production of myelin, and the sprouting of new axons. All of these factors may contribute to the observed enlargement of the white matter near the injury site after a graft.

Other mechanisms of study include revascularization. Revascularization begins around 3d after injury and reaches its maximum around 14d after injury¹⁰⁴. OECs, in particular, appear to increase vascularization and enhance its directionalization along the graft and or spinal cord. Immunomodulation is similarly of interest, as correlative studies demonstrate grafting decreases harmful inflammation.

A general concern is where implanted cells may migrate. Therefore, you'll likely see the mention of halting migration in further reading. One strategy to doing so is encasing the stem cells within a matrix, typically of fibrin.

21.1.1 Long Distance Growth of Stem Cells

Stated in the 2019 Giovanni Review: "We believe that the most promising preclinical strategy to promote long-distance regeneration of axons in the spinal cord has come from recent studies in the **Tuszynski laboratory**, which used human spinal cord-derived NSC grafts combined with a cocktail of growth factors." Indeed—let's begin with such a study¹⁰⁵. The idea of this paper is to use stem cells cultured in a fibrin matrix, containing a cocktail of growth factors, and then graft this entity into rats after SCI. Growth was mTOR dependent, but not Nogo dependent¹⁰⁶.

Rats underwent complete T₃ transection. Rat embryonic stem cells were labeled with GFP and differentiated primarily into neurons after grafting. Cells did not migrate much beyond the graft / lesion site either. Grafted neurons were capable of growing long distances, with axons extending multiple vertebrae away both rostrally and caudally. They determined approximately 29,000 axons grown after grafting, and a similar density among all subjects tested. In fact, grafted neurons even became wrapped by host oligodendrocytes! Their justification for the growth not being Nogo dependent is that grafted cells still expressed Nogo, so therefore it is unlikely that Nogo inhibition promoted the growth. They tried inhibiting mTOR and found a significant decrease in axonal growth.

They then repeated these studies using human-derived stem cells. I didn't see this question answered directly in the text (maybe I just missed it) but I am wondering how much the neurons actually matter, especially for functional recovery. I.e., the matrix contained growth factors—could the growth factors alone be promoting growth, independent of the stem cells?

21.1.2 3D Printed Spinal Scaffolds

The ability to create 3D structures of cells is becoming ever more popular. One such example is again from the Tuszynski lab¹⁰⁷. The goal of this paper is to generate a scaffold capable of promoting growth, more so than creating a CNS mimic. They essentially designed a cross section of the spinal

¹⁰⁴Take this with a large grain of salt.

¹⁰⁵[https://www.cell.com/fulltext/S0092-8674\(12\)01018-5](https://www.cell.com/fulltext/S0092-8674(12)01018-5)

¹⁰⁶Dr. Strittmatter will be upset!

¹⁰⁷<https://www.nature.com/articles/s41591-018-0296-z>

cord with pores / channels where axons can grow into, synapse onto neural progenitor cells, and those cells can grow in the opposite direction and synapse onto neurons below the injury site. It is kind of like a well structured relay station for signals. They call their method microscale continuous projection printing (μ CPP), and remarkably it is able to print such scaffolds in a matter of seconds. They showed an interesting potential application where a 3D model of a patient's SCI lesion was taken and then a corresponding scaffold was printed to fill the gap.

The device itself is quite impressive. They are able to print on a $1\mu\text{m}$ level. In their proof of concept runs, they printed scaffolds that resemble different modes of SCI. Notably, this is meant as an almost complete replacement for the spinal cord—i.e., it requires a very invasive surgery to implant and the similar removal of leftover nervous tissue. The ones they used were 2mm in length and made of polyethylene glycol-gelatin methacrylate (PEG-GelMA). Fortunately, this paper had some of the most in-depth controls, including comparisons to stem cell only injections and scaffolds made of agarose. Another key control was that the implantation did not worsen inflammation. However, at the inflammation site there was still a reactive astrocyte layer. While it was less prominent in the PEG-GelMA scaffold than in agarose, it was still present.

Very interestingly, implantation of stem cells often requires waiting many weeks. This is because dissociated cells like this, which do not have support from blood vessels and are exposed to reactive oxygen and immune hurdles, do not survive well. The group wondered if by providing a supportive scaffold, if implantation can be done earlier after injury—and indeed it could. Acutely implanted scaffold retained their stem cells a month later. It seems like in general, the results were a bit inconsistent. In long term studies they found that some neural progenitor cells became myelinated and the tubes became vascularized. In fact, they even claim that astrocytes' feet lined the vessels, signaling a restored blood brain barrier. Interestingly, the walls of the scaffold thinned by $\approx 50\%$ at the 60 months post implantation mark. It is unclear if this has any meaningful impact, though, as once neural connections are made, perhaps the scaffold itself is not needed.

Onto the part that matters most. Animals with the scaffolds exhibited significant functional recover, reaching a Basso score of $\approx 6 - 7$, compared to the controls reaching $\approx 1 - 2$ at 5 months after injury¹⁰⁸. They also used an electrophysiological method where they stimulated the motor cortex and read motor neuron outputs, and again found the scaffold to exhibit significantly better outcomes¹⁰⁹.

¹⁰⁸This is a sidenote, but geez—it is kind of inhumane to keep a mouse alive with complete immobility for 5 months, solely to ensure it doesn't recover.

¹⁰⁹As another sidenote, this whole thing is really... odd, in a sense. Of course, the FDA and medical boards cannot allow researchers to do whatever they want. But, these mice had a complete transection and were able to get significant recovery. Surely it can do some good in humans? This is some serious motivation for an enhanced Right to Try bill. If one is completely paralyzed, the option should be open.

Part V

Brain-Spine Interfaces

When we stand at the edge of the ocean, we can not understand its vastness. We know only that it is big. Ittō Ittosai is big. And what about Kojirō?

– Reworded from Vagabond by Takehiko Inoue

21.2 Perspective

Papers to Read:

- Neuroimaging guidelines: <https://www.nature.com/articles/s41393-019-0309-x>
- munc13 <https://www.sciencedirect.com/science/article/pii/S0896627321007753>
- courtine in NHP <https://www.nature.com/articles/nature20118>
- Myelin: <https://www.nature.com/articles/s41577-023-00907-4>
- Another scaffold: <https://www.science.org/doi/10.1126/science.abh3602>
- CD8 t cell paper <https://www.science.org/doi/full/10.1126/science.abd5926>
- Growth cone review 1 <https://www.nature.com/articles/nrm2679>
- Growth cone review 2 <https://www.nature.com/articles/nrn3176>
- a third, focusing on mechanics <https://www.frontiersin.org/articles/10.3389/fncel.2015.00244/full>
- literally focuses on glia-neuron growth cone lol <https://www.frontiersin.org/articles/10.3389/fnins.2020.00203/full>
- you **MUST** read this asap <https://www.nature.com/articles/s41586-023-06377-x>

Chapter 22

Interfacing with Nerves

22.1 Historical Dealings

A proverb in a writing called *Testament* by Daitō Kokushi reads:

I beg you, try to find the fundamental source.

...

Like our great predecessors,

Do not merely pinch off the leaves

Or concern yourselves only with the branches.

The field of neuron regeneration feels novel, as investigating its complexities appears to require new age technology. However, greatness spans time. In the 1930s, one of the most brilliant neuroscientists the world has ever known, Ramón y Cajal, suspected restoration of neural circuits after injury required the emulation of developmental conditions. Using electronics to study neural circuits, too, has a long and storied history. One can think of Hodgkin and Huxley, whose ubiquitous achievements evades a need for citation, using an operational amplifier to clamp the voltage of giant squid axons, they revealed the fundamentals of action potentials in the 50s. Or, one can think of Fitzhugh, whose work inspired Nagumo to devise analog circuits to model excitable systems in the 60s. In the case of solving spinal cord circuits, so too have electronics long been used, with examples dating back to the 40s¹¹⁰. Similarly, stimulating the spinal cord originates from the theory of central pattern generation, first characterized in the 1980s¹¹¹. A large part of what we must do as modern scientists is to not forget the questions posed by our predecessors. While they were limited by technology in their ability to investigate, the validity of their curiosities can never be lost.

Note: These next two paragraphs deserve their own sections. These labs are instrumental. Find the fundamental source!

Restoration of the signals which pervade severance in spinal cord injury through therapeutics has been equally explored. For example, drugs such as clonidine, α_2 receptor agonist, can promote walking in cats with spinal cord injury¹¹². This effect can be blocked completely by yohimbine, an α_2 receptor antagonist¹¹³.

¹¹⁰<https://journals.physiology.org/doi/epdf/10.1152/jn.1943.6.2.111>

¹¹¹https://nyaspubs.onlinelibrary.wiley.com/doi/full/10.1111/j.1749-6632.1998.tb09062.x?casa_token=squhz5qGCxsAAAAA%3A1_eFcl105AQAUdyU1ZoGqmSoCeMnjfpNpvBrnf5Nezmg-AwmwujHWj04NNH5lHWlrYRurC3HlTbh8phW

¹¹²<https://journals.physiology.org/doi/full/10.1152/jn.1998.79.6.2941>

¹¹³<https://www.ncbi.nlm.nih.gov/pmc/articles/PMC2278596>

The ability to generate walking-like movements from electrical stimulation of the lower spine, the T10-L1 region, has been long known^{114,115}. In these instances, “tonic” stimulation was able to generate step-like movements. Although the term “tonic” is dubious because other papers by the same lab identified frequency dependence in their stimulation¹¹⁶. While one can generate step-like movements at once frequency, continued extension can be generated with another.

22.2 Electrostimulation

22.2.1 Background

Stimulating nerves is not straightforward. The amount of current necessary to stimulate a nerve is highly dependent on the location. For electrodes especially close to myelinated fibers, currents as small as $0.1 \mu A$ have been successful in depolarizing neurons¹¹⁷. It seems that as a general trend, the faster conduction velocity of a neuron, the lower amount of current is required to simulate it. Too, throwing off one’s measurements is often that you may indirectly stimulate a neuron of interest by depolarizing nearby cells. For direct stimulation, the distance from electrode to the closest Node of Ranvier seems to be essential metric. Figure 3 of the paper footnoted earlier in this paragraph shows a fascinating plot. The current supplied by an electrode resembles something of a double-sided Lenhert-Jones plot. Therefore, for an anode¹¹⁸, one would actually expect a core of cells to be depolarized, while those of the periphery would actually be hyperpolarized. The inverse would be true for a cathode. This makes me wonder if oscillating, $\pm A$ has been applied, and the outcomes. If one were to use two electrodes (i.e., an anode and a cathode nearby) then one has the option of longitudinal stimulation or transverse stimulation (i.e., either parallel or perpendicular to the axon).

Note: Perhaps it would be good to go through the different electrode options? I.e., where one places ground, whether current or voltage is applied, etc. Though, I have had trouble finding information on this.

Ramblings.

In a strange sense, the human body can be considered the infinite resistor lattice mentioned in the electronics section.

22.2.2 Biomaterials Used

A primary focus in finding suitable biomaterials are those that are conducting, flexible, and non-reactive¹¹⁹. Polypyrrole (PPy) is one such option. PPy alone is quite rigid, but is a good accompaniment with other materials. For example, you may coat some glass or fabric in PPy in order to make it more biocompatible and conducting. Too, PPy seems a good candidate for boosting cell adhesion to your biomaterials. Others have used PPy in a tubular fashion, applied some current, and used it to

¹¹⁴<https://www.sciencedirect.com/science/article/pii/B9780444521378000188>

¹¹⁵<https://journals.sagepub.com/doi/pdf/10.1177/1073858417699790>

¹¹⁶<https://link.springer.com/article/10.1007/s00422-004-0511-5>

¹¹⁷<https://www.sciencedirect.com/science/article/pii/S0006899375903649>

¹¹⁸Fascinatingly, a quick Google search for ‘anode’ provides two definitions, one stating it is positively charged and one stating it is negative. Regardless, you only need to know that it supplies electrons.

¹¹⁹<https://onlinelibrary.wiley.com/doi/epdf/10.1002/term.383>

guide regenerating axons. Another similar product is polyaniline (often called PANI). Polyaniline can be oxidized and reduced, providing an additional usage. PPy and PANI are two of the most studied conducting polymers, but many more exist.

Carbon nanotubes (CNTs) are another way one can manipulate the direction of growth. Interestingly CNTs appear to be cytotoxic when suspended in media, but strongly promote growth when integrated into a scaffold, keeping them immobilized¹²⁰. CNTs frequently have diameters similar to axons themselves.

The use of piezo-electric materials too provides interesting avenues of study. Piezo-electric materials being those that convert mechanical energy to electrical energy. An example is poly(vinylidene fluoride) (PVDF). Generally, piezoelectric materials are considered inferior to standard conducting polymers because external control is limited and activation is often too localized.

Ramblings.

The axon-like size of CNTs seems very interesting to me, as they provide a neat route of usage, i.e., as artificial myelination. Perhaps one can develop a CNT with a membrane permeable enough for extracellular signaling to get through, but conductive enough to function like myelin. I am curious if you could produce a multi-layered scaffold, where certain tracts fit axons, certain tracts fit glia, etc, and it can act like repaired oligodendrocytes after SCI.

Another interesting thought is the deep implantation of Piezoelectric materials and then activating them using sonication. It would be neat to develop some kind of material that can be mechanically stimulated at specific sonic frequencies, preventing random stimulation from body movement.

22.2.3 Flexible Brain-Computer Interfaces

For the moment, I'm not sure where to put this, so I'm adding it here. We will discuss¹²¹. The key idea of this work is that hard electronics present a geometric mismatch with the body's tissues. An amazing fact mentioned right away is that the dura mater, skull, and scalp function as low-pass filters! Which, now we know about in considerable depth from chapter 2. This leads low frequency signals, like alpha and beta waves, to be detected. Another interesting point made right away is that billions of neurons are distributed over volumes on the order of centimeters to meters, while neurons themselves are on the order of tens of microns to hundreds of microns. Similarly, neurons fire on the order of milliseconds, yet brain wave changes and behavioral outcomes take months to manifest.

Hard electronics are less flexible and adaptable. If BCIs are to improve, it'll mean that they must interface with more neurons and capture more data. Such a request is not feasible with hard electronics. Similarly, hard electronics offer potential harm to neural tissue via mechanical damage. Slight migration in hard electronics on the order of microns is inevitable. Therefore, the tracking of single neurons over long periods is impossible without re-calibrating and accounting for such migration. This work also harps that single unit recordings is not possible over long periods anyway, as gliosis and scarring will eventually worsen the signal-to-noise ratio so that individual neurons become invisible in the static.

¹²⁰I am a bit confused by this. Who would ever leave the tubes just floating around in the media? What would be the point?

¹²¹<https://www.nature.com/articles/s41928-022-00913-9>

The mismatch between hard electronics and neural tissue is often measured by Young's modulus, which designates the flexibility in response to applied force. Much thinner electronics are required to match the electronic and neural tissue moduli. Indeed, such attempts have been done, which require reducing transistors down to nanometer thicknesses. Tissue-like electronics that have been produced prove to be much better at recording single neuron activity over long periods. A considerable consequence of shrinking and shrinking electronics is that there may be accidental crosstalk between nearby transistors.

The brain expands and contracts in a non-negligible way. This is especially true in the developing brain, or in a highly degenerative brain. Thus, electronics would ideally be stretchable to accommodate volumetric changes. This is similarly true for segments of neural tissue that may require flexion, such as peripheral nerves or spinal nerves. Stretchable electronics have been achieved in the past when made as a mesh. Well designed meshes with channels can integrate optogenetics and chemogenetics as well, allowing for the possibility of cell-type specific neural recording and modulation.

Soft electronics like this come with considerable design and production challenges. For example, scaling up high densities of transistors embedded in meshes is extremely difficult. Similarly, these devices are very sensitive to ion or water influx. Further, parasitic capacitance (capacitance due to electronics proximity to one another) is largely unavoidable at small scale. When dielectrics are used as insulators, again possible mechanical damage due to flexion is a possible source of ion influx and thus worsened function.

Chapter 23

Peripheral Nerve Stimulation

Peripheral nerve stimulation¹²² has shown promise in treating nerve damage, but naturally is greatly limited by technology. One such limitation is the difficulty in targeting peripheral nerves that may be lodged deep within the body. Too, once reached, one must avoid off-target stimulation, movement of the electrodes over time, and swelling in surrounding regions. Removal of leads after the completion of neurorehabilitation can cause further damage as well, as tissue may become attached to it, resulting in a second injury.

23.0.1 Adaptive, Conductive, and Electrotherapeutic Scaffolds

Adaptive, conductive, and electrotherapeutic scaffolds (ACESs) is one implementation of electrical neurorehabilitation after injury¹²³. The primary structure is electrodes embedded in alginate (an anionic polymer, which creates a maleable gel-like structure when combined with water, and is often used for creating molds) and polyacrylamide (a cationic polymer most known for its use in SDS page gels, and can be used to suspend solvents at various stiffnesses)—which can be dissolved, allowing for removal of leads with minimal damage to tissue. Because the electrodes are located within the gel, glial encapsulation is not to occur (or, if it does, it will be at the borders of the gel and not the electrodes themselves)—therefore, stimulation should be un-dampened. Gold particles were used to increase conductivity of the gel.

In rats, in order to test accessible nerves, sciatic nerve transection was performed, and electrodes were used for 6 weeks. Stimulation was delivered every other day for 30 minutes in **anesthetized** rats. It was delivered to each electrode at 20 hz (every 200 ms), 2 mA¹²⁴ amplitude, and a 100 μ s pulse width. They used a stainless steel electrode by Plastics One¹²⁵. Stimulation was powered using the Intan system¹²⁶. As two electrodes were used, their pulses were offset by 100 ms. The two stimulating electrodes were proximal and distal to the injury site, and a third, ground electrode was located at the tibialis anterior muscle. EMG recordings and response to sensory stimulation were used to validate functional success of regeneration, as well as axon counts. To test percutaneous nerve stimulation, they performed a similar procedure on the vagus nerve of swine.

¹²²Annoyingly, peripheral nerve stimulation is often abbreviated as PNS, so do not get confused with peripheral nervous system vs. nerve stimulation.

¹²³<https://www.sciencedirect.com/science/article/pii/S2666634023001654?via%3Dihub>

¹²⁴It is not clear to me why they choose to deliver current rather than voltage.

¹²⁵Interestingly, I can't seem to find a product that resembles the one found in their supplemental images. Still it is probably comparable: <https://www.protechp1.com/search?q=MS303&type=products>

¹²⁶https://intantech.com/RHS_system.html

23.0.2 Vagus Nerve Modulates Circuits via Acetylcholine

Vagus nerve stimulation seems to be much more complex than you'd expect on surface. One such example is¹²⁷. Vagus nerve stimulation (VNS) has shown to enhance motor recovery after nerve injury when paired with rehabilitation. Canonically, VNS is used to treat epilepsy and depression—but new treatment options are expanding, such as recent papers looking into treatment after a stroke. Notably, VNS leads to widespread brain activity, but seemingly had a narrow, targeted effect. This paper identifies M1 neurons as being partly responsible for enhanced motor control following VNS. **Importantly, this was tested only in healthy mice, and not any form of nerve injury.** Their work found that VNS specifically *after* successful completion of a task helped reinforce learning of this task—therefore, it may not work as a therapeutic in the case of total injury, but could help recover partial injuries back to normal levels.

Awake, active mice were stimulated via cuff which wrapped the Vagus nerve. Machinery was mounted on the skull, from which wires would extend. They tested a few different methods, and found stimulation following success to be the only positive difference from the sham. Stimulation was done with 100 μ s pulses at a frequency of 30hz (or, every 33.3ms) a total of 15 times (entire duration summing to 500ms) at an amplitude of \approx 0.5mA. Looking at their figure 1, there are some questions. Firstly, what they decide as early and late in the training days seems arbitrary (i.e., first 4 days is early, second 10 is late). I am curious if you thresholded this differently, if their significance levels would change. Secondly, the VNS stimulation results were significant, but the % increase in task completion from WT to stimulated seems only to be about 10-15%. Similarly, the difference in early vs. late trials seems to be about 10% as well—making me wonder how physiologically relevant this is¹²⁸.

To determine what is downstream of VNS, they used a tetrode implanted into the brain to read the response of neurons in the basal formation, as they wondered if it was here that encoded for reinforcement. They found that about 43% of neurons showed some response (either suppression or activation), and about 28% showed an increased activity due to VNS. Now, I'm no expert, but those don't seem like great odds to me. That seems like a coin toss. I didn't see much mention in this paper of trying different VNS parameters. I would postulate that they'd get a much better response in tweaking this. An experiment they could run right away is using the tetrode, and varying peak duration, amplitude, and frequency of stimulation to maximize this increased activity parameter. They could then repeat their behavioral studies and see if it increases success rate. Interestingly, they did something similar in the motor cortex, investigating temporal relationship of activation or suppression of neurons over a range of amplitudes. They found that neuronal activation and suppression occurred at disparate times succeeding VNS. Fascinatingly, to test if this observed interaction was ACh dependent, they injected ACh antagonists and allowed them to act globally—effectively invalidating the entire experiment¹²⁹.

As a concluding remark, it seems from their data that VNS may contribute to motor learning reinforcement, but certainly is not the essential driving factor. Similarly, I did not see a “negative control” anywhere in their paper (i.e., a vagotomy, for example) demonstrating that motor learning was severely hindered when this pathway was stopped¹³⁰. Many of the decisions made in this paper are quite confusing to me.

¹²⁷[https://www.cell.com/neuron/fulltext/S0896-6273\(22\)00555-4#%20](https://www.cell.com/neuron/fulltext/S0896-6273(22)00555-4#%20)

¹²⁸I.e., would a patient consider brain surgery to have a 10% increase in some motor activity? Absolutely not.

¹²⁹I must be missing something, because this experiment makes no sense.

¹³⁰Perhaps it is buried in the supplements, or done in a previous paper, though.

23.0.3 Hand Movement Recovery via Intrafascicular Stimulation

This group utilized intrafascicular, rather than intramuscular, stimulation as a means to recover fine motor skills in the hand of primates¹³¹. Of course, Courtine is also on this paper. A drawback to intramuscular surgery is it requires electrodes placed on multiple muscles and is typically quite invasive. Very interestingly, intramuscular stimulation has been found to recruit large efferent nerves before small, contrary to normal function and leading to faster fatigue. In other words, faster fatiguing muscles are activated earlier than expected in this case. Stimulating an entire nerve fascicle requires high amplitude and is prone to overstimulation or recruitment of unintended nerve fibers. Intrafascicular stimulation is an opportunity to resolve this.

Such a method requires first identifying the ideal implantation site and building an electrode design accordingly. They call their device a transverse intrafascicular multichannel electrode (TIME). They developed a model of the monkey's fascicles in order to model recruitment¹³². They settled on a 16-electrode design, withheld in a polyimide shaft.

The bulk of the paper is stimulating individual or combination fibers to initiate a variety of different grips. The end is when they take it to the next level, so-to-speak, in giving the monkeys some voluntary control. They pharmacologically block the monkey's spinal cord circuitry. They used intracortical recordings to modulate hand stimulating, using what they describe as a simple program. Their design was too simplified to activate complex grips, but did prove to work in simple grasping tasks.

¹³¹<https://www.science.org/doi/10.1126/scitranslmed.abg6463>

¹³²I don't know how they did this, but it would be good to learn.

Chapter 24

Spinal Cord Stimulation

A large part of spinal cord stimulation, particularly epidural electrical stimulation (EES), is in fact not neural stimulation directly, but rather CSF stimulation¹³³. EES requires the implantation of electrodes onto the dorsal surface of the spinal cord. As was identified through this computational model, depolarizing signals spreading through the CSF are capable of triggering large, afferent fibers. Such fibers are most easily accessible at their dorsal root entry zones. Their activation leads to motor neuron activation, or the conversion of an inactive circuit to an excitatory one. The bulk of this investigation is done at the lumbar level, as its focus is on restoring walking after SCI. However, other studies have replicated the idea in hand dexterity when stimulating the cervical dorsal root entry zones.

An unsung hero which operates by similar means is transcutaneous stimulation—done through the skin, making it non-invasive and easily performed. Of course, it lacks the precision of EES, but has been used to promote motor recovery after SCI.

24.0.1 Electronic Dura Mater

A couple years ago now, Courtine and Lacour groups developed a framework for electronic dura mater¹³⁴. One of the primary problems addressed here is that dura mater is hard and protective while neural tissue is soft—so if one were to remove the dura and replace it with an electronic, it would need to meet both of these criteria. Their “invention” is called e-dura. It is meant to go beneath the dura mater, and is composed of silicone with gold wiring¹³⁵. The silicone has a similar kPa to the dura itself. Most implant are done above the dura, so the soft nature allows for implantation beneath it.

One of their comparisons is in implantation of soft vs. hard electronics in locomotion (this is without spinal cord injury). Notably, the soft electronics performed the same as the sham—while the hard electronics were much worse. They similarly quantified damage to the spinal cord, and expectedly found that soft electronics did less damage, and similarly that there was more inflammation in hard electronics. They also made a model of the linak cord using a hydrogel to show similar effects—perhaps useful to keep in mind.

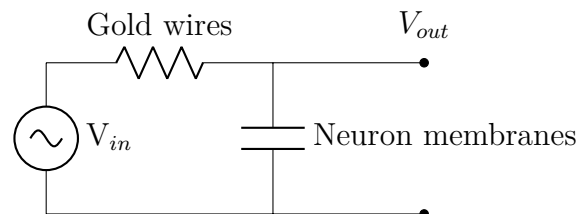
I’ve noticed this same thing in a few papers. But, they make the claim that impedance stays constant over the course of a few weeks. However, the error bars show an impedance of $\approx 50\text{k}\Omega \pm 30\text{k}\Omega$. Firstly,

¹³³<https://www.jneurosci.org/content/33/49/19326.short>

¹³⁴<https://www.science.org/doi/abs/10.1126/science.1260318>

¹³⁵I didn’t realize this until just now, but the increased impedance over time is due to micro-cracks in the gold. Interesting to keep in mind.

this is quite high impedance—but that may be a protective feature. Secondly, and more crucially, the spread is humongous. My wonder is if the Reviewers did not notice or understand this, and saw that the average stayed around the same. Impedance does seem to be quite variable / strange in every paper. So it also may be that controlling this is quite hard. There is also quite a large phase angle, reaching $\approx -30^\circ$. Notably, *in vitro* there is no phase shift nor is the impedance near $50\text{k}\Omega$. The $\approx -40^\circ$ shift is suggestive of this being a low-pass filter at their tested 1kHz . Very fascinatingly, the circuit may look something like this¹³⁶:



In vitro, you would see this phase shift because there are no capacitors to ground. Let us take this a step further, even. If:

$$\begin{aligned}
 A_{out} &= A_{in} \sin(\omega t + \phi) \\
 \frac{V_{out}}{V_{in}} &= \frac{1}{\sqrt{1 + (2\pi f RC)^2}} \\
 \sin(\omega t + \phi) &= \frac{1}{\sqrt{1 + (2\pi f RC)^2}} \\
 \sin(-40^\circ) &= \frac{1}{\sqrt{1 + (2\pi \times 1\text{kHz} \times 6\text{k}\Omega \times C)^2}}
 \end{aligned} \tag{24.1}$$

I estimated R to be $6\text{k}\Omega$ by eyeballing their graphs. I couldn't find any raw data in the paper. Solving this gives us a C value of $3.16 \times 10^{-8}\text{F}$, or 31.6nF . This does seem a bit low, as I believe the standard estimate for a cell membrane is around $100\mu\text{F}$. However, there are likely many factors at play.

I digress. The functional tests they did were using a 3×3 array of electrodes, and the motor cortex of mice were stimulated using channelrhodopsin-2. The e-dura demonstrated the ability to record signals sent from the cortex. They then tried delivering stimulation after spinal cord injury, induced via severe contusion. They delivered serotonergic replacement therapy through microfluidic chambers in the e-dura and delivered continuous stimulation at 40Hz , 0.2ms , and 50 to $150\mu\text{A}$. Naturally, stimulation improved locomotion.

24.0.2 Electronics with Shape Actuation

The goal of this paper is to address the gap in stimulation devices¹³⁷. That is, one can choose either percutaneous electrodes (i.e., puncturing through the skin and covering a small area) or a large paddle requiring invasive surgery. This paper developed a flexible paddle, which can be rolled up to a diameter of less than 2mm , and injected similar to an electrode but expands upon entrance. Too, the flexible shape is fitted with microchannels. Applying air pressure to such channels causes expansion.

¹³⁶This is why you should read the electronics section.

¹³⁷<https://www.science.org/doi/10.1126/sciadv.abg7833>

It is composed of materials like gold, parylene-C, silicone, polyethylene, and polyimide.

The device is made in two stages, but is monolithic. The first silicone layer is laid, and before it is fully cured, secondary materials are added. Then, the final layer of silicone is laid, and the entire device cures together. To validate it electrically, they used “electrical impedance spectroscopy techniques”¹³⁸. Interestingly, the impedance was calculated to be around 1000 Ω ! And it was quite variable; their box plots show an IQR of about 600 to 1200 Ω . This is, indeed, not ideal. One concern is how much power will be dissipated by current running through the device, thereby generating heat (and possibly causing device expansion). They also tracked increase in impedance due to mechanical stress, and it seems to increase from about 500 to 1000 Ω —representative of an approximately new device vs. approximately 6 years old within the body¹³⁹.

The device has a diode-like IV curve¹⁴⁰. They look exactly like a diode would in the positive half (i.e., current exponentially increases at about 0.8V). But the negative voltage range looks quite strange. To apply voltage, they used the Intan device, like in the ACES paper.

The claim is that they are able to implant the entire device using a syringe (presumably under the lamina) into cadavers and then expand the device over the dura mater. Somehow, the how the device is able to spread over the spinal cord while, despite all of the connective tissue and fat filling the lamina-dura space¹⁴¹. To find the desired site of implantation required fluoroscopy, meaning the device itself had to be visible under fluoroscopy. Another confusing aspect of this paper is the biphasic nature of SCS to treat neuropathy. As one always undergoes a trial period, the question is will this device complement the trial phase properly?

The big takeaways, to me, are that expansive devices seem possible, and fitting it with microfluidic channels is a fascinating way to apply therapeutics in addition to electrical stimulation. The next question is, of course, can we do the same thing with ECoG—thereby not requiring a highly invasive procedure to record brain waves?

24.0.3 SCI Specific Cells

Using a simplified device similar to what will be discussed in the upcoming Lorach *et al.* 2023 section, the Courtine group used electrical therapy to re-establish walking in a number of SCI patients¹⁴². Their paper goes into depth on the cell-type specific response to this electrical modulation. They called this model epidural electrical stimulation (EES) + rehab, or EES^{REHAB}. They first approached by measuring metabolic consumption in the spinal cord before and after EES^{REHAB} using PET scanners, and found that metabolism actually **decreases** in the face of EES^{REHAB}, despite regaining the ability to walk. Therefore, they hypothesized that EES^{REHAB} “cleans up” the circuits a bit, causes activity to become targeted for walking.

To investigate which specific neurons undergo changes, they used a mouse model and performed RNAseq. They found excitatory interneurons as being enriched upon EES^{REHAB}. These neurons

¹³⁸It is not clear to me what they are referring to, beyond simply driving different currents. There is a paper discussing this here, though.

¹³⁹How they could approximate a 6 year old device is questionable to me.

¹⁴⁰For lack of a better word, the IV curves look insane.

¹⁴¹All of this is very odd to me. I am having trouble understanding how this is possible mechanically.

¹⁴²<https://www.nature.com/articles/s41586-022-05385-7>

were identified by the markers *Vsx2* and *Hoxa10*, and thought to be *V2a* neurons. These neurons projected exclusively to the ventral spinal cord and formed synapses with varying neuron types (glutamatergic, GABAergic, and cholinergic in no preferred proportion). The synapses were found in dense appositions (i.e., many synapses side-by-side) and SCI caused a reduction in such appositions. Ablating/inactivating these neurons alone in non-SCI mice did not halt their ability to walk. However, inactivating them did halt walking under EES^{REHAB}. Therefore, it is hypothesized that these neurons are specific to the injury condition and required for recovery after SCI.

The main takeaway from this paper, in my opinion, is simply the recapitulation that excitatory interneurons play a key role in recovery from SCI. This has been established now through many routes, and is certainly of considerable interest in the future. There are a few open questions, with the biggest being: how exactly does electric modulation drive circuit reformation through these interneurons?

24.1 Clinical Applications

Reduction of Pain.

This description comes from Dr. Iahn Cajigas, and this video¹⁴³. In reducing neuropathic pain, the mechanism by which it works is postulated to be Gate-Control Theory¹⁴⁴. After this publication, spinal cord stimulators became available in 1965. The hypothesis was painful signals can be overridden by other pathways. Namely, fast, large A β nerves can override the smaller, pain carrying A δ and C fibers. It is thought to occur at the level of the dorsal horn through inhibitory interneurons, but this is not known with certainty.

Failed back surgery is the most common need for spinal stimulation of this kind. Stimulation is a good treatment option if the patient's pain is localized, and no identifiable structural defects are found. That is, if one's spinal cord is still improperly aligned, stimulation should not be considered. It is essential to attain extensive pre-operative imaging, as structural issues can also lead to hardware malfunction. For example, a slipped disc may cause unforeseen warping of hardware. Interestingly, psychiatric symptoms is a common indicator of poor patient outcome. Repeated operations usually indicate less effects as well.

Implanting an electrodes is done in two stages:

1. Trial: A lead is inserted in order to find the site of pain. That is, exactly where to place the electrode permanently is found first in a trial. In the trial phase, patients are usually kept awake.
2. Permanent: After such place is found, a permanent surgery can be scheduled for long-term treatment.

A variety of stimulators exist, ranging from linear leads to paddles. Paddles will require laminectomy by a neurosurgeon, but less invasive leads do not necessarily need this.

The stimulation itself has changed greatly. That is, the frequency, amplitude, etc. has been widely investigated. For example, bursts of stimulation, as opposed to continuous stimulation, has been recently tried. Notably, burst stimulation is usually imperceptible to patients, making it preferable in

¹⁴³https://www.youtube.com/watch?v=MULbgftczf8&ab_channel=CongressofNeurologicalSurgeons

¹⁴⁴<https://pubmed.ncbi.nlm.nih.gov/5320816/>

many cases. It is hypothesized that burst stimulation may inhibit both the physical and emotional aspects of pain.

Regaining Motor Control.

This is from this video¹⁴⁵. EES is performed on SCI patients following a long period of physical therapy. The physical therapy has two purposes. First, it is to determine whether or not someone can recover at all without surgery. Two, it is to “prime” the cells for rehabilitative EES.

The operation requires complete anesthesia, placement of the electrode on the outside of the dura (i.e., epidural stimulation). It requires a laminectomy. The device they used is the same one as is used in treatment of chronic neuropathies. Importantly, the electrode is not placed nearby the injury site. In this patient, the injury was in the upper thoracic area, but the electrode was placed in the T_{12} area. They also used an EMG with electrodes in the muscles in order to trial and error the placement of the electrode. The entire surgery took ≈ 6 h. The battery pack is also added within the patient a few days later.

Absolutely remarkably, the patient was able to regain some motor control the first time the device was turned on.

24.2 Advancements in Parkinson’s Disease

Founding Works.

In large part, tremors induced by PD have already been well solved through deep brain stimulation and high intensity focused ultrasound. However, this paper focuses on some of the non-tremor symptoms of PD, and the idea that one can use spinal cord stimulation to fix degenerative diseases is generally interesting, so let us learn from¹⁴⁶. The premise of this experiment is somewhat surprising, as stimulation is often thought to interrupt signals (as is the case in deep brain stimulation for PD, and SCS for neuropathy). In this case, though, they believe SCS **enhances locomotor signals**. That is, they are not treating PD tremors, but rather are treating PD induced akinesia. Experiments were performed in mice using dopamine-transporter knockout (DAT-KO) as their PD model. They also injected tyrosine hydrolase inhibitor (called AMPT)¹⁴⁷ to further deplete dopamine. Dorsal root stimulation was performed using electrodes into the upper thoracic levels of the spinal cord. The greatest locomotor improvement in locomotion was found at 300 Hz stimulation.

Notably, some hospitals are currently attempting clinical trials for spinal cord stimulation’s use in treating Parkinson’s. Some efforts include blocking pain and treating akinesia. [Note from future Jackson: When I first read this paper a few months ago, I thought it was a bit silly. It was difficult for me to see why one would attempt this, when DBS is already so powerful. I figured it would go no where. Yet, read on:](#)

¹⁴⁵https://www.youtube.com/watch?v=0ubpMu-2EcE&ab_channel=MayoClinic

¹⁴⁶<https://www.science.org/doi/10.1126/science.1164901>

¹⁴⁷I didn’t bother Googling what this is, but intuition would suggest it aids in the conversion of tyrosine to catecholamines.

24.2.1 SCS-DBS Intersection

Here we discuss¹⁴⁸. Dr. Ramayya, an MD-PhD neurosurgeon I had the pleasure of talking to, commented that after seeing this work his first thought was “you don’t have to be the best at everything.” Indeed, this work is so awe inspiring that it makes one question their place in the field.

DBS treats a very small subset of symptoms associated with PD. Because of the success of EES in treating SCI, these groups wondered if a similar feat can be accomplished in PD patients. The first bit of this work was done in an NHP model (rhesus macaque). Because of differences in monkey and human mobility, they developed a scoring technique to analyze PD models in NHPs and compare them to human PD symptoms. The preferred PD model for them was administration of MPTP, a drug able to mimic the death of dopamine producing neurons. They compared spinal circuits before and after MPTP and identified “hot spots” in the spinal cord. In implanting these devices, they stimulated different electrodes in the array in order to test their ability to cause muscle contraction.

After these tests, they then aimed to use a brain-spine-muscle interface as they had in their other foundational works. Microelectrode arrays were inserted into the cortexes of RHPs and were able to regularly decode motor signals. They then furthered this by inserting EMG electrodes into the legs of NHPs¹⁴⁹. The neuroprosthesis together improved natural movement and posture. Finally, they added DBS to their circuit and found further improvement of movement.

In humans, the ability to decode motor movement may be difficult in people with PD. Therefore, their first step was to recruit participants willing to get electrodes implanted into their cortex for reading their intended movements. They considered this a success and moved forward. They enrolled a patient in their STIMO-PARK clinical trial. The patient already had DBS, but still had some severe symptoms. They used a SCS paddle used in treating pain, connected to an Activa RC IPG, guided in location by CT and MRI. Rather than implanting an ECoG to read the patient’s motor cortex, they instead used motion sensors and attempted to read motor intentions and send updated pulses to the stimulator that way. Fascinatingly, DBS and EES seemed to treat different symptoms at times, and act synergistically. That is, DBS^{ON} - EES^{OFF} showed no improvement in “fraction of time frozen,” while DBS^{OFF} - EES^{ON} showed total recovery. Their benefits were generally additive, though.

Questions: feasibility of this surgery on a large scale—that is, it is a hefty surgery, patients will typically be older, perhaps it sucks a ton of power and thus requires more frequent battery replacements, etc.

¹⁴⁸<https://www.nature.com/articles/s41591-023-02584-1>

¹⁴⁹I am really wondering if some nice code can use this kind of data to iterate and self correct. Need feedback, of course.

Chapter 25

Brain Stimulation

25.1 Deep Brain Stimulation

Deep brain stimulation is an ever increasing field of study. First popularized for treatment of tremors, it is not becoming generalized for many more disorders, including OCD. In the case of nerve injury, noninvasive methods like transcranial direct current stimulation and transcranial magnetic stimulation have been done with some success, especially when combined with rehabilitation, particularly in recovery of hand dexterity after injury. It is thought that recovery occurs through growth of descending corticospinal tract neurons. Needless to say, brain stimulation is an expanding field with many routes of exploration.

25.1.1 Technology Overview

Primarily drawn from¹⁵⁰. Deep brain stimulation was first performed at Columbia by Dr. Lawrence Pool for psychiatric patients. It's use in treating Parkinson's disease was coined by Dr. Carl Wilhelm Sem-Jacobsen. Early usages were based on cardiac pacemakers. The first closed-loop works were done in 1980.

Electrode Design.

The linear electrodes we know and love are composed of platinum-iridium wires and nickel alloy connectors.

Questions for Dr. Cajigas:

1. "...integration with the extension cable surgically challenging"—what?
2. Why current over voltage? Surely you're depolarizing the extracellular space, so a clamped voltage makes more sense. I'd think you'd want a unipolar device driving voltage. Note from future Jackson: It's because current is considered to be more consistent in delivering charge. It is also easier to channel current, and or, ensure it is applied over a region. That is, you could supply a constant voltage, but said voltage drop may occur over an ambiguous region. Another comment, which is probably worth putting elsewhere, is that the "impedance" measured by technicians is very ambiguous. Presumably they perform a frequency sweep, but it is difficult to nail them down on what they are exactly doing. It's also not clear that impedance will rise over time.

¹⁵⁰<https://www.nature.com/articles/s41582-020-00426-z>

If we take the cell membrane to be a capacitor in series with a resistor, driving a voltage to one side seems to give much more reproducible results than does current—especially when you consider different membranes to have different capacitance.

25.1.2 In the Clinic—Parkinson’s and Essential Tremor

For this section, I’ll discuss broadly how deep brain stimulation works clinically, including an outline of the procedure. I’ll discuss primarily from my experiences with neurosurgeons Dr. Casey Halpern and Dr. Iahn Cajigas.

Before Surgery Begins.

Candidacy (which drugs to try), HiFUS vs. DBS, etc.

25.1.3 The Surgery Itself

Deep brain stimulation is done in two steps. The first step is the primary brain surgery itself, which constitutes implantation and initial testing of the electrodes. The second is implanting the battery, somewhere in the chest, and connecting it to the electrodes. The steps are split because the duration of surgery is highly correlated with infection rate, so minimizing total length is helpful in suppressing infection whenever possible.

The first surgery takes approximately 4 hours total, from bed, to operating room, and back to bed (4 hours bed-to-bed, as I call it). It begins with a pre-operative CT scan, which is required to guide the electrodes into place. The beginning portion of the surgery is done while the patient is under anesthesia, but the later stages allow the patient to be awake. A frame is placed on the patient’s head, and a rotating coordinate system allows the team to precisely mark where the electrodes will enter. A surgeon scrapes away the outer layers of the skull, dura, and arachnoid space to reveal the brain. Using the frame, an electrode is inserted and slowly transverses the layers of the brain until it reaches the desired target. Such transversing is accomplished with a nearby physiologist, who records brain activity from the electrode as it is lowered into the deeper segments. Naturally, the way one does this depends on which target you are aiming for. A fascinating metric one can use, if the GPi is the target, is that just below the GPi is the optic tract. Thus, the team may turn all the lights off in the room and flash a light on the patient’s face. In doing so, they’ll stimulate the optic nerves, and a faint signal can be seen when reaching the bottom of the GPi.

Once the electrode is in place, and its location is confirmed with a second scan, the patient can be awoken. The purpose of this is to do some initial testing and verify that the stimulation is not impacting nearby sites. The current is slowly ramped, and you ensure that the patient is cognitively intact and doesn’t experience any tingling. If the patient has strong tremors, there is sometimes an immediate benefit. Typically, though, initial benefits are to be taken with a grain of salt. This is because the entrance of the electrode itself can cause inflammation and damage to the site, which may in turn halt symptoms. Benefits in stimulating the STN may arise quickly, but stimulating the GPi usually requires more time.

Targets.

Device Options.

Boston Scientific has most up-to-date rechargeable battery, which lasts approximately 15 years.

25.1.4 Living Electrodes

This is from the work by Dr. K. Cullen, and featuring Dr. I. Chen¹⁵¹. Part of the problem they are trying to solve is the rigidity of standard, mechanical electrodes. To solve it, they developed implantable cortical neurons embedded within a hydrogel tract. This paper mentioned another drawback of standard, inorganic designs causing overheating of surrounding tissues—this is the first time I’ve seen this mentioned, and I have frequently wondered about it.

The platform they use is called microtissue engineered neural networks (μ TENN). The gist is they make a hydrogel tube, culture neurons in kind of a cluster (or, aggregate), place this aggregate at one end of the tube, fill the tube with ECM-like compounds to promote axonal growth across it, and then implant the tubes where the synapses will be formed at the end opposite of the cell bodies. The columns are $\approx 400\mu\text{m}$ wide, with only the inner $\approx 180\mu\text{m}$ being made up of cells. They are made between 2 and 9mm in length. Action potentials can propagate bi-directionally in some models, or uni-directionally, depending on how it is made. Their experimental setup in this paper, for example, is to use a uni-directional setup with optically activated neurons, and record the induced activity through a second, bi-directional column (that is not optically activated). Channelrhodopsin-2 (ChR2) was used as their optic input, while RCaMP was used as their output reader.

In vitro, interestingly, they show that the max $\Delta F/F$ increases with increased optic power. However, they do not show it levelling off at any point—which would have good to know (i.e., where the point of max stimulation is). They also didn’t show the baseline intensity over time (for more than 20 seconds, that is), which might have been interesting to see. The fluorescence plots over time seem quite variable. That is, RCaMP $\Delta F/F$ is not uniformly affected at the point of each stimulation. *In vivo*, the non-uniformity is even worse. I would assume there is some accumulation of RCaMP fluorescence over time, as repeat stimulations slowly build up more calcium. Parallely, one might expect the baseline intensity to go down as RCaMP becomes bleached.

There are many limitations to consider. For example, RCaMP’s k_{on} or k_{off} , reset time for ChR2, refractory period of neurons, the time it takes to grow neurons (which seems to be closer to a week or more), necrosis within the aggregate, etc. Too, you lack any real understanding of the neuron if using living electrodes as sensors. That is, you don’t get much localization or intensity information (if any). Confusingly, from watching their supplemental videos, the potential seem to be wave-like, flowing horizontally across the columns rather than one instantaneous pulse. Perhaps this is due to the k_{on} of the calcium indicator used, but it seems to indicate some strange temporal differences in activation—i.e., the depolarizing of one neuron within the aggregate may cause the depolarization of another nearby that is independent of its intent as a sensor. This would be comparable to a spreading depression one might expect in a migraine, but instead of being within a brain, it is within this cultured cluster.

¹⁵¹<https://www.science.org/doi/full/10.1126/sciadv.aay5347>

Ramblings.

What is fascinating about reading papers like this is I go into them every time thinking “Wow, this method sounds remarkable! Perhaps this will be the secret to next-gen BCIs.” Yet, I always finish the paper with more questions / critiques than I began with.

Chapter 26

Reading Thoughts

At present, I am unsure if reading one's thoughts is a requirement at all for overcoming SCI. I am unconvinced that electrical stimulation controlled by one's brain is better than electrical neurorehabilitation—or if it is better by any measurable margin. In investigating this, I believe the limiting factor in bridging from the stimulation applied by Tator and Minassian is a reliable way to read one's objective through their brain waves. The Lorach *et al.* 2023 solved this using the WIMAGINE system¹⁵². But, let's begin by discussing the options and a bit of history.

26.0.1 Different Reading Devices

As you would imagine, there is a tradeoff between the resolution and the damage you will confer upon one's brain. This is described well by Schwartz in 2006, so notably technology may have advanced since then¹⁵³. The four classes of devices are:

1. Electroencephalography (EEG)
2. Electrocorticography (ECoG)
3. Local field potentials (LFPs)
4. Single Unit AP

EEGs, naturally, are non-invasive and have a reading range on the order of a few centimeters. ECoG is on the tenths of centimeters level, while LPS is millimeters level. Single unit AP is as the name describes, and reads individual action potentials. EEGs sit far above the cortex, outside of the skull, and ECoG come in contact with it. Both LPS and single unit require the electrodes to be buried within the cortex itself, thus causing damage to the brain tissue. Therefore, EEG is typically preferable, as it does not require surgery. It is highlighted by Schwartz that many negatives can occur long term from invasive procedures, such as degeneration, volume displacement, or glial encapsulation. Therefore, it is for this reason that I presume the ability to read one's objective was the limiting factor in progressing the field.

For the moment, I will avoid describing individual technologies between the four groups, as it is likely that the tech progresses greatly each year, and it would be pointless to attempt to describe the reading ranges of any without being totally up-to-date. Instead, we will discuss the WIMAGINE in depth here.

¹⁵²<https://www.frontiersin.org/articles/10.3389/fnins.2019.00847/full>

¹⁵³<https://www.sciencedirect.com/science/article/pii/S0896627306007264>

Soft vs. Hard Electronics.

The importance of the electronic's physical form has been considered by the Courtine group as well¹⁵⁴. In their case, they looked specifically at the electrode paddly inserted into the spinal cord. Notably, they did not use this device in their recent, Lorach *et al.* 2023 paper. One problem I personally find is that in using hard electronics, one immediately resolves to doing massive cranioplasty in order to add their device. If one goes the soft-only electronics route, perhaps you can insert the electronics beneath the skull itself.

26.0.2 Reading LFPs Without Surgery

A very recent article devised injectable electrodes for reading brain activity¹⁵⁵. It is injected through blood vessels, and requires vessels of $\approx 100\mu\text{m}$. For reference, the smallest arteries are around $\approx 100\mu\text{m}$, and arterioles below this threshold. Therefore, this is usable in a wide range of vasculatures. Such a device is considered a micro-endovascular (MEV) probe. Other attempts at this have been done in the past, but a primary limiting feature is that metal electrodes are inflexible and thus cannot be navigated through the array of vessels in the brain. One of this paper's primary advancements, then, was making it ultra-flexible. I'm actually having trouble understanding how many electrodes the device has—in some graphs they show 16, in others only 5. It seems that they too use an Intan device to read and process data.

The device is injected through a microcatheter, which itself has a much wider diameter. Therefore, the location of implantation is limited in that it must be accessible by a wider vessel nearby. In their example, a large vessel branched off into two directions. To select between the two branches, they had to change the mechanical properties of the device itself¹⁵⁶. My understanding of their method of inducing this was by stressing part of the mesh making up the device.

Their testing was done in anesthetized mice in both wildtype and disease models (such as induced seizures). In such circumstances, they were able to record local LFPs. In some instances, though, they were able to get single AP recordings on individual electrodes. Interestingly, this paper included both the filtered and unfiltered readings, providing some nice insight into the benefit of bandpass filtering!

Some confusions: I'm not sure exactly if this is meant to be a permanent addition or not, or if it is removable atraumatically. Similarly, I'm not understanding how they are actually reading from the device. Their setup in the supplements seems to require anesthetizing the mice and doing surgery to attach the electrodes to the Intan device—which I assume cannot be true, lest the whole purpose is defeated. So my wonder is: are the mice walking around with wires hanging from their skulls, or are the wires inaccessible without surgery? I should probably read more closely to understand.

NOTE: A K. Cullen paper cited in the above article¹⁵⁷. Read later.

¹⁵⁴<https://www.science.org/doi/10.1126/science.1260318>

¹⁵⁵<https://www.science.org/doi/10.1126/science.adh3916>

¹⁵⁶This is likely a considerable limitation. It is unlikely that this sort of device will ever become generalized or patient specific. However, its use in research might be considerable.

¹⁵⁷<https://www.frontiersin.org/articles/10.3389/fnins.2019.00269/full>

26.0.3 Neurograin

Neurograin (a type of ECoG) is an interesting development that includes both the ability to read and stimulate the brain from small, rice-grain sized chips¹⁵⁸. Neurograins are individual pieces, providing the immensely powerful ability to scale your device. They verified their method using 48 electrodes, but suggested the ability to scale to up to 770—providing quite impressive resolution.

The core achievement of this paper is in developing microchips of less than 1mm in size, that are able to read and transmit information. However, I am slightly confused by the intended use. In their Figure 1, they show the neurograin array beneath the dura, and a wireless power/download port wirelessly connect from above the skull. It isn't clear to me how they intend to use this—as they'll need to remove the dura in order to implant the device. A possibility application would be to make a network that can be “woven” into the spinal cord, allowing you get to readings with minimal (if any) laminectomy.

One large question I have is how they are processing this data. In the case of a PET scanner, which has a similar 1GHz+ sampling, instead of overloading the computer with billions of data points a second, it has a 2-step sampling approach, where data is discarded unless it is “non-zero.” That is, data is transmitted only when light hits a receiver. In this case, I'm not sure if that is possible, since brain waves will not be binary.

The bulk of the paper is very electronics heavy, so it will be good to reference in future builds.

26.0.4 Robotic Control with Eye.

Here we discuss¹⁵⁹. Usually, when we think of neural prosthetics or brain-computer interfaces, we think of their use in treating spinal cord or traumatic brain injury. However, there are many of really fascinating uses of brain computer interfaces beyond this. One such example is in ALS. Interestingly, muscles of the eye are unaffected by ALS. Therefore, while the rest of the body loses motor control, theoretically eye movements can be used to interact with the world. This paper used EEG signals and resolved eye movements—which are normally considered noise in an EEG.

EEG, being a non-invasive reading technique, is ideal for patients. Notably, unintentional, automatic blinks produce a smaller spike on an EEG than do intentional, voluntary blinks. These researchers used 5 subjects and attempted to monitor voluntary blinks as well as left and right looks in order to control a robot. They did so through some basic thresholding algorithms, followed by a training algorithm. They used this approach for real-time processing of EEG data. As a side comment, they wrote this in Python, which is surprising to me, because EEG produces a ton of data, so I'm surprised Python is fast enough to process it all “real time.” They did mention, though, that their real-time algorithm is much less accurate than their “offline” algorithm, which may be due to differences in how they process data to speed it up. Their accuracy was in the 75-80 % range for the three movements they tested.

Long term investigation and optimization of eye tracking will be helpful for a variety of neurodegenerative diseases, so this is a helpful step in this path.

¹⁵⁸<https://www.nature.com/articles/s41928-021-00631-8>

¹⁵⁹<https://www.nature.com/articles/s41598-023-44645-y>

26.0.5 WIMAGINE ECoG

As the name suggests, the device requires the skull to be torn away and must sit directly upon the dura, above the motor cortex. It features 64 electrodes, and a human patient would need to have two implanted in order to read both sides of one's cortex. The device lacks a bit of the spatial resolution, as it does not directly touch the brain—but it is surely an improvement on current clinical devices.

The device was tested longest in sheep, which was a 10 month trial. Surprisingly, at the end of the 10 month trial, through GFAP staining, they still found a great deal of glial migration/build-up around the site. They did not quantify this, but in my personal opinion, this does not bode well for our patient—as they will have to spend a lifetime with the device. Secondly, calcification of the skull over the device had begun. This is not inherently surprising, and perhaps is a good sign that the bone was not irreversibly damaged. However, as the device is wirelessly charged, and wirelessly transmits brain information, one must wonder how years of calcium buildup may impact the ability to send or receive information. Too, if the technology needs a dust-up, the surgeons will have to re-destroy these calcified layers. There is quite a lot of fuss made about the fact that the device is wireless, and how it was a decision made to best serve patient comfort. But, in my opinion, it may spell out more long-term harm than good. It is not clear to me yet whether the 8×8 resolution of the electrodes is sufficient to delineate all necessary information. Though, this is the trade-off one must make in choosing between EEG, ECoG, and LPS. The WIMAGINE system digitizes information with 12 bits of resolution. Data is processed through pwelch spectral analysis. From what I can gather, this is simply another implementation of the FFT.

Chapter 27

Synthesis

The purpose of synthesizing the aforementioned parts together to create a brain-machine interface is so that you may skip over the injury altogether, and transmit from brain to body.

27.1 Lorach et al. 2023

27.1.1 Overview

This is the most recent iteration of an ongoing project by the Courtine group. The group used surgical implantation into the skull, over the motor cortex, to record patient movements and wirelessly transmit this to the spinal cord. The technology used to capture these electrocorticographic (ECoG) signals is the WIMAGINE. The design features two antennas, and the second of which transmits motor signals that are to be decoded and sent to a pulse generator. The pulse generator is ACTIVA RC, the same that is used in deep brain stimulation (DBS) or pacemakers in the heart. There is no mention of having the patient replace this in future years, but my assumption is that a new battery will require a new surgery in years to come.

27.1.2 Shortcomings

The three shortcomings explicitly mentioned in the **Introduction** are that **(1)** one using this BSI must have motion sensors on in order to compensate (a sort of PID controller, perhaps), **(2)** that the patient's movement was not perceived as natural, and **(3)** that there was still considerable hurdles in traversing variable terrain. Many more shortcomings exist than this, and we will go through them below.

Motion Sensors.

I suppose it is obvious why one would use a motion sensor rather than an EMG—as it would be too difficult to discern whether the motion itself, or strength of contraction, is too high using an EMG alone. Still, though, I wonder if this is a feasible alternative. Perhaps one can simply predict motion based on EMG patterns.

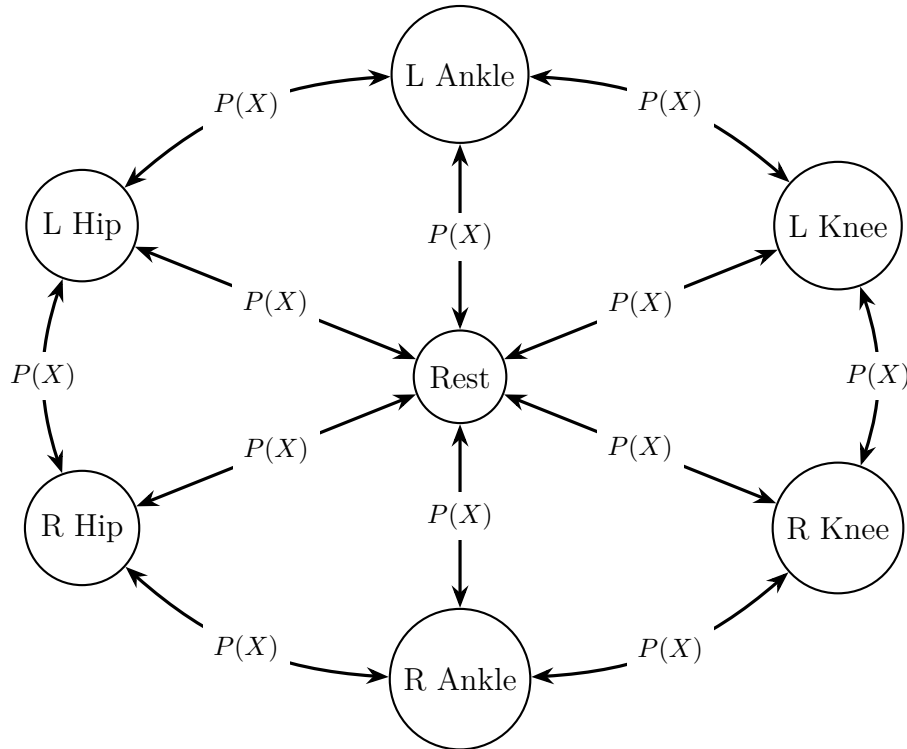
The largest drawback, in my opinion, is their desire to make it quickly programmed/calibrated. As with DBS, one would actually prefer longer calibration time. That is, one would be happy to wait a few extra hours or days if it makes their ability to walk improve.

Similarly, they commented that the patient tested was able to walk without the BSI turned on (using crutches) after some time. This signals three things to me, **(1)** this patient's injury was not, per se, insurmountably severe, **(2)** the plastic abilities of a damaged spinal cord may be better than we had thought—especially since the patient's injury predated this treatment by 10 years, **(3)** that there was likely some important tuning being done by the brain-spine endogenous connection (i.e., their BSI was not doing all of the work), and **(4)** in some cases, no BSI is likely needed at all, and electrical stimulation may be sufficient. This in itself is a quite interesting, alternative patient state. For example, one can imagine a scenario where a patient's brain-spine communication is deeply dampened, but not entirely ceased by damage. Therefore, one would only need amplification of signals as opposed to complete generation of new ones. There may be some of that here. Another comment to make is that their signals are incredibly un-sophisticated, as presented in this paper. That is, they use 16 random electrodes, which do not have connections to synapses themselves. Perhaps this design is to hijack a more reflex-based approach to walking—hence why one can not traverse variable terrain that goes beyond reflexive movement.

A comment regarding the surgery itself: The patient's are having two large, 50mm arrays placed into their skull. Naturally, most would agree to this in order to restore their ability to walk. However, it surprises me that they chose to make the device wireless, given that the surgery is already quite invasive.

Seven States.

Data is processed and used to edit the probability distribution of a Markov chain, which progresses the electrode paddle through seven defined states defined below.



Notably, they did not explicitly mention that one of the progressions could be from state to self state, but one can only assume this is true. So too, only seven states seems to limit the mobility of a patient.

Part VI

Some Ideas

Man takes up the sword in order to shield the wound in his heart sustained in a far-off time beyond remembrance. Man wields the sword so that he may die smiling in some far-off time beyond perception.
– Berserk by Kentaro Miura

Chapter 28

Ramblings

This section will largely be messy—likely for the coming years. It is for me to jot down ideas I have through reading.

28.1 Idealized World

Regarding ECoGs.

Better ECoGs are really the path to incredible options. Of course, we have the mechanics already. Theoretically, one could simply build a mech-suit to accomplish any task—the trouble is getting it to respond. Somehow, it seems certain groups are able to resolve speech patterns and handwriting from brain data—so certainly it is within the realm of possibility. In this same way, ECoGs must become less invasive. The route to accomplishing this is likely through extremely intelligently made soft electronics. The resolution must be greatly improved by the inclusion of many, many more electrodes. In this way, powerful machine learning will be needed to process this data¹⁶⁰.

There are a few things to consider. First, glial encapsulation will probably destroy you if you try to use too small of electrodes. Second, hard electronics seem to have many drawbacks. If you are using ultra-micro electronics, they are still limited by their ability to read within the gyri, given that the electronics will be hard. Similarly, you simply cannot afford to do massive cranioplasties on a regular basis. It'll need to be improved. Accompanying this issue is the ability to test on humans. One must first test on mice, which parallelly means that the device must be scalable.

Some Experiments.

1. Inhibit L-type VGCCs—likely need to use some kind of hydrogel with antagonists built in.
2. Optimize stiffness of paddles—or hydrogel, if we use the ACES system.
3. Optimize ECoG—that is, take up less space, maintain resolution, etc. to minimize invasiveness of surgery.

¹⁶⁰I should really start teaching myself ML.

Inhibit L-type VGCCs.

It is well known by now that electrical stimulation combined with rehabilitation improves patient's ability to walk after SCI.

ACES Method.

I like the ACES method as a starting point. It seems easy enough to implement, and can be built upon to arrive at some SCI method. Of course, I like that it is already integrated into a hydrogel setup. Some mild concerns are the 2 mA applied. It seems like quite a bit.

Biomaterials.

The biomaterials possibilities are quite cool too.

CSF-cNs.

A great, easy experiment is CSF-cNs ablation with EES, compare vs. WT, and see if recovery is similar.

Waveforms for Neuropathic Pain.

Perhaps one can use a feedback mechanism, where the frequency of stimulation can be altered in order to dampen neural signals. You'd need to both read and write, essentially. Surely you can record brain waves responsible for feeling pain, and have a circuit edit itself to minimize them? — > actually, dampening neural signals is a great example of a time to use the peak detection method, because you're only interested in magnitude.

28.2 Device Idea

28.2.1 Motivation

Much is made of the frequency and amplitude of neuropathic pain stimulators. Dr. Ben-Haim even called the search for such as being the “waveform revolution.” Perhaps one can avoid this investigation altogether by simply connecting the entire pain pathway to the feedback loop of an opamp. That is, an opamps v_+ is grounded, the V_{out} is tied to a electrode in the spine, and the v_- is connected to some form of ECoG in the brain. Theoretically, the opamp's V_{out} will do whatever it can to cause the signal read at the brain to go to 0. Of course, you cannot assume the opamp's feedback will be predictive, nor can you assume it will fix sharp pains. But, it may be able to fix chronic pain. Let's think of an overall build.

28.2.2 Framework

Processing Brain Waves.

To process the brain waves we will likely:

1. Filter out background from individual electrodes.
2. Subtract and amplify from some reference.

3. Do some summing amplification from each of our electrodes.
4. Rectify our signal.
5. Convert via peak detection.

Feedback.

To implement, we will then:

1. Feed processed signal to a PID controller of some sort.

The only thing I am not sure about is if we will need a separate PID controller for each electrode in the spinal cord. I am not sure if we can just take all of the brain signals and combine them together, but I would assume that is fine. Another question is how much current we will need. If too low, we can add a push-pull to boost, but I doubt we will need a high current.

THANK YOU.

A FINAL NOTE:

The world is always full of the sound of waves.

The little fishes, abandoning themselves to the waves, dance and sing and play, but who knows the **heart** of the sea, a hundred feet down? Who knows its depth?

– Musashi by Eiji Yoshikawa

Part VII

Addendum

Overview

Hello there! You've reached not only the end of the book, but actually the parts beyond its conclusion! At least for the moment, there are topics I'd like to discuss, but they're only tangentially related (if at all) to the idea of brain-machine interfaces. Therefore, consider this the bonus parts that are not worth reading, unless you are immensely inclined.

One such topic is that of neurodegeneration. Naturally, there are not many direct parallels to be drawn from diseases like Alzheimer's and spinal cord injury. Yet, I do believe strongly in Musashi's epithet, that once you know the way broadly, you can see it in all things. For this reason, I think there is unknowable value in learning about degeneration. As it turns out, there are considerable parallels between the pathologies of traumatic SCI and neurodegenerative diseases, like degenerative cervical myelopathy (DCM) as covered in other sections like **17.3**. Thus, it is certainly worth understanding in-depth. Oh, and I because I am taking a class on it and I need somewhere to take notes ;)

Chapter 29

Neurodegeneration

This is more of a historical dive into the research, because so much of what we know about neurodegenerative diseases is likely wrong, overstated, or misinterpreted. You will hear some, like Dr. Rothstein at JHU, argue that there is a viral component. There is many fascinating theories and little agreement. You will hear some, like the Wallace lab at Penn, claim that Alzheimer's is due to mitochondrial dysfunction and not aggregated. So for now, let's call this a historical work.

This is all extremely messy and disgusting for the moment. Will clean up later (hopefully).

Alzheimer's

Alzheimer's disease (AD) is a degenerative disorder present in many demented, elderly patients. It must be diagnosed after death because of considerable symptom overlap. Diagnosis after death is on the basis of extracellular amyloid plaques and intracellular tau tangles.

Holtzman Lecture

This is from a video featuring Holtzman called Sleep & the Pathophysiology of Alzheimer's Disease¹⁶¹. To start, dementia is considered a decline in cognitive abilities sufficient to impair daily life. Approximately 50% of people over the age of 80 have some form of dementia.

The role of glia has been understated for a long time in the progression of AD. It seems that Tau and β -amyloid buildup activates a glial / autoimmune response. Like most neurodegenerative diseases, symptom onset marks the end stages of it. Pathology beginnings occur far before symptom onset.

APP is enriched at synapses in the brain. Interestingly, endocytosis occurring at the membrane leads to membrane bound APP being taken back up by vesicles into the synapse. It is here that, while in endosomes, APP is cleaved, leaving behind its β unit. These are then exocytosed. This can occur both pre- and postsynaptically.

The A β peptide is somehow higher in the dark and lower in the light. The A β presence is also closely correlated with the amount of lactate, which sometimes serves as a proxy for synaptic activity. A β can be measured in the CSF. Chronic sleep deprivation leads to significantly increased A β plaque buildup,

¹⁶¹<https://www.youtube.com/watch?v=zCmngDk9VDU>

and the converse was true in sleep induced mice. Essentially, this idea was repeated in humans and was conserved. These researchers also determined that it was due, in fact, to production and release as opposed to clearance (done using labeled $A\beta$). This is quite interesting because ApoE is thought to help clear $A\beta$. Also fascinatingly, $A\beta$ seems to further worsen sleep.

While $A\beta$ accumulation precedes symptoms by many years, tau buildup seems to correlate strongly with symptom onset. Acute neuronal activity increase and chronic increase both lead to buildup of tau. As wakefulness increases neuronal activity, so too does it increase tau.

Overview by Bonini

Regarding drugs and tools, Alois Alzheimer's used dyes to stain tissues and reveal their histology. Aricept blocks acetylcholine degradation, which can slow symptoms for a short time. Measuring amyloid buildup, or other markers, in the CSF is a tool to determine disease progression and or drug efficacy. Congo red is used to stain amyloid buildup (any β -pleated sheet)—i.e., it is non-specific to β -amyloid of AD. It also seems capable of staining tau tangles. Another method is using (thioflavin T) ThT, which also interacts with β -pleated sheets. This has been used to make a radioactive version called Pittsburgh compound B (PiB) and quantify the amount of plaques. This helps identify dementia years before it begins. This is primarily used to track disease progression.

Trisomy 21 patients almost ubiquitously get AD, and specifically early onset AD—which suggested there must be some association with Chr21. β -amyloid was purified in 1984 by Glenner and Wong, which allowed it to be sequenced early. They then generated an antibody against it, allowing them to stain certain regions of the brain. After the β -amyloid protein was identified, other groups sequenced the surrounding nucleotides and found it to be part of a larger transmembrane protein—which was eventually called the amyloid precursor protein (APP), mapped to Chr21. Thus, it was intuited that this little peptide was cleaved from the larger transmembrane protein.

Goate et al, 1991

Overview / Background

$A\beta$ was first sequenced in 1984. In 1987, four groups cloned the APP gene.

Previously, Chr21 was found to contain an AD locus. The authors identified a site on Chr21 that seems to segregate, sometimes, with early onset Alzheimer's disease and in the gene encoding amyloid precursor protein (APP), specifically at the β -amyloid site. However, as this mutation does not seem to be ubiquitous, they concluded that there is considerable heterogeneity even among early AD patients. This is an important note, because it was originally believed that the APP gene was not disease causing, as some linkage studies did not find APP to be causative. Though, they've identified two families with this mutation and believe it to be causative in some cases.

Table 1

Table 1 contains the LOD scores for markers along Chr21 against the proposed AD locus. APP clearly exhibited the most likely among the markers.

Figure 1

Figure 1 is a pedigree chart. The majority of it is uninformative, as many of the family members have one or two alleles for the APP gene and surrounding markers. Depending on the allele, family members either do or do not have AD. However, two family members exhibit recombinant alleles at different sites. The first individual shares the same allele at the telomeric end of the chromosome to the affected parent. This suggests the AD causing gene is not, in this family, telomeric to the APP gene. Second, another individual shared the same allele as the affected parent only centromeric to APP, and at the time of the study was unaffected. It's possible this individual would develop AD later in life. Therefore, based on their current pedigree, APP was the clearest possible disease causing gene, which motivated their Fig. 2 work.

Figure 2

Figure 2A used PCR to identify the site of mutation, and determined a valine to isoleucine polymorphism specifically in the β APP encoding portion. They sequenced the β unit first because it appeared causative in other diseases. Figure 2B used a *Bcl*I restriction site induced by the polymorphism in order to cut DNA and detect, by the number of base pairs, the presence of the mutation on a gel. That is, a non-affected person will have an uncut sequence of DNA of 319 bp in length, while those affected individuals will have a band at 199 bp and 120 bp. This allowed them to quickly screen for affected individuals in other families, of which they found. While sequencing may take closer to weeks, such enzyme gels can be done in a day. To verify these families were not related, they checked other polymorphic sites and found divergence, suggesting they are not related.

As some final comments, they did not sequence the entire APP gene. Thus, it's possible that the true disease-causing mutation is not within the β encoding portion. They suggest that APP's lack of causative support may be due to previous studies misdiagnosing AD (and or phenocopies) and or AD's heterogeneity. They also made a somewhat silly, in retrospect, suggestion that the mutation makes the APP transmembrane domain anchored more tightly to the membrane. They did correctly postulate that the deposition of β amyloid is associated with a worsened disease, and based on the phenotype of trisomy 21, is somehow dose dependent.

Follow-Up

After this work, many of the labs around the world began sequencing from their brain banks, and a host of mutations was found. There seems to be a correlation between the location of mutations and the site that a protease cleaves APP. α -secretase precedes γ -secretase cleavage, which leads to two fragments—this is not pathogenic. When β -secretase precedes γ -secretase, that is when problems arise! γ -secretase is not hyper-specific to a given site, and thus some variable cleavages too lead to worsened disease.

Sherrington et al, 1995

Overview / Background

Genetic studies identified an AD3 gene as being associated with an aggressive form of AD. AD3, along with ApoE and β APP are the three loci so far identified as being genetically related to AD. Within the defined region is a transcript they call S182, encoding for a newly identified, transmembrane protein.

They identified mutations in this new protein that are conserved between families, indicating these defects are causative.

Figure 1

Using a group of familial pedigrees and previously published data, they analyzed a set of genetic markers on Chr14. By analyzing the recombination events, they were able to conclusively narrow the causative region to between two markers. To clone the gene, they started by generating contigs. **Table 1** expands on this, denoting the shared alleles within boxes (i.e., the identical partial halotypes). Two clusters of genes were found to be shared between families of common ethnic origins. This indicated to them the heritability of the gene, and allowed them to make more direct comparisons as the families will be under similar “genetic backgrounds” so to speak. They analyzed the cDNA clones of this region and determined 151 of them to reflect spliced mRNA. Using RT-PCR from AD affected brains and non-affected brains allowed them to narrow their field of interest down to 7 transcripts. Among these was a novel gene, represented by fragment S182.

Figure 2

Using a Northern Blot, they identified 2 major transcripts and expression in most regions of the brain. Notably, mouse tissue only identified one of the two, specifically the 3kb region—which the authors suspect may be the normal mRNA, and the other the other transcript may represent a more rare, alternatively spliced version.

Figure 3 & 4

Figure 3 shows the sequence homology between mice and humans, and some other features geneticists probably care about. Algorithmic predictions show 7 transmembrane domains, and an example structure is shown in Figure 4. Two other non-polar regions were found that appear unstructured and unlikely to form transmembrane helices. They identified potential glycosylation sites, which they suspect may help order these regions into structures along the membrane. Not shown in a figure directly, but they did comment on sequence homology with *C. elegans* proteins. No great candidates stand out among those identified. SPE-4 seemed to be the most similar, which plays a role in spermatogenesis specifically through a golgi derived organelle formation—thus the authors throw out the possibility of S182 altering β APP or Tau golgi trafficking. Of course, we know in hindsight that this is untrue. A similarly funny hypothesis is that this S182 is the mammalian equivalent of Ca- α 1D¹⁶²!

Figure 5

Within the ORF of this gene was mutations in multiple AD affected individuals. Among families with such mutations, no unaffected family members were ever found to have these mutations.

Strul & Greenwald, 1999

Background

Soon after PSEN1 was identified, another gene was found on Chr1, which happened to be quite similar to PSEN1! We now know this to be PSEN2. Then, a *C. elegans* paper came out in which a worm

¹⁶²This is funny to no one but myself, as my first published paper was on Ca- α 1D function in *Drosophila*, a cool 28 years after this paper came out.

homolog was found. It was identified through their investigation of Notch signaling. In hindsight, we know that γ -secretase and PSEN are indeed one and the same (or rather, that it is the proteolytic subunit of the complex).

Notch signaling is a key developmental path in many organisms. Notch is especially important in cell-to-cell communication during development, aiding in cross talk between cells and driving cell differentiation. A ligand released by a cell will bind to Notch's extracellular domain, inducing a conformational change and allowing Notch's intracellular domain to be cleaved. Cleavage is done by γ -secretase, which cleaves the Notch intracellular domain (NICD). The NICD is trafficked to the nucleus, which it interacts with g inhibitors, turns them off, and allowed genes to be transcribed.

Overview

Prenesilin (PSEN) is a transmembrane protein known to contribute to AD progression, and thought to play a role in amyloid processing. In *Drosophila*, PSEN modulates Notch activity, which thereby can influence transcription. This paper identifies PSEN as aiding in Notch cleavage, allowing it to exit the membrane and enter the nucleus where it can exert its control.

By this point, it was known that β -secretase is required for APP's conversion to β -amyloid and such cleavage occurs in the extracellular space. Similarly, it was known that γ -secretase cleaves APP in the transmembrane domain. It was shown that Notch cleavage occurs in a similar way. PSEN mutations cause AD by increasing the amount of $A\beta$. PSEN knockdown inhibits the activity of γ -secretase. It was not known at this point if PSEN was an activator or a component of γ -secretase. Notably, they specifically comment on PSEN in relationship to an $A\beta_{42}$ (42 aa in length) variant, which is mentioned in other literature.

Figure 1

Figure 1 analyzes the phenotypes of PSEN (PS in flies) knockdown. They generated two truncated alleles, which both showed identical phenotypes. PS^- embryos exhibited clustered neuroblasts, which should typically be spread out. Midline cells, thought to be controlled by Notch, did not differentiate as they do in WT. Homozygous PS loss is pupal lethal. Clones of PS^- cells causes abnormal wing development, thought to be through Notch's role in dorsal-ventral cell communication. Finally, embryos of PS^- flies show normal accumulation / membrane localization of Notch, which indicates that it is not upstream of Notch expression—suggesting a role in Notch signaling.

Figure 2

I'm a tad confused by the exact method they used. My rough understanding is they performed a Gal4 knock-in into the intracellular side of the Notch protein. In the absence of a ligand, and in PS^- , Notch is not trafficked to the nucleus. This is marked by a UAS, which drives β -Gal expression that they can stain for. My understanding is this: They have 3 lines, which they call N^+ -GV3, N^{ECN} -GV3, and N^{intra} -GV3. N^+ -GV3 is like their WT control, which functions normally. In the absence of either PSEN (PS^-) or Notch's ligand (Delta, DI^-), no nuclear transport occurs, marked by no β -Gal staining. N^{ECN} -GV3 includes a large deletion of the extracellular domain, which essentially decouples Notch from its ligand and makes it constitutively active. Thus, in this case they found DI^- embryos to still have considerable trafficking to the nucleus, while PS^- did not. Finally, N^{intra} -GV3 is missing both the extracellular and transmembrane domains—therefore suggesting it will never be trafficked

to the membrane at all, causing it to remain cytosolic. In this case, neither DI^- nor PS^- prevented Notch trafficking to the nucleus, so all embryos could be stained by the β -Gal.

These experiments led them to the conclusion that PSEN was specifically involved in cleavage of Notch, as opposed to acting as a ligand or aiding in its downstream signaling cascade. They also concluded that PSEN is cleaving Notch somewhere in its transmembrane domain. So naturally, the big takeaway is the suggestion that PSEN may play a similar role in APP processing, producing $A\beta$ in a similar way.

Ye et al. 1999

Figure 1

To investigate the role of PSEN in Notch signaling, they developed 5 *Df* lines. To verify the phenotypes of these lines are PSEN dependent, they used a variety of DNA rescues, one of which omitted the PSEN DNA and did not phenotypically rescue such fly lines.

Figure 2

Based on their mutants, they identified a pupal lethal phenotype they considered to be similar to a *Su(H)* mutant, an effector of the Notch signaling path. Using a few different larva wing disc markers (driven by expression of various genes related to wing development), they determined β -Gal expression was missing in their *Df* lines, but not elsewhere.

Similarly, sensory organ precursor (SOP) cells were found to cluster together with limited lateral inhibition, determined by enlarged territories and increased *achaete* and *scabrous* expression (early SOP markers).

Figure 3

They determined, using ELAV staining, that paternal PSN partially rescues neurodevelopmental troubles.

Figure 4

Notch protein localization and expression was similar across their PSEN mutants and wildtype larva. This was consistent between both the intracellular and extracellular components of Notch, and for the Notch ligand, Delta. In retrospect, the finding that intracellular PSEN is unchanged may be considered surprising, since PSEN is now known to cleave Notch. The authors attribute this to the small intracellular quantity that is actually trafficked to the nucleus, and which remains undetectable using immunostaining.

Figure 5

To investigate how PSEN may process notch, the authors used Western blots. Figure 5A suggests the largest, $\approx 120K$ piece migrates more slowly in the PSEN mutants, suggesting the piece is slightly larger. Figure 5B shows that among the 120K fragments, the largest one dominates in the PSEN knockout, compared to the WT. Figure 5D & E serves to prove the phenotype is specific to PSEN knockdown, as in the *Su(H)* mutant background, this phenotype is not observed (i.e., Notch is processed as WT is),

and similarly in mutant Notch background the large 120K band is absent. Figure 5F showed that the same fragments are unaltered in other proteolytic knockdown (specific to Notch's processing in the golgi), demonstrating a specificity for PSEN and that the cleavage observed occurs after its membrane targeting. Figure 5G & H verified the intracellular domain is unaffected by the PSEN knockdown. Finally, Figure 5I shows that PSEN knockdown did not affect Delta levels.

Figure 6

Figure 6A shows that inactive Notch confers proneural clustering in both WT and PSEN mutants. Figure 6B demonstrates, using only the intracellular Notch domain, that no SOP differentiation occurs in both WT and PSEN mutants. Figure 6C shows suppression of most SOP differentiation in a membrane tethered background. It is supposed by the authors that PSEN is not required for membrane trafficking nor nuclear trafficking of Notch. Rather, they supposed PSEN is needed in some activation mechanism that follows ligand binding.

Games et al. 1995

Despite some attempts, no successful AD model had been established. This group used a modified, transgenic APP gene in mice which reproduced many of the AD phenotypes. Such a model drove increased expression in many mouse tissues, but especially within the brain. They consider the promoter they used, PDGF- β , and the familial AD mutation they used (V717F), to be the two prime contributors to success.

Figure 1

Figure 1 serves to validate their model. Figure 1B shows 3 different alternatively spliced forms of APP mRNA. Figure 1C & D show via western blots that the amount of protein is greatly increased in the transgenic mice vs. wildtype mice. Figure 1E demonstrates that A β was indeed being produced too.

Figure 2 & 3

A β buildup occurs only at 6-9 months of age and worsened from there. It was primarily local to the hippocampus, corpus callosum, and cerebral cortex. A β buildup took a variety of forms, including irregularly shaped bundles and other more characteristic, dense plaques. Figure 3D demonstrated that reactive astrocytes often surrounded such plaques via GFAP staining.

Immensely important: tau was not found. It was commented that tau is notoriously absent from rodent tissues, which is surprising because I'd certainly expect mice to have similarly structured tau.

Figure 4

Using more immunostaining, A β plaques were associated with synaptophysin, suggesting their specific localizing to sprouting axons. Staining for MAP-2 in addition to synaptophysin showed plaques disrupting and de-densifying nearby regions. Plaques also seemed to compress the surrounding neuropil (the unmyelinated, cell dense regions of neural tissue).

Tau

To summarize to this point. At present, there is the belief that the ratio of A β 42 to 40 indicates the progression of the disease. This is part of the amyloid cascade hypothesis. All of this work has been focused on the plaques, but no insight whatsoever into the tangles.

Tangled up in Blue

In the 60s, tangles were purified to the point of visual analysis, indicating they were helical in nature and likely two filaments coiled around one another. This gave them the name paired helical filaments (PHF). In 1992, this PHF was tested against tau antibodies and stained with Coomassie Brilliant Blue, showing different forms of tau at variable molecular weights. Normal, wildtype tau was largely unaffected by dephosphorylation by a generic phosphatase. But dephosphorylating PHF substantially lowers the molecular weight of tau. In short, this suggested PHF is a heavily phosphorylated version of tau. This principle is generally conserved in diseases, where a protein becomes abnormally phosphorylated. Notably, tau mutations are never associated with familial AD—but are associated with other degenerative diseases.

Tau binds to microtubules and is thought to help stabilize them. When phosphorylated, it unbinds from the microtubules, thought to cause axonal regeneration. Notably, tangle burden progresses with the disease more so than does plaque burden. In general, this created a rift among scientists on what the root of the disease was—A β or tau.

Lewis et al. 2000

Initially it was thought that tau tangles was solely a symptom, and or, a result of already dying neurons.

The paper overexpressed mutant tau protein that can be found in frontotemporal dementia and parkinsonism (FTDP). The mice exhibited a wide variety of degeneration linked to the tau protein buildup. This included symptoms even in the spinal cord and peripheral nerves. Mutant tau (P301L) was expressed by the mouse prion promoter (MoPrP). They found that hemizygous lines expressed tau at approximately the same level as WT, and mice homozygous for the mutant expressed it at levels $\approx 2 \times$ WT.

Figure 1-4

Their Figure 1 was a composite of behavioral assays, including escape responses, motor defects, and the inability to right (flipping over from its back onto its feet again). Hemizygous mice had symptom onset at about 6.5 months, while homozygous at around 4.5 months. Eventually they were unable to walk.

Figure 4 showed spinal cord defects, namely fibrillary gliosis, axonal degeneration, and axonal spheroids (bleb). GFAP immunoreaction was found throughout the brain, signifying gliosis. Importantly, degeneration was global, including skeletal muscle and peripheral nerves. In Figure 2, neurofibrillary tangles were found throughout the brain, including in the brainstem and diencephalon. Interestingly, so-called “pretangles” were found in other regions of the brain, including the hippocampus. In Figure 3, the fibrils were irregular in shape and specifically phosphorylated.

Figure 5

Figure 5 investigated the solubility of tau. In the mutant lines, a greater proportion was insoluble and shifted toward a higher molecular weight. This is consistent with being heavily phosphorylated, of course, which was verified by dephosphorylating the protein causing the elimination of such bands. They seemed proud of the similarity between AD bands and their model's bands.

Follow-Up

To follow-up, whether or not APP modulates the tau protein buildup became a focus. Indeed crossing this tau mouse with an APP mouse led to increased NFT formation. This suggest tangles are needed for neural loss? Later, groups tried combining multiple familial AD mutations in APP with PSEN mutants, leading to very early onset and more powerful, clear behavioral defects. After these tau models were verified, tau too was added.

In clinical trials, antibodies against $A\beta$ showed the ability to decrease plaques. However, no obvious clinical benefit was found. Naturally, this could be because degeneration had already run its course, or it could be that tau is directing progression at this point. Some take this as evidence against the amyloid cascade hypothesis.

Jonsson et al. 2012

Background

Iceland keeps quite good genealogy records, and because people are quite related due to population isolation, their genetics are ripe for this sort of testing.

This paper identifies an APP mutation that protects against AD. Fascinatingly, they claim it also protects against age-related dementia in non-AD patients. This seems very fishy to me, but hey, whatevs. Beginning with a pool of ≈ 2000 people, they identified SNPs in elderly people compared to AD patients. They identified the A673T mutation to be higher in the non-AD people, suggesting it is protective. They then chip-genotyped more people (i.e., used a probe against this SNP) to increase sample size. They also showed an increased risk in late onset AD vs. early onset, which demonstrated some mechanistic differences. **Understand better?** Mutations in APP have not been implicated in early onset AD before.

Table 1

Table 1 shows that the odds of having the mutation are significantly higher for those that are 85 and older, and cognitively intact than those with AD.

The genotype is relatively rare, on the order of one per couple hundred people, or rarer depending on the continent. Because the mutation is neuroprotective, carriers have markedly longer life spans. Fascinatingly, they even suggest the genotype is substantially beneficial even compared to those without AD. In cognitive scores they performed much better. Notably, though, the error bars are so insane they go off the screen (like literally, some error bars are cutoff from the graph).

Huntington's

Overview

There's 30-40 human diseases due to CAG repeats. For HD, it is within the coding region of an exon, which encodes glutamine—which becomes a polyGlu. Though, notably, there's a bunch of diseases with the same mechanism. These genes normally have CAG repeats, but in disease phenotypes the repeats become elongated. HD is typically characterized as a movement disorder. For very long expansions, one can get juvenile HD. In patients, the caudate and putamen (which make up the striatum) are especially damaged, which causes enlarged central ventricles.

Interestingly, in diseases like spinocerebellar ataxia, another exon CAG repeat disease, many present clinically in the same way. However, their mutations are in different genes and the cell types affected are different. This causes degeneration in slightly different regions of the brain. Ataxic gait is classified by a lack of balance, which causes patients to widen their legs to maintain balance and jerk-like movement with stepping. It is especially clear upon asking patients to close their stance, in which case you'll see them lose balance. HD has less extreme, jerky movements and more stiffness, dis-coordination, and difficulty balancing¹⁶³.

Huntington's is characterized by an autosomal dominant mutation, and symptom onset begins around age 30 to 50 and is completely penetrant. Chorea (large muscle jerks, resulting in dance-like movement) and cognitive decline are two marked symptoms. Genetic anticipation is a feature where diseases get worse, with earlier onset, every generation. While Huntington's was first recognized in the 1900's, it was largely ignored—people didn't know what to make of it, because the gene changing over time seemed confusing. Repeat expansion was first identified in DM1 disease, which was a CTG expansion. You cannot precisely predict the age of onset by the length of the CAG repeats, for HD.

Nancy Wexler was one of the first to “set out” to characterize HD. She traveled around the world and met many HD patients, looking for someone who was homozygous. She specifically went to Venezuela because they had a very large HD population. The median repeat length in this population was around 45 repeats. Most fall in the range of 40-50, but some rare outliers exist. Juvenile onset median was closer to 60 repeats.

Repeat expansion occurs more commonly in sperm production, so it is more common for an affected father to worsen the disease. Interestingly, as HD most severely affects the striatum, movement is expectedly impacted. However, conversely to Parkinson's, dopamine levels actually increase, while GABA and acetylcholine decrease. Therefore, dopamine inhibitors are a way to treat the symptoms (not the disease progression) of HD.

RFLPs

The benefits of RFLPs are that mutations cause a restriction enzyme cut site. This allows you to get a broad sense of the genotypes of those in a pedigree. Thus, researchers started looking for RFLPs nearby disease causing genes.

¹⁶³A rude comparison is to someone who is tweaking.

Gusella et al. 1983

Overview

Prior to this study, nothing was known about the disease pathology of Huntington's disease. In fact, the closest that had been achieved before is that 20% of the chromosome was excluded from the disease-causing locus.

They generated cell lines from their derived tissues for future use. Picking a high quality of patients was essential, which included using experienced neurologists and people with verified HD over the course of a couple of years. They used 12 DNA probes from genes that already existed, which could not hybridize to multiple places in the genome. Only the G8 marker gave a suggestion of linkage to the HD gene.

Figure 1 & 2

These figures are simply illustrations of large pedigrees they found. Finding large families with well documented Huntington's disease and available tissue samples, evidently, was quite hard then.

Figure 3

Really, a large roadblock in investigating HD was the lack of genetic linkages. The G8 marker showed the first promising results. Figure 3 (top) shows the cut sites for *HindIII* (H) and *EcoRI* (R) restriction sites. The actual probe that they have is quite small. The G8 polymorphic sites are very close to one another. They want to prove individuals that are heterozygous, so that they can differentiate between affected and non-affected chromosomes.

Haplotype A is associated with HD in the American family. It is haplotype C in the Venezuelan family. The fact that the haplotypes are different between people either suggests it's two different genes or that the mutations arose independently in the two families. There are a few instances in which individuals have haplotype C, but do not have HD. This could be due to different age of onset or that some recombination event separated this polymorphism from the HD gene.

Table 1

Table 1 shows that G8 does not hybridize without Chr4 present. In fusing human-mouse cell hybrids, they essentially generate mouse cells with human chromosomes. They score which chromosomes each cell has and too if it hybridizes with the G8 marker. Because all cells with Chr4 have the G8 marker, they assumed G8 must be on Chr4. They tried testing recombination events of the HD gene with other Chr4 markers and found no association.

G8 is not the HD gene, but it is certainly close to it!

Implications

This had considerable implications, as you can now test haplotypes of offspring and predict if they'd get HD. Moving forward, more markers and more segregation analysis will be helpful in narrowing down the gene. Then, you have to start sequencing nearby genes.

Questions

What insight allowed them to map a gene by RFLPs? Polymorphisms in RFLPs allowed them to test using restriction enzymes and map different lengths via southern blotting. This was beneficial as they were heritable and could be found in regions that were not protein coding.

how many DNA probes did they use to detect RFLPs before they found an association? 12?

What does it mean that the haplotype of the two families with HD are different? They're at different locations on the chromosome?

They don't have the gene so of what use is a piece of DNA linked to the HD gene? A jumping off point to start sequencing.

HDRCG 1993

Overview

For many years, they had to make markers and compare recombination of events around this G8 area. Through continual investigation of recombination events in HD families, they were able to rule out different regions of Chr4. This meant the genome was narrowed down more and more until it became time to sequence. They were able to narrow it down to 2.2Mb. By comparing the haplotypes of HD kindreds, they narrowed it further to 500Kb. They look specifically for genes that become expressed by screening with a cDNA library.

Northern blot showed that the IT15 gene is expressed in HD patients as well as controls. This gene, as it turns out, was quite big. They didn't have a single cDNA which covered it, so they pieced together a couple cDNAs. It was predicted to be 3144 amino acids!

They find CAG repeats and that more than some number of repeats (42 in this case) was perfectly correlated with HD. They then tested as many HD families as they could. PCR and southern showed very variable repeat lengths.

Figure 1

Figure 1 mapped the HD gene to somewhere between two markers on Chr4 by recombination events. Restriction enzyme cut sites are also shown. These restriction sites were helpful in mapping the haplotype of different HD kindreds, allowing them to narrow down their range of interest.

Figure 2

They generated exon clones and therefore cDNAs IT15A and IT16A. Northern blotting showed hybridization with a similarly sized sequence, suggesting the sequences are derived from the same mRNA. My understanding of Figure 2 is that they are simply verifying the existence of an 11kb RNA strand characteristic of the IT15 gene in both homozygous HD patients and normal samples.

Figure 3

Using the cDNA they had (IT16A and IT15A) they did a walk, where they used overlapping cDNAs to get the entire IT15 sequence.

Figure 5

After sequencing, they generated primers for the regions flanking the CAG repeats. Of the 173 chromosomes they sequenced, the vast majority had below 25 repeats, and chromosomes had 80% heterozygosity. Figure 5 shows a comparison of normal cosmids and normal cDNA compared to HD cosmids. Recall that a cosmid is made by digesting DNA, implanting into viruses, and then these viruses infect bacteria, while cDNA is from reverse transcription.

Figure 6 & 7

Their Figure 5 showed PCR products of different family members in the kindred, hoping to show that one allele was unaffected and one allele was affected in the HD group. Notably, though, some do not show a HD allele, which they write off as being due to the repeat lengths being too long to amplify. They verified this by southern blot in Figure 7, which showed that the repeat length was 100—and this patient had HD onset at age 2. Some people show more than 2 HD alleles. The hypothesis for why this occurs is that the cell lines, lymphocytes, are likely a bit more mosaic, since they actively divide much more.

Figure 8

They were interested in testing sporadic cases of HD to see if this repeat expansion was still the driving cause. Indeed, they found parents with higher-end repeat expansion, and thus the offspring had repeats reaching the stereotypical 44+ range. They identify a similar haplotype in these chromosomes as in 1/3rd of all HD chromosomes, which suggests that this haplotype may predispose individuals for HD.

Takeaways

The key findings were that there is this correlation between repeats and HD. This could be used as a diagnostic tool, or describe those who are pre-disposed to getting HD. At present, they do not know the mechanism by which HD acts, but they suspect it may be gain of function. They cannot say anything with certainty about this gene's corresponding protein, nor can they say that the repeats are translated at all. If it is translated, the polyQ would have considerable effects, and if it were untranslated, the effects are likely at the mRNA level. The next step that they propose is, indeed, to understand the endogenous function of this protein which they call huntingtin (with gene HTT).

Mangiarini et al. 1996

Overview

Prior to this point, questions regarding the nature of HD existed. It was unclear how the CAG repeat was affecting patients, but by then it was known that the glutamine residues corresponding to CAG were indeed translated. Generating a mouse model was difficult, as the HTT gene is incredibly long so cloning was almost un-doable then. In this work, they generated a model with only the beginning portion of the HTT gene (a single exon), including (CAG)₁₁₅—(CAG)₁₅₀. Their model, using a fragment from the human genome, in fact used the endogenous HTT gene promoter.

This work made the comment that 70% of juvenile cases are inherited from fathers.

How do you even maintain these mice? Won't the HTT gene always get purified, else the lines will die due to their instability.

Figure 1

Figure 1A shows the region of human genomic DNA inserted into the mice. Figure 1B shows a Southern blot of the genomic DNA of F1 progeny from their successful transgenic mouse. They probe with a piece of DNA that hybridizes to the C terminus of their inserted sequence. The purpose of this was to better understand where their insertion integrated into the genome. Figure 1C shows the predicted transgenes. It doesn't really make sense to me, though.

Figure 2

Figure 2 shows the number of CAG repeats in each of their transgenic lines via PCR amplification and an ABI sequencer—in other words, amplified and then sequenced. The ABI sequencer plots show peaks corresponding to the length of the repeats—which were all in the range of about 110-150. Table 1 showed a frequency of the various genotypes in F1 progeny.

Figure 3

Age of onset was usually around 9-11 weeks, and death around 10-13 weeks, meaning death followed symptoms quickly. The phenotype is described as complex, and that at birth no differences are observed. Symptoms include motor jerks and resting tremors, which worsened under stress. Significant weight loss is noticed by death, which is strangely confounded by the fact that their appetites are not reduced. Indeed, upon death food is found in their stomachs and stool seems to be normally produced, but their bodies have atrophied. Strangely, too, they seem to urinate excessively.

Figure 4 & 5

Figure 4 attempts to determine location of expression. In some lines, transgene expression was found in all tissues analyzed, suggesting to them that it was expressed under the promoter within the injected DNA fragment. Figure 5 used an antibody called 1C2 and performed Westerns to analyze protein translation patterns—which appeared to be global. In one case, they identified a lack of translation, which they attribute to the protein not expressing the necessary epitope—which seems odd since it is meant to bind to polyQ.

Figure 6 & 7

How did they separate out the cytosolic and nuclear? Figures 6 and 7 characterized the neuropathologies of the mice. They identified universal shrinkage of the brain, not necessarily degeneration nor shrinkage localized to the striatum, on the order of about 20% smaller than normal brains—however, there was clear ventricular expansion. They observed no neural or glial loss, nor did they see reactive gliosis. In fact, even the basal ganglia and striatum had normal neural morphology, aside from shrinkage. **Without hindsight, I'd have thought HD was a metabolic disorder...** This shrinkage was observed early in the disease progression, and did not worsen with age. This, obviously, contrasts to human HD. One hypothesis they suggest is that disease progression is so rapid in mice that there is not time for atrophy to occur—seems fishy.

Future Directions

Afterwards, they further investigated the neuropathology associated with the phenotype. By EM, they found large clumps present in the nucleus, where HTT is not expected to be. They found these

clumps stained for both HTT and ubiquitin, meaning it was tagged for degradation. It seemed that degradation was failing. Almost all neurological diseases are characterized by ubiquitinated proteins, including AD, and thus it is a strong marker for the buildup of aberrant proteins. Notably, they did not see staining for congo red, which suggested it was not amyloid.

They also found that brain weight decreased weeks before total body weight decreased—but up to this point, everything is normal. Further correlative data suggested neuropathology was induced by HTT accumulation in the nucleus, which was causal for brain weight decrease and therefore causal for whole body phenotypes. This suspected mechanism linked it to AD.

In other works from different groups, protein context was found to be critical. It was shown that only when polyQ proteins are trafficked into the nucleus does a phenotype manifest. If a polyQ protein stays in the cytosol—it will not be pathogenic.

Scherzinger et al. 1997

Overview

This work focused on *in vitro* and *in vivo* model development and subsequent investigation of supposed amyloid plaque-like structures that form as a result of polyQ translation. Prior works had shown the huntingtin protein is associated with the cytosol, possibly around vesicles and or microtubules. Notably though, the HTT protein is expressed widely, which presents a strange problem when considering that degeneration is relatively specific to the striatum. Some hypothesized a gain of function as a result of the increased expansion, and some predicted that it was due to conformational changes in the HTT protein. Notably, polyQ are capable of forming β -pleated sheets. I'll let you connect the dots with that one.

Using the model presented in the previous section, this work found morphological changes on a neuronal level. Small granular structures can be seen, and indentations in the nuclear membrane are found along with increased density of nuclear pores.

Figure 1

To build their model they used expression of exon 1 of the HD gene with expanded repeats fused to glutathione S-transferase (GST), which could be cleaved to produce free polyQ repeats. Such fusion proteins were made into plasmids, expressed in *E. coli*, and purified. Proteins were purified and stained using a Coomassie blue dye and an anti-Huntingtin antibody, both of which verified expected expression and variable sized bands predicted by their sequence.

Figure 2 & 3

In Figure 3A, via digesting the proteins to cleave off the GST domain, lower molecular weight products are found in GST-HD20,30. However, a group of high molecular weight particles was present after GST-HD51 cleavage, suggesting there is some aggregation occurring. This also suggested that GST increased solubility of the protein when un-cleaved. This difference was stronger in Figure 3B, which included complete digestion of the GST tag.

In Figure 3C, they developed a method of quantifying aggregation by collection of insoluble components on an acetate filter, which existed in their longer repeat line (GST-HD51). They find GST-HD

present in both the cleaved and uncleaved state on the nitrocellulose membrane. This contrasts to the acetate membrane, in which they only find protein in the cleaved GST-HD51 group. Therefore, they assumed only this group can be forming aggregates.

Figure 4 & 5

Via electron microscopy, they found uniform, oligomeric particles without aggregates in undigested GST-HD51. Upon digestion, many non-uniform, ribbon-like aggregates were found. Clot-like structures were found on the end of fibrils. Based on their Figure 4E, it appears the clots were due to incomplete digestion. This contrasts with GST-HD20,30, which did not form aggregates with or without cleavage.

Notably, this protein stained with Congo Red, shown in Figure 5. The staining was similar to that would be seen in prions or in amyloid. To determine if these products are found *in vivo*, they used transgenic mouse lines mentioned in Mangiarini et al. 1996. They indeed found, via SDS page gel and Western Blots using the anti-HD antibody, that there is some fraction of peptide present at a high molecular weight. This product was found in the nuclear fraction. They also used an anti-ubiquitin antibody, and found that it reacted with the aggregates, suggesting it is ubiquitinated.

Notably, the less aggressive transgenes they used showed characteristic fibrils, while the most aggressive forms did not. They think this may be because fibrils do not have time to form, in these cases.

They literally have 2 pages of discussion.

Yamamoto et al. 2000

Overview

The premise of this paper is that they've used a conditional expression system to drive mutant HTT. Upon blocking its expression, Huntington's disease symptoms disappeared—leading to the hypothesis that continuous production of HTT is required for the phenotype.

Figure 1

The technology they use is called a tet-regulated system. A promoter drives the expression of tTA, which binds to the TetO elements, allowing for expression of the transgene that follows, which, in this case, was a HD(CAG)₉₄. A molecule called tetracycline (and the analog doxycycline) is able to bind to tTA, which blocks its binding to the TetO element, shutting off transcription. TetO is actually bidirectional, so the opposite side contained a β -galactosidase (lacZ) reporter, used to validate everything. Initially, they observed a strong lethality phenotype which they attributed to strong expression of HTT in the developing fetus. To ameliorate this, they gave pregnant mothers doxycycline, which did the trick.

Figure 2 & 3

Figure 2 validated expression. Strong expression was found in the striatum, septum, cortex, and hippocampus. They validated this both with β -gal staining, and with antibodies against HTT. They found diffuse nuclear staining as well, including aggregates of varying sizes. Though, they did find

a significant amount of extra-nuclear aggregates as well, including those that were highly ubiquitinated.

Figure 3 analyzed broad phenotypes, including finding a significant size reduction in mice with HTT expression, and a narrowing of the striatum. Reactive astrogliosis was observed via GFAP staining, particularly in the striatum. Interestingly, they also observed D1 receptor loss—though, it's unclear to me how this can be attributed to anything other than a product of less cells.

Figure 4 & 5

Clasping behavior was observed here as well. Interestingly, the average lifespan of mice was still comparable to WT (approx. 2 years). That's a good indication of what it means to be a scientist, I suppose. 2 years for a single metric, which ended up having no difference from WT.

Figure 5 is where things get interesting. In comparing mice without dox treatment, and those that began treatment at 18 weeks, no HTT was found in the brains of mice experiencing treatment. However, some buildup was seen in other areas. Similarly, no brain weight reduction was seen after the dox was administered.

Figure 6 & 7

Figure 6 showed that, after dox administration, the caudate and putamen no longer shrunk. GFAP staining did not increase, and in fact seemed to reduce. Finally, D1 receptor loss did not further decrease. In Figure 7, clasping score actually improved quite significantly. Therefore, blocking aggregate progression indicates an overall blocking of disease progression, and or an improvement in symptoms.

Discussion

They commented in their discussion that there is a significant volume loss in the R6 transgenic lines, without decreasing the cell number. It is thought, then, that other factors may be decreasing, like the volume of the cells or their ECM.

Xia et al. 2004

Overview

This work focused on spinocerebellar ataxia type 1 (SCA1), induced by a polyQ in the ataxin-1 gene. SCA1 manifests itself primarily in the cerebellum, perhaps lending it to easier access by injection. One interesting thing to note is that SCA1 does not seem to require nuclear inclusion. An important step of this paper is applying RNAi technology *in vivo*, as its efficacy was already established *in vitro*.

Notably, they mentioned in the discussion that the Huntingtin RNA, and particularly the CAG region, did not lend itself to RNAi (or was not accessible by the RNAi degrading mechanism). Another worthwhile comment is that RNAi would target both mutant and WT RNA in individually. For SCA1, this is not predicted to cause problems, as mice with Ataxin-1 knockout seem healthy. Similarly, RNAi is not expected to completely ablate protein levels.

Figure 1

The group screened for a number of hairpins formed against ataxin-1 RNA and used HEK cells with shLacZ used as their control. The most effective they identified were called F10 and F11, directly adjacent to the CAG repeats. In Figure 1B, this was verified through Western blots, which showed a decrease in protein expression, via probing for a flag tag. Figure 1C showed that this was dose-dependent decreases. Figure 1D identified the modified CMV promoter (Pol II) was more effective in knockdown, as well as recapitulated the phenotype in neurons. In Figure 1E,F, knockdown efficiency was further improved via using a miRNA hairpin, rather than their original hairpin—they assumed this may be better because it more closely mimicks endogenous miRNA, and therefore might be processed easier (increasing expression). This is hypothesized to be due to enhanced nuclear transport. This held true for both mutant and non-mutant Ataxin.

Figure 2

After verifying their model works *in vitro*, they sought to replicate it *in vivo* via generating AAVs including it. The AAV included hrGFP, allowing for visualization of the transfected cells. Figure 2B shows successful transfection. Expression of hairpins was shown in Figure 2C via Northern blotting after 10 days.

Figure 2D begins the real paper, with functional studies. Using SCA1 transgenic mice, motor symptoms are assayed. Particularly, improper foot placement is noticed, which causes mice to struggle with rotarod tests. Indeed, mice treated with RNAi had significantly better performances on the rotarod test. They were not as strong as WT mice, but exhibited obvious improvements over saline treated mice.

Figure 3

The natural next step is, of course, test the neuropathology. Calbindin staining, a molecule used as a proxy of Ca^{2+} , was used to survey the transduced and untransduced brains. Indeed, Figure 3A includes an overlay of GFP and Calbindin, and it is clear that transduced neurons were robust against SCA1. The width of this region of the cortex was quantified in Figure 3B, and again was smaller in untransduced mice. The images are meant to show that on the left side, which is not transduced, the region thins. But, on the right side, which is transduced and marked by GFP, is robustly maintained.

Figure 4

In an online supplement, they showed that nuclear inclusions of Ataxin-1 decreased, even 1 week after AAV injection. They attribute this to the rapid turnover of the Ataxin protein and because AAV expression is quick. It was also shown in Figure 4. Figure 4A,B showed a reduction in nuclear inclusions of Ataxin-1.

Discussion

Their construct showed expression in 5 – 10% of all cerebellar Purkinje fibers, but 100% of targeted lobules? Using lentiviruses can be bad—early clinical applications integrated into the genome in places that caused lymphoma. Adeno-associated viruses (AAVs) are preferable and can be made cell-specific.

Add more info about RNAi-AAV technology.

Fragile X

Background

Fragile X is a developmental disorder characterized by immensely long repeat expansions on the X chromosome. It's associated with some degree of mental disability and clear visual markers, like a longer face and larger ears. Fragile X is considered to fall on the autism-spectrum disorder, and causes multiple unrelated phenotype (pleiotropic). As autism is becoming increasingly common, it is of considerable interest.

I thought I'd mention this, since it is interesting. There's been considerable, considerable, considerable work over the years solving all these neural circuits, on a single or clustered neuronal level. In general, it seems unclear how this information may be useful clinically. Dr. Bonini commented that TMS treatment for someone with autism indeed helps alleviate some of their social symptoms—so indeed, the ability to resolve individual neural circuits is important.

The fragile X site itself can be visually seen, due to the nature and number of repeats. There are little nub-like structures on the ends of the chromosome. Using these cytogenetic techniques, you can identify carriers before there is an effected son. However, this visual marker was not found in all cells—only in close to 40%. Though, knowing the gene is on the X chromosome provides a great basis to start research—much easier than finding the HTT gene. Fragile X is characterized by (CGG)_n repeats in the FMR-1 gene—interestingly, it is specifically in the 5'-UTR, rather than an exon. A normal number of repeats includes the range from 6 to 54, and one can have no phenotypes for up to 200 repeats. Fragile X is the most common form of inherited mental disability, and the second most common total (behind Down's syndrome). It is considered X-linked dominant—yet, around 30% of female carriers show symptoms, and 20% of males with a fragile X show no phenotypes. This is referred to as the Sherman paradox—genetic anticipation in the fragile X context. Notably, a reduction in FMR-1 mRNA is noted in fragile X patients. Specifically, a CpG island in the FMR-1 gene is associated with methylation, and such methylation is associated with decreased expression. It was thought, then, that the fragile X mutation alters methylation patterns in this region. Due to increased repeats, the chromosome is unstable and thus mosaic genotypes are observed.

Notably, patenting is very important to garner company interest.

Yu et al. 1991

Figure 1

Okay, so it seems prior to this point, very little was known about the location of the gene, and the genetics of it was mystifying. Through isolating a chunk of human DNA using a yeast artificial chromosome, they generated a probe they called XTY26. Via *in situ* hybridization, they found that this probe spanned the entire X chromosome region thought to be responsible for this phenotype. At one end of this probe, which they identified through generating contigs, is a marker called Alu2, and at the other end is VK16. They keep narrowing down their scope until they find an *EcoR1* fragment which segregates with the fragile site.

Figure 4

They now use Southern blotting and probe with segments of the previously mentioned *EcoR1* strand in Figure 4. They find that when they probe with various segments, some hybridize to longer or shorter regions of DNA. They're hybridizing against patient genes that were digested with *Pst 1*.

Notably, because this region is very G-C rich, it was very difficult to PCR amplify.

Fu et al. 1991

Figure 1 & 3

In Figure 1, via a shotgun approach (splicing the gene up into parts), they sequenced the region predicted to contain the fragile X gene. They compared this sequence with one previously reported and found discrepancies, which they suspect are due to various cloning steps. They generated a PCR test to quickly sequence the variability of genes in patients, which they validated via Southern blotting in Figure 3. Of those they sequenced, they found a range of 5 to 54 repeats encoding arginine. Of the ≈ 500 chromosomes they sequenced, 29 repeats was the most common.

Figure 4

They plotted the distribution of repeat lengths in Figure 4A. Notably, non-affected carriers show mosaic genotypes ranging from 200 to 600 base pairs (they call the pre-mutation), and affected individuals of 600 to 4,000 base pairs with greater mosaicism (they call the full mutation). Naturally, such long repeats make PCR difficult, and using a Southern blot limits one's ability to determine the size. Their Figure 4B includes PCR products of such patients, but indeed may have inaccuracies. Regardless, they find repeat lengths centered around 70-80. They mention having sequenced some over 200, but chose not to include them due to their questionable PCR accuracy.

Figure 5 & 6

Figure 5 examined a pedigree with their PCR assay. They found that affected males did not generate a product at all, unless they were mosaic for lesser alleles as well. Lanes 7 and 8 of their first test used PCR for a CAG repeat region of an androgen receptor as a method of control. Figure 5A is used as an example of repeat expansion and or inheritance. The effected grandmother passed along a 73 repeat, which expanded to 83 in the mother. The two sons recieved a full mutation, which expanded to be not visible by PCR. Pedigree B showed a reversal of the repeats. The mother showed an allele which could not be amplified, which contracted in the son to only 73 repeats (a premutation form)—which is quite curious. Individual 4 in Pedigree C is thought to be mosaic for the full mutation, but shows a smear for the pre-mutation form in the PCR. Mosaic females are shown in Pedigrees D and E.

Figure 6 performs a southern blot on family 5C mentioned in the previous figure. They include both *EcoR1* and *BssHII* restriction enzymes—which would help differentiate between size and methylation patterns of the gene. They probe with the pE5.1 probe utilized in Pieretti et al. 1991—a cosmid.

Figure 7, 8, & 9

Figure 7 studies a family in which a 54 repeat length allele was found with none expressing fragile X. Offspring from the 54 repeat mother all had varying lengths, some of which expanded to 60, and

other which shrunk to 52.

Figure 8 demonstrates that as the parental # of repeats increases, so too does the instability which causes altered size in the next generation. Figure 9 similarly demonstrates that the frequency of expansion is size-dependent.

Figure 10

Is simply a graphical demonstration of the Sherman paradox.

Pieretti et al. 1991

Figure 1

This work focuses on methylation patterns of the FMR-1 gene in the context of fragile X. A CpG fragment (cytosine preceding guanine) in the FMR-1 gene is preferentially methylated in fragile X patients. They use an RT-PCR assay to determine the amount of mRNA, and identified very low levels in fragile X patients. Figure 1 shows the primers used in their assay. Both were designed for RNA only, and do not overlap with the variable CGG region.

Figure 2 & 3

Shows the RT-PCR products of affected males. Notably, in comparing affected, carriers, and unaffected, it is obvious that FMR-1 expression is lowest in the affected population. However, there is also a marked reduction in the carriers as well. Though, they don't call attention to this and rather say that they do demonstrate some product.

Figure 3 attempts to be more quantitative by limiting the PCR cycles and normalizing to their control gene expression. Essentially, they find no FMR-1 in affected individuals—but they do not compare this to heterozygous females and or carriers.

Figure 4

Figure 4 uses a restriction enzyme that normally cuts at a GCGCGC site, but is incapable of doing so when these cytosines are methylated. The Southernblots shown that there is significantly less *BssHII* digestion occurring in affected patients.

Jin et al. 2003

Fragile X patients have significantly more dendritic spines, and this was preserved in mouse models with FMR-1 knockouts. Yet, those with FMR-1 knockout experience no degeneration, while those with the CGG repeats do. This is evidenced even by patients with the premutation, who may not experience developmental delays but show tremor or parkinsonism later in life. Thus, it's hypothesized that the repeats confer degeneration. Studies after patient death showed that these patients had intranuclear inclusions that stained for ubiquitin. Interestingly, in the premutation the levels of mRNA are actually increased. This seems to contradict previously discussed works. This work achieves evidence for this in a *Drosophila* model, in which they express varying length CGG repeats of the human FMR-1 gene.

Figure 1

They use the UAS-Gal4 system was used, and a premutation of 90 CGG repeats was added to a UAS-EGFP sequence. **Ask if it is a fusion protein.** By both RT-PCR and Western Blot, in which they used *GMR-Gal4*, expression of the human FMR-1 gene and EGFP was found in the retina.

Table 1 & Figure 2

Both of these demonstrate the results of their CGG-EGFP expression. They expressed, at varying levels, in a few different tissues. **Am I stupid? How do they get strong / weak / moderate expression levels?**

Figure 4

Figure 4A-C shows nuclear Hsp70 inclusions in the face of the (CGG)₉₀ repeats. Figure 4D shows OE of Hsp70 and demonstrates its ability to rescue the disease phenotype. This is not so when overexpressing a dominant negative Hsp70.

Morales et al. 2002

Figure 1

Figure 1A compares the sequence homology of different species FMR-1 gene, and compares the evolutionary origin of it as well (the family tree, that is). Figure 1C is a Western blot for the protein, and they find that their deletion lines show no expression, and one mutation is a hypomorph.

Figure 2

Figure 2 showed staining for neurons, glia, and the *dfxr* gene. They find no overlap in glia. Figure 2D shows that *dfxr* is expressed most in the cytoplasm, rather than nuclei.

Figure 3

Figure 3 A-D shows that less fibers exist in *dfxr* deletion. Figure 3 E and F show that fibers extend erroneously, with poor guidance.

Amir et al. 1999

Overview

Rett syndrome is an X-linked developmental disease, where symptom onset begins around 6-18 months of age and affects only girls. At this point, there is a rapid deterioration, where children may lose their previously acquired skills. It is considered the severest form of the autism spectrum disorders. Communication and motor function delays are some of the earliest signs. Patients may also get seizures or other more severe symptoms. It is a lifelong disease with no treatments.

The incidence is $\approx 1/10000$. It was determined that Rett syndrome is indeed lethal in males, hence only females get it. 99% of cases are sporadic. However, some very rare Mendelian cases allowed for insights into the gene of interest. The mutations were in a gene called MECP2, which aids in methylation of CpG islands. It was the first disease found to be caused by mutations in a *trans*-acting

factor, i.e. a gene that modulates other gene expression at the level above DNA. The protein has a methyl-binding domain and a nuclear localization domain, which is flanked by transcriptional repression domains, which recruits proteins to help shut off transcription. It is predicted that the mutations are loss-of-function. The hypothesis is that genes that would normally be repressed are now being expressed.

Fascinatingly, early mouse models with homozygous knockouts demonstrated phenotypes similar to human disease—i.e., were not lethal, but rather were born normal. Further interestingly, more sophisticated models including *Cre*-based knockouts in only mature neural tissue phenocopied these models.

Figure 1

Figure 1 used PCR amplification to scan for mutations in the MECP2 gene. These mutations were shown to be *de novo* by comparing the mother's sequence to the daughters. While the mutations are sporadic, it is possible to have a mosaic germline, in which a mother can pass on the gene to multiple offspring (at a probability impossible if it were chance alone).

Guy et al. 2007

Figure 1

They used a *lox-Stop* site in order to create a null-allele for *Mecp2*, but which can be activated by tamoxifen (TM) treatment. Figure 1A shows the efficacy via Western blotting, and 1B shows similar results using in situ immunostaining. Figure 1C compared the survival rates of *stop* and *Stop-cre* groups to demonstrate that the *Stop-cre* does not confer any extra survival when off. In Figure 1D, I have no idea what they are probing for. I think they're just Southern blotting for the *Mecp2* allele, and they find WT when the Stop and CreER are both present.

Figure 3

Figure 3A & E show the treatment regime used, and that there is actual recovery after injecting the TM.

Amyotrophic lateral sclerosis

Overview

ALS was identified by Jean-Martin Charcot around 1825 in France. His style was innovative at the time, which was to interview, record, and imitate many symptoms in order to demonstrate them to training physicians. This is also around the time photography became possible, so in addition to his drawings, pictures allowed for further diagnostic insight. Amyotrophic refers to the degeneration of muscles, lateral refers to the region in the spinal cord, and sclerosis refers to the glial scarring in the nervous system. Charcot characterized other diseases as well, including multiple sclerosis.

Motor neurons are lost in the motor cortex and throughout the spinal cord. Interestingly, some subsets of neurons, like those in the neck, do not degenerate. This provides a pathway for developing therapeutics, as we can look for what is unique about these neurons. The typical onset is around 45 to

65. Initially, it was thought to be purely motor-related. However, it is now known that dementia can be a symptom as well. There is a genetic correlation between this (i.e., depending on which ALS-causing mutation you have). Specifically, some forms can segregate with fronto-temporal dementia, where one can present with both diseases, or only one. There was some initial support for environmental factors causing ALS, but we now know there's 20 or so genes which can cause it.

Rosen et al. 1993

ALS can either be inherited as an autosomal dominant disease (about 10% of cases), or is sporadic. The two manifest clinically in a very similar manner, causing them to become interested in using fALS for insight into sporadic ALS. Linkage studies have shown a correlation between ALS and Chr21. This work furthers this by identifying the gene ALS is caused by to be Cu/Zn-binding superoxide dismutase (SOD1). This was a key, remarkable finding because SOD1 was already known at the time. Very few proteins / genes were understood, but in fact this was one of them! Therefore, many thought ALS would be cured quickly. SOD1 is helpful in clearing reactive oxygen species, and thus the immediate hypothesis was its dysfunction leads to ROS buildup and thus cell death. Interestingly, they comment that this may be counterintuitive because the allele is dominant, and it seems unlikely that a loss of function allele would be dominant.

Figure 1

Fortunately for them, the sequence of SOD1 was already known and published. This allowed them to easily design primers for SOD1 exons. One metric they used was single-strand conformation polymorphism—which uses the structure of single stranded DNA and looks for differences due to polymorphism. They identified conformational changes in a small group of fALS families, but none in non-affected individuals in the SOD1 gene. This is shown both in Table 2 and Figure 1A. Figure 1A focused on exons 2 and 4, and used an audiogram to show DNA differences. **I am confused by what we are looking at here.** Figure 1B shows their Sanger sequencing results and identifies mutation sites. Importantly, these were all heterozygous, as indicated by the multiple base pairs found.

Gurney et al. 1994

Figure 1

This work develops a mouse model for ALS using human WT and mutant SOD1. Their model was verified first through Western and Southern blotting. Figure 1E shows that the G1 mice become impaired between 60 and 150 days and die between 150 and 180 days. Their stride significantly worsens between 150 and 180 days, as shown in Figure 1F. Table 1 also quantified the total amount of SOD1 protein being produced, and found that it is comparable between WT and G1, suggesting that the G1 phenotype is due to the mutation rather than expression alone.

Figure 2 & 3

Figure 2A-D showed their neuropathological studies. They found decreased ChAT staining in the G1 mice. They also stained for the presence of SOD1 in the spine and found a high degree in the horns. Figure 3 showed neurofibrillary tangles in many, but not all, motor neurons.

Clement et al. 2003

The key takeaway here is that both glia and neurons must express mutant SOD1. Mutant neurons can be salvaged by many wildtype neurons in the surrounding regions.

Figure 2A & 3

Chimeras between SOD1 mutants and those expressing low levels of human neurofilament subunits were generated. Loss of motor neurons was found to be symmetric, which was odd considering all motor neurons express mutant SOD1. It was found that the neuronal sparing seemed higher on sides of the spinal cord where the proportion of wildtype, non-neuronal cells was greater. This signified some potential neuroprotection associated with non-neuronal cells.

A key finding is that nearly no WT motor cells may still have no phenotype. The hypothesis being that other cell types, namely glia, also require dysfunction before an ALS phenotype can emerge. Interestingly, they actually found asymmetry among the two sides of the spinal cord. Importantly, in heavily degenerating sections of the spinal cord, nearly no WT non-neuronal cells are found, compared to those sections of the spinal cord that survive. Similarly, mutant SOD1 expressing non-neuronal cells seem capable of killing motor neurons as well.

Nagai et al. 2007

Figure 1A, 3G, 4

Figure 3G shows that transgenic astrocytes caused more cell death in both transgenic and non-transgenic motor neurons. Fascinatingly, media conditioned by transgenic astrocytes kills neurons more than does normal media or media conditions by non-transgenic astrocytes. This suggests mutant astrocytes release toxic elements, causing neurons to die.

This paper also found that non-astrocytes have no effect whatsoever on motor neurons. Similarly, non-spinal motor neurons are not affected at all by transgenic astrocytes. Even other motor neurons derived from other parts of the body are unaffected by these mutants.

Eventually, in 2021, it seems that the toxic product in the media is lipids—specifically non-saturated lipids? Part of the theory may be that non-saturated lipids are preventing membrane fluidity, somehow impacting their membranes globally.

Neumann et al. 2006

Some of the background here is that frontotemporal dementia and ALS are two of the most common degenerative diseases for those under 65. They present with similar symptoms, suggesting possible mechanistic crossover. About 30% of FTDs are familial and many show linkage to chromosome 17. While the inclusions in FTD are hyper-ubiquitinated, FTD does not present with any tauopathies, leaving the protein unknown. The key result of this paper is that both frontotemporal lobar degeneration (FTLD) and ALS have inclusions due to TDP-43. These inclusions are marked by hyperphosphorylated, ubiquitinated TDP-43.

Interestingly, FTD and ALS are frequently found together in families, so therefore it may be possible that there is some mechanistic or genetic conservation between the two.

Figure 1

Figure 1 begins by showing that they developed antibodies which specifically bind to patients with either FTLN type 1 or type 2, and that these antibodies mark ubiquitinated inclusions. To develop these they would have had to inject ubiquitinated inclusions into mice and isolate single cells within the spleen. To screen these possible antibodies they tested on slices from human brains. In other words, a robust and large brain bank played a key role in this. On a Western blot, these antibodies show an $\approx 24\text{kD}$ band and an $\approx 26\text{kD}$ band for type 1 and type 2 respectively. Using a urea-based purification technique was essential for removing any and all soluble proteins so that only the insoluble aggregates remain. These bands were not found in controls or AD brains, and similarly tau staining was not found in FTLN brains.

To determine what these antibodies might be binding to, they performed, in SFigure 1, a 2D page gel and looked for a bands around 25kD . Because similar spots of $\approx 3.5\text{pI}$ were found on both type 1 and type 2, they predicted this was correct. They performed mass spectrometry and identified the protein as being TDP-43. Both fragments of TDP-43 are truncated at the C-termini. Notably, this gene is on chromosome 1.

Figure 2

Figure 2 uses immunostaining to further prove their TDP-43 hypothesis. In type 1 and type 2 FTLN, as many inclusions as were labeled by TDP-43 antibodies were labeled by ubiquitin. Interestingly, type 3 FTLN had inclusions not labeled by these antibodies. Additionally, other degenerative diseases did not show any TDP-43 staining.

Figure 3

Figure 3 found TDP-43 only in the urea fraction after Western blotting. Non-aggregate TDP-43 was found in all fractions. Figure 3B showed that the molecular profile of TDP-43 was different in FTLN than it was in other degenerative diseases. Specifically, extra bands around 45kD were found. Figure 3C showed that dephosphorylation of these bands collapsed them into a single band. Figure 3D also demonstrated the higher weight TDP-43 band is ubiquitinated.

Figure 4

Figure 4 extended this work to ALS by verifying TDP-43 also labels ALS inclusions. Interestingly, they suggest TDP-43 is normally a nuclear protein, but in disease pathologies is cytosolic. Figure 4L shows that the cleaved products seem only present in the frontal cortex. However, phosphorylated TDP-43 can be found throughout other regions of the brain and spinal cord. Additionally, some of the FTLN families were mutant for a different gene called PGRN. The relation between PGRN and TDP-43 is unknown. Regardless, TDP-43 aggregates characterize nearly all diseased ALS brains.

Rothstein, 2007

Soon after the publication of Neumann et al. detailing the potential role of TDP-43 aggregates, this piece from Rothstein was published criticizing it. He comments largely on the over-statements frequently made regarding aggregates. He comments that some nuclear inclusions have been shown to be protective, rather than disease-causing, in some CAG repeat diseases. Rothstein comments that TDP-43 inclusions were found in non-motor cells and in regions clinically unaffected by ALS.

Therefore, this calls in to question their relevance in disease progression. Similarly, because these inclusions are not found in fALS mutant for SOD1, there is further questions. This author proposes that, because sALS is a slower progressing disease than fALS, more time is given for aggregates to build up. Therefore, they are not necessary for disease progression, but rather another symptom.

Perhaps the cells with inclusions are the survivors rather than the sick ones.

Follow-Up

Follow-up work looked to sequence TDP-43, and many mutations were found in the glycine-rich region (near the C-terminus) of TDP-43. Other similarly structured proteins, which had RNA-recognition motifs (RRMs) include proteins like FUS—which was later found to aggregate in ALS as well. Interestingly, FUS did not have many mutations in the glycine-rich region, but rather it was in its C-terminus. Similarly, in FUS' mutation it is trafficked outside of the cell. The C-terminus area, then, was determined to be relevant in nuclear localization. However, TDP-43's mutations are not often in its nuclear localization sequence. Both FUS and TDP-43 have NLS and NES, meaning they can be trafficked back and forth between the cytoplasm and nucleus as needed—but both spend much more time in the nucleus.

Interestingly, both FUS and TDP-43 are localized to stress granules in these diseases. Important insight came from *C. elegans* embryos. In early stages, granules in these worms get trafficked from scattered around the cell and are then trafficked to one side of the cell. Fascinatingly, though, these granules do not get moved, per se, but rather disappear and reappear. Thus, they are not being pulled like you might expect. Rather, they are phase-separated liquid droplets. Stress granules are similar to the nucleolus—they are effectively membrane-less organelles. Both TDP-43 and FUS have “low complexity domains” which allow for the gel-like formations of these proteins. It's hypothesized that liquid droplets and then transition somehow into being hard, solid aggregates. One of the most fascinating questions, then, is how non-mutant TDP-43 still exhibits these stress granule to aggregate conversions. Somehow, continued stress in the neurons leads to this. What causes this?

So what is TDP-43 anyway? It is a nucleic acid binding protein which is capable of doing a lot in RNA maintenance and processing, including splicing. TDP-43 is considered a repressor, helping to prevent expression of certain exons. Therefore, both TDP-43 loss of function and gain of function is capable of producing different, new proteins with either extra or less than intended exons. TDP-43 especially represses “cryptic exons” which are not found in mice. Therefore, we can only use RNAseq from humans to determine how TDP-43 dysfunction alters the transcriptome. Broadly, TDP-43 seems to make transcription more accurate and precise. Thus, it is wise to hypothesize that improper transcription of critical genes may lead to neuron death. One example of this is stathmin-2 (STMN2), which has a cryptic exon and is known to play a role in motor function and motor neuron outgrowth. Again, this is not preserved in mice—so we cannot investigate it properly in a mouse model. As a final comment, TDP-43 is autoregulated, so it is not an ideal therapeutic target.

DeJesus-Hernandez et al. 2011

It was shown years prior that ALS and FTD are linked to a gene on Chr9. Yet, finding this gene proved impossible. A large reason for this is the advent of next generation sequencing, which caused researchers to miss the key mutations. All of the exons were sequenced, so the Rademaker group questions if the causative mutations could be in the introns. Via attempts to PCR these introns, one

intron failed to amplify. This work identifies this gene as *C9ORF72*, and that the causative mutation is a repeat expansion in a non-coding region.

Figure 1 & 2, Table 1

Figure 1 shows brain tissue from affected family members showing Chr9 linkage. These stains clearly show TDP-43 inclusions. Figure 2 shows a pedigree that implies a lack of transmission from affected parent to affected offspring. Via PCR amplification, they size different alleles in their suspected gene and find that affected individuals only show one size. This is curious, and suggests affected individuals are homozygous—which cannot be true. This means instead that it cannot be amplified. They then turned to a Southern blot, and by probing this region, they found that diseased individuals had very long alleles. The expansions they found were on the order of thousands of base pairs. Table 1 shows that this mutation is more common than any other ALS or FTD mutation, even more so than SOD1, FUS, and TDP-43, etc. At many clinics around the world, it was on the order of 50% of cases are due to this repeat expansion.

Figure 4 & 5

Based on a single SNP, the group can tell how the RNA is cut. In variant 2 and variant 3, both alleles are seen. It is not seen in variant 1, which could suggest expanded repeats turn off expression of variant 1. Thus, Figure 4 demonstrates the possibility that these expanded repeats cause alternative splicing. It shows that those with the expanded repeat have a much higher % of the V2 splice. Figure 5 shows that expanded repeat RNA forms nuclear inclusions.

Renton et al. 2011

The Traynor lab used extensive next generation sequencing to look for the changes in the critical region of Chr9. Next generation sequencing specifically creates a shotgun library of genomic DNA, sequences it, and aligns them together. Each fragment is on the order of 50 to 100 base pairs. This is not *de novo* sequencing, but rather comparative sequencing, where one compares and or aligns with a reference sequence from the original human genome project. A read depth describes how often an individual base is read. In affected individuals, they were reading with a depth around 170, meaning each individual nucleotide was read around 170 times—i.e., this is great depth. Part of the computation done is to align uniquely mapped reads, meaning segments of DNA which are conserved in different parts of the genome, it cannot be mapped—hence a struggle with repeat expansions. The Traynor group therefore was able to see a massive gap in the reads done by their sequencing, suggesting some error in computation, which they supposed was due to repeat expansion.

One of the strategies employed was “repeat primed PCR,” where a reverse primer and an anchor primer are used. Part of the reverse primer is homologous to the variable repeat, and the anchor is homologous to a non-repeat expansion. The reverse primer will then be capable of binding anywhere along the repeat, generating various amplification products. Adding the anchor primer after allows you to amplify all of these fragments. You will then, in short, see a wide variety of products when there are repeats.

Fallout

One possible implication would be that a long repeat leads to RNA accumulation that soaks up tons and tons of RNA binding proteins, leading to a dual kind of gain of function-loss of function result.

Notably, no point mutations have ever been found in this disease. Unlike something like FMR-1, it must be true that repeat expansions alone are causing the disease. Therefore, it may also be that the protein is translated strangely, including translation through introns, leading to aberrant proteins.

This gene is now part of the common disease haplotype that characterizes ALS. Again, note that healthy individuals have 2-23 units of the GGGGCC repeats, while affected individuals have nearly 700-1600. Yet, while this gene is extremely unstable, there is no observed anticipation. It thus remains unknown what the “minimum” length is required to cause disease, as there is no “middle” cases. Interestingly, the A haplotype has more repeats seen than does the G haplotype. However, this is still well within the normal range.

Another fascinating thing to note is this mutation can confer both FTD or ALS, or both. Different family trees seem to be biased toward one disease or another, suggesting more genetic factors are involved, or environmental factors. Because of the similarity in this haplotype, and the localization to certain countries, it's thought that this repeat expansion may have originated in Europe from Viking times. I.e., it's possible this repeat expansion occurred only once.